
Application of Effective Field Theory Methods in the Case of HEFT and SMEFT

Florian Pandler



München 2025

Application of Effective Field Theory Methods in the Case of HEFT and SMEFT

Florian Pandler

Dissertation
der Fakultät für Physik
der Ludwig-Maximilians-Universität
München

vorgelegt von
Florian Pandler
aus Freising

München, den 17.06.2025

Erstgutachter: Prof. Dr. Gerhard Buchalla

Zweitgutachter: PD Dr. Michael Haack

Tag der mündlichen Prüfung: 30.07.2025

Contents

Publications	viii
Zusammenfassung	xiii
Abstract	xiv
1. Introduction	1
I. Foundations	5
2. The Standard Model	7
2.1. The SM Lagrangian	7
2.2. Higgs Sector in the SM	9
2.2.1. Custodial Symmetry	11
2.2.2. Experimental Constrains	12
2.3. Beyond the SM	13
2.3.1. Experimental hints for BSM physics	13
2.3.2. Theoretical hints for BSM physics	14
3. Effective Field Theories	17
3.1. The EFT paradigm	17
3.2. Top-Down vs. Bottom-Up Approach to EFTs	19
3.3. SMEFT	19
3.3.1. Dimension 5	20
3.3.2. Dimension 6	21
3.3.3. Dimension 7 and above	23
3.4. HEFT	23
3.4.1. Leading order chiral Lagrangian	23
3.4.2. Power Counting and NLO operators	25
3.5. SMEFT vs. HEFT	25
4. Functional matching techniques	29
4.1. A simplified approach to One Loop Matching	29
4.2. Universal One Loop Effective Action	31
4.2.1. Covariant diagram method	32
4.2.2. Effective Lagrangian	34
4.2.3. Example: Euler-Heisenberg Lagrangian	34

II. Applications	37
5. Loop Counting in SMEFT	39
5.1. Toy Model analysis of $e^+e^- \rightarrow t\bar{t}$	40
5.1.1. Diagrammatic matching	40
5.1.2. Strategy of regions	42
5.1.3. Top-down EFT	44
5.1.4. Bottom-Up EFT	46
5.1.5. Functional matching	47
5.2. SMEFT	48
5.2.1. Example: Higgs Production via Gluon Fusion	49
5.2.2. Power Counting in General EFTs	51
5.2.3. Loop counting in SMEFT	52
5.2.4. Amplitude for $gg \rightarrow h$ with leading dim 6 corrections in SMEFT	55
5.3. Heuristic approach to chiral dimensions	57
5.4. Example for SMEFT in a UV Model: $u\bar{u} \rightarrow t\bar{t}$ via gluon exchange in the 2HDM	58
5.4.1. 2HDM in the decoupling limit	58
5.4.2. Top-Down EFT	63
5.4.3. Bottom-Up SMEFT calculation	65
5.5. Discussion	66
6. Linear Sigma Model: Nondecoupling EFT	69
6.1. The model	70
6.2. EFT	71
6.2.1. Tree-Level EFT	72
6.2.2. SMEFT-like EFT	73
6.3. Integrating the scalar out at the one-loop level	74
6.3.1. Inverting Δ_L	75
6.3.2. Calculation of \mathcal{L}_H	76
6.4. Renormalization	78
6.4.1. Background scalar self-energy	79
6.4.2. Elimination of the background scalar S	80
6.5. Goldstone scattering at NLO	81
6.6. Discussion	84
7. 2HDM: Nonlinear EFT	85
7.1. Nondecoupling Regime - Higgs-EWChL	85
7.2. Tree-level matching in the nondecoupling regime	89
7.2.1. Algorithm for tree-level matching	89
7.2.2. Other Yukawa interactions	93
7.2.3. Four-fermion operators in the alignment limit	94
7.3. Nondecoupling effects at one loop	96
7.3.1. Functional matching	96
7.3.2. Diagrammatic matching	98
7.4. Custodial symmetry breaking	102
7.5. Parameter Range - Decoupling vs. Nondecoupling Limit	106
7.6. Phenomenological considerations	108

7.7.	Linear EFT	108
7.8.	Discussion	112
7.9.	Appendix: Exact solution for $H_0(h)$	112
8.	Anomalous HEFT couplings for Off-shell Higgs in $gg \rightarrow Z_L Z_L$	115
8.1.	Effective field theory framework for $gg \rightarrow ZZ$	116
8.1.1.	Electroweak chiral Lagrangian	116
8.1.2.	EFT applied to $gg \rightarrow ZZ$ - overview	117
8.2.	Anomalous Higgs couplings in $t\bar{t} \rightarrow ZZ$	119
8.3.	Anomalous Higgs couplings in $gg \rightarrow Z_L Z_L$	120
8.3.1.	General Structure	121
8.3.2.	Form factors at leading order	122
8.3.3.	Subleading EFT corrections	123
8.3.4.	Toy models for c_{ggh}	126
8.3.5.	RGE effects	128
8.4.	Phenomenological considerations	129
8.5.	Discussion	131
8.6.	Appendix: Details of the calculation	132
III.	Conclusion	135
9.	Conclusion and Outlook	137
IV.	Appendix	139
A.	Parameters of the 2HDM potential	141
B.	Explicit computation of the scalar masses in the 2HDM	145
C.	Useful relations for one-loop integrals	149
D.	SU(2) identities and operator reduction	153
E.	Scalar Integrals	155
F.	Feynman Rules	159

Relevant Publications

The thesis is based on the following publications:

- [1] G. Buchalla, G. Heinrich, Ch. Müller-Salditt, and F. Pandler. “Loop counting matters in SMEFT”. in: *SciPost Phys.* 15.3 (2023), p. 088. DOI: 10.21468/SciPostPhys.15.3.088. arXiv: 2204.11808 [hep-ph]
- [2] G. Buchalla, F. König, Ch. Müller-Salditt, and F. Pandler. “Two-Higgs-doublet model matched to nonlinear effective theory”. In: *Phys. Rev. D* 110.1 (2024), p. 016015. DOI: 10.1103/PhysRevD.110.016015. arXiv: 2312.13885 [hep-ph]
- [3] Gerhard Buchalla and Florian Pandler. “Anomalous Couplings from the Electroweak Chiral Lagrangian for Off-Shell Higgs in $gg \rightarrow Z_L Z_L$ ”. In: (July 2025). arXiv: 2507.23658 [hep-ph]

Chapter 5 relies on [1], Chapter 7 on [2] and Chapter 8 on [3].

List of Figures

3.1.	General concept underlying top-down and bottom-up EFTs	19
4.1.	Covariant diagrams corresponding to dimension six operators	32
5.1.	$e^+e^- \rightarrow t\bar{t}$ in a toy model. (a) Lowest-order amplitude. (b), (c): Leading corrections from S -scalar exchange in the full theory. (d), (e): Contributions needed to reproduce the $1/M^2$ corrections of the full theory within the EFT, where the black dots represent the local dimension 6 EFT operators. Q_2 and Q_3 enter at tree-level in (d), whereas Q_1 contributes at one loop in (e).	41
5.2.	Higgs production through gluon fusion. (a) SM amplitude at leading order (two diagrams with opposite fermion flows are understood). (b)–(g): Representative SMEFT diagrams with insertions of dimension-six operators (black dots). (1)–(3): Examples of radiative corrections.	50
5.3.	Sample diagrams in a generic UV theory that generate the various operator classes after integrating out the heavy fields: (a): $\kappa^4(\phi^\dagger\phi)^3$, (b): $\kappa^2(\phi^\dagger D\phi)^2$, (c): $\kappa^3\phi^\dagger\phi\bar{\psi}\phi\psi$, (d): $\kappa^2(\phi^\dagger D\phi)\bar{\psi}\psi$, (e): $\kappa^2(\bar{\psi}\psi)^2$. The dashed double line denotes a generic heavy boson	54
5.4.	The (dashed) double line denotes a generic heavy (boson) fermion	54
5.5.	Three bases for the neutral scalar degrees of freedom taken from [170]	61
5.6.	One loop diagram for $u(k_1)\bar{u}(k_2) \rightarrow t(p_1)\bar{t}(p_2)$ with one loop correction due to heavy 2HDM states to the top quark vertex function	63
5.7.	Contributions needed to reproduce the $1/M^2$ correction to the full theory within the EFT. The black square represents the insertion of a SMEFT dimension 6 operator.	65
6.1.	Background scalar self-energy diagrams of $\mathcal{O}(M^4)$	80
6.2.	One-loop diagrams for $\varphi\varphi \rightarrow \varphi\varphi$ scattering. Black circles denote vertices from the LO Lagrangian.	82
8.1.	Diagrams for $gg \rightarrow ZZ$ at leading order in the chiral counting. Black circles and black squares denote vertices from the LO and NLO Lagrangian, respectively. Additional diagrams with permutations of the external legs are not explicitly shown.	117
8.2.	Representative diagrams for $gg \rightarrow ZZ$ at next-to-leading order in the chiral counting. Black circles, black squares and crossed squares denote vertices from the LO, NLO and NNLO Lagrangian, respectively.	118
8.3.	Sample diagrams for $gg \rightarrow ZZ$ with operators from the Lagrangian at chiral dimension 4, which would only contribute at next-to-next-to-leading (3-loop) order to this process. Black squares denote vertices from the NLO Lagrangian, respectively.	118

8.4.	Diagrams for $t\bar{t} \rightarrow ZZ$ at leading order in the chiral counting. Black circles denote vertices from the LO Lagrangian.	120
8.5.	Tree-level and triangle graphs. Black circles and black squares denote vertices from the LO and NLO Lagrangian, respectively. Additional diagrams with permutations of the external legs are not explicitly shown.	120
8.6.	Box graphs, Background	121
8.7.	Energy dependence of the scattering cross section at $\cos\theta = 0$ in units of fb. Here only the LO anomalous couplings are varied while all other coefficients are set to their SM values.	131
8.8.	Energy dependence of the scattering cross section at $\cos\theta = 0$ in units of fb. Here only the HEFT coefficient $C_{\psi S1} = -\xi m_t/16\pi^2 v^2$ is varied while all other coefficients are set to their SM values.	131
8.9.	Energy dependence of the scattering cross section at $\cos\theta = 0$ in units of fb. Here only the NLO anomalous couplings $C_{GU1} = c_{ggH}/32\pi^2 M^2$ varied while all other coefficients are set to their SM values.	132
8.10.	Energy dependence of the scattering cross section at $\cos\theta = 0$ in units of fb. Here we plot the SM scattering cross section for the processes $gg \rightarrow \varphi^0\varphi^0$ and $gg \rightarrow Z_L Z_L$. For large \sqrt{s} we find good agreement between the two processes validating our choice to use the Goldstone limit.	132

Zusammenfassung

Effektive Feldtheorien (EFTs) haben sich als unverzichtbare Werkzeuge in der Suche nach Physik jenseits des Standardmodells (BSM) etabliert. Sie ermöglichen eine modellunabhängige Parametrisierung der indirekten Effekte neuer Physik. Um konsistente Vorhersagen zu erhalten, ist es jedoch entscheidend, die zugrunde liegenden Annahmen klar zu formulieren und die EFTs systematisch anzuwenden. Im Bereich der BSM-Physik sind zwei EFTs besonders weit verbreitet: die Standardmodell-Effektive-Feldtheorie (SMEFT) und die elektroschwache chirale Lagrangedichte, oft als Higgs-Effektive-Feldtheorie (HEFT) bezeichnet. Diese basieren auf unterschiedlichen Ordnungsprinzipien. Diese Arbeit widmet sich der systematischen Anwendung beider Ansätze.

Für die SMEFT argumentieren wir, dass eine Powercountingvorschrift, die sich ausschließlich auf kanonische Dimensionen stützt, unzureichend ist. Sie muss durch eine Zählung der Schleifenordnung ergänzt werden, die sich durch die Einführung chiraler Dimensionen darstellen lässt. Die gleichzeitige Berücksichtigung kanonischer und chiraler Dimensionen führt zu einer klaren Hierarchie der Operatoren und erlaubt es, dominante Beiträge in Hochenergieprozessen gezielt zu identifizieren. Als konkretes Beispiel untersuchen wir das Zusammenspiel beider Zählweisen durch das Matching des schwach gekoppelten Zwei-Higgs-Doublett-Modells (2HDM) auf die SMEFT.

Ein einfaches Modell auf Basis des $SO(4)$ linearen Sigma-Modells dient zur weiteren Verdeutlichung der beiden Entwicklungsparameter. Durch das Ausintegrieren des schweren Freiheitsgrads leiten wir die entsprechende Niederenergie-EFT her und vergleichen das Ergebnis für schwache und starke Kopplung.

Danach kehren wir zum 2HDM zurück, diesmal im Nicht-Entkopplungsregime. Durch das Ausintegrieren der schweren Skalarfelder zeigen wir, wie HEFT als Niederenergie-Grenzfall entsteht. Mithilfe funktionaler Methoden leiten wir die chirale Lagrangedichte in führender Ordnung der chiralen Zählweise auf effiziente und transparente Weise her. Dies umfasst auch lokal generierte Schleifenbeiträge wie $h \rightarrow \gamma\gamma$ und $h \rightarrow \gamma Z$, die in derselben Ordnung wie ihre Standardmodell-Gegenstücke auftreten. Darüber hinaus präsentieren wir einen Algorithmus zur Berechnung der charakteristischen Koeffizientenfunktionen bis zur beliebigen Ordnung im Higgsfeld h .

Abschließend untersuchen wir die Produktion longitudinaler Z -Bosonenpaare in Gluonfusion mit anomalen HEFT-Kopplungen. Unter Betonung der Rolle des Organisationssprinzips analysieren wir detailliert die führenden und nächstführenden EFT-Beiträge zur Streuamplitude. In führender Ordnung hängen die Beiträge neuer Physik von drei EFT-Kopplungen ab, die sich auf zwei unabhängige Parameter reduzieren lassen. Effekte höherer Ordnung werden innerhalb des Gültigkeitsbereichs der EFT als vernachlässigbar erwartet.

Die vorliegende Arbeit stellt heraus, dass eine konsistente Powercountingvorschrift notwendig bei der Anwendung von EFT Methoden ist.

Abstract

Effective Field Theories (EFTs) have become indispensable tools for physics beyond the Standard Model (BSM) to parameterize new physics in a model-independent way. To obtain consistent predictions, the underlying assumptions have to be specified, and the EFT has to be applied systematically. For BSM physics, two particular EFTs are widely used: the Standard Model Effective Field Theory (SMEFT) and the electroweak chiral Lagrangian, often referred to as the Higgs Effective Field Theory (HEFT). These two approaches are based on distinct organizing principles. This thesis is dedicated to investigating the systematic application of both frameworks.

For SMEFT, we argue that a power-counting scheme based solely on canonical dimensions is insufficient. It must be supplemented by a loop-order counting scheme, conveniently expressed through the assignment of chiral dimensions. By accounting for both canonical and chiral dimensions, a clear hierarchical structure emerges among the operators, enabling a more meaningful identification of potentially dominant contributions in high-energy processes. As a concrete example, we explore the interplay between these two counting schemes by matching the Two-Higgs Doublet Model (2HDM) to SMEFT in the decoupling limit.

To further illuminate the role of the two expansion parameters, we analyze a toy model based on the $SO(4)$ linear sigma model. By integrating out the heavy degrees of freedom, we derive the corresponding low-energy EFT and compare the resulting theories in both the strongly and weakly coupled regimes.

Subsequently, we revisit the 2HDM, this time focusing on the non-decoupling regime. We integrate out the heavy scalars and demonstrate how HEFT naturally arises as the low-energy EFT. Using functional methods, which provide a transparent and efficient approach, we derive the chiral Lagrangian at leading order in the chiral counting. We include loop-induced local terms such as $h \rightarrow \gamma\gamma$ and $h \rightarrow \gamma Z$, which appear at the same order as their SM counterparts. Additionally, we present an algorithm that allows us to compute the characteristic coefficient functions to all orders in the Higgs field h .

Finally, we investigate the production of longitudinal Z boson pairs via gluon fusion with anomalous HEFT couplings. Emphasizing the role of power counting, we perform a detailed analysis of the leading and next-to-leading EFT contributions to the amplitude at leading order in QCD. We demonstrate that the new physics effects at leading order depend on three EFT couplings, which can be reduced to two independent parameters. Subleading corrections are expected to remain small within the range of validity of the EFT.

The thesis shows that a consistent power counting prescription is crucial when using EFT methods.

1. Introduction

“Dass ich erkenne, was die Welt / Im
Innersten zusammenhält.”

*Johann Wolfgang von Goethe
Faust I*

The timeless question posed by Goethe’s *Faust* has been a driving force for humanity throughout the centuries, trying to understand “what holds the world together in its inmost folds.” Since the Presocratic philosophers of the 6th and 5th centuries BCE, the question of the basic constituents of matter has remained at the forefront of scientific inquiry.

In essence, modern particle physics continues this quest, now armed with sophisticated theoretical frameworks and powerful experimental tools. Many of the most significant experimental advances of the past century have come from high-energy particle colliders, where subatomic particles such as protons are accelerated and collided to probe the structure of matter at ever-smaller scales.

The two cornerstones of modern physics, special relativity (SR) and quantum mechanics (QM), are needed to theoretically describe such processes. They can be combined in a single mathematical framework known as quantum field theory (QFT). QFT predicts the existence of antiparticles and the spontaneous pair creation of particles from the vacuum and explains the connections of spin and statistics. None of these phenomena can be explained by quantum mechanics alone. For instance, the uncertainty principle tells us that energies can fluctuate over short time scales. Yet, we need the insight from relativity that energy can be converted into matter and vice versa to explain the phenomenon of pair creation. Elementary particles are described as excitations of matter *fields* by QFT. Despite its successes, early QFT was plagued by the appearance of infinities in calculations involving interacting particles, leading to doubts about its consistency. It was later understood that these divergences arise from the idealization of local interactions at arbitrarily small distances. The infinities can be tamed by *regularizing* the divergent integrals. Then, the divergences can be removed by systematically redefining the physical observables, a procedure known as *renormalization*. Used in such a way, QFTs provide the most accurate predictions of any scientific theory. For instance, the quantum electrodynamics (QED) [4–6] prediction for the anomalous magnetic moment of the electron agrees with the experimentally measured value to within 10 significant figures [7].

All known elementary particles and their interactions can be described within a QFT framework, the Standard Model of particle physics (SM). It combines the theory of the strong interaction, quantum chromodynamics (QCD) [8–11], and the theory of electroweak interactions [12–14], that unifies the electromagnetic and weak interactions. So far, it has withstood all experimental tests and is rightfully known as the most successful scientific theory in history. For the theory to remain consistent at high energies and facilitate the breaking of the electroweak symmetry, the SM contains the Higgs mechanism [15–19] and

the corresponding particle, the scalar *Higgs boson*. With the discovery of the Higgs boson at the LHC collider [20, 21] in 2012, the last missing puzzle piece of the SM was experimentally discovered.

However, not all open questions were answered with the discovery of the Higgs boson. It opened a wide range of questions regarding the nature of the discovered boson and the precise mechanism of electroweak symmetry breaking. While all the experiments so far are consistent with a SM-like Higgs, deviations from the SM in the Higgs sector of $\mathcal{O}(10\%)$ are still possible.

Evidence for new physics can come from *direct* or *indirect* sources. Since there have been no direct discoveries, i.e., new particles, since the Higgs, we depend on the indirect effects of new physics. From the theory side, we need a calculational framework to constrain the effects of new physics. This is where effective field theories (EFTs) come into play. EFTs are not renormalizable as QFTs in the traditional sense, i.e., an infinite amount of counterterms is required to remove all divergences. For this reason, the pioneers of QFT discarded EFTs as viable theories, as their goal was to formulate fundamental theories valid up to arbitrarily high energies. Steven Weinberg, in his seminal article "Phenomenological Lagrangians" [22], rehabilitated EFTs. He noted that the most general, analytic, unitary, Lorentz invariant, and cluster decomposition satisfying Lagrangian will yield the most general S-matrix elements consistent with these principles. Thus, an EFT Lagrangian contains all possible terms consistent with the aforementioned principles and, as a result, contains an infinite tower of operators parameterizing the effects of new physics. However, not all operators are equally important. This is where the *power counting prescription* enters. It defines an expansion parameter $\delta \ll 1$ and tells us which operators are required for consistent calculation up to $\mathcal{O}(\delta^n)$. A consistent power counting scheme is, therefore, vital to obtain meaningful predictions from an EFT. The consistent and systematic application of EFT methods is the subject of this thesis.

To illustrate our argumentation, we employ two widely used EFT frameworks that are particularly suited for physics beyond the SM. The Standard Model Effective Field Theory (SMEFT) [23–28] is the most general theory with the SM matter content and gauge symmetry. The Electroweak Chiral Lagrangian (EwChL, also known as HEFT) [28–46], on the other hand, is the most general EFT to describe electroweak symmetry breaking and contains the physical Higgs boson as a gauge singlet. The underlying ordering principle for the two EFTs is different. We will highlight the differences and discuss the consistent application of both EFTs by examining several examples.

The structure of this thesis is as follows. The first three chapters serve as an introduction, where all the necessary foundations on which this thesis rests are covered. In Chapter 2, we give a brief overview of the Standard Model and its Lagrangian. The Higgs sector of the SM and the description of electroweak symmetry breaking are covered in more depth, as the Two-Higgs-Doublet Model (2HDM), a model for an extended scalar sector, is featured prominently in this thesis. We motivate the use of EFT methods for Higgs physics by discussing the experimental and theoretical indications for new physics beyond the SM. Chapter 3 serves as an introduction to EFTs in general and the SMEFT and HEFT in particular. We specifically point out how the Higgs sectors of both EFTs differ. A convenient and efficient framework for one-loop matching using functional methods, developed in [47], is presented in Chapter 4, which we frequently employ in the subsequent chapters. After covering the foundations, we turn to applications. All the applications serve as examples of a systematic and consistent usage of the SMEFT and the HEFT.

First, we discuss the power-counting prescription for the SMEFT in Chapter 5 and argue that power counting based solely on canonical dimension is incomplete. It has to be extended to include loop orders or, equivalently, *chiral dimensions*. In Chapter 6, we take the $SO(4)$ linear σ -model and integrate out the massive degree of freedom at one loop to obtain nondecoupling EFT effects. We also study nondecoupling effects in Chapter 7, which is dedicated to matching the 2HDM in the strongly coupled, nondecoupling regime to the HEFT. The study of the process $gg \rightarrow Z_L Z_L$ with anomalous couplings in Chapter 8 showcases the systematic application of HEFT for a phenomenologically interesting high-energy process. Finally, in Chapter 9, we conclude.

Part I.

Foundations

2. The Standard Model

Our goal in this section is to provide a brief, yet self-contained, review of the Standard Model of particle physics (SM). Readers already familiar with the SM are free to skip this section and jump directly to the next section on EFTs. However, the notation used throughout the thesis will be largely set in this chapter.

2.1. The SM Lagrangian

Since the advent of modern science, the goal of physics has been to understand what holds the world together at its core on increasingly smaller scales. Specifically, this meant identifying the fundamental building blocks of nature and understanding their interactions with one another. The road to such a unitary framework of elementary particle interactions was not straightforward. It took decades of groundbreaking experimental and theoretical work, beginning with the pioneers of quantum mechanics, to develop a theory that describes all known elementary particles and their interactions with astonishing precision. That framework, finalized in the 1970s, is the Standard Model of particle physics (SM). Except for gravity, it describes all known fundamental particles and interactions. Furthermore, all measurements performed at energies accessible to current colliders are in excellent agreement with its predictions. It is fair to regard the SM as the foundational achievement of physics in the 20th century.

The SM is formulated as a Quantum Field Theory (QFT) based on 19 input parameters. Although the SM describes such a wide range of particles and interactions, its mathematical description is relatively simple. Hence, its Lagrangian fits nicely on a coffee mug (albeit in a highly simplified form). To formulate the SM Lagrangian, all the necessary theoretical input is the underlying symmetries and the particle content, making it a triumph of theoretical elegance and empirical success. The SM is a gauge theory based on the gauge group

$$G_{SM} = SU(3)_C \times SU(2)_L \times U(1)_Y \quad (2.1)$$

Here $SU(3)_C$ is the gauge group of quantum chromodynamics (QCD) the theory of strong interactions [8–11] and $SU(2)_L \times U(1)_Y$ the gauge group of the electroweak interactions [12–14] which is broken by the Higgs mechanism [15–19] to $U(1)_{em}$. Pedagogical introductions to the SM can be found e.g. in [48–53]. To finally write down the SM Lagrangian one has to write down all renormalizable (up to canonical dimension 4), Lorentz and gauge invariant terms

$$\begin{aligned} \mathcal{L}_{SM} = & -\frac{1}{2}\langle G_{\mu\nu}G^{\mu\nu} \rangle - \frac{1}{2}\langle W_{\mu\nu}W^{\mu\nu} \rangle - \frac{1}{4}B_{\mu\nu}B^{\mu\nu} + \frac{\theta}{32\pi^2}\langle \tilde{G}_{\mu\nu}G^{\mu\nu} \rangle \\ & + \bar{q}_L i \not{D} q_L + \bar{l}_L i \not{D} l_L + \bar{u}_R i \not{D} u_R + \bar{d}_R i \not{D} d_R + \bar{e}_R i \not{D} e_R \\ & + (D_\mu \phi)^\dagger (D^\mu \phi) + \mu^2 \phi^\dagger \phi - \frac{\lambda}{2} (\phi^\dagger \phi)^2 \end{aligned}$$

$$- \left(\bar{q}_L Y_u u_R \tilde{\phi} + \bar{q}_L Y_d d_R \phi + \bar{l}_L Y_e e_R \varphi + \text{h.c.} \right) \quad (2.2)$$

where we introduce the complex conjugate of the Higgs doublet $\tilde{\phi}$ as $\tilde{\phi}_j = \varepsilon_{jk}(\phi^k)^*$ ($\varepsilon_{12} = 1$). Here and in the following $\langle M \rangle$ denotes the trace of any matrix M . The covariant derivative acting on a generic field χ is given by

$$D_\mu \chi = \partial_\mu \chi + i g_s T^A G_\mu^A \chi + i g T^a W_\mu^a \chi + i g' Y B_\mu \chi \quad (2.3)$$

Here $T^A = \lambda^A/2$ and $T^a = \sigma^a/2$ are the generators of the fundamental representations of $SU(3)_C$ and $SU(2)_L$ respectively, where λ^A are the Gell-Mann matrices and σ^a the Pauli matrices. The generators are normalized in the usual way $\langle T^a T^b \rangle = \delta^{ab}/2$. The gauge fields for $SU(3)_C$ and $SU(2)_L$ are Lie algebra valued matrix fields $G_{\mu\nu} = G_{\mu\nu}^A T^A$ and $W_{\mu\nu} = W_{\mu\nu}^a T^a$. The gauge field strength tensors are constructed as follows

$$\begin{aligned} G_{\mu\nu}^A &= \partial_\mu G_\nu^A - \partial_\nu G_\mu^A - g_s f^{ABC} G_\mu^B G_\nu^C \\ W_{\mu\nu}^a &= \partial_\mu W_\nu^a - \partial_\nu W_\mu^a - g \epsilon^{abc} W_\mu^b W_\nu^c \\ B_{\mu\nu} &= \partial_\mu B_\nu - \partial_\nu B_\mu \end{aligned} \quad (2.4)$$

For a generic field strength X we define the dual field strength tensor $\tilde{X}_{\mu\nu} = \frac{1}{2} \varepsilon_{\mu\nu\rho\sigma} X^{\rho\sigma}$ ($\epsilon_{0123} = +1$).

The first line comprises the kinetic terms of the gauge fields and the theta term. The interactions, induced by the local $SU(3)_C \times SU(2)_L \times U(1)_Y$ gauge symmetry are mediated by spin 1 vector bosons. Here G_μ^A denotes the gluon field, the gauge bosons corresponding to the $SU(3)_C$ gauge group, W_μ^a denotes the $SU(2)_L$ gauge boson. The third gauge boson B_μ mediates the $U(1)_Y$ hypercharge interactions. The last term in the first line is known as the theta term; it is a total derivative, and thus neither appears in the equations of motion nor perturbation theory. However, it has non-perturbative implications for the vacuum structure of QCD [54].

The second line of (2.2) gives the kinetic terms for the chiral spin- $\frac{1}{2}$ fermions. They can be divided into quarks and leptons that transform in different representations of G_{SM} . Only the quarks carry color charge and transform as the fundamental representation of $SU(3)$. Every quark and lepton comes in three copies, known as generations, only differing by the strength of their Yukawa couplings. In the broken electroweak phase, they then acquire different masses. The SM is a chiral theory i.e., it distinguishes particles of different chirality. For massless particles, chirality is equivalent to helicity and is the sign of the projection of the spin vector on the momentum vector. The quarks can be further divided into left-handed and right-handed quarks. Only the former carry $SU(2)_L$ charge and participate in the weak interaction. Once the quarks acquire mass through the Higgs mechanism, the resulting Dirac mass term mixes the chiralities. It should be noted that quarks and gluons are only good degrees of freedom at energies above $\Lambda_{QCD} \sim 200 \text{ MeV}$ where perturbation theory is applicable. QCD exhibits asymptotic freedom [55, 56] meaning that the effective $SU(3)$ coupling constant decreases for large energy scales. Below Λ_{QCD} the theory becomes strongly coupled, and one must use nonperturbative EFTs such as Chiral Perturbation Theory (ChPT) [57, 58].

The third line of (2.2) is the Higgs Lagrangian, where the mass parameter μ^2 is the only dimensional input in the SM, hinting at physics beyond the SM (see Section 2.3). When spontaneous symmetry breaking occurs (SSB), the Higgs doublet acquires a vacuum

expectation value, splitting into the physical Higgs boson and the would-be Goldstone bosons that become the longitudinal W^\pm and Z modes. Fermion masses then arise from Yukawa couplings to this vev. The phenomenology of electroweak symmetry breaking is discussed in Section 2.2. The full SM matter content is summarized in Table 2.1.

	Quarks			Leptons		Higgs
field	$q_{Lp}^{\alpha j} = \begin{pmatrix} u_{Lp}^\alpha \\ d_{Lp}^\alpha \end{pmatrix}$	u_{Rp}^α	d_{Rp}^α	$l_{Lp}^j = \begin{pmatrix} \nu_{Lp} \\ e_{Lp} \end{pmatrix}$	e_{Rp}	$\phi^j = \begin{pmatrix} \phi^+ \\ \phi^0 \end{pmatrix}$
$SU(3)_C$ rep.	3	3	3	1	1	1
$SU(2)_L$ rep.	2	1	1	2	1	2
hypercharge Y	$\frac{1}{6}$	$\frac{2}{3}$	$-\frac{1}{3}$	$-\frac{1}{2}$	1	$\frac{1}{2}$

Table 2.1.: The matter content of the SM. Here $j = 1, 2$ is an isospin index, $\alpha = 1, 2, 3$ is a color index and $p = 1, 2, 3$ is a generational index.

2.2. Higgs Sector in the SM

Although (2.2) exhibits an $SU(2)_L \times U(1)_Y$ gauge symmetry, the same symmetry is broken in the ground state of the theory. If the symmetry were present in the ground state, four massless electroweak gauge bosons should be in the spectrum. Phenomenologically, however, the W^\pm - and Z bosons are observed to be massive, whereas only the photon, mediating the electromagnetic interaction, remains massless. In other words, at energies below $v = 246\text{GeV}$ the $SU(2)_L \times U(1)_Y$ symmetry of the SM is spontaneously broken to $U(1)_{em}$.

As a result of spontaneous symmetry breaking (SSB) the fermions obtain their masses. However, it should be noted that the Higgs particle is not strictly needed to explain the fermion masses. It is needed to unitarize the theory, since theories with massive vector bosons are known to be inconsistent at high energies. In the SM, electroweak symmetry breaking $SU(2)_L \times U(1)_Y \rightarrow U(1)_{em}$ is achieved through the Higgs mechanism, where an $SU(2)_L$ doublet ϕ with hypercharge $Y = 1/2$, the Higgs doublet, is introduced. In unitary gauge, ϕ is given by

$$\phi = \begin{pmatrix} 0 \\ \frac{1}{\sqrt{2}}(v + h) \end{pmatrix} \quad (2.5)$$

where h is the physical Higgs particle. The Higgs potential in the SM is given by

$$V(\phi) = -\mu^2 \phi^\dagger \phi + \frac{\lambda}{2} (\phi^\dagger \phi)^2 \quad (2.6)$$

Note that in the broken electroweak phase the mass term has the "wrong" sign such that the minimum of the potential is no longer at zero but rather the Higgs doublet acquires

a vacuum expectation value.

$$\langle \phi \rangle = \frac{1}{\sqrt{2}} \begin{pmatrix} 0 \\ v \end{pmatrix}, \quad \text{with} \quad v = \sqrt{2} \frac{\mu^2}{\lambda} \quad (2.7)$$

After SSB the Higgs Lagrangian is given by

$$\begin{aligned} \mathcal{L}_{Higgs} = & \frac{1}{2} \partial_\mu h \partial^\mu h - \frac{m_h^2 v^2}{2} \left[\left(\frac{h}{v} \right)^2 + \left(\frac{h}{v} \right)^3 + \frac{1}{4} \left(\frac{h}{v} \right)^4 \right] \\ & + g^2 \frac{(v+h)^2}{8} \left[(W_\mu^1)^2 + (W_\mu^2)^2 + \left(\frac{g'}{g} B_\mu - W_\mu^3 \right)^2 \right] \end{aligned} \quad (2.8)$$

where $m_h^2 = \lambda v^2$. To diagonalize the mass-terms, the gauge fields can only be rotated and not rescaled since the kinetic terms for B_μ and W_μ^a are already canonically normalized. Only one linear combinations of B_μ and W_μ^3 picks up a mass whereas the orthogonal combination remains massless. These are the massive Z boson and the massless photon A_μ . They are related by the rotation matrix

$$\begin{pmatrix} Z_\mu \\ A_\mu \end{pmatrix} = \begin{pmatrix} \cos \theta_W & -\sin \theta_W \\ \sin \theta_W & \cos \theta_W \end{pmatrix} \begin{pmatrix} W_\mu^3 \\ B_\mu \end{pmatrix} \quad (2.9)$$

where θ_W is the Weinberg angle with

$$\tan \theta_W = \frac{g'}{g}, \quad \sin \theta_W = \frac{g'^2}{\sqrt{g^2 + g'^2}} \quad (2.10)$$

The kinetic terms for the Z -boson Z_μ and the photon A_μ are then given by

$$\mathcal{L}_{kin} = -\frac{1}{4} F_{\mu\nu} F^{\mu\nu} - \frac{1}{4} Z_{\mu\nu} Z^{\mu\nu} + \frac{1}{2} m_Z^2 Z^\mu Z_\mu \quad (2.11)$$

with $m_Z = gv/2 \cos \theta_W$, $Z_{\mu\nu} = \partial_\mu Z_\nu - \partial_\nu Z_\mu$ and $F_{\mu\nu} = \partial_\mu A_\nu - \partial_\nu A_\mu$. While the photon and Z boson do not carry $U(1)_{em}$ charge, the remaining two gauge degrees of freedom do. The couplings of the gauge bosons among themselves are determined by commutators and since W_μ^3 contains the photon we have

$$D_\mu W_\nu \supset g[W_\mu^3 T^3, W_\nu] \supset g \sin \theta_W A_\mu W_\nu^a [T^3, T^a] \quad (2.12)$$

We can read off the electromagnetic charge

$$e = g \sin \theta_W = g' \cos \theta_W \quad (2.13)$$

Defining the combination of generators $T^\pm = \frac{1}{\sqrt{2}}(T^1 \pm iT^2)$ that satisfies $[T^3, T^\pm] = \pm T^\pm$ we can deduce that W boson that couples to T^\pm has electric charge ± 1 . Writing $W^a T^a = W^+ T^+ + W^- T^- + W^3 T^3$ we observe that the linear combinations

$$W_\mu^\pm = \frac{W_\mu^1 \mp iW_\mu^2}{\sqrt{2}} \quad (2.14)$$

have charges ± 1 . Inserting the mass eigenstates into (2.8) we arrive at

$$\begin{aligned} \mathcal{L}_{Higgs} = & \frac{1}{2} \partial_\mu h \partial^\mu h - \frac{m_h^2 v^2}{2} \left[\left(\frac{h}{v} \right)^2 + \left(\frac{h}{v} \right)^3 + \frac{1}{4} \left(\frac{h}{v} \right)^4 \right] \\ & + m_W^2 \left(1 + \frac{h}{v} \right)^2 W_\mu^+ W^{-\mu} + \frac{m_Z^2}{2} \left(1 + \frac{h}{v} \right)^2 Z_\mu Z^\mu \end{aligned} \quad (2.15)$$

The gauge boson masses are given by

$$m_W = \frac{g v}{2}, \quad m_Z = \frac{m_W}{\cos \theta_W} \quad (2.16)$$

The SM predicts therefore that the W^\pm bosons should be lighter than the Z boson which is also realized in nature [59] ($m_W = 80.37$ GeV and $m_Z = 91.19$ GeV). It is reasonable to wonder if the tree-level relation of the gauge bosons masses $m_W/m_Z \cos \theta_W = 1$ has a deeper origin. The next section is dedicated to this question.

2.2.1. Custodial Symmetry

In the SM, the Higgs potential in the unbroken electroweak phase is invariant under a global $SO(4) \simeq SU(2) \times SU(2)$ symmetry. To see this introduce the Higgs bi-doublet

$$\Phi = \frac{1}{\sqrt{2}} \begin{pmatrix} \tilde{\phi} & \phi \end{pmatrix} \quad (2.17)$$

where $\tilde{\phi} = i\sigma_2 \phi^*$ is the conjugated doublet, such that $\langle \Phi^\dagger \Phi \rangle = \phi^\dagger \phi$. Writing the Higgs potential as

$$V(\Phi) = \frac{\lambda}{2} \left(\langle \Phi^\dagger \Phi \rangle - \frac{v^2}{2} \right)^2 \quad (2.18)$$

it is easy to see that the potential is invariant under the global symmetry transformation

$$\Phi \rightarrow g_L \Phi g_R^\dagger = e^{-i\epsilon_L^a T^a} \Phi e^{i\epsilon_R^a T^a} \quad (2.19)$$

where $g_{L/R} \in SU(2)_{L/R}$. The SM gauge group $SU(2)_L \times U(1)_Y$ is a subgroup of $SU(2)_L \times SU(2)_R$ and acts on the bi-doublet Φ as

$$\Phi \rightarrow e^{-i\epsilon_L^a T^a} \Phi e^{i\epsilon_Y T^3} \quad (2.20)$$

where now $\epsilon_{L,Y}(x)$ are functions of spacetime. The $U(1)_Y$ gauge coupling g' , thus, also violates custodial symmetry but the effect is very small. If we had $g' = 0$ then W - and Z -bosons would have equal masses. When the Higgs bi-doublet acquires a vacuum expectation value

$$\Phi = \frac{1}{2} \begin{pmatrix} v & 0 \\ 0 & v \end{pmatrix} \quad (2.21)$$

the global symmetry $SU(2)_L \times SU(2)_R$ is broken to the diagonal subgroup $SU(2)_V$ since the vacuum is only invariant if $g_L = g_R$. This residual symmetry is known as custodial isospin or custodial $SU(2)$ [60]. Custodial symmetry protects the ρ parameter

$$\rho = \frac{m_W^2}{\cos^2 \theta_W m_Z^2} \quad (2.22)$$

from receiving large corrections. Note that the custodial-symmetry violating effect of g' is already incorporated in the definition of ρ . Plugging in the tree level values of m_Z and m_W (2.16) we see that $\rho_0 = 1$ in the SM. At the loop level there are deviations from this value mainly due to top-quark loops. Custodial symmetry is explicitly broken by the Yukawa sector, which is a small effect with the exception of the top quark Yukawa coupling ($y_t \approx 1$).

Even if there were no Higgs sector altogether, there would be electroweak symmetry breaking and custodial symmetry through nontrivial nonperturbative effects in QCD. Taking the limit of massless u and d -quarks, the QCD Lagrangian has a $SU(2)_L \times SU(2)_R$ symmetry where the left- and right-handed fields transform independently. Due to the quark condensate $\langle \bar{q}q \rangle$, this symmetry is broken to the diagonal subgroup $SU(2)_L \times SU(2)_R \rightarrow SU(2)_V$, where the $SU(2)_V$ symmetry is precisely the custodial symmetry relating the gauge boson masses to the gauge charges. In this case, the pions play the role of would-be Goldstone bosons, which would end up as the longitudinal degrees of freedom for the gauge bosons. This suggests that the Higgs and QCD vacuum structure may be more deeply connected [50, 61].

2.2.2. Experimental Constrains

At present experimental accuracy, the SM solution to electroweak symmetry breaking is consistent with experiments. However, there is still much room for deviations from the SM. In contrast to electroweak precision data, the Higgs sector is relatively weakly constrained, especially the Higgs self-couplings. The Higgs boson trilinear self-coupling is the most important direct probe of the Higgs potential and can give insight into the nature of the electroweak phase transitions [59]. The trilinear self-coupling may be probed by double Higgs production. The signal process involves a virtual single Higgs produced from a top quark loop, which splits into two Higgs bosons in the final state through the triple self-coupling. The experimental constraints are usually reported using the "kappa-framework" [62] where the SM coupling is multiplied by a coupling modifier κ_i ($\kappa_i=1$ in the SM). The ATLAS [63] and CMS [64] results for the triple self-coupling are

$$\kappa_\lambda \in [-0.6, 6.6] \text{ (ATLAS)}, \quad \kappa_\lambda \in [-1.2, 6.5] \text{ (CMS)} \quad (2.23)$$

where the bounds correspond to the 95% confidence limit. To measure the quartic self-couplings would require a hh final state, which is out of reach for the LHC. In addition, the ATLAS measurements [65] for the $hhVV$ coupling are

$$\kappa_{2V} \in [0.1, 2.0] \quad (2.24)$$

where again the bounds correspond to the 95% confidence limit. In contrast, the modifier for the gauge boson coupling hVV is rather well constrained [66]

$$\kappa_V = 1.035 \pm 0.031 \quad (2.25)$$

Given the loose constraints on many couplings in the Higgs sector, there is still ample room for models of extended Higgs sectors, such as composite Higgs models [67]. We will, however, pursue a model-independent EFT approach in this thesis. The Electroweak Chiral Lagrangian (EwChL) is the most general EFT that describes electroweak symmetry breaking and allows for $\mathcal{O}(1)$ deviations from the SM in the Higgs couplings. We introduce the EwChL in the next chapter.

2.3. Beyond the SM

Even though the SM is an extremely successful theory, there are several theoretical and experimental indicators for physics beyond the SM (BSM) which we will discuss in the following.

2.3.1. Experimental hints for BSM physics

While neutrinos in the SM are massless, they are, in fact, massive. Neutrino masses were first observed indirectly in oscillations of solar neutrinos [68–70]. The observation constituted the first direct evidence of BSM physics. The number of measured electron neutrinos was only a third of the expected number, indicating that flavor eigenstate neutrinos oscillate as they propagate through spacetime. Only in the mass basis, the propagators are diagonal. Note that oscillation experiments cannot measure the absolute masses but are only sensitive to differences in squares of neutrino masses. Therefore, the mass hierarchy is not fixed.

To give mass to neutrinos via the Higgs mechanism, right-handed or *sterile neutrinos* can be added to the SM. Since the electroweak symmetry does not forbid a Majorana mass term, neutrinos could be Dirac or Majorana fermions. Neutrino oscillation experiments alone cannot determine whether neutrinos are Dirac or Majorana fermions. A Majorana mass term would violate lepton number L . A lepton number violating process that could establish the Majorana nature of neutrinos is *neutrinoless double β -decay* in which two neutrons inside a nucleus turn into two protons with the emission of two electrons and zero neutrinos, violating L by two units [71]. So far, neutrinoless double β -decay has not been observed.

To generate the observed matter-antimatter asymmetry of the universe, the three Sakharov conditions must be satisfied [72]. First, baryon number B violation is required. Second, both charge conjugation symmetry C and the combined symmetry of charge conjugation and parity CP must be violated. Third, the universe must undergo a period of departure from thermal equilibrium. At first glance, these conditions seem to hold in the SM. B is violated in the SM by the chiral anomaly and the weak interaction breaks CP through the non-zero phase in the CKM phase. Additionally, the universe naturally experiences periods out of thermal equilibrium during its cooling history. It turns out, however, that the extent to which these conditions are satisfied is not enough. There needs to be more baryon number violation, CP violation and the electroweak phase transition needs to be first order to explain baryogenesis. For these reasons, baryogenesis remains a compelling motivation for exploring BSM physics [50].

2.3.2. Theoretical hints for BSM physics

Additionally, from the theoretical perspective, there are several indicators that SM should not be viewed as a fundamental theory, but rather as the leading term in an effective description. First of all, the SM does not include gravity, and the formulation of gravity as an EFT [73] breaks down at the Planck scale $M_{Pl} \sim 10^{19}$ TeV. Thus, new physics has to enter at the latest at that scale. The discrepancy between the Planck and the electroweak scales is also known as the *hierarchy problem*, which we will discuss in the following. The hierarchy problem relies on the notion of naturalness, and as an example for an unnaturally small parameter, we also briefly discuss the θ -angle and the *strong CP problem*.

Naturalness and the Hierarchy problem

First of all, one may regard the large number of input parameters of the SM as theoretically unappealing as their deeper origin is not explained by the theory. Accepting this, one may still want to explain the smallness of certain parameters. To do so, t'Hooft introduced the notion of *technical naturalness* [74].

A small parameter p in a physical theory is said to be *technically natural* if radiative corrections to said parameter are multiplicative, implying that the quantity stays small under radiative corrections. This is the case if there is custodial symmetry protecting the parameter in the sense that setting $p = 0$ would lead to an enhanced symmetry prohibiting radiative corrections from inducing a nonzero value of the parameter [75].

For instance, in two-flavor QCD, setting the up- and down-quark masses to zero restores the chiral symmetry $SU(2)_L \times SU(2)_R$ rotating left- and right-handed quarks independently. In the massless limit, chiral symmetry forbids the radiative generation of quark masses. In the massive case, all radiative corrections will be proportional to the bare mass, which stays small as long as the bare mass was once set small. For the gauge bosons, the gauge symmetry plays the role of custodial symmetry.

There is, however, no custodial symmetry to explain the value of the Higgs mass parameter. Recall that there are only two fundamental scales in the SM: the Higgs mass parameter $\mu^2 \sim 10^2 \text{ GeV}$ and the Planck scale $M_{Pl} \sim 10^{19} \text{ GeV}$. The hierarchy problem refers to the vast discrepancy between the two scales, which has no theoretically satisfying answer. In principle, a fundamental scalar could enjoy a shift symmetry $\phi \rightarrow \phi + f$, which would render its mass technically natural. However, the Higgs sector of the SM explicitly breaks any such shift symmetry in multiple interaction terms. This absence of a custodial symmetry for μ^2 is the essence of the electroweak hierarchy problem.

Strong CP problem

While the weak interaction violates CP invariance through a non-zero phase in the CKM matrix, it is a relatively small effect referred to as weak CP violation. The strong interactions, on the other hand, should exhibit strong CP violation, which, however, is not realized in nature. This discrepancy is known as the strong CP problem. The origin of this problem can be traced back to the subgroup $U(1)_A$ of the chiral symmetry, which acts on the quark fields as $\psi \rightarrow e^{i\gamma_5\theta}\psi$. While this constitutes a symmetry of the classical

theory, the path integral is not invariant

$$\int \mathcal{D}\bar{\psi}\mathcal{D}\psi \rightarrow \int \mathcal{D}\bar{\psi}\mathcal{D}\psi \exp\left(i\theta \int \frac{g_s^2}{32\pi^2} G_{\mu\nu}^A G^{A\mu\nu}\right) \quad (2.26)$$

The symmetry is said to be anomalous, since the path integral is not invariant under a chiral rotation. Instead it generates the theta term that we encountered previously and is also generated non-perturbatively by QCD. The theta terms corresponding to the gauge groups $SU(2)_L$ and $U(1)_Y$ can be rotated away. Phenomenologically relevant is the basis invariant combination

$$\mathcal{L}_\theta = \bar{\theta} \frac{g_s^2}{32\pi^2} G_{\mu\nu}^A G^{A\mu\nu}, \quad \bar{\theta} = \theta_{QCD} - \theta_F \quad (2.27)$$

where $\theta_F \equiv \arg \det(Y_d Y_u)$. $Y_{u,d}$ are the Yukawa matrices for up- and down-type quarks respectively. The parameter is related to the electric dipole moment of the neutron and the experimental current limits give $|\bar{\theta}| \leq 10^{-9}$ [76]. Since there is no symmetry protecting the theta parameter, it is considered technically unnatural. The Peccei-Quinn solution [77, 78] solves the CP problem by introducing axions.

3. Effective Field Theories

We now turn to the subject of effective field theories (EFTs), focusing especially on the SMEFT and the HEFT. In Sec. 3.1 we elucidate the basic philosophy behind EFTs and in Sec. 3.2 we discern top-down and bottom-up EFTs. The SMEFT and explicit operator bases of dimension five and six operators are discussed in Sec. 3.3. Sec. 3.4 is devoted to a brief review of the Electroweak Chiral Lagrangian also known as the HEFT and the corresponding power counting based on chiral dimensions. In the last Sec. 3.5 we take a glance at the difference between HEFT and SMEFT comparing their respective Higgs sectors. Pedagogical introductions to EFTs may be found in [79, 80].

3.1. The EFT paradigm

Despite the conceptual elegance of the SM, practical calculations involving its degrees of freedom, particularly in systems with complex bound states, can become increasingly difficult or even straight up impossible. Fortunately, it is not necessary to fully resolve the microscopic details of a system in order to accurately describe its macroscopic behavior. To put it drastically: when designing a bridge, the dynamics of the Higgs boson are entirely irrelevant. What matters instead is identifying the appropriate energy scales and degrees of freedom for the problem at hand. This is the essential idea behind effective field theories (EFTs).

EFTs exploit the existence of a hierarchy of scales by systematically separating the physics of light and heavy degrees of freedom. The heavy fields associated with a high-energy scale Λ are integrated out, and their effects are encoded in a tower of higher-dimensional operators involving only the light fields. The resulting low-energy theory is constructed to reproduce the same infrared (IR) observables as the full theory, up to a given accuracy in m/Λ , where m is the characteristic IR scale of the physical process.

Consider an observable $\mathcal{A}(m, \Lambda)$ depending on two scales, with $m \ll \Lambda$. The EFT allows for an expansion of the form

$$\mathcal{A}(m, \Lambda) = m^{[\mathcal{A}]} a\left(\frac{m}{\Lambda}\right), \quad (3.1)$$

where $[\mathcal{A}]$ denotes the mass dimension of the observable. The function $a(m/\Lambda)$ can include logarithms and is typically not a Taylor series but an asymptotic series. In this way, EFTs may be understood as a sophisticated form of dimensional analysis, controlled by the small power-counting parameter $\delta = m/\Lambda \ll 1$. Observables can therefore be computed in a systematic and predictive expansion in δ , with uncertainties quantifiable by the size of omitted higher-order terms.

EFT methods also appear throughout classical physics. For instance, general relativity itself can be understood as the leading-order term in an EFT valid below the Planck scale [73]. Also problems in classical mechanics that exhibit scale separation can be treated in an EFT framework. For an illustrative example of EFT methods applied to a classical

mechanical system, see [81].

The well-known multipole expansion of an electrostatic potential serves as a great model to illustrate important features of EFTs [61, 80]. We consider the electrostatic potential due to a complicated charge distribution $\rho(\mathbf{r})$, which is given by the well-known expression

$$\Phi(\mathbf{r}) = \int d^3x' \rho(\mathbf{r}') \frac{1}{|\mathbf{r} - \mathbf{r}'|} \quad (3.2)$$

The integral can be very hard to solve in practice but fortunately it is not necessary to do so if the observer sits far away from the charge distribution. To first approximation the charge distribution is simply a point charge

$$\Phi(x) \approx \frac{Q}{r} \quad (3.3)$$

where $Q = \int_V d^3x \rho(x)$ is the total charge. As we get closer we can resolve more details

$$\Phi(\mathbf{r}) = \frac{Q}{r} + \frac{q_i r_i}{r^3} + \frac{q_{ij} r_i r_j}{r^5} + \dots \quad (3.4)$$

This is of course nothing else than the familiar multipole expression, which can be written schematically

$$\Phi(\mathbf{r}) = \frac{1}{r} \sum_{lm} b_{lm} \frac{1}{r^l} Y_{lm}(\Omega) \quad (3.5)$$

where the $Y_{lm}(\Omega)$ denote the spherical harmonics. Assuming that ρ is enclosed by a sphere with radius a we can write

$$\Phi(\mathbf{r}) = \frac{1}{r} \sum_{lm} c_{lm} \left(\frac{a}{r}\right)^l Y_{lm}(\Omega) \quad (3.6)$$

where we introduced the dimensionless coefficients $b_{lm} \equiv c_{lm} a^l$. This example illustrates several key points about EFTs [80]

- The expression (3.6) contains two scales, the infrared (IR) scale a and the ultraviolet (UV) scale r where $a \ll r$. The multipole expansion is an expansion in the ratio $\delta \equiv a/r$ which is the power counting parameter in this case. In high-energy physics it is common to work in momentum space. Here the IR scale in momentum space is $p \sim 1/r$ and the UV scale $\Lambda \sim 1/a$ and $\delta = p/\Lambda$. In an EFT treatment of BSM physics the IR scale is $v \sim 246$ GeV and mass of new resonances Λ serves as the UV scale
- An observer located far away can determine the dimensionful short-distance coefficients $b_{lm} = c_{lm} a^l \sim c_{lm}/\Lambda^l$ by Fourier analyzing the measured potential. With increasing l the coefficients become more and more suppressed. In a high-energy physics context, the Wilson coefficients (the analog of the c_{lm}) of operators at higher order in the EFT expansion are more strongly suppressed by the new physics scale Λ .

- Including more multipole moments will result in more accurate value for the potential. Since the experimental resolution is finite, the UV coefficients can only be determined up to some finite maximum value l_{max} . On the theory side the expression for the potential (3.6) can be consistently expanded up to $\mathcal{O}(\delta^{l_{max}})$. The error is then of $\mathcal{O}(\delta^{l_{max}+1})$. Also in the SMEFT it is vital to calculate observables consistently in the $1/\Lambda$ expansion to obtain a meaningful prediction that can be compared with experiments.

3.2. Top-Down vs. Bottom-Up Approach to EFTs

There are two general approaches to EFTs. If the underlying theory is not known, then a *bottom-up* EFT may be used to parametrize the effects of the unknown sector. Such an EFT is the most general nonrenormalizable QFT with the assumed symmetries and particle content [82]. If the underlying UV theory is known, it can still be helpful to construct a *top-down* EFT. The procedure to obtain a top-down EFT is known as integrating out the heavy degrees of freedom. The path integral over the heavy fields has to be performed to derive the Lagrangian of a top-down EFT. Hence the name "integrating out." At the tree level, this is equivalent to solving the classical equations of motion for the heavy fields. At the one-loop level, a Gaussian integration over the heavy field fluctuation is needed. We discuss this topic in detail in Chapter 4. Top-down EFTs are used, e.g., if the fundamental theory contains too many scales and unsuitable degrees of freedom. Sometimes, the EFT has an emergent low-energy symmetry, and the EFT can be used to resum large logarithms. For instance, top-down EFTs are often used for QCD as calculations within perturbative QCD are limited. Examples include Heavy Quark Effective Theory (HQET) [83], Soft Collinear Effective Theory (SCET) [84], and Chiral Perturbation Theory for mesons and baryons (ChPT) [57, 58]. The basic idea behind top-down and bottom-up EFTs is summarized in Fig. 3.1.

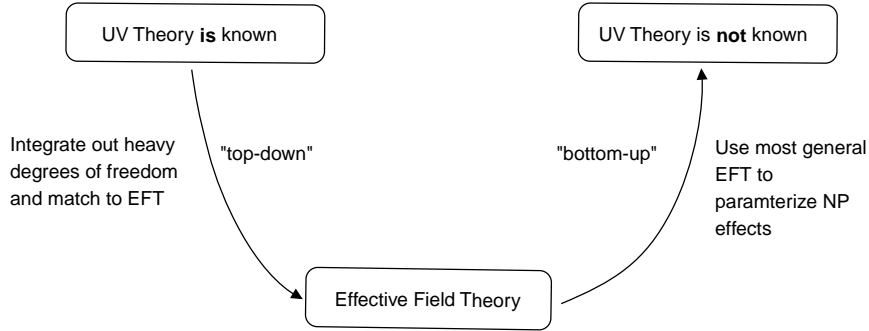


Figure 3.1.: General concept underlying top-down and bottom-up EFTs

3.3. SMEFT

As discussed, the SM should not be seen as a fundamental theory valid up to arbitrary high energies but rather as an effective theory valid up to some energy scale Λ where new physics should enter. The direct detection of new physics resonances might be out of reach for the current generation of colliders. To parametrize indirect new physics effects in a

model independent way an EFT framework is necessary. It is, therefore, well-motivated to construct a bottom-up EFT based on the SM gauge group and the SM particles as degrees of freedom. This EFT is known as the Standard Model Effective Theory (SMEFT) [23–28]. The SMEFT contains the renormalizable SM as the leading term and adds higher dimensional operators, which are suppressed by powers of the new physics scale Λ . The EFT operators are constructed out of the SM degrees of freedom and are singlets under the SM gauge group. Schematically we may write

$$\mathcal{L}_{SMEFT} = \mathcal{L}_{SM} + \frac{1}{\Lambda} \sum_i C_i^{(5)} Q_i^{(5)} + \frac{1}{\Lambda^2} \sum_i C_i^{(6)} Q_i^{(6)} + \mathcal{O}\left(\frac{1}{\Lambda^3}\right) \quad (3.7)$$

Here $C_i^{(d_c)}$ are the dimensionless Wilson coefficients of the d_c -dimensional EFT operators $Q_i^{(d_c)}$. The effects of new physics are encoded in the Wilson coefficients of the higher-dimensional operators. Definitively establishing $C_i \neq 0$ for a single Wilson coefficient would imply a deviation from the SM and an indirect discovery of new physics. Although (3.7) is not renormalizable in the traditional sense, it may be renormalized consistently order by order in $1/\Lambda$. In practice, this implies calculating matrix elements up to a fixed order in the $1/\Lambda$ expansion, e.g. $\mathcal{O}(\Lambda^{-2})$. The divergences of such diagrams may then be removed by other dimension-six operators that act as counterterms. The SMEFT is an example of a *decoupling EFT* [85]; sending Λ to ∞ recovers the SM.

Integrating out the heavy degrees of freedom of mass $M \gg v$ from a weakly coupled new physics model, the resulting effective Lagrangian can always be brought into a SMEFT form with $\Lambda \sim M$. There can be, of course, several new physics scales Λ_i . In that case, the parameter Λ in (3.7) should be identified as the smallest such scale. The leading deviations from the SM are given by dimension five and six operators, which we discuss in the following.

3.3.1. Dimension 5

At mass dimension 5 there is only one possible operator structure, the so-called "Weinberg operator" [22],

$$Q_{\nu\nu} = (C_{\nu\nu})_{pr} \left(\tilde{\phi}^\dagger l_p \right)^T C \left(\tilde{\phi}^\dagger l_r \right) \quad (3.8)$$

where C is the charge conjugation matrix. The Wilson coefficient of $C_{\nu\nu}$ is a 3x3 matrix in flavor space assuming three lepton generations. This operator violates lepton number and after SSB generates a Majorana mass term for left-handed leptons

$$m_{pr} = (C_{\nu\nu})_{pr} \frac{v^2}{2\Lambda} \quad (3.9)$$

An explicit model where the operator arises in an EFT treatment of right-handed neutrinos. Right-handed neutrinos can have a Dirac mass term and a Majorana mass term. If the latter is large they can be integrated out and the Weinberg operator is generated. This is known as the *Seesaw Mechanism* [86]. Experimental constraints inferred from neutrino masses indicate a very high effective scale $\Lambda \sim 10^{14}$ GeV [59, 87–90].

3.3.2. Dimension 6

The leading effects of new physics (NP) at energies $E \ll \Lambda$ can be parameterized by dimension-six operators,

$$\mathcal{L}_{SMEFT} \supset \sum_i \frac{C_i}{\Lambda^2} O_i. \quad (3.10)$$

For most applications, the new-physics scale Λ is taken to be in the range of several TeV. Note that only the combination C_i/Λ^2 can be constrained and not the C_i or Λ individually. Global fits [91] of the Wilson coefficients C_i remain compatible with zero, indicating that present data are not yet sensitive to NP effects.

At a given operator dimension, bases are not unique: integration by parts and field redefinitions (via the equations of motion) can eliminate redundant structures. We employ the ‘‘Warsaw basis’’ [24], which, assuming baryon-number conservation, contains 59 independent operator classes. With three fermion generations this yields 2499 independent Wilson coefficients; allowing baryon-number violation adds four more classes. We display the Warsaw basis in Tabs. 3.1 and 3.2.

To reduce this parameter space, one often imposes additional flavor-symmetry assumptions. A standard choice is *Minimal Flavor Violation* (MFV) [87, 92], which postulates that the only sources of breaking of the SM’s global flavor symmetry

$$\mathcal{G}_f = U(3)_q \times U(3)_u \times U(3)_d \times U(3)_\ell \times U(3)_e \cong SU(3)^5 \times U(1)^5 \quad (3.11)$$

are the Yukawa matrices Y_u , Y_d , and Y_e , treated as spurions. In the limit $Y_{u,d,e} \rightarrow 0$, \mathcal{G}_f is exact; turning them on breaks it to

$$U(1)_{e-\mu} \times U(1)_{\tau-\mu} \times U(1)_B \times U(1)_L \times U(1)_Y. \quad (3.12)$$

Under MFV, higher-dimensional operators must include Yukawa spurion insertions, suppressing flavor-changing effects. At leading order in this expansion, off-diagonal CKM entries can be neglected in four-fermion operators.

Often only the expansion in inverse powers of Λ is made explicit when writing the SMEFT Lagrangian. Accordingly, the Wilson coefficients C_i are treated as $\mathcal{O}(1)$ numbers. Such a power counting prescription is, however, not entirely consistent. As we show in Chapter 5, if the ultraviolet (UV) completion is weakly coupled and renormalizable, operators involving gauge field strengths are further suppressed by loop factors [1].

Here we defined

$$\phi^\dagger \overleftrightarrow{D}_\mu \phi = \phi^\dagger D_\mu \phi - (D_\mu \phi)^\dagger \phi \quad (3.13)$$

and

$$\phi^\dagger \overleftrightarrow{D}_\mu^I \phi = \phi^\dagger \tau^I D_\mu \phi - (D_\mu \phi)^\dagger \tau^I \phi \quad (3.14)$$

In the Higgs sector the operators $Q_H, Q_{H\Box}$ preserve custodial symmetry whereas Q_{HD} contains a custodial symmetry violating part. Sometimes it is convenient to eliminate Q_{HD}

$$Q_{HD} = -\frac{1}{4} \left(Q_{H\Box} + (\phi^\dagger \overleftrightarrow{D}_\mu \phi)(\phi^\dagger \overleftrightarrow{D}^\mu \phi) \right) \quad (3.15)$$

X^3		ϕ^6		$\psi^2\phi^3$	
Q_G	$f^{ABC}G_\mu^{A\nu}G_\nu^{B\rho}G_\rho^{C\mu}$	Q_H	$(\phi^\dagger\phi)^3$	Q_{eH}	$(\phi^\dagger\phi)(\bar{l}_p e_r \phi)$
$Q_{\tilde{G}}$	$f^{ABC}\tilde{G}_\mu^{A\nu}G_\nu^{B\rho}G_\rho^{C\mu}$	$Q_{H\Box}$	$(\phi^\dagger\phi)\Box(\phi^\dagger\phi)$	Q_{uH}	$(\phi^\dagger\phi)(\bar{q}_p u_r \tilde{\phi})$
Q_W	$\varepsilon^{IJK}W_\mu^{I\nu}W_\nu^{J\rho}W_\rho^{K\mu}$	Q_{HD}	$(\phi^\dagger D^\mu\phi)^*(\phi^\dagger D^\mu\phi)$	Q_{dH}	$(\phi^\dagger\phi)(\bar{q}_p d_r \phi)$
$Q_{\tilde{W}}$	$\varepsilon^{IJK}\tilde{W}_\mu^{I\nu}W_\nu^{J\rho}W_\rho^{K\mu}$				
$X^2\phi^2$		$\psi^2 X\phi$		$\psi^2\phi^2 D$	
Q_{hG}	$\phi^\dagger\phi G_{\mu\nu}^A G^{A\mu\nu}$	Q_{eW}	$(\bar{l}_p\sigma^{\mu\nu}e_r)\tau^I\phi W_{\mu\nu}^I$	$Q_{Hl}^{(1)}$	$(\phi^\dagger i\overleftrightarrow{D}_\mu\phi)(\bar{l}_p\gamma^\mu l_r)$
$Q_{H\tilde{G}}$	$\phi^\dagger\phi\tilde{G}_{\mu\nu}^A G^{A\mu\nu}$	Q_{eB}	$(\bar{l}_p\sigma^{\mu\nu}e_r)\phi B_{\mu\nu}$	$Q_{Hl}^{(3)}$	$(\phi^\dagger i\overleftrightarrow{D}_\mu\phi)(\bar{l}_p\tau^I\gamma^\mu l_r)$
Q_{HW}	$\phi^\dagger\phi W_{\mu\nu}^I W^{I\mu\nu}$	Q_{uG}	$(\bar{q}_p\sigma^{\mu\nu}T^A u_r)\tilde{\phi} G_{\mu\nu}^A$	Q_{He}	$(\phi^\dagger i\overleftrightarrow{D}_\mu\phi)(\bar{e}_p\gamma^\mu e_r)$
$Q_{H\tilde{W}}$	$\phi^\dagger\phi\tilde{W}_{\mu\nu}^I W^{I\mu\nu}$	Q_{uW}	$(\bar{q}_p\sigma^{\mu\nu}u_r)\tau^I\tilde{\phi} W_{\mu\nu}^I$	$Q_{Hq}^{(1)}$	$(\phi^\dagger i\overleftrightarrow{D}_\mu\phi)(\bar{q}_p\gamma^\mu q_r)$
Q_{HB}	$\phi^\dagger\phi B_{\mu\nu} B^{\mu\nu}$	Q_{uB}	$(\bar{q}_p\sigma^{\mu\nu}u_r)\tilde{\phi} B_{\mu\nu}$	$Q_{Hq}^{(3)}$	$(\phi^\dagger i\overleftrightarrow{D}_\mu\phi)(\bar{q}_p\tau^I\gamma^\mu q_r)$
$Q_{H\tilde{B}}$	$\phi^\dagger\phi\tilde{B}_{\mu\nu} B^{\mu\nu}$	Q_{dG}	$(\bar{q}_p\sigma^{\mu\nu}T^A d_r)\phi G_{\mu\nu}^A$	$Q_{\phi u}$	$(\phi^\dagger i\overleftrightarrow{D}_\mu\phi)(\bar{u}_p\gamma^\mu u_r)$
Q_{HWB}	$\phi^\dagger\tau^I\phi W_{\mu\nu}^I B^{\mu\nu}$	Q_{dW}	$(\bar{q}_p\sigma^{\mu\nu}d_r)\tau^I\phi W_{\mu\nu}^I$	Q_{Hd}	$(\phi^\dagger i\overleftrightarrow{D}_\mu\phi)(\bar{d}_p\gamma^\mu d_r)$
$Q_{H\tilde{W}B}$	$\phi^\dagger\tau^I\phi\tilde{W}_{\mu\nu}^I B^{\mu\nu}$	Q_{dB}	$(\bar{q}_p\sigma^{\mu\nu}u_r)\phi B_{\mu\nu}$	Q_{Hud}	$i(\tilde{\phi}^\dagger D_\mu\phi)(\bar{u}_p\gamma^\mu d_r)$

Table 3.1.: Dimension-six operators other than the four-fermion operators taken from [24]

$(\bar{L}L)(\bar{L}L)$		$(\bar{R}R)(\bar{R}R)$		$(\bar{L}L)(\bar{R}R)$	
Q_{ll}	$(\bar{l}_p\gamma_\mu l_r)(\bar{l}_s\gamma^\mu l_t)$	Q_{ee}	$(\bar{e}_p\gamma_\mu e_r)(\bar{e}_s\gamma^\mu e_t)$	Q_{le}	$(\bar{l}_p\gamma_\mu l_r)(\bar{e}_s\gamma^\mu e_t)$
$Q_{qq}^{(1)}$	$(\bar{q}_p\gamma_\mu q_r)(\bar{q}_s\gamma^\mu q_t)$	Q_{uu}	$(\bar{u}_p\gamma_\mu u_r)(\bar{u}_s\gamma^\mu u_t)$	Q_{lu}	$(\bar{l}_p\gamma_\mu l_r)(\bar{u}_s\gamma^\mu u_t)$
$Q_{qq}^{(3)}$	$(\bar{q}_p\gamma_\mu\tau^I q_r)(\bar{q}_s\gamma^\mu\tau^I q_t)$	Q_{dd}	$(\bar{d}_p\gamma_\mu d_r)(\bar{d}_s\gamma^\mu d_t)$	Q_{ld}	$(\bar{l}_p\gamma_\mu l_r)(\bar{d}_s\gamma^\mu d_t)$
$Q_{lq}^{(1)}$	$(\bar{l}_p\gamma_\mu l_r)(\bar{q}_s\gamma^\mu q_t)$	Q_{eu}	$(\bar{e}_p\gamma_\mu e_r)(\bar{u}_s\gamma^\mu u_t)$	Q_{qe}	$(\bar{q}_p\gamma_\mu q_r)(\bar{e}_s\gamma^\mu e_t)$
$Q_{lq}^{(3)}$	$(\bar{l}_p\gamma_\mu\tau^I l_r)(\bar{q}_s\gamma^\mu\tau^I q_t)$	Q_{ed}	$(\bar{e}_p\gamma_\mu e_r)(\bar{d}_s\gamma^\mu d_t)$	$Q_{qu}^{(1)}$	$(\bar{q}_p\gamma_\mu q_r)(\bar{u}_s\gamma^\mu u_t)$
		$Q_{ud}^{(1)}$	$(\bar{u}_p\gamma_\mu u_r)(\bar{d}_s\gamma^\mu d_t)$	$Q_{qu}^{(8)}$	$(\bar{q}_p\gamma_\mu T^A q_r)(\bar{u}_s\gamma^\mu T^A u_t)$
		$Q_{ud}^{(8)}$	$(\bar{u}_p\gamma_\mu T^A u_r)(\bar{d}_s\gamma^\mu T^A d_t)$	$Q_{qd}^{(1)}$	$(\bar{q}_p\gamma_\mu q_r)(\bar{d}_s\gamma^\mu d_t)$
				$Q_{qd}^{(8)}$	$(\bar{q}_p\gamma_\mu T^A q_r)(\bar{d}_s\gamma^\mu T^A d_t)$
$(\bar{L}R)(\bar{R}L)$ and $(\bar{L}R)(\bar{L}R)$		B -violating			
Q_{ledq}	$(\bar{l}_p^j e_r)(\bar{d}_s q^j)$	Q_{duq}	$\varepsilon^{\alpha\beta\gamma}\varepsilon_{jk}[(d_p^\alpha)^T C u_r^\beta][(q_s^{\gamma j})^T C l_t^k]$		
$Q_{quqd}^{(1)}$	$(\bar{q}_p^j u_r)\varepsilon_{jk}(\bar{q}_s^k d_t)$	Q_{qqqu}	$\varepsilon^{\alpha\beta\gamma}\varepsilon_{jk}[(q_p^{\alpha j})^T C q_r^{\beta k}][(u_s^\gamma)^T C e_t]$		
$Q_{quqd}^{(8)}$	$(\bar{q}_p^j T^A u_r)\varepsilon_{jk}(\bar{q}_s^k T^A d_t)$	Q_{qqq}	$\varepsilon^{\alpha\beta\gamma}\varepsilon_{jn\epsilon km}[(q_p^{\alpha j})^T C q_r^{\beta k}][(q_s^{\gamma m})^T C l_t^n]$		
$Q_{lequ}^{(1)}$	$(\bar{l}_p^j e_r)\varepsilon_{jk}(\bar{q}_s^k u_t)$	Q_{duu}	$\varepsilon^{\alpha\beta\gamma}[(d_p^\alpha)^T C u_r^\beta][(u_s^\gamma)^T C e_t]$		
$Q_{lequ}^{(3)}$	$(\bar{l}_p^j\sigma_{\mu\nu}e_r)\varepsilon_{jk}(\bar{q}_s^k\sigma^{\mu\nu}u_t)$				

Table 3.2.: Four-fermion dimension-six SMEFT operators taken from [24]

The electroweak T and S parameters are directly related to the Wilson coefficients of two Warsaw basis operators [93]

$$\alpha T = -\frac{1}{2}v^2 C_{HD} \quad (3.16)$$

$$\alpha S = 4v^2 \sin \theta_W \cos \theta_W C_{HWB} \quad (3.17)$$

The renormalization group equations for dimension 6 operators have been computed [94–98] and have the general structure

$$\frac{d}{d \ln \mu^2} C_i = \gamma_{ij} C_j \quad (3.18)$$

The parametric size of the RGE effects is $\sim 1/16\pi^2 \cdot v^2/\Lambda^2$, thus they are subleading compared to the insertion of dimension six operators in tree level diagrams. Feynman rules for the Warsaw basis have been compiled in [99].

3.3.3. Dimension 7 and above

Operators of canonical dimension seven and above are suppressed with respect to dimension six operators and can therefore be expected to be phenomenologically negligible in most cases. There are, however, certain processes where the leading new-physics effects are given by dimension eight operators. The number of basis elements at every dimension can be derived using Hilbert series [100]. The construction of operator bases for a given mass dimension can be automatized [101, 102]. All odd-dimensional operators violate $B - L$. Explicit bases have been worked out for dimension 7 [103–105], dimension 8 [106, 107] and dimension 9 [108, 109] SMEFT operators.

3.4. HEFT

As we explained in the first chapter the SM solution to electroweak symmetry breaking appears for many reasons to be unsatisfactory and therefore one expects new physics to enter the picture. Although, at present, the SM Higgs mechanism appears to be an accurate description of electroweak symmetry breaking there are several theoretical shortcomings. The electroweak hierarchy problem motivated the construction of numerous new-physics models with new dynamics typically around the TeV scale. To study electroweak symmetry breaking in a model independent way one is inevitably drawn to EFT methods. The most general EFT for electroweak dynamics with the SM matter content and the Higgs particle as a gauge singlet under $SU(2)_L \otimes U(1)_Y$ is known as the electroweak chiral Lagrangian (EwChL) or Higgs effective field theory (HEFT) [28–46].

3.4.1. Leading order chiral Lagrangian

The construction principle for this EFT is reminiscent of Chiral Perturbation theory (ChPT) for mesons and parametrizes the minimal coset $SU(2)_L \times U(1)_Y / U(1)_{em}$ in a non-linear manner. The Goldstone matrix U then transforms linearly under $SU(2)_L \times SU(2)_R$

$$U \rightarrow g_L U g_R^\dagger, \quad h \rightarrow h \quad (3.19)$$

whereas the physical Higgs boson h is an electroweak singlet, implying that the covariant derivative reads

$$D_\mu U = \partial_\mu U + ig W_\mu U - ig' B_\mu U T_3, \quad D_\mu h = \partial_\mu h \quad (3.20)$$

The leading-order HEFT Lagrangian can be written as

$$\mathcal{L}_{LO} = \mathcal{L}_{SM0} + \mathcal{L}_{Uh,2} \quad (3.21)$$

where

$$\begin{aligned} \mathcal{L}_{SM} = & -\frac{1}{4} G_{\mu\nu}^A G^{A\mu\nu} - \frac{1}{4} W_{\mu\nu}^a W^{a\mu\nu} - \frac{1}{4} B_{\mu\nu} B^{\mu\nu} \\ & + \bar{q}_L i \not{D} q_L + \bar{l}_L i \not{D} l_L + \bar{u}_R i \not{D} u_R + \bar{d}_R i \not{D} d_R + \bar{e}_R i \not{D} e_R \end{aligned} \quad (3.22)$$

The Lagrangian in the Higgs sector reads

$$\begin{aligned} \mathcal{L}_{Uh,2} = & \frac{v^2}{4} \langle D_\mu U^\dagger D^\mu U \rangle (1 + F_U(h)) + \frac{1}{2} \partial_\mu h \partial^\mu h - V(h) \\ & - v \left[\bar{q}_L \left(\hat{Y}_u + \sum_{n=1}^{\infty} \hat{Y}_u^{(n)} \left(\frac{h}{v} \right)^n \right) U P_{+q_R} + \bar{q}_L \left(\hat{Y}_d + \sum_{n=1}^{\infty} \hat{Y}_d^{(n)} \left(\frac{h}{v} \right)^n \right) U P_{-q_R} \right. \\ & \left. + \bar{l}_L \left(\hat{Y}_e + \sum_{n=1}^{\infty} \hat{Y}_e^{(n)} \left(\frac{h}{v} \right)^n \right) U P_{-l_R} + \text{h.c.} \right] \end{aligned} \quad (3.23)$$

where

$$F_U(h) = \sum_{n=1}^{\infty} F_n \left(\frac{h}{v} \right)^n, \quad V(h) = \frac{m_h^2 v^2}{2} \left[\left(\frac{h}{v} \right)^2 + \sum_{n=3}^{\infty} V_n \left(\frac{h}{v} \right)^n \right] \quad (3.24)$$

The function $F_U(h)$ is sometimes known as the Flare function and encapsulates the couplings of a pair of (longitudinal) gauge bosons to any number of Higgs fields (and Goldstone fields) [44]. Here, the right handed quark fields and leptons are collected as $q_R = (u_R, d_R)^T$ and $l_R = (\nu_R, e_R)^T$ respectively and the projectors

$$P_{\pm} = \frac{1}{2} \pm T_3 \quad (3.25)$$

are used. The SM is recovered in the limit

$$\begin{aligned} F_U(h) = & 2 \frac{h}{v} + \frac{h^2}{v^2}, \quad V(h) = \frac{m_h^2 v^2}{2} \left(\left(\frac{h}{v} \right)^2 + \left(\frac{h}{v} \right)^3 + \frac{1}{4} \left(\frac{h}{v} \right)^4 \right) \\ \hat{Y}_f = & \hat{Y}_f^{(1)}, \quad \hat{Y}_f^{(n \geq 2)} = 0 \end{aligned} \quad (3.26)$$

The relation between the matrix U and the Goldstone fields φ^a is

$$U = \exp \left(\frac{2i\varphi^a T^a}{v} \right), \quad \varphi^a T^a = \frac{1}{2} \begin{pmatrix} \varphi^0 & \sqrt{2}\varphi^+ \\ \sqrt{2}\varphi^- & -\varphi^0 \end{pmatrix} \quad (3.27)$$

where $T^a = \sigma^a/2$ are the generators of $SU(2)$ and $\varphi^\pm = 1/\sqrt{2}(\varphi^1 \mp i\varphi^2)$. The anomalous couplings in (3.23) contain at least one Higgs fields such that all couplings without Higgs fields like the fermion-gauge couplings are SM like at LO. Pure fermionic operators only appear in the NLO in the form of four-fermion operators.

3.4.2. Power Counting and NLO operators

The leading order EwChL is not renormalizable and contains operators of arbitrary mass dimensions. It is a nondecoupling EFT similar to ChPT for mesons. Thus, in contrast to the SMEFT, its power counting is not governed by canonical dimensions. It is governed by a loop expansion, which can be conveniently grasped by chiral dimensions. The power counting for the EwChL was discussed in [110, 111]. It is similar to the power counting for ChPT coupled to photons [112]. To see how chiral dimensions arise, consider a generic L -loop diagram \mathcal{D} built from (3.21), with H external Higgs fields, B external Goldstone bosons, $F_{L(R)}^{1(2)}$ external left-/right-handed (anti)fermions, and V external gauge fields, which can only appear as field-strength tensors $X_{\mu\nu}$. Such a diagram scales as [37, 40]

$$\mathcal{D} \sim \frac{(yv)^\nu (gv)^{m+2r+2x+u+z}}{v^{F_L+F_R-2-2\omega}} \frac{p^d}{\Lambda^{2L}} \bar{\psi}_L^{F_L^1} \psi_L^{F_L^2} \bar{\psi}_R^{F_R^1} \psi_R^{F_R^2} \left(\frac{X_{\mu\nu}}{v} \right)^V \left(\frac{\varphi}{v} \right)^B \left(\frac{h}{v} \right)^H \quad (3.28)$$

Here m is the total number of gauge-boson-Goldstone vertices, ν the number of Yukawa vertices with Goldstones and/or Higgs bosons, $u(x)$ the total number of cubic (quartic) gauge-boson vertices, r the number of vertices of type $X_\mu^2 \varphi^s$, ω the number of Higgs self-interaction vertices and $z_{L/R}$ the number of fermion-gauge-boson interactions $\bar{\psi}_{L/R} \psi_{L/R} X_\mu$. The power of external momenta p or superficial degree of divergence is

$$d \equiv 2L + 2 - \frac{F_L + F_R}{2} - V - \nu - m - 2r - 2x - u - z - 2\omega \quad (3.29)$$

Note that the number of external Higgs and Goldstone bosons does not enter d . Therefore, counterterms with an arbitrary number of Goldstone and Higgs bosons are required. Rearranging this formula gives

$$2L + 2 = d_p + X + \frac{F_L + F_R}{2} + V + \nu + m + 2r + 2x + u + z + 2\omega \equiv \chi \quad (3.30)$$

The right-hand side of (3.30) for any given operator can be grasped by assigning it a *chiral dimension* $d_\chi = 2L + 2$. Chiral dimensions are defined as

$$[X_\mu]_\chi = [h]_\chi = [\varphi]_\chi = 0, \quad [\psi]_\chi = \frac{1}{2}, \quad [\partial_\mu]_\chi = [g]_\chi = 1 \quad (3.31)$$

i.e. fermion bilinears, small couplings and derivatives each carry one unit of chiral dimension. Bosonic fields do not carry chiral dimension. It is straightforward to verify that the leading order EwChL has $[\mathcal{L}_{Uh,2}]_\chi = 2$. The operators in the next-to-leading order Lagrangian at chiral dimension $d_\chi = 2L + 2 = 4$ or equivalently at loop order $L = 1$ have been compiled in [37, 40] and can be divided into several classes schematically given by

$$UhD^4, \quad X^2Uh, \quad XUhD^2, \quad \psi^2UhD, \quad \psi^2UhD^2, \quad \psi^4Uh \quad (3.32)$$

3.5. SMEFT vs. HEFT

Assuming the SM symmetry and field content, the SMEFT contains the physical Higgs as part of an electroweak doublet. HEFT, on the other hand, as the most general EFT

parameterizing the minimal coset $SU(2)_L \times U(1)_Y / U(1)_{em}$ with the physical Higgs h as an electroweak singlet, is more general than SMEFT in the sense that the anomalous Higgs couplings are uncorrelated and $\mathcal{O}(1)$ numbers a priori. In the SMEFT these couplings are correlated. The relation of SMEFT and HEFT has been discussed extensively in the literature [28, 113]. Geometric methods have been developed to make statements independent of the chosen field basis [43, 114]. The Geometric Standard Model Effective Field Theory (GeoSMEFT) [115–117] can be regarded as an interpolating case between the SMEFT and the HEFT where certain operator structures are summed to all orders in $\phi^\dagger \phi$. Positivity constraints [118] on amplitudes can also serve to clarify the distinction between the two EFTs.

Thus, the relation between SMEFT may be characterized in a schematic way

$$\text{SMEFT} \subset \text{HEFT} \quad (3.33)$$

As a result the SMEFT Higgs sector can always be cast in HEFT-like form [44]. However, the contrary is not true. In the remainder of this section, we illustrate this statement up to $\mathcal{O}(1/\Lambda^2)$. To achieve this we use the exponential parametrization for the doublet

$$\phi = \frac{v+h}{\sqrt{2}} U \begin{pmatrix} 0 \\ 1 \end{pmatrix} \quad (3.34)$$

where U is the Goldstone matrix and h the physical Higgs. Working with the exponential parameterization, we make use of the following identity

$$\begin{pmatrix} 0 & 1 \end{pmatrix} M \begin{pmatrix} 0 \\ 1 \end{pmatrix} = \frac{1}{2} \langle M(\mathbb{1} - 2T_3) \rangle \quad (3.35)$$

In the Warsaw basis, there are three operators containing only the Higgs doublet

$$\mathcal{O}_H = (\phi^\dagger \phi)^3, \quad \mathcal{O}_{H\Box} = (\phi^\dagger \phi) \Box (\phi^\dagger \phi), \quad \mathcal{O}_{HD} = (\phi^\dagger D_\mu \phi)^* (\phi^\dagger D^\mu \phi) \quad (3.36)$$

where \mathcal{O}_H is a contribution to the Higgs potential whereas $\mathcal{O}_{H\Box}$ and \mathcal{O}_{HD} modify the kinetic term. Using the exponential parametrization and (3.35) we obtain

$$\mathcal{O}_H = \frac{v^6}{8} \left(1 + \frac{h}{v} \right)^6 \quad (3.37)$$

$$\mathcal{O}_{H\Box} = -v^2 \left(1 + \frac{h}{v} \right)^2 \partial_\mu h \partial^\mu h \quad (3.38)$$

$$\mathcal{O}_{HD} = \frac{v^2}{4} \left(1 + \frac{h}{v} \right)^2 \partial_\mu h \partial^\mu h + \frac{v^2}{4} \left(1 + \frac{h}{v} \right)^2 \langle \tau_L L_\mu \rangle^2 \quad (3.39)$$

where we used integration by parts in the case of $\mathcal{O}_{H\Box}$. We used the notation [40]

$$L_\mu \equiv iU D_\mu U^\dagger, \quad \tau_L = UT_3 U^\dagger \quad (3.40)$$

The operators $\mathcal{O}_{H\Box}, \mathcal{O}_{HD}$ with derivatives affect the kinetic term

$$\mathcal{L}_{h,kin} = \frac{1}{2} \left(1 - 2 \frac{v^2}{\Lambda^2} C_{H,kin} \left(1 + \frac{h}{v} \right)^2 \right) \partial_\mu h \partial^\mu h \quad (3.41)$$

where we defined the combination

$$C_{H,kin} \equiv C_{H\Box} - \frac{1}{4}C_{HD} \quad (3.42)$$

To bring the kinetic term to its canonic form (up to $\mathcal{O}(\Lambda^{-4})$ terms) the field redefinition

$$h \rightarrow h + \frac{v^2}{\Lambda^2} C_{H,kin} \left(h + \frac{h^2}{v} + \frac{h^3}{3v^2} \right) \quad (3.43)$$

is needed. Inserting the field redefinition and including \mathcal{O}_H in the potential we obtain the SMEFT predictions (up to $\mathcal{O}(1/\Lambda^2)$) for the Higgs functions in (3.23). The potential

$$\begin{aligned} V = \frac{m_h^2 v^2}{2} & \left[\left(\frac{h}{v} \right)^2 + \left(1 + 3\bar{C}_{H,kin} - 2\bar{C}_H \frac{v^2}{m_h^2} \right) \left(\frac{h}{v} \right)^3 + \left(\frac{1}{4} + \frac{25}{6}\bar{C}_{H,kin} - 3\bar{C}_H \frac{v^2}{m_h^2} \right) \left(\frac{h}{v} \right)^4 \right. \\ & \left. + \left(2\bar{C}_{H,kin} - \frac{3}{2}\bar{C}_H \frac{v^2}{m_h^2} \right) \left(\frac{h}{v} \right)^5 + \left(\frac{1}{3}\bar{C}_{H,kin} - \frac{1}{4}\bar{C}_H \frac{v^2}{m_h^2} \right) \left(\frac{h}{v} \right)^6 \right] \end{aligned} \quad (3.44)$$

the flare function

$$F_U(h) = 1 + (2 + 2\bar{C}_{H,kin}) \frac{h}{v} + (1 + 4\bar{C}_{H,kin}) \left(\frac{h}{v} \right)^2 + \frac{8}{3}\bar{C}_{H,kin} \left(\frac{h}{v} \right)^3 + \frac{2}{3}\bar{C}_{H,kin} \left(\frac{h}{v} \right)^4 \quad (3.45)$$

and the Yukawa Higgs function

$$\mathcal{M}(h) = \mathcal{M}_0 \left[1 + (1 + \bar{C}_{H,kin}) \frac{h}{v} + \bar{C}_{H,kin} \left(\frac{h}{v} \right)^2 + \frac{\bar{C}_{H,kin}}{3} \left(\frac{h}{v} \right)^3 \right] \quad (3.46)$$

receive correction from $\mathcal{O}_H, \mathcal{O}_{H\Box}, \mathcal{O}_{HD}$ where we use the short-hand notation $\bar{C} \equiv C v^2 / \Lambda^2$. It is easy to see that the Higgs self-couplings are correlated as opposed to the EwChL where the potential coefficients are $\mathcal{O}(1)$ parameters. However, these correlations are modified when including higher dimensional operators. The Higgs mass in terms of the potential parameters is given by

$$m_h^2 = \lambda v^2 (1 + 2\bar{C}_{H,kin}) + 3\bar{C}_H v^2 \quad (3.47)$$

Our result can be validated using the linear EFT Lagrangian in [119] and setting $\bar{C}_{H,kin} = -1/2\alpha^2$.

4. Functional matching techniques

Constructing a top-down EFT from an extension of the SM allows for the parametrization of indirect effects of new physics as an expansion in inverse powers of the heavy scale. Tasked with integrating out the heavy degrees of freedom from a particular UV model to obtain the Wilson coefficients of the low-energy EFT, there are two approaches one can choose. The diagrammatic matching approach involves calculating Green functions with light particle external legs in the full theory, where heavy fields can only appear as internal lines, and then calculating the same Green function in the EFT. By equating the two (matching condition), the expressions for the Wilson coefficients are obtained. The functional matching approach, on the other hand, does not reference Green functions or diagrams. Instead, the functional integral over the heavy fields is directly performed at the level of the path integral. In this way, the effective action can be calculated directly. The functional approach has obvious advantages; there is no need to compute specific diagrams or consider symmetry factors. The matching calculation becomes, therefore, much more efficient and transparent. Additionally, we do not need to work out an EFT operator basis in advance to perform the matching; everything follows from the functional integration. As we repeatedly employ the functional matching approach, we dedicate this chapter to a brief review of the technique. In addition, we will discuss the *Universal One-Loop Effective Action*.

4.1. A simplified approach to One Loop Matching

In [47] an efficient and systematic functional matching procedure has been developed, that includes the one-loop contributions, where heavy and light quantum fluctuations appear in the same loop. Since we employ the technique in the following chapters, we summarize the most important ingredients. We start by considering a general theory with heavy (η_H) and light (η_L) degrees of freedom, which we denote collectively by $\eta = (\eta_H, \eta_L)$. Our task is to calculate the one-loop effective Lagrangian resulting from integrating out η_H . As is well known, the first step is to split each component of $\eta \rightarrow \eta + \tilde{\eta}$ into classical background fields η satisfying the classical equations of motion and quantum fluctuations $\tilde{\eta}$. To compute the one-loop effective action, the Lagrangian needs to be expanded up to quadratic order in $\tilde{\eta}$.

$$\mathcal{L} = \mathcal{L}^{tree}(\eta) + \mathcal{L}^{(\tilde{\eta}^2)} + \mathcal{O}(\tilde{\eta}^3) \quad (4.1)$$

The zeroth order term is just the classical tree-level Lagrangian and the term linear in $\tilde{\eta}$ is proportional to the classical equations of motion and can thus be discarded. The quadratic term can be written as

$$\mathcal{L}^{(\tilde{\eta}^2)} = \frac{1}{2} \tilde{\eta}^\dagger \frac{\partial^2 \mathcal{L}}{\partial \eta^* \partial \eta} \tilde{\eta} \equiv \frac{1}{2} \tilde{\eta}^\dagger \mathcal{O} \tilde{\eta} \quad (4.2)$$

where the fluctuation operator has the generic form

$$\mathcal{O} = \begin{pmatrix} \Delta_H & X_{LH}^\dagger \\ X_{LH} & \Delta_L \end{pmatrix} \quad (4.3)$$

The fluctuation operator depends only on the classical background fields. To obtain the one-loop effective action the Gaussian integral over the heavy fluctuation fields have to be computed

$$e^{iS} = \mathcal{N} \int \mathcal{D}\tilde{\eta}_L \mathcal{D}\tilde{\eta}_H \exp \left[i \int d^4x \mathcal{L}^{(\tilde{\eta}^2)} \right] \quad (4.4)$$

The fluctuation operator is not block diagonal and thus the path integral over the heavy fields does not include the contributions that correspond to diagrams with heavy *and* light particles in the loop. Therefore, we proceed in the following to diagonalize the fluctuation operator in order to perform the functional integration. The field transformation

$$P = \begin{pmatrix} I & 0 \\ -\Delta_L^{-1} X_{LH} & I \end{pmatrix} \quad (4.5)$$

transforms the fluctuation operator into block-diagonal form

$$P^\dagger \mathcal{O} P = \begin{pmatrix} \tilde{\Delta}_H & 0 \\ 0 & \Delta_L \end{pmatrix} \quad (4.6)$$

with

$$\tilde{\Delta}_H = \Delta_H - X_{LH}^\dagger \Delta_L^{-1} X_{LH} \quad (4.7)$$

We can now perform the functional integration over the heavy fields η_H yielding

$$e^{iS} = \left(\det \tilde{\Delta}_H \right)^{-c} \mathcal{N} \int d\eta_L \exp \left[i \int dx \frac{1}{2} \eta_L^\dagger \Delta_L \eta_L \right] \quad (4.8)$$

where $c = 1/2, (-1)$ for bosonic (fermionic) heavy fields and \mathcal{N} is an unimportant multiplicative constant. The determinant factor in front represents the one-loop effective action coming from loops involving heavy fields

$$\exp [iS_H] = \left(\det \tilde{\Delta}_H \right)^{-c} \quad (4.9)$$

or equivalently

$$S_H = i c \ln \det \tilde{\Delta}_H \quad (4.10)$$

Using the identity $\det A = \exp \text{Tr} \ln A$ we arrive at

$$S_H = i c \text{Tr} \ln \tilde{\Delta}_H \quad (4.11)$$

where Tr denotes the full trace of the operator including the integration over spacetime. In the next step we insert momentum eigenstates to compute the trace

$$\begin{aligned} S_H &= i c \text{tr} \int \frac{d^d p}{(2\pi)^d} \langle p | \ln \tilde{\Delta}_H | p \rangle \\ &= i c \text{tr} \int d^d x \frac{d^d p}{(2\pi)^d} e^{-ipx} \ln \left(\tilde{\Delta}_H(x, \partial_x) \right) e^{ipx} \\ &= i c \text{tr} \int d^d x \frac{d^d p}{(2\pi)^d} \ln \left(\tilde{\Delta}_H(x, \partial_x + ip) \right) \mathbb{1} \end{aligned} \quad (4.12)$$

As $\tilde{\Delta}_H$ contains the kinetic term of the heavy fields and in the special case of scalar fields it takes the generic form

$$\tilde{\Delta}_H = -\hat{D}^2 - m_H^2 - U \quad (4.13)$$

Then performing the shift $\partial_x \rightarrow \partial_x + ip$ one arrives at

$$S_H = \frac{i}{2} \text{tr} \int d^d x \int \frac{d^d p}{(2\pi)^d} \ln \left(p^2 - m_H^2 - 2ip\hat{D} - \hat{D}^2 - U(x, \partial_x + ip) \right) \mathbb{1} \quad (4.14)$$

To obtain the final expression, we expand the logarithm and obtain the effective Lagrangian

$$\mathcal{L}_{eff} = \mp \frac{i}{2} \sum_{n=1}^{\infty} \frac{1}{n} \int \frac{d^d p}{(2\pi)^d} \text{tr} \left\{ \left(\frac{2ip\hat{D} + \hat{D}^2 + U(x, \partial_x + ip)}{p^2 - m_H^2} \right)^n \mathbb{1} \right\} \quad (4.15)$$

where the (minus) plus corresponds to a (bosonic) fermionic fluctuation operator. For determinants of fermionic fluctuation operators of the general form

$$\mathcal{O} = i\hat{D} - M - \Sigma \quad (4.16)$$

further care is needed. The matrix U in this case is given by

$$U_{ferm} = -\frac{i}{2} \sigma^{\mu\nu} [\hat{D}_\mu, \hat{D}_\nu] - i [\hat{D}, \Sigma_e] + i \{ \hat{D}, \Sigma_o \} + 2m_H \Sigma_e + \Sigma(\Sigma_e - \Sigma_o) \quad (4.17)$$

Here $\Sigma \equiv \Sigma_e + \Sigma_o$ and $\Sigma_{e,(o)}$ contains an even (odd) number of gamma matrices. To evaluate (4.15) we need to determine the inverse of Δ_L , which can be formally expanded in a Neumann series expansion

$$\Delta_L^{-1} = \sum_{n=0}^{\infty} (-1)^n \left(\tilde{\Delta}_L^{-1} X_L \right)^n \tilde{\Delta}_L^{-1} \quad (4.18)$$

Here $\Delta_L = \tilde{\Delta}_L + X_L$, where $\tilde{\Delta}_L$ corresponds to the fluctuations coming from the kinetic term, i.e. $\tilde{\Delta}_L^{-1}$ is the light field propagator.

The methods can be generalized to two loops [120, 121].

4.2. Universal One Loop Effective Action

In case the matrix U does not contain any derivatives, (4.15) can be computed up to the desired order in the $1/M$ expansion. The resulting expression is known as the *Universal One Loop Effective Action* (UOLEA) [122–126]. The UOLEA is universal in the sense that it is applicable for any given UV model. Only the quadratic fluctuation operator has to be computed and the resulting expression for U has to be plugged into the UOLEA. In the following, we sketch how the UOLEA can be computed efficiently.

4.2.1. Covariant diagram method

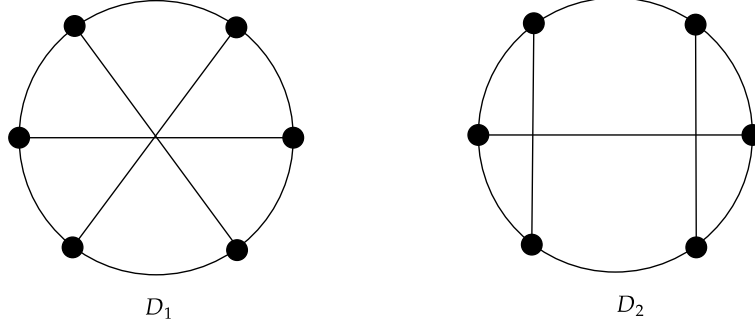


Figure 4.1.: Covariant diagrams corresponding to dimension six operators

In this section we present an efficient method to compute the integral (4.15). We slightly adapt the trick explained in the appendix of [127] and evaluate (4.15) in the special configuration $\partial_\mu \hat{X}_\nu = \partial_\mu \hat{U} = 0$, allowing us to drop all derivatives. In this case

$$D_\mu \hat{G} \rightarrow [\hat{X}_\mu, \hat{G}], \quad \hat{X}_{\mu\nu} \rightarrow [\hat{X}_\mu, \hat{X}_\nu] \quad (4.19)$$

where $D_\mu = \partial_\mu + \hat{X}_\mu$ and \hat{G} is any matrix-valued function of \hat{U} and \hat{X}_μ . In the final result, we can then express everything again in terms of D and $\hat{X}_{\mu\nu}$. Furthermore, we may choose a gauge condition, where

$$\hat{X}_\mu \hat{X}^\mu = 0 \quad (4.20)$$

For this specific choice of gauge, (4.15) becomes

$$\mathcal{L}^{(1)} = c_s \sum_{n=1}^{\infty} \frac{(-1)^{n+1}}{n} \text{tr} \left[i \int_p \frac{(2ip_\mu \hat{X}^\mu - \hat{U})^n}{(p^2 - M^2)^n} \mathbb{1} \right] \quad (4.21)$$

Certain operator structures can be summed to all orders in n . Setting $\hat{X}_\mu = 0$ we easily sum the operators of type \hat{U}^n

$$\begin{aligned} \mathcal{L} = \frac{c_s}{(4\pi)^2} & \left[M^2 \left(1 + \ln \frac{\mu^2}{M^2} \right) \langle \hat{U} \rangle + \frac{1}{2} \ln \frac{\mu^2}{M^2} \langle \hat{U}^2 \rangle \right. \\ & \left. + M^4 \sum_{n=3}^{\infty} \frac{(-1)^n}{n(n-1)(n-2)} \left\langle \left(\frac{\hat{U}}{M^2} \right)^n \right\rangle \right] \end{aligned} \quad (4.22)$$

where the divergent operator coefficients were renormalized in the $\overline{\text{MS}}$ scheme. In Chapter 7 we are interested in the terms of the form $\hat{U}^n \hat{X}_{\mu\nu} \hat{X}^{\mu\nu}$. Setting $[\hat{X}_\mu, \hat{U}] = 0$ automatically removes all terms containing $D_\mu \hat{U}$. The terms with 4 derivatives (i.e. 4 factors of X_μ) in (4.21) and n factors of U then reduce to the terms of interest due to the formal gauge invariance of the functional integral. Finally, we obtain

$$\mathcal{L} = \frac{c_s}{(4\pi)^2} \sum_{n=1}^{\infty} \frac{(-1)^n}{12nM^{2n}} \langle \hat{X}_{\mu\nu} \hat{X}^{\mu\nu} \hat{U}^n \rangle = -\frac{c_s}{192\pi^2} X_{\mu\nu} X^{\mu\nu} \ln \left(1 + \frac{U}{M^2} \right) \quad (4.23)$$

where we assumed $\hat{X}_\mu = X_\mu \cdot 1$ and $\hat{U} = U \cdot 1$ are scalar valued in the last step. The pure gauge operators may be computed from (4.21) by setting $\hat{U} = 0$ and we obtain the expression

$$\mathcal{L} = \frac{c_s}{(4\pi)^2} \sum_{n=3}^{\infty} \frac{1}{(M^2)^{n-2}} \frac{2^n(n-3)!}{(2n)!} S_n^{\mu_1\mu_2\cdots\mu_{2n}} \langle X_{\mu_1} \cdots X_{\mu_{2n}} \rangle \quad (4.24)$$

Here S_n is the completely symmetric tensor with $2n$ indices constructed purely from the metric tensor $g_{\mu\nu}$. For instance $S_1^{\mu_1\mu_2} = g^{\mu_1\mu_2}$ and $S_2^{\mu_1\mu_2\mu_3\mu_4} = g^{\mu_1\mu_2}g^{\mu_3\mu_4} + g^{\mu_1\mu_3}g^{\mu_2\mu_4} + g^{\mu_1\mu_4}g^{\mu_2\mu_3}$. It contains $(2n-1)!!$ terms in general. The term with $n=2$ has a divergent coefficient and has to be treated separately. The *covariant diagram method* [128, 129] is a convenient way to evaluate (4.24). We illustrate this method by evaluating the $n=3$ term in the sum (4.24) i.e. computing the coefficients of dimension six operators. There are two linearly independent trace structures

$$\mathcal{L} = \frac{c_s}{(4\pi)^2} \frac{1}{M^2} \frac{1}{90} \left(\langle \hat{X}_{\mu_1} \hat{X}_{\mu_2} \hat{X}_{\mu_3} \hat{X}_{\mu_1} \hat{X}_{\mu_2} \hat{X}_{\mu_3} \rangle + 3 \langle \hat{X}_{\mu_1} \hat{X}_{\mu_2} \hat{X}_{\mu_1} \hat{X}_{\mu_3} \hat{X}_{\mu_2} \hat{X}_{\mu_3} \rangle \right) \quad (4.25)$$

These two strings of X s can be visualized by two circle diagrams, known as covariant diagrams. We have displayed the two diagrams

$$D_1 = \langle X_{\mu_1} X_{\mu_2} X_{\mu_3} X_{\mu_1} X_{\mu_2} X_{\mu_3} \rangle, \quad D_2 = \langle X_{\mu_1} X_{\mu_2} X_{\mu_1} X_{\mu_3} X_{\mu_2} X_{\mu_3} \rangle \quad (4.26)$$

in Fig. 4.1. The diagrams correspond to the two linearly independent pure gauge operator structures. They read

$$Q_1 = \langle \hat{X}_{\mu\nu} \hat{X}^{\nu\rho} \hat{X}_\rho^\mu \rangle, \quad Q_2 = \langle J_\mu J^\mu \rangle \quad (4.27)$$

where we defined

$$J_\mu = D_\nu \hat{X}^{\nu\mu} \quad (4.28)$$

Making use of our special gauge configuration ($\hat{X}_\mu \hat{X}^\mu = 0$) we can write the operators as our string of X s

$$Q_1 = 3D_2 - D_1 \quad (4.29)$$

$$Q_2 = 4D_2 \quad (4.30)$$

Inverting this relation, we arrive at

$$D_1 = \frac{3}{4}Q_2 - Q_1, \quad D_2 = \frac{1}{4}Q_2 \quad (4.31)$$

such that the effective Lagrangian up to $\mathcal{O}(1/M^2)$ reads

$$\mathcal{L}_{eff} = \frac{c_s}{(4\pi)^2} \frac{1}{M^2} \frac{1}{6} \left[-\langle \hat{U}^3 \rangle - \frac{1}{2} \langle (D_\mu \hat{U})^2 \rangle - \frac{1}{2} \langle \hat{U} \hat{X}_{\mu\nu}^2 \rangle + \frac{1}{15} \langle \hat{X}_{\mu\nu} \hat{X}^{\nu\rho} \hat{X}_\rho^\mu \rangle - \frac{1}{10} \langle J_\mu J^\mu \rangle \right] \quad (4.32)$$

where we include the operators involving \hat{U} . This example can be generalized to higher dimensions. First, one needs to evenly distribute $2n$ nodes on a circle and connect all

nodes pairwise with each other. Connecting two neighboring nodes is forbidden since this corresponds to trace structures involving $\hat{X}_\mu \hat{X}^\mu$, which vanish for our chosen gauge configuration. Additionally, diagrams related by point reflection with respect to the center of the circle are equivalent, reflecting the cyclicity of the trace. All the independent diagrams are then multiplied by a symmetry factor. For instance, the "pizza" diagram D_1 gets a factor 1 since there is precisely one such structure for every n . The diagram D_2 , on the other hand is less symmetric than D_1 and gets a factor 3, i.e. there are three terms in the sum $S_3^{\mu_1 \mu_2 \dots \mu_6} \langle X_{\mu_1} \dots X_{\mu_6} \rangle$ that correspond to this diagram. After drawing all independent diagrams, one has to work out all possible independent operator structures, write them as linear combinations of covariant diagrams, and then invert the relation to compute the operator coefficients.

4.2.2. Effective Lagrangian

Using the covariant diagram methods allows the computation of the UOLEA up to the desired order in the $1/M^2$ expansion. We display here the UOLEA up to $\mathcal{O}(1/M^4)$ [129]

$$\begin{aligned} \mathcal{L} = \frac{c_s}{(4\pi)^2} \Bigg\{ & M^2 \left(1 + \ln \frac{\mu^2}{M^2} \right) \langle \hat{U} \rangle + \frac{1}{2} \ln \frac{\mu^2}{M^2} \left[\langle \hat{U}^2 \rangle + \frac{1}{6} \langle \hat{X}_{\mu\nu} \hat{X}^{\mu\nu} \rangle \right] \\ & + \frac{1}{M^2} \frac{1}{6} \left[-\langle \hat{U}^3 \rangle - \frac{1}{2} \langle \hat{U} \hat{X}_{\mu\nu} \hat{X}^{\mu\nu} \rangle - \frac{1}{10} \langle J_\mu J^\mu \rangle + \frac{1}{15} \langle \hat{X}_\mu^\nu \hat{X}_\nu^\rho \hat{X}_\rho^\mu \rangle \right] \\ & + \frac{1}{M^4} \frac{1}{24} \left[\langle \hat{U}^4 \rangle - \langle \hat{U}^2 (D^2 \hat{U}) \rangle + \frac{4}{5} \langle \hat{U}^2 \hat{X}_{\mu\nu} \hat{X}^{\mu\nu} \rangle + \frac{1}{5} \langle (\hat{U} \hat{X}_{\mu\nu})^2 \rangle \right. \\ & - \frac{2}{5} \langle \hat{U} (D_\mu \hat{U}) J^\mu \rangle + \frac{2}{5} \langle \hat{U} J^\mu J_\mu \rangle - \frac{2}{15} \langle D^2 \hat{U} \hat{X}_{\mu\nu}^2 \rangle + \frac{1}{35} \langle (D_\mu J_\nu)^2 \rangle \\ & - \frac{4}{15} \langle \hat{U} \hat{X}_\mu^\nu \hat{X}_\nu^\rho \hat{X}_\rho^\mu \rangle - \frac{8}{15} \langle (D_\mu D_\nu \hat{U}) \hat{X}^{\mu\rho} \hat{X}_\rho^\nu \rangle + \frac{16}{105} \langle \hat{X}_{\mu\nu} J^\mu J^\nu \rangle \\ & + \frac{17}{210} \langle (\hat{X}^{\mu\nu} \hat{X}_{\mu\nu})^2 \rangle + \frac{1}{420} \langle (\hat{X}_{\mu\nu} \hat{X}_{\rho\sigma})^2 \rangle + \frac{2}{35} \langle (\hat{X}_{\mu\nu} \hat{X}_{\nu\sigma})^2 \rangle \\ & \left. + \frac{1}{105} \langle \hat{X}_{\mu\nu} \hat{X}^{\nu\sigma} \hat{X}_{\sigma\rho} \hat{X}^{\rho\mu} \rangle + \frac{16}{105} \langle (D_\mu J_\nu) \hat{X}^{\nu\sigma} \hat{X}_\sigma^\mu \rangle \right] \Bigg\} \end{aligned} \quad (4.33)$$

where again the divergent operator coefficients were renormalized in the $\overline{\text{MS}}$ -scheme. For a real scalar we have $c_s = 1/2$, a complex scalar $c_s = 1$ and a fermion $c_s = -1$.

4.2.3. Example: Euler-Heisenberg Lagrangian

To illustrate our result we integrate out a first scalar and then a Dirac fermion coupled to electromagnetism using the UOLEA. We then obtain the familiar Euler-Heisenberg Lagrangian [130] for (scalar) spinor QED up to $\mathcal{O}(1/M^4)$. We can neglect operator structures with factors of J_μ since those can be reduced using the equations of motion for the gauge field. First, we take scalar QED and the Lagrangian for a scalar ϕ coupled to electromagnetism is

$$\mathcal{L}_{UV} = -\frac{1}{4} F_{\mu\nu} F^{\mu\nu} + \phi^* (-D^2 - M^2) \phi \quad (4.34)$$

where $D_\mu = \partial_\mu + ieA_\mu$ and $F_{\mu\nu} = \partial_\mu A_\nu - \partial_\nu A_\mu$. The scalar QED example is particularly simple since $U = 0$. Using (4.33) the effective Lagrangian is given by [131]

$$\mathcal{L}_{eff} = \frac{e^4}{(4\pi)^2} \frac{1}{M^4} \left[\frac{1}{288} (F_{\mu\nu} F^{\mu\nu})^2 + \frac{1}{360} F_{\mu\nu} F^{\nu\rho} F_{\rho\sigma} F^{\sigma\mu} \right] \quad (4.35)$$

where we set $J_\mu = 0$. Using the dual field strength tensor $\tilde{F}_{\mu\nu} = \frac{1}{2}\epsilon_{\mu\nu\rho\sigma} F^{\rho\sigma}$ our result takes the form

$$\mathcal{L}_{eff} = \frac{e^4}{(4\pi)^2} \frac{1}{M^4} \left[\frac{7}{1440} (F_{\mu\nu} F^{\mu\nu})^2 + \frac{1}{1440} (F_{\mu\nu} \tilde{F}^{\mu\nu})^2 \right] \quad (4.36)$$

Here we used the useful relation

$$F_{\mu\nu} F^{\nu\rho} F_{\rho\sigma} F^{\sigma\mu} = \frac{1}{2} (F_{\mu\nu} F^{\mu\nu})^2 + \frac{1}{4} (F_{\mu\nu} \tilde{F}^{\mu\nu})^2 \quad (4.37)$$

Next, we consider a heavy Dirac fermion Ψ coupled to a non-abelian gauge field A_μ , i.e. we have

$$\mathcal{L}_{UV} = -\frac{1}{2} \langle G_{\mu\nu} G^{\mu\nu} \rangle + \bar{\Psi} (i\not{D} - M) \Psi \quad (4.38)$$

where $D_\mu = \partial_\mu - igA_\mu$ and $[D_\mu, D_\nu] = -igG_{\mu\nu}$. The one-loop effective action is then given by

$$S_{EFT}^{1-loop} = -i \text{Tr} \log (i\not{D} - M) = -\frac{i}{2} \text{Tr} \log \left(D^2 + M^2 - \frac{g}{2} G_{\mu\nu} \sigma^{\mu\nu} \right) \quad (4.39)$$

where $\sigma_{\mu\nu} = (i/2) [\gamma_\mu, \gamma_\nu]$. The pure gauge operators without derivatives at mass dimension eight read

$$\begin{aligned} \mathcal{L}_{dim8} = \frac{1}{(4\pi)^2} \frac{g^4}{48} \frac{1}{M^4} & \left[-\frac{76}{105} \langle (G^{\mu\nu} G_{\mu\nu})^2 \rangle - \frac{64}{105} \langle (G_{\mu\nu} G_{\rho\sigma})^2 \rangle + \frac{272}{35} \langle (G_{\mu\nu} G_{\nu\sigma})^2 \rangle \right. \\ & \left. - \frac{424}{105} \langle G_{\mu\nu} G^{\nu\sigma} G_{\sigma\rho} G^{\rho\mu} \rangle \right] \end{aligned} \quad (4.40)$$

Note that the trace over the identity matrix in Dirac space gives a factor 4. Specializing to $U(1)$ as a gauge group, we can compute the Dirac traces using the identities

$$(\sigma_{\mu\nu} F^{\mu\nu})^2 = \mathcal{F} \mathbb{1} + i\gamma_5 \mathcal{G} \quad (4.41)$$

$$\text{tr} (\sigma_{\mu\nu} F^{\mu\nu})^{2n} = 4 \sum_{k=0}^{\lfloor \frac{n}{2} \rfloor} \binom{n}{2k} (-1)^k \mathcal{F}^{n-2k} \mathcal{G}^{2k} \quad (4.42)$$

with

$$\mathcal{F} = 2F_{\mu\nu} F^{\mu\nu}, \quad \mathcal{G} = 2\tilde{F}_{\mu\nu} F^{\mu\nu} \quad (4.43)$$

and obtain (setting $g = e$ and $M = m_e$)

$$\mathcal{L}_{dim8} = \frac{e^4}{(4\pi)^2} \frac{1}{m_e^4} \left[-\frac{1}{36} (F_{\mu\nu} F^{\mu\nu})^2 + \frac{7}{90} F_{\mu\nu} F^{\nu\rho} F_{\rho\sigma} F^{\sigma\mu} \right] \quad (4.44)$$

Using (4.37), we recover the well-known Euler-Heisenberg Lagrangian up to dimension eight operators

$$\mathcal{L}_{dim8} = \frac{e^4}{(4\pi)^2} \frac{1}{m_e^4} \left[\frac{1}{90} (F_{\mu\nu} F^{\mu\nu})^2 + \frac{7}{360} (F_{\mu\nu} \tilde{F}^{\mu\nu})^2 \right] \quad (4.45)$$

Part II.

Applications

5. Loop Counting in SMEFT

We have introduced the SMEFT in Chapter 3 as a widely used and well-motivated framework for parameterizing the indirect effects of new physics. In this chapter, we take a closer look at its organizing principle: the power-counting prescription. A clear and consistent power-counting scheme is essential for systematically expanding and truncating the EFT. In particular, it should guide whether a given operator should be included or omitted in a bottom-up EFT calculation at a specified order of approximation.

The power counting relies on general assumptions about the underlying UV theory. While these assumptions and the resulting power-counting rules are not unique, they must be explicitly stated to consistently use the EFT. This is especially important for SMEFT.

In most applications, only the expansion in inverse powers of the scale of new physics Λ is made explicit where each operator of canonical dimension d_c is suppressed by a factor of Λ^{4-d_c} . As a result, operators of higher dimension are increasingly suppressed. However, as previously noted, a power-counting prescription based solely on canonical dimensions may lead to inconsistencies. To be consistent, it must be supplemented by specifying whether the SM particles are weakly or strongly coupled to the UV sector.

Effectively, this implies a counting of loop orders. Loop orders can be systematically accounted for by assigning a chiral dimension d_χ to each operator. By "inconsistent" we do not mean that a canonical-dimension-based SMEFT with $\mathcal{O}(1)$ Wilson coefficients is nonviable as an EFT under perturbative renormalization. Rather, such an approach may fail to match a broad class of weakly coupled UV completions and fails to provide a justification for the expected size of operator coefficients.

In this chapter, we review the fundamental rules of power counting. Although these rules are not new, they are often left implicit or applied inconsistently in the literature. We emphasize the importance of loop counting in SMEFT and illustrate its role through concrete examples and calculations.

This chapter is structured as follows. In Section 5.1, we introduce a toy model featuring a fermion, the "top quark" t , coupled to a heavy scalar S . We construct a top-down EFT by integrating out the scalar and analyze the process $e^+e^- \rightarrow t\bar{t}$ both in the full theory and in the EFT.

This example demonstrates how a magnetic-moment-type operator, $m_t \bar{t} \sigma_{\mu\nu} t F^{\mu\nu}$, and a four-fermion operator, $\bar{t} t \bar{t} t$, contribute at the same order in the EFT expansion (both being dimension-six operators), even though the former appears at tree level and the latter at one loop. We show that this distinction is naturally explained by loop counting. A complementary analysis within a bottom-up EFT confirms these findings.

In Section 5.2, we discuss the general power-counting rules of SMEFT, emphasizing the importance of loop-order counting. This can be conveniently expressed using the concept of chiral dimensions d_χ . To illustrate the counting scheme in practice, we examine Higgs boson production via gluon fusion ($gg \rightarrow h$), a process that elegantly highlights the interplay between canonical operator dimensions and loop orders in SMEFT. The general SMEFT power-counting formula can also be derived by distinguishing between couplings

and scales in the EFT Lagrangian, as discussed in Section 5.3.

In Section 5.4, we consider a more realistic scenario and analyze the process $u\bar{u} \rightarrow t\bar{t}$ in a decoupling Two-Higgs Doublet Model (2HDM) as the UV completion of SMEFT, thereby connecting our discussion to SMEFT in a phenomenologically relevant context. Finally, we summarize and conclude in Section 5.5.

The discussion in this chapter follows closely Ref. [1], where the author of this thesis is a co-author. A similar treatment also appeared in the Ph.D. thesis of another co-author [132].

5.1. Toy Model analysis of $e^+e^- \rightarrow t\bar{t}$

To illustrate how loop counting enters standard EFT calculations we consider a toy UV model and show that certain effective low-energy EFT operators are loop suppressed. The toy model consists of two fermions coupled to electromagnetism, an electron ψ with mass $m_e \approx 0$ and a heavy "top quark" t with mass m . They which represent "standard" physics. In addition, the role of "non standard" physics is taken by a real scalar field S with mass $M \gg m$ which has renormalizable self-interactions and a Yukawa coupling to the "top-quark" t . The toy model Lagrangian is given by

$$\begin{aligned} \mathcal{L} = & \bar{\psi} (i\not{D} - m_e) \psi + \bar{t} (i\not{D} - m) t - \frac{1}{4} F_{\mu\nu} F^{\mu\nu} \\ & + \frac{1}{2} \partial_\mu S \partial^\mu S - \frac{1}{2} M^2 S^2 - \frac{b}{3!} S^3 - \frac{\lambda}{4!} S^4 - g \bar{t} t S \end{aligned} \quad (5.1)$$

where

$$D_\mu = \partial_\mu + ieq_f A_\mu, \quad q_e = -1, \quad q_t = \frac{2}{3}, \quad F_{\mu\nu} = \partial_\mu A_\nu - \partial_\nu A_\mu \quad (5.2)$$

The first line of our toy model is simply quantum electrodynamics with two fermions. The scale of "new physics" M is assumed to be much larger than m and the typical energies \sqrt{s} accessible in experiments. The dimensionful coupling b can be $\mathcal{O}(M)$, while the dimensionless couplings λ, g are of $\mathcal{O}(1)$. Integrating out the heavy scalar produces new-physics effects modifying the top quark dynamics, suppressed by powers of s/M^2 . A similar toy model has been discussed in [133].

5.1.1. Diagrammatic matching

To illustrate our argumentation we examine the process $e^-(k_1)e^+(k_2) \rightarrow t(p_1)\bar{t}(p_2)$ and compute the amplitude in the full theory and in the EFT, thus we perform diagrammatic matching. At tree-level the amplitude for the process arises from s-channel photon exchange shown in Fig. 5.1 (a). The tree-level amplitude is given by

$$\mathcal{A}_{LO} = -i \frac{e^2 q_t}{q^2} \bar{v}(k_2) \gamma_\mu u(k_1) \bar{u}(p_1) \gamma^\mu v(p_2) \quad (5.3)$$

where $q = k_1 + k_2 = p_1 + p_2$ and $s = q^2$. Let us now consider the leading corrections to this amplitude due to the heavy scalar. Due to the Yukawa coupling S modifies the

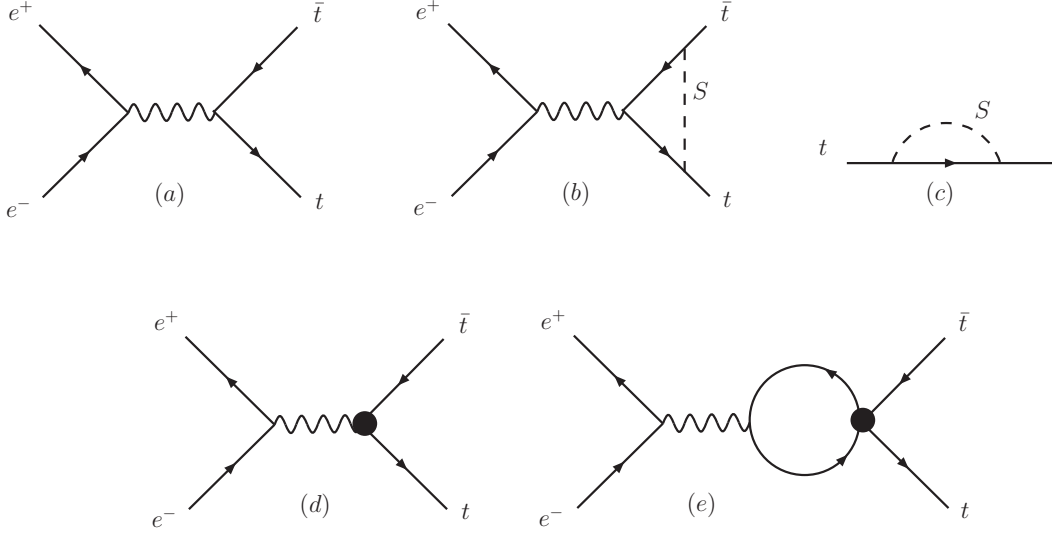


Figure 5.1.: $e^+e^- \rightarrow t\bar{t}$ in a toy model. (a) Lowest-order amplitude. (b), (c): Leading corrections from S -scalar exchange in the full theory. (d), (e): Contributions needed to reproduce the $1/M^2$ corrections of the full theory within the EFT, where the black dots represent the local dimension 6 EFT operators. Q_2 and Q_3 enter at tree-level in (d), whereas Q_1 contributes at one loop in (e).

$t\bar{t}$ -photon vertex function. The corresponding one-loop diagram is depicted in Fig. 5.1 (b) and the amplitude is

$$\mathcal{A}_{LO} + \delta\mathcal{A} = -i \frac{e^2 q_t}{q^2} \bar{v}(k_2) \gamma_\mu u(k_1) \bar{u}(p_1) \Gamma^\mu v(p_2) \quad (5.4)$$

We write the one-loop vertex function as

$$\Gamma^\mu = \gamma^\mu + \delta\Gamma^\mu \quad (5.5)$$

where $\delta\Gamma^\mu$ contains the effect of S -boson exchange. To compute $\delta\Gamma^\mu$ we need to compute the following one-loop integral

$$\bar{u}(p_1) \delta\Gamma^\mu v(p_2) = ig^2 \int \frac{d^d k}{(2\pi)^d} \frac{\bar{u}(p_1) (\not{k} + \not{p}_1 + m) \gamma^\mu (\not{k} - \not{p}_2 + m) v(p_2)}{(k^2 - M^2)((k + p_1)^2 - m^2)((k - p_2)^2 - m^2)} \quad (5.6)$$

Up to $\mathcal{O}(M^{-2})$ the correction to the vertex function due to the heavy scalar is given by

$$\delta\Gamma^\mu = -\frac{g^2}{16\pi^2} \frac{1}{M^2} \left[\left(\frac{\ln r}{3} + \frac{4}{9} + h_1(z) \right) q^2 \gamma^\mu + \left(\ln r + \frac{7}{6} + h_2(z) \right) im \sigma^{\mu\nu} q_\nu \right] \quad (5.7)$$

where we defined

$$r \equiv \frac{m^2}{M^2}, \quad z \equiv \frac{q^2}{4m^2} \quad (5.8)$$

and ($\bar{x} = 1 - x$)

$$h_1(z) = \int_0^1 dx \, 2x\bar{x} \ln(1 - 4x\bar{x}z - i\eta) = \left(\frac{1}{3} + \frac{1}{6z} \right) h_2(z) + \frac{1}{9} \quad (5.9)$$

$$h_2(z) = \int_0^1 dx \ln(1 - 4x\bar{x}z - i\eta) = -2 + \sqrt{1 - z^{-1}} \ln \frac{\sqrt{1 - z^{-1}} + 1}{\sqrt{1 - z^{-1}} - 1} \quad (5.10)$$

In the Euclidean region $z < 0$ the second expression for $h_2(z)$ is immediately applicable. For $z > 0$ it holds with the prescription $z \rightarrow z + i\eta$. The function $h_2(z)$ comes from the Passarino-Veltman scalar bubble function (E.4)

$$B_0(q^2; m^2, m^2) = \frac{1}{\epsilon} + \ln \frac{\mu^2}{m^2} - h_2(z) \quad (5.11)$$

5.1.2. Strategy of regions

In this section, we demonstrate how the expression in (5.7) can be obtained without computing the exact all-orders result in M first, as discussed in [132]. Specifically, we evaluate (5.6) in two distinct momentum regions, thereby illustrating key features of EFTs. In particular, this analysis highlights how the EFT reproduces the nonanalytic terms in the infrared (IR) scale that appear in the full theory. This approach is equivalent to the method of regions [84, 134] in this context.

Since the full theory and the EFT share the same IR degrees of freedom, their results must agree in the soft region, where $k^2 \ll M^2$. In this momentum region, the heavy scalar can be integrated out, which amounts to expanding its propagator as

$$\frac{1}{k^2 - M^2} = -\frac{1}{M^2} \left(1 + \frac{k^2}{M^2} + \frac{k^4}{M^4} + \dots \right) \quad (5.12)$$

Expanding in the UV scale M using dimensional regularization isolates the momentum region $k^2 \ll M^2$ in (5.6). Each term in the series corresponds to the IR contribution of higher-dimensional operators.

Working to $\mathcal{O}(M^{-2})$, we retain only the first term in the expansion, corresponding to operators of canonical dimension six. In the soft momentum region ($k, p_1, p_2, m \ll M$), the integral becomes

$$\bar{u}(p_1) \delta\Gamma_{EFT}^\mu v(p_2) = \frac{-ig^2}{M^2} \int \frac{d^d k}{(2\pi)^d} \frac{\bar{u}(p_1)(\not{k} + \not{p}_1 + m)\gamma^\mu(\not{k} - \not{p}_2 + m)v(p_2)}{((k + p_1)^2 - m^2)((k - p_2)^2 - m^2)} \quad (5.13)$$

Since we have expanded in the UV scale M , this result does not contain any nonanalytic dependence on M , such as $\ln M$ terms, that appear in the full theory. The order of expansion and integration matters clearly matters here.

Evaluating the integral in the EFT region yields

$$\delta\Gamma_{EFT}^\mu = -\frac{g^2}{16\pi^2 M^2} \left[\left(-\frac{1}{3\epsilon} + \frac{1}{3} \ln \frac{m^2}{\bar{\mu}^2} + h_1(z) \right) q^2 \gamma^\mu + \left(-\frac{1}{\epsilon} + \ln \frac{m^2}{\bar{\mu}^2} + h_2(z) \right) i m \sigma^{\mu\nu} q_\nu \right], \quad (5.14)$$

where $\bar{\mu}^2 = \mu^2 4\pi e^{-\gamma_E}$. The divergences here are formally IR in origin. Crucially, the logarithmic IR terms $\ln m^2$ in (5.14), which are nonanalytic in m , agree exactly with those in (5.7), as required since the EFT must reproduce the IR behavior of the full theory.

To fully reconstruct the amplitude, we must also evaluate (5.6) in the hard momentum region ($k \sim M \gg m, p_1, p_2$). This contribution is known as the *matching contribution*,

as it determines the Wilson coefficients in the EFT by matching the UV behavior and nonanalytic terms in M .

The matching contribution $\delta\Gamma_M^\mu$ can be computed by expanding $\delta\Gamma^\mu$ in the IR scale m . We can safely set $m = 0$ in the propagators:

$$\bar{u}(p_1)\delta\Gamma_M^\mu v(p_2) = ig^2 \int \frac{d^d k}{(2\pi)^d} \frac{\bar{u}(p_1)(\not{k}\gamma^\mu\not{k} + 4mk^\mu + 4m^2\gamma^\mu)v(p_2)}{(k^2 - M^2)k^4 \left(1 + \frac{2k \cdot p_1}{k^2}\right) \left(1 - \frac{2k \cdot p_1}{k^2}\right)} \quad (5.15)$$

To extract the $\mathcal{O}(M^{-2})$ terms, we expand the integrand up to $\mathcal{O}(k^{-6})$:

$$\begin{aligned} \frac{\not{k}\gamma^\mu\not{k} + 4mk^\mu + 4m^2\gamma^\mu}{\left(1 + \frac{2k \cdot p_1}{k^2}\right) \left(1 - \frac{2k \cdot p_1}{k^2}\right)} &= \not{k}\gamma^\mu\not{k} + 4m^2\gamma^\mu - \frac{8mk^\mu k \cdot (p_1 - p_2)}{k^2} \\ &+ \frac{4\not{k}\gamma^\mu\not{k} [(k \cdot p_1)^2 + (k \cdot p_2)^2 - (k \cdot p_1)(k \cdot p_2)]}{k^4} + \mathcal{O}\left(\frac{1}{k^2}\right) \end{aligned} \quad (5.16)$$

Evaluating the integral in d dimensions gives:

$$\delta\Gamma_M^\mu = \left(\frac{2-d}{d} M^2 \gamma^\mu + 8 \frac{d-1}{d(d+2)} m i \sigma^{\mu\nu} q_\nu + \frac{4(d-4)(d-1)}{d(d+2)} m^2 \gamma^\mu + \frac{2}{d+2} q^2 \gamma^\mu \right) I_B \quad (5.17)$$

where the basis integral is

$$I_B = \int \frac{d^d k}{(2\pi)^d} \frac{1}{(k^2 - M^2)k^4} = \frac{i}{16\pi^2 M^2} \left(\frac{1}{\epsilon} + \ln \frac{\bar{\mu}^2}{M^2} \right) \quad (5.18)$$

Thus, the matching contribution becomes

$$\begin{aligned} \delta\Gamma_M^\mu &= \frac{g^2}{16\pi^2 M^2} \left[\frac{M^2}{2} \gamma^\mu \left(\frac{1}{\epsilon} + \ln \frac{\bar{\mu}^2}{M^2} + \frac{1}{2} \right) - m i \sigma^{\mu\nu} q_\nu \left(\frac{1}{\epsilon} + \ln \frac{\bar{\mu}^2}{M^2} + \frac{7}{6} \right) \right. \\ &\quad \left. + m^2 \gamma^\mu - \frac{q^2}{3} \gamma^\mu \left(\frac{1}{\epsilon} + \ln \frac{\bar{\mu}^2}{M^2} + \frac{4}{3} \right) \right] \end{aligned} \quad (5.19)$$

Adding the soft and hard contributions yields:

$$\begin{aligned} \delta\Gamma_{EFT}^\mu + \delta\Gamma_M^\mu &= -\frac{g^2}{16\pi^2 M^2} \left[\left(\frac{1}{3} \ln r + \frac{4}{9} + h_1(z) \right) q^2 \gamma^\mu + \left(\ln r + \frac{7}{6} + h_2(z) \right) m i \sigma^{\mu\nu} q_\nu \right. \\ &\quad \left. - m^2 \gamma^\mu - \frac{M^2}{2} \gamma^\mu \left(\frac{1}{\epsilon} + \ln \frac{\bar{\mu}^2}{M^2} + \frac{1}{2} \right) \right] \end{aligned} \quad (5.20)$$

One might worry that the intermediate momentum region $m \ll k \ll M$ has been double-counted by summing $\delta\Gamma_{EFT}^\mu$ and $\delta\Gamma_M^\mu$. However, this region corresponds to scaleless integrals when (5.6) is expanded in both $1/M$ and m . Scaleless integrals vanish identically in dimensional regularization so that the intermediate region does not contribute.

This is consistent with the interpretation of dimensional regularization as a generalization of residue calculus. The integrand of (5.6) has both UV poles at M and IR poles at m . Expanding in $1/M$ isolates the IR poles (EFT), while expanding in m captures the UV structure (matching). Their sum gives the full result [80].

To cancel the remaining divergence, we renormalize the vertex function. The contribution of the heavy scalar to the top-quark self-energy [Fig. 5.1 (c)] is:

$$\Sigma(\not{p}) = \frac{1}{16\pi^2} \int_0^1 dx (x\not{p} + m) \left(\frac{1}{\epsilon} + \ln \frac{\bar{\mu}^2}{M^2} - \ln \left(x + \bar{x} \frac{m^2}{M^2} - x\bar{x} \frac{p^2}{M^2} \right) \right) \quad (5.21)$$

Using the Ward identity, the renormalization constant δ_2 in the on-shell scheme is:

$$\delta_2 = - \left. \frac{d\Sigma(\not{p})}{d\not{p}} \right|_{\not{p}=m} \quad (5.22)$$

which evaluates to

$$\delta_2 = -\frac{g^2}{16\pi^2} \left[\frac{1}{2} \left(\frac{1}{\epsilon} + \ln \frac{\bar{\mu}^2}{M^2} \right) - \int_0^1 dx x \ln \left(x + \bar{x}^2 \frac{m^2}{M^2} \right) + \frac{m^2}{M^2} \int_0^1 dx \frac{2\bar{x}(1+x)}{x + \bar{x}^2 \frac{m^2}{M^2}} \right] \quad (5.23)$$

Expanding δ_2 to $\mathcal{O}(M^{-2})$ gives:

$$\delta_2 = -\frac{1}{16\pi^2 M^2} \left[\frac{M^2}{2} \left(\frac{1}{\epsilon} + \ln \frac{\bar{\mu}^2}{M^2} + \frac{1}{2} \right) + m^2 \right] + \mathcal{O}(M^{-4}) \quad (5.24)$$

Adding this counterterm to (5.20) cancels the remaining divergence and reproduces the full result:

$$\delta\Gamma^\mu = \delta\Gamma_{EFT}^\mu + \delta\Gamma_M^\mu + \delta_2\gamma^\mu \quad (5.25)$$

5.1.3. Top-down EFT

Knowing the full UV result, we can match onto an EFT operator basis at canonical dimension six in a top-down approach. This requires calculating the vertex function to order $1/M^2$ in both the full theory and the EFT. By comparing the two, the expressions for the Wilson coefficients can be extracted. To reproduce the full vertex function within the EFT, we need a complete basis of dimension-six operators:

$$\Delta\mathcal{L}_6 = \frac{1}{M^2} \sum_i C_i Q_i \quad (5.26)$$

Typically, one constructs a complete basis of EFT operators, derives the corresponding Feynman rules, and identifies which operators are required to match the full theory result. In our case, however, the relevant EFT operators can be essentially inferred directly from the functional form of the vertex function in (5.7):

$$Q_1 = \bar{t}t\bar{t}t, \quad Q_2 = \partial_\mu F^{\mu\nu} \bar{t}\gamma_\nu t, \quad Q_3 = m \bar{t}\sigma_{\mu\nu} t F^{\mu\nu} \quad (5.27)$$

The operator Q_2 can be eliminated using the equation of motion for A_μ , yielding an equivalent form involving four-fermion operators:

$$Q'_2 = -e \bar{\psi}\gamma^\nu \psi \bar{t}\gamma_\nu t + eq_t \bar{t}\gamma^\nu t \bar{t}\gamma_\nu t \quad (5.28)$$

It is straightforward to verify that the local four-fermion operator $-e\bar{\psi}\gamma^\nu\psi\bar{t}\gamma_\nu t$ gives the same contribution to the vertex function as Q_2 . Using these three operators we can reproduce $\delta\Gamma^\mu$ up to $\mathcal{O}(M^{-2})$. Their coefficients are determined by equating the amplitudes in the full theory and the EFT:

$$-ieq_t\delta\Gamma^\mu = -ieq_t\delta\Gamma_{Q_1}^\mu + \frac{C_2}{M^2}(-iq^2\gamma^\mu) + \frac{C_3}{M^2}(-2\sigma^{\mu\nu}q_\nu m) \quad (5.29)$$

Note that Q_1 must be inserted into the one-loop diagram shown in Fig. 5.1 (e), yielding the vertex function:

$$\delta\Gamma_{Q_1}^\mu = -\frac{1}{16\pi^2}\frac{2C_1}{M^2}\left[\left(\frac{1}{3}\ln\frac{m^2}{\bar{\mu}^2} + h_1(z)\right)q^2\gamma^\mu + \left(\ln\frac{m^2}{\bar{\mu}^2} + h_2(z)\right)i\sigma^{\mu\nu}q_\nu m\right] \quad (5.30)$$

This expression matches (5.14) and correctly reproduces all non-analytic terms in the infrared scale m as seen in (5.7). Since the local operators Q_2 and Q_3 generate only analytic terms, the one-loop contribution from Q_1 is essential to reproduce the full $\mathcal{O}(1/M^2)$ amplitude in the EFT.

The vertex function in (5.30) is renormalized in the $\overline{\text{MS}}$ scheme. The matching condition in (5.29) then implies:

$$C_1 = \frac{g^2}{2}, \quad C_2 = -eq_t\frac{g^2}{16\pi^2}\left(\frac{1}{3}\ln\frac{\bar{\mu}^2}{M^2} + \frac{4}{9}\right), \quad C_3 = eq_t\frac{g^2}{16\pi^2}\left(\frac{1}{2}\ln\frac{\bar{\mu}^2}{M^2} + \frac{7}{12}\right) \quad (5.31)$$

Here we see explicitly how the factorization of IR and UV scales in the EFT works. The physics from large momentum regions ($k \sim M$) is encoded in the Wilson coefficients C_2 and C_3 . Together they form the matching contribution

$$-ieq_t\delta\Gamma_M^\mu = \frac{C_2}{M^2}(-iq^2\gamma^\mu) + \frac{C_3}{M^2}(-2\sigma^{\mu\nu}q_\nu m) \quad (5.32)$$

whereas contribution from small scales are reproduced by the matrix element of the local operator Q_1 . The two regions are separated by a renormalization scale $\bar{\mu}$ that cancels when adding the two. Together with (5.4) and (5.5), the relations (5.29)–(5.31) reproduce the leading $1/M^2$ corrections to the process $e^+e^- \rightarrow t\bar{t}$ in the EFT.

Under renormalization, the operator Q_1 mixes into Q_2 and Q_3 , and the corresponding renormalization group equations can be extracted from (5.31):

$$\beta_i \equiv 16\pi^2\frac{dC_i}{d\ln\mu} \quad \Rightarrow \quad \beta_2 = -\frac{4}{3}eq_tC_1, \quad \beta_3 = 2eq_tC_1 \quad (5.33)$$

Additionally, the Wilson coefficients C_2 and C_3 act as counterterms that absorb the UV divergences originating in (5.30).

Even in this simple toy model, it becomes clear that relying solely on canonical dimension is insufficient. Although all three operators have canonical dimension six, they appear at different loop orders in the calculation: all contribute corrections of order $\sim g^2/(16\pi^2 M^2)$ to the amplitude, but Q_1 appears at the one-loop level, while Q_2 and Q_3 contribute at tree level, as shown in Fig. 5.1 (d) and (e). The loop suppression of Q_2 and Q_3 distinguishes them from Q_1 , despite sharing the same canonical dimension. This demonstrates the necessity of chiral dimensions d_χ (3.31) to account for loop orders. In our example:

$$d_\chi[C_1Q_1] = 4, \quad d_\chi[C_2Q_2] = d_\chi[C_3Q_3] = 6 \quad (5.34)$$

We will examine the assignment of weak couplings to dimension-six operators in detail in Sec. 5.2. For the present discussion, it suffices to recall that each gauge field strength contributes at least one weak coupling, a tensor fermion current contributes two, and a vector current contributes one. Counting chiral dimension correctly captures the relative suppression of $Q_{2,3}$ with respect to Q_1 by a loop factor $1/(4\pi)^2$.

5.1.4. Bottom-Up EFT

Typically one uses the SMEFT as a bottom-up EFT where the Wilson coefficients of the higher dimensional operators are unknown. Assuming a power counting scheme based on canonical dimensions alone would result in treating all coefficients C_i as $\mathcal{O}(1)$ numbers. We again point out the inconsistency of such an approach by constructing a bottom-up EFT in the context of our toy model. We assume the standard physics at energies $\sim m$ is still given by the first line of (5.1) but we have no knowledge this time of the heavy sector presumed to reside at $M \gg m$. Working again to order $1/M^2$ the EFT Lagrangian has the form of (5.26), where the operators remain to be determined. To perform a consistent bottom-up calculation we need a complete EFT operator basis. At canonical dimension six there are two operator classes; four-fermion operators and magnetic-moment type operators. Starting with the four-fermion operators we have to write down all possible combinations while eliminating redundant operators using Fierz identities. The independent structures are given by

$$Q_{S1} = \bar{t}t \bar{\psi}\psi, \quad Q_{S2} = i\bar{t}t \bar{\psi}\gamma_5\psi, \quad Q_{S3} = i\bar{t}\gamma_5t \bar{\psi}\psi, \quad Q_{S4} = \bar{t}\gamma_5t \bar{\psi}\gamma_5\psi, \quad (5.35)$$

$$\begin{aligned} Q_{V1} &= \bar{t}\gamma_\mu t \bar{\psi}\gamma^\mu\psi, & Q_{V2} &= \bar{t}\gamma_\mu t \bar{\psi}\gamma^\mu\gamma_5\psi \\ Q_{V3} &= \bar{t}\gamma_\mu\gamma_5t \bar{\psi}\gamma^\mu\psi, & Q_{V4} &= \bar{t}\gamma_\mu\gamma_5t \bar{\psi}\gamma^\mu\gamma_5\psi \end{aligned} \quad (5.36)$$

$$Q_{T1} = \bar{t}\sigma^{\mu\nu}t \bar{\psi}\sigma_{\mu\nu}\psi, \quad Q_{T2} = i\bar{t}\sigma^{\mu\nu}t \bar{\psi}\sigma_{\mu\nu}\gamma_5\psi \quad (5.37)$$

and, with $\eta = t, \psi$,

$$Q_{\eta S1} = \bar{\eta}\eta \bar{\eta}\eta, \quad Q_{\eta S2} = i\bar{\eta}\eta \bar{\eta}\gamma_5\eta, \quad Q_{\eta S4} = \bar{\eta}\gamma_5\eta \bar{\eta}\gamma_5\eta \quad (5.38)$$

$$Q_{\eta V1} = \bar{\eta}\gamma^\mu\eta \bar{\eta}\gamma_\mu\eta, \quad Q_{\eta V2} = \bar{\eta}\gamma^\mu\eta \bar{\eta}\gamma_\mu\gamma_5\eta \quad (5.39)$$

The magnetic moment type operators are given by

$$Q_{tF} = m\bar{t}\sigma_{\mu\nu}t F^{\mu\nu}, \quad Q_{\psi F} = m_e\bar{\psi}\sigma_{\mu\nu}\psi F^{\mu\nu} \quad (5.40)$$

Note that all operators with $F_{\mu\nu}$ and derivatives may be reduced via the equations of motion to those listed above. Out of those three independent combinations give corrections to the vertex function: $Q_1 = Q_{tS1}$, $Q_3 = Q_{tF}$ and $Q'_2 = -eQ_{V1} + 2/3eQ_{tV1}$. We now try to parametrize the leading order corrections to the $e^+e^- \rightarrow t\bar{t}$ amplitude using our bottom-up EFT. We would write ($\bar{v} = \bar{v}(k_2)$ etc.)

$$\delta A = \frac{i}{M^2} \sum_i C_i \langle Q_i \rangle = \frac{i}{M^2} \bar{v}\gamma_\mu u \bar{u}\sigma^{\mu\nu}v 2ie \frac{mq_\nu}{q^2} C_{tF} + \frac{i}{M^2} \bar{v}\gamma_\mu u \bar{u}\gamma^\mu v C_{V1} + \dots \quad (5.41)$$

where $\langle Q_i \rangle$ denotes the matrix element of Q_i . Here C_{V1} serves as a representative for all four-fermion operators of the type $((\bar{\psi} \dots \psi)(\bar{t} \dots t))$ contributing at tree level. Four-top operators, on the other hand, such as $Q_{tS1} = \bar{t}t \bar{t}t$ would contribute to δA at one loop. Assuming $C_{tS1} = \mathcal{O}(1)$ would imply $\delta A_{tS1} \sim 1/16\pi^2 M^2$ which would appear to be sub-leading with respect to the terms $\sim 1/M^2$ in (5.41). Several conclusions can be drawn from our example. While the toy model is a specific realization of a UV sector it clearly demonstrates that counting canonical dimensions alone is not enough. A bottom-up EFT constructed as the most general low-energy theory should be able to reproduce any specific model of new-physics at the scale M at any given order in the EFT approximation. Furthermore, the distinction between Q_{tS1} and Q_{tF} is generic in the sense that any model with a heavy boson coupled to the top quark will induce four-top interactions such as Q_{tS1} at tree level and generate Q_{tF} at one loop.

While the toy model assumed weak coupling to the heavy sector the ratio of the coefficients of the magnetic-moment operator and the four-top operator $C_3/C_1 = \mathcal{O}(1/16\pi^2)$ is independent of the coupling g . For strong coupling $g \sim 4\pi$ we could have $C_3 = \mathcal{O}(1)$ but only at the price of a four-fermion coefficient $C_1 = \mathcal{O}(16\pi^2)$.

It is, of course, not necessary to assume a weakly-coupled UV completion for an EFT. We illustrate this by assuming that the top quark is strongly coupled to the new physics at scale M . The vertex function in its full generality can be written as

$$\Gamma^\mu = \gamma^\mu G_1(q^2) + \frac{i\sigma^{\mu\nu} q_\nu}{2m} G_2(q^2) \quad (5.42)$$

where $G_{1,2}$ are formfactors where $G_1 = 1 + \mathcal{O}(M^{-2})$, $G_2 = \mathcal{O}(M^{-2})$. The leading new-physics effects which enter at $\mathcal{O}(M^{-2})$ can be parameterized by a bottom up EFT

$$\Delta\mathcal{L}_6 = \frac{1}{M^2} [C_1 \bar{t}t \bar{t}t + C_2 \partial_\mu F^{\mu\nu} \bar{t}\gamma_\nu t + C_3 m \bar{t}\sigma_{\mu\nu} t F^{\mu\nu} + \dots] \quad (5.43)$$

where the ellipsis denotes the remaining four-fermion operators in the full basis. One then finds

$$G_1(q^2) = 1 + \frac{q^2}{M^2} \left[\frac{C_2}{eq_t} - \frac{C_1}{8\pi^2} \left(\frac{1}{3} \ln \frac{m^2}{\bar{\mu}^2} + h_1(z) \right) + \dots \right] \quad (5.44)$$

$$G_2(q^2) = -\frac{m^2}{M^2} \left[4 \frac{C_3}{eq_t} + \frac{C_1}{4\pi^2} \left(\ln \frac{m^2}{\bar{\mu}^2} + h_2(z) \right) + \dots \right] \quad (5.45)$$

Assuming the top-quark is strongly coupled no weak couplings are associated with C_1 and the first term in (5.43) has $d_\chi = 2$. The second and third terms in (5.43) will have $d_\chi = 4$ since $C_{2,3}$ will come with at least a factor of e that is necessarily associated with $F_{\mu\nu}$ in $Q_{2,3}$. Again $C_{2,3}$ will have a loop suppression with respect to C_1 and all coefficients will contribute at the same order in (5.44) and (5.45). A similar reasoning may be applied to the remaining terms in (5.43). For instance, four-top operators $(\bar{t} \dots t)(\bar{t} \dots t)$ contribute analogously to Q_1 . The amplitude $e^+ e^- \rightarrow \bar{t}t$ will also receive contributions from operators of the type $(\bar{\psi} \dots \psi)(\bar{t} \dots t)$.

5.1.5. Functional matching

For completeness we include the complete one-loop matching results employing the functional approach. Integrating out the heavy scalar S at the tree level amounts to solving

the equation of motion

$$(\square + M^2) S = -\frac{b}{2} S^2 - \frac{\lambda}{6} S^3 - g \bar{t} t \quad (5.46)$$

iteratively in inverse powers of M . To first order the solution is given by

$$S = -\frac{g}{M^2} \bar{t} t + \mathcal{O}(M^{-4}) \quad (5.47)$$

Plugging this solution back into the Lagrangian generates the tree-level effective Lagrangian up to canonical dimension 6

$$\mathcal{L}_{EFT}^{tree} = \bar{\psi} (i\not{D} - m_e) \psi + \bar{t} (i\not{D} - m) t - \frac{1}{4} F_{\mu\nu} F^{\mu\nu} + \frac{g^2}{2M^2} (\bar{t} t)^2 \quad (5.48)$$

To perform the one-loop matching, the formalism laid out in Chapter 4 can be used. The formalism has been automatized in the software package **Matchete** [126]. Implementing our toy model in **Matchete** produces the effective Lagrangian

$$\begin{aligned} \mathcal{L}_{EFT}^{loop} = & \bar{\psi} (i\not{D} - m_e) \psi + \bar{t} (i\not{D} - m) t - \frac{1}{4} F_{\mu\nu} F^{\mu\nu} \\ & + C_1 (\bar{t} t)^2 + C_2 F^{\mu\nu} \bar{t} \sigma_{\mu\nu} t + C_3 (\bar{t} \gamma_\mu t)^2 + C_4 (\bar{t} \sigma_{\mu\nu} t)^2 + C_5 (\bar{t} \gamma_\mu t) (\bar{\psi} \gamma^\mu \psi) \end{aligned} \quad (5.49)$$

where the Wilson coefficients up to one loop in the $\overline{\text{MS}}$ -scheme are given by

$$\begin{aligned} C_1 &= \frac{g^2}{2M^2} + \frac{g^2}{16\pi^2 M^2} \left[\frac{\lambda}{4} \left(\ln \frac{\bar{\mu}^2}{M^2} + 1 \right) - g^2 \left(\frac{3}{2} \ln \frac{\bar{\mu}^2}{M^2} + \frac{5}{4} \right) \right] \\ C_2 &= q_t e \frac{g^2}{16\pi^2 M^2} \left(\frac{1}{2} \ln \frac{\bar{\mu}^2}{M^2} + \frac{7}{12} \right), \quad C_3 = -q_t^2 e^2 \frac{g^2}{16\pi^2 M^2} \left(\frac{1}{3} \ln \frac{\bar{\mu}^2}{M^2} + \frac{4}{9} \right) \\ C_4 &= -q_t^2 e^2 \frac{g^2}{16\pi^2 M^2} \left(\frac{1}{2} \ln \frac{\bar{\mu}^2}{M^2} + \frac{3}{4} \right), \quad C_5 = q_t e^2 \frac{g^2}{16\pi^2 M^2} \left(\frac{1}{3} \ln \frac{\bar{\mu}^2}{M^2} + \frac{4}{9} \right) \end{aligned} \quad (5.50)$$

where we neglected factors of m_e in the matching results. These results agree with (5.31), confirming the equivalence between the functional and diagrammatic approaches.

5.2. SMEFT

While bottom-up EFTs such as SMEFT aim to remain as general as possible, certain assumptions are unavoidable and must be applied consistently. In particular, the following key ingredients must be specified to construct and apply a bottom-up EFT coherently:

- (a) the low-energy degrees of freedom (particle content),
- (b) the relevant local and global symmetries,
- (c) the power-counting scheme.

The power-counting prescription plays a central role in establishing a hierarchy among new-physics effects and enables a systematic expansion and truncation in a well-defined expansion parameter. Assumptions about the UV completion directly impact the power-counting rules. Frequently, only the existence of a mass gap between the known particles

and the new physics scale is assumed, which justifies an expansion in inverse powers of that scale. However, it is equally important to specify whether SM particles are weakly or strongly coupled to the UV sector, as we discuss in the following.

In general, any relativistic EFT can be organized as a double expansion in powers of the heavy scale Λ and loop orders [135]. For SMEFT, the natural expansion parameters are:

$$\frac{E^2}{\Lambda^2} \quad \text{and} \quad \frac{1}{16\pi^2}, \quad (5.51)$$

where E is the typical energy scale of the process, usually of the order of a few times the electroweak scale v , and $1/(16\pi^2)$ represents the loop factor in four dimensions.

In most applications, only the expansion in $1/\Lambda$ is made explicit when writing the SMEFT Lagrangian. Up to order $1/\Lambda^2$, it takes the form:

$$\mathcal{L}_{\text{SMEFT}} = \mathcal{L}_{\text{SM}} + \sum_i \frac{C_i}{\Lambda^2} Q_i. \quad (5.52)$$

Here, we neglect the lepton-number violating dimension-five Weinberg operator. The operators Q_i are of dimension six, constructed from SM fields, and respect the full SM gauge symmetry. Additional simplifying assumptions, such as baryon and lepton number conservation or minimal flavor violation (MFV), may also be imposed. Notably, the “traditional” SMEFT formulation does not account for the loop expansion. This constitutes a limitation that, as we will show, can lead to inconsistencies. We illustrate this with the example of SMEFT corrections to Higgs production via gluon fusion.

5.2.1. Example: Higgs Production via Gluon Fusion

To illustrate our reasoning, we examine the $\mathcal{O}(1/\Lambda^2)$ corrections to Higgs production via gluon fusion, which is the dominant Higgs production mechanism at the LHC. This process is loop-induced in the SM, with the top-quark loop providing the leading contribution (Fig. 5.2(a)). Fig. 5.2 (b)–(g) shows sample SMEFT diagrams with single insertions of dimension-six operators. The relevant operators (see Tabs. 3.1 and 3.2) are:

$$\begin{aligned} \text{(b)} : Q_{HG}, \quad \text{(c)} : Q_{uH}, \quad \text{(d)} : Q_{uG}, \quad \text{(e)} : Q_{uu}, Q_{qq}^{(1)}, Q_{qq}^{(3)}, Q_{qu}^{(1)}, Q_{qu}^{(8)}, \\ \text{(f)} : Q_H, Q_{H\Box}, \quad \text{(g)} : Q_G \end{aligned} \quad (5.53)$$

A consistent power-counting scheme should dictate which operators must be included at a given order in the $1/\Lambda^2$ expansion. Importantly, the diagrams shown span tree-level, one-loop, and two-loop topologies, and therefore differ in the number of explicit loop factors. This strongly suggests that loop-order counting should be incorporated into SMEFT power counting; just as it is in the SM, where perturbative expansions are organized in powers of loop factors or equivalently weak couplings. Fig. 5.2 (1)–(3) illustrates how the perturbative and the EFT expansion have to be combined to obtain radiative corrections to the leading diagrams.

One might naively attempt to include all contributions from dimension-six operators (i.e., all diagrams in Fig. 5.2 (b)–(g)) regardless of topology. This would imply treating the Wilson coefficients C_i as arbitrary dimensionless numbers that compensate the loop suppression. However, such an approach is unsatisfactory: it makes any consistent truncation of the EFT impossible, as dimension-eight or higher operators with large coefficients could

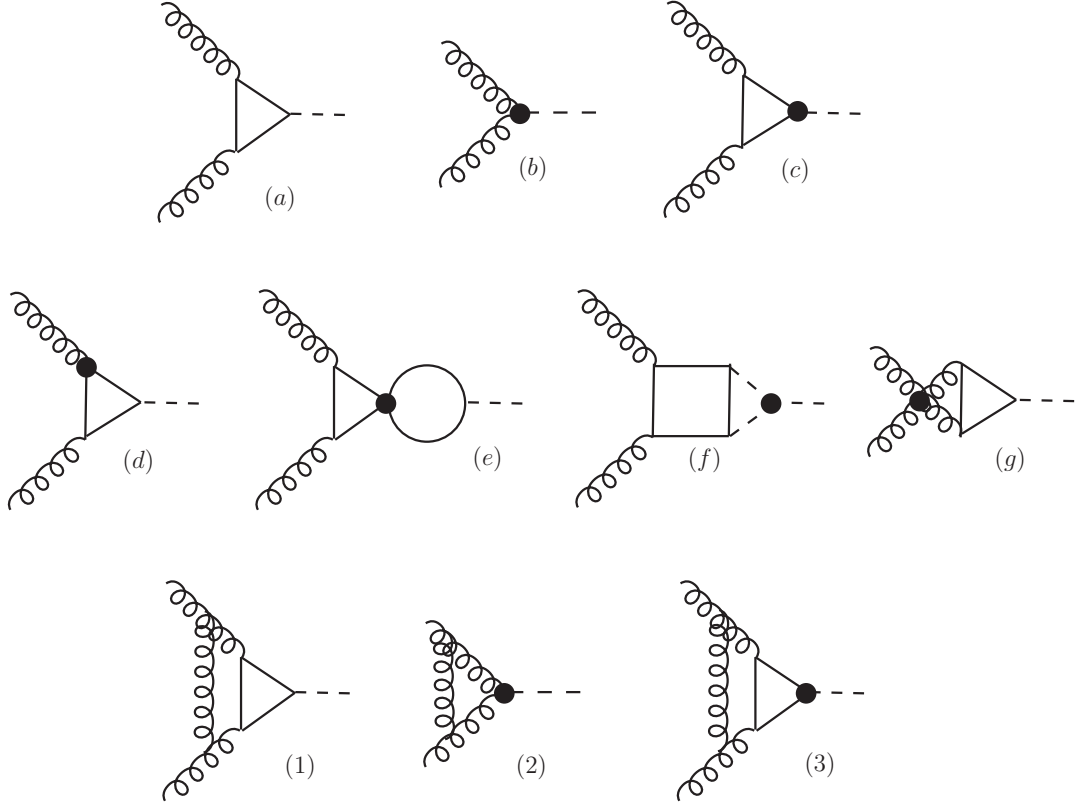


Figure 5.2.: Higgs production through gluon fusion. (a) SM amplitude at leading order (two diagrams with opposite fermion flows are understood). (b)–(g): Representative SMEFT diagrams with insertions of dimension-six operators (black dots). (1)–(3): Examples of radiative corrections.

generate effects of similar or even larger size. Without power-counting assumptions, the EFT expansion loses predictive power.

The standard SMEFT power-counting approach, based solely on canonical dimensions, assumes $C_i = \mathcal{O}(1)$, and considers only suppression by powers of Λ . In this scheme, diagram (e) in Fig. 5.2 would appear to be subleading relative to diagram (d), due solely to its loop topology. However, as shown in our previous toy model, such a classification fails to capture the effects of a heavy resonance (weakly or strongly) coupled to the top quark. For a framework intended to be model-independent, this is a serious shortcoming. Additionally, the same logic would suggest that diagram (b) provides the leading SMEFT correction to $gg \rightarrow h$, as it is the only tree-level diagram. Yet, this conclusion is at odds with common new-physics scenarios [136, 137], where corrections arise at loop level. We thus conclude that assuming $C_i = \mathcal{O}(1)$ is inadequate. A meaningful and consistent power-counting prescription must incorporate loop-order counting alongside the EFT expansion.

5.2.2. Power Counting in General EFTs

Before specializing to the SMEFT, we first review general power counting rules for relativistic EFTs. As noted in our previous discussion, it is essential to keep track of both the expansion in powers of E^2/Λ^2 and loop factors of $1/16\pi^2$. This can be systematically achieved by considering both the *canonical* and *chiral* dimensions of EFT operators. This framework, discussed in [111], is equivalent to well-known results in the literature on EFT power counting [82, 110, 138, 139].

We consider a general relativistic EFT of scalar fields φ , gauge fields A , and fermions ψ , valid at energies well below a cutoff scale Λ . It is convenient to define a reference energy scale

$$f \equiv \frac{\Lambda}{4\pi} \quad (5.54)$$

which is well within the domain of validity of the EFT ($f \ll \Lambda$). This scale allows us to treat the expansions in E^2/Λ^2 and $1/16\pi^2$ on an equal footing: at energies $E = f$, the energy expansion parameter becomes $f^2/\Lambda^2 = 1/16\pi^2$ equal to a loop factor.

We now estimate the size of the coefficient for a generic EFT operator of the form

$$\partial^{N_p} \varphi^{N_\varphi} A^{N_A} \psi^{N_\psi} \kappa^{N_\kappa} \quad (5.55)$$

involving N_p derivatives, N_φ scalar fields, N_A vector fields, N_ψ fermions, and N_κ insertions of weak couplings, denoted generically by κ .

To estimate the coefficient, both the canonical and chiral dimensions of the operator must be taken into account. Since the Lagrangian must have canonical dimension 4, dimensional analysis gives a factor f^{4-d_c} . Meanwhile, loop factors $1/16\pi^2$ are associated with loop order $L = (d_\chi - 2)/2$, where d_χ is the chiral dimension. The general form of the coefficient is therefore

$$C(d_c, d_\chi) = \frac{f^{4-d_c}}{(4\pi)^{d_\chi-2}} \quad (5.56)$$

For the operator above, the canonical and chiral dimensions are given by

$$d_c = N_p + N_\varphi + N_A + \frac{3}{2}N_\psi \quad (5.57)$$

$$d_\chi = N_p + \frac{1}{2}N_\psi + N_\kappa \quad (5.58)$$

These formulae are valid for general EFTs, regardless of whether the UV completion is weakly or strongly coupled. However, the interpretation of f differs in each case. In weakly coupled EFTs, $f \equiv \Lambda/4\pi$ serves primarily as a bookkeeping device. In strongly coupled theories, however, f acquires a physical meaning. For example, in chiral perturbation theory (ChPT), $f = f_\pi$ is the pion decay constant, related to the QCD scale via the NDA relation $\Lambda_{\text{QCD}} = 4\pi f_\pi$ [138].

Focusing now on the SMEFT, we may rewrite equation (5.56) in terms of the cutoff scale Λ as

$$C(d_c, d_\chi) = \frac{1}{\Lambda^{d_c-4}} \left(\frac{1}{16\pi^2} \right)^{(d_\chi-d_c)/2+1} \quad (5.59)$$

As expected, powers of Λ are determined by canonical dimension, while loop factors are governed by

$$\frac{2 + d_\chi - d_c}{2} = \frac{2 + N_\kappa - N_F}{2} \quad (5.60)$$

where we used equations (5.57) and (5.58), and introduced the total number of fields $N_F \equiv N_\varphi + N_A + N_\psi$. Thus, the number of loop factors is dictated by the difference between the chiral and canonical dimensions, or equivalently, by the difference between the number of weak couplings and the number of fields.

For dimension-6 operators, such as those in the Warsaw basis, this formula simplifies to

$$C(6, d_\chi) = \frac{1}{\Lambda^2} \left(\frac{1}{16\pi^2} \right)^{(d_\chi-4)/2} \quad (5.61)$$

To determine the expected size of an operator coefficient, knowledge of its chiral dimension (or equivalently, the number of weak couplings N_κ) is essential. Without this information, power counting remains incomplete. While the general formula 5.56 applies to both ChPT and SMEFT, the two differ in how weak couplings are assigned to fields and interactions. Therefore, any consistent power-counting prescription must specify which fields are weakly or strongly coupled to the heavy sector. Various assignment schemes can be considered, but such a classification is unavoidable. The exactly solvable model in [140] nicely illustrates this fact. The parametric size of the operator coefficients obtained from a weakly or strongly coupled heavy sector are consistent with the general power-counting rules. In the next section, we discuss the assignment of weak couplings to dimension-6 SMEFT operators.

5.2.3. Loop counting in SMEFT

Let us now consider the standard scenario underlying SMEFT. In this setting, SMEFT arises as the low-energy EFT valid at the electroweak scale, after integrating out the heavy degrees of freedom associated with a UV extension of the SM. These heavy fields are characterized by a scale $\Lambda \gg v$, where v is the electroweak scale. We assume a generic extension of the SM with new physics at the scale Λ , weakly coupled to the SM fields and describable by a renormalizable Lagrangian (in the traditional sense). Weak coupling implies that the characteristic mass scale of the heavy particles aligns with the cutoff scale Λ .

Of course, a weakly coupled UV sector is not a necessary assumption. As discussed in Sec. 3.4, if the Higgs sector is strongly coupled, the resulting EFT at the electroweak scale takes the form of an electroweak chiral Lagrangian (HEFT). A typical example is provided by composite Higgs models with a characteristic scale f . When expanded in the parameter v/f , such models yield a SILH-type version of SMEFT [141], as discussed in [135].

In the following, we focus on SMEFT under the assumption of a weakly coupled UV sector and aim to determine the minimal number of weak couplings associated with dimension-six operators. This classification enables us to distinguish operators that may be generated at tree level from those that necessarily arise at loop level. In part, we rederive the results of [142], employing the convenient formalism of chiral dimensions. A comprehensive classification of potentially tree- and loop-level generated operators up to canonical dimension

eight can be found in [143].

A generic UV theory of this type is a renormalizable QFT involving bosons (scalars and gauge bosons) and fermions. The field content includes the SM bosons b and fermions f , as well as new heavy bosons B and fermions F . Weak coupling implies that the SM fields f and b interact with the heavy fields F and B through coupling constants of order unity. In a renormalizable theory, only a limited set of interaction vertices is allowed. Denoting a generic fermion (boson) by $\Psi = f, F$ and $\beta = b, B$, the allowed interaction classes include: $\bar{\Psi}\Psi\beta, \beta^3, \beta^4$ and $\beta^2\partial\beta$.

We summarize the possible vertices involving both heavy and light fields in Table 5.1. For triple boson vertices the mass scale μ is required by dimensional analysis which may

$\bar{\Psi}\Psi\beta:$	$\bar{f}fB$	$\bar{f}Fb$	$\bar{F}fb$	$\bar{f}FB$	$\bar{F}fB$	$\bar{F}Fb$	$[\kappa]$
$\beta^3:$	b^2B	bB^2					$[\kappa\mu]$
$\beta^4:$	b^3B	b^2B^2	bB^3				$[\kappa^2]$
$\beta^2\partial\beta:$	$b\partial bB$	$B\partial Bb$					$[\kappa]$

Table 5.1.: Possible interaction vertices coupling heavy and light fields in a generic, renormalizable UV theory and the associated coupling

be taken as a heavy or light scale. In addition, there are vertices that consist only of heavy or light fields such as B^3 . For a given operator we need to determine the number of weak couplings N_κ . We use the notation $A \sim \kappa^n$ indicating that a building block A is associated with (at least) n powers of weak couplings. From Tab. 5.1 we can read off

$$b \sim \kappa, \quad b^2 \sim \kappa, \quad b\partial b \sim \kappa, \quad b^3 \sim \kappa^2 \quad (5.62)$$

For fermion bilinears we have to differentiate between scalar, vector and tensor currents. In a renormalizable theory only scalar and vector fermion currents are allowed. As a result, only those may come with a single weak coupling, tensor currents carry at least two factors of weak coupling

$$\bar{f}\Gamma f \sim \kappa, \quad \text{for } \Gamma = 1, \gamma^\mu \quad \bar{f}\sigma^{\mu\nu}f \sim \kappa^2 \quad (5.63)$$

The (minimal) number of weak-couplings for the various operator classes in the Warsaw basis is given by

$$\kappa^4(\phi^\dagger\phi)^3, \quad \kappa^2(\phi^\dagger D\phi)^2, \quad \kappa^3\phi^\dagger\phi\bar{\psi}\phi\psi, \quad \kappa^2(\phi^\dagger D\phi)\bar{\psi}\psi, \quad \kappa^2(\bar{\psi}\psi)^2 \quad (5.64)$$

The assignment of weak couplings can be understood by drawing sample diagrams in a generic UV theory with the vertices described in Tab. 5.1 that generate the operator classes after integrating out the heavy particle(s). Consider e.g. diagram (a) in Fig. 5.3 which consists of three vertices of type b^2B and one vertex B^3 . Integrating out the heavy boson gives, assuming $\mu \sim M$, the Wilson coefficient of an operator of the class $(\phi^\dagger\phi)^3$ would scale as

$$C_{(a)} \sim \kappa^4 \frac{\mu^4}{M^4} \frac{1}{M^2} \sim \kappa^4 \frac{1}{M^2} \quad (5.65)$$

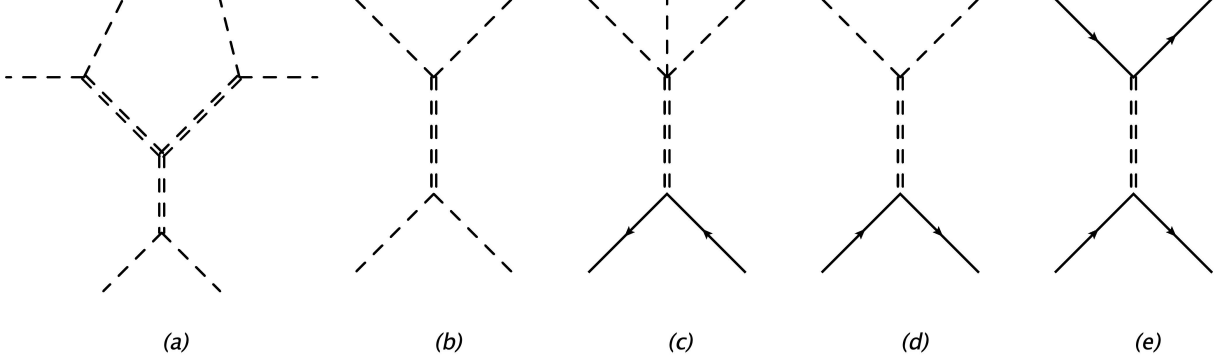


Figure 5.3.: Sample diagrams in a generic UV theory that generate the various operator classes after integrating out the heavy fields: (a): $\kappa^4(\phi^\dagger\phi)^3$, (b): $\kappa^2(\phi^\dagger D\phi)^2$, (c): $\kappa^3\phi^\dagger\phi\bar{\psi}\phi\psi$, (d): $\kappa^2(\phi^\dagger D\phi)\bar{\psi}\psi$, (e): $\kappa^2(\bar{\psi}\psi)^2$. The dashed double line denotes a generic heavy boson

The generalization to the other operator classes is straightforward. While the operators listed in (5.64) are potentially generated at tree level this is not the case for the operator classes with field strengths

$$\kappa^3 X_\mu^\nu X_\nu^\lambda X_\lambda^\mu, \quad \kappa^4 \phi^\dagger \phi X_{\mu\nu} X^{\mu\nu}, \quad \kappa^4 \bar{\psi} \sigma_{\mu\nu} \psi X^{\mu\nu} \phi \quad (5.66)$$

Those operators cannot be generated from tree-level diagrams in a renormalizable UV theory. Sample one-loop diagrams generating the classes in (5.64) are displayed in Fig. (5.66) Diagram (c) nicely illustrates that a fermionic tensor current comes with at least

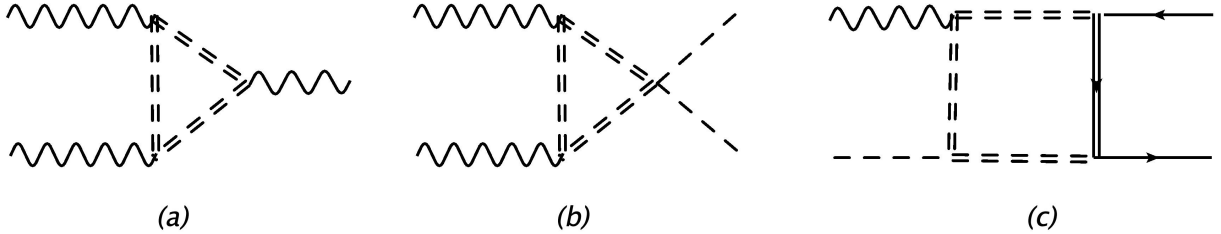


Figure 5.4.: The (dashed) double line denotes a generic heavy (boson) fermion

two factors of weak couplings since there is no vertex of type $B^2 f \bar{f}$ in a renormalizable UV theory.

It is now easy to read off the chiral dimensions of the various operator classes.

$$\begin{aligned} d_\chi[\kappa^4(\phi^\dagger\phi)^3] &= d_\chi[\kappa^2(\phi^\dagger D\phi)^2] = d_\chi[\kappa^3\phi^\dagger\phi\bar{\psi}\phi\psi] = d_\chi[\kappa^2(\phi^\dagger D\phi)\bar{\psi}\psi] = d_\chi[\kappa^2(\bar{\psi}\psi)^2] = 4 \\ d_\chi[\kappa^3 X_\mu^\nu X_\nu^\lambda X_\lambda^\mu] &= d_\chi[\kappa^4 \phi^\dagger \phi X_{\mu\nu} X^{\mu\nu}] = d_\chi[\kappa^4 \bar{\psi} \sigma_{\mu\nu} \psi X^{\mu\nu} \phi] = 6 \end{aligned} \quad (5.67)$$

Using the power-counting formula (5.61) this implies coefficients of order $1/\Lambda^2$ for the operators in (5.64) and coefficients of order $1/16\pi^2\Lambda^2$. Equivalently, assuming weak coupling to the heavy sector, all Warsaw basis operators with gauge field strength factors are additionally suppressed by a loop factor [24, 142].

Returning to our example process $gg \rightarrow h$ from Sec. 5.2.1 we can assign a clear ordering to the SMEFT contributions

$$\frac{1}{16\pi^2} : (a), \quad \frac{1}{16\pi^2\Lambda^2}, (b), (c), \quad \frac{1}{(16\pi^2)^2\Lambda^2} (d), (e), (f), \quad \frac{1}{(16\pi^2)^3\Lambda^2} (g) \quad (5.68)$$

The leading contribution comes from the SM in Fig. 5.2 (a) contains a loop factor but is unsuppressed in $1/\Lambda$. An additional factor of $1/\Lambda^2$ carry the SMEFT corrections in (b),(c). Diagram (b) is a tree level graph but the operator Q_{HG} carries an implicit loop factor while diagram (c) is a genuine one-loop graph. Similarly, (d) - (f) have the same power counting size despite their different topology. In accordance with our toy model the magnetic-moment type vertex in Fig. 5.2 (d) enters at the same order as the 4-fermion operators in Fig. 5.2 (e).

A power-counting prescription that incorporates both canonical and chiral dimensions enables a consistent truncation of the SMEFT expansion. For instance, if we aim to compute only the leading SMEFT corrections to the Standard Model, then only the diagrams shown in Fig. 5.2 (b) and (c) need to be considered, while the contributions from diagrams (d)–(f) can be systematically omitted. Radiative corrections to these leading SMEFT contributions, as illustrated in Fig. 5.2 (1)–(3), can also be consistently included within the same power-counting framework, up to the desired level of accuracy.

The power-counting scheme discussed here is broadly applicable to a wide range of high-energy collider processes and observables. It provides a systematic means of identifying potentially dominant SMEFT effects. Moreover, by enforcing a consistent truncation of subleading terms, the scheme helps reduce the number of free parameters in practical SMEFT analyses, thereby enhancing the interpretability and predictive power of the EFT framework.

Examples for the application of the power-counting scheme can be found in the literature. Single Higgs production in SMEFT has been studied in [117, 144–147]. Studies of Higgs-boson pair production at NLO and beyond include [148–156]. In [153] the systematic loop counting for SMEFT has already been discussed for the process under consideration. A systematic discussion of top-quark pair production via gluon in SMEFT has appeared in [157]. The pattern of SMEFT effects in $g \rightarrow hh$ or $h \rightarrow gg$ is similar in $h \rightarrow \gamma\gamma$ decay which has been treated in [158–160]. Zh production in pp collisions including SMEFT corrections was investigated in [161, 162]. A systematic study of $h \rightarrow gg$ and $h \rightarrow \gamma\gamma$ with anomalous HEFT couplings including NLO QCD effects has appeared in [163].

5.2.4. Amplitude for $gg \rightarrow h$ with leading dim 6 corrections in SMEFT

Having identified the leading dimension-six SMEFT corrections in Fig. 5.2 (b) and (c), we now present the explicit $gg \rightarrow h$ amplitude including these contributions as an illustrative example of a consistent application of SMEFT. The relevant operators for the process $gg \rightarrow h$ in the Warsaw basis (Table 3.1) are:

$$\mathcal{O}_{H\Box}, \mathcal{O}_{HD}, \mathcal{O}_{uH}, \mathcal{O}_{HG} \quad (5.69)$$

After performing the field redefinition to canonically normalize the Higgs kinetic term (3.43), the anomalous couplings relevant for Higgs boson production via gluon fusion can be parameterized by the interaction Lagrangian [153]:

$$\Delta\mathcal{L}_h = -m_t c_t \frac{h}{v} \bar{t}t + \frac{\alpha_s}{8\pi} c_{ggh} \frac{h}{v} G_{\mu\nu}^A G^{A\mu\nu} \quad (5.70)$$

The same interaction Lagrangian is also applicable in the HEFT framework, where the anomalous couplings c_t and c_{ggh} are $\mathcal{O}(1)$ parameters. In SMEFT, however, deviations

from the SM are assumed to be small. The relation between the anomalous Higgs couplings and the SMEFT coefficients in the Warsaw basis is given by:

$$c_t = 1 + \frac{v^2}{\Lambda^2} C_{H,\text{kin}} - \frac{v^3}{\sqrt{2} m_t \Lambda^2} C_{uH} \equiv 1 + \delta_{c_t}, \quad (5.71)$$

$$c_{ggh} = \frac{v^2}{\Lambda^2} \frac{8\pi}{\alpha_s} C_{HG} \quad (5.72)$$

Note that the deviations from the SM values are suppressed by powers of the new physics scale Λ . We observe that three Warsaw basis operators contribute to δ_{c_t} . While c_t and c_{ggh} are invariant under QCD renormalization, the SMEFT coefficients C_{uH} and C_{HG} are not [94, 96, 98]. Additionally, the operators $C_{H,\text{kin}}$, C_{uH} , and C_{HG} carry different chiral dimensions, $d_\chi = 2, 3$, and 4 respectively; that is, they are not homogeneous in d_χ . Nevertheless, under the assumption of a weakly coupled SMEFT power counting, both δ_{c_t} and c_{ggh} are effectively of chiral dimension $d_\chi = 2$. For a consistent EFT treatment, the amplitude involving vertices from $\Delta\mathcal{L}_h$ must be expanded to leading order in v^2/Λ^2 , with all higher-order terms discarded.

Numerically, the corrections from δ_{c_t} and c_{ggh} are expected to be small. For a representative value of $\Lambda = 3$ TeV, we obtain $v^2/\Lambda^2 \approx 7 \cdot 10^{-3}$, without yet accounting for further suppression due to weak couplings. Current global fits show that δ_{c_t} and c_{ggh} are still compatible with zero, indicating that current experimental precision is insufficient to detect these SMEFT effects rather than pointing to a need to include dimension-8 operators.

The amplitude for the process $g(k_1, \mu) + g(k_2, \nu) \rightarrow h(q)$ can be decomposed as:

$$\mathcal{M}^{AB} = \delta^{AB} \epsilon_\mu(k_1) \epsilon_\nu(k_2) \mathcal{M}^{\mu\nu} \quad (5.73)$$

$$\mathcal{M}^{\mu\nu} = \frac{\alpha_s}{8\pi v} \mathcal{F}_1 T^{\mu\nu} \quad (5.74)$$

where A, B are color indices, $\epsilon_\mu, \epsilon_\nu$ are gluon polarization vectors, and

$$T^{\mu\nu} = g^{\mu\nu} - \frac{k_1^\nu k_2^\mu}{k_1 \cdot k_2} \quad (5.75)$$

The form factor \mathcal{F}_1 is given by [164–167]:

$$\mathcal{F}_1 = 2q^2 \left\{ (1 + \delta_{c_t}) \tau_t \left[1 - (1 - \tau_t) \frac{f(\tau_t)}{4} \right] + c_{ggh} \right\} \quad (5.76)$$

where $\tau_t = 4m_t^2/q^2$ and $q^2 = 2k_1 \cdot k_2 = m_h^2$ for on-shell Higgs production. The loop function $f(\tau_t)$ is defined in (E.10).

In addition to the SMEFT corrections above, the amplitude also receives v^2/Λ^2 contributions from the operators $Q_{Hl}^{(3)}$ and Q_{ll}^{1221} , which modify the muon decay rate and thus the Fermi constant G_F used to determine v . Denoting G_F as the Fermi constant measured from muon decay and defining $G_{F0} = 1/(\sqrt{2}v^2)$, the relation is expressed as [160, 168]:

$$G_{F0} = G_F (1 - 2\delta_G) \quad (5.77)$$

with

$$2\delta_G = \frac{v^2}{\Lambda^2} \left(C_{Hl,1}^{(3)} + C_{Hl,2}^{(3)} - C_{1221}^{ll} \right) \quad (5.78)$$

where the numerical subscripts denote lepton generation indices.

Phenomenologically, the impact of this correction to (5.76) from first- and second-generation fermion operators is negligible, being constrained to well below the percent level [169]. Consequently, δ_{c_t} and c_{ggh} remain the leading SMEFT corrections to the $gg \rightarrow h$ process.

5.3. Heuristic approach to chiral dimensions

We rederive the chiral counting formula for SMEFT carefully differentiating between masses and scales. Here we follow the concept explained in [61]. Essentially, this concept can be derived when trying to restore the appropriate factors of \hbar in calculations. Factors of \hbar not only appear due to loops, they are also present in the propagator; this can be already seen in the Klein-Gordon equation of a real scalar field ϕ with explicit factors of \hbar and c

$$\frac{1}{c^2} \partial_t^2 \phi - \Delta \phi + \frac{m^2 c^2}{\hbar^2} \phi = 0 \quad (5.79)$$

Unlike in natural units we do not set $\hbar = 1$ but retain it in the following. Upon setting $c = 1$ we see that the mass parameters are conveniently written as $\tilde{m} = m/\hbar$. When retaining \hbar we distinguish between units of energy (E) and length (L). The quantities of interest for a canonically normalized 4d Lagrangian (\mathcal{L}) with scalars (φ), gauge bosons (A_μ) and fermions (ψ) including small couplings, which we collectively denote as κ have the following energy and length units

$$[\hbar] = E L, \quad [\mathcal{L}] = E L^{-3}, \quad [\varphi] = [A_\mu] = E^{1/2} L^{-1/2}, \quad [\psi] = E^{1/2} L^{-1} \quad (5.80)$$

$$[\partial] = [\tilde{m}] = L^{-1}, \quad [\kappa] = E^{-1/2} L^{-1/2} \quad (5.81)$$

Here gauge and Yukawa couplings are considered small couplings whereas quartic scalar couplings are of order κ^2 . The bottom line is that now not only masses are dimensionful quantities but couplings as well. We introduce the following convenient units of *mass* $\tilde{M} \equiv L^{-1}$ and *coupling* $C \equiv E^{-1/2} L^{-1/2}$.

We consider a generic EFT operator

$$\partial^{N_p} \varphi^{N_\varphi} A_\mu^{N_A} \psi^{N_\psi} \kappa^{N_\kappa} \quad (5.82)$$

with a certain number of fields (φ, A_μ, ψ), derivatives and weak couplings. The canonical dimension d_c and chiral dimension d_χ of this generic operator are given by

$$d_c = N_p + N_\varphi + N_A + \frac{3}{2} N_\psi \quad (5.83)$$

$$d_\chi = N_p + \frac{1}{2} N_\psi + N_\kappa \quad (5.84)$$

Our task is to estimate the size of the coefficient of this operator. From naive dimensional analysis our generic operator is suppressed by some mass $1/\Lambda^{d_c-4}$ and following general considerations by some power of the loop factor in four dimensions $1/16\pi^2$. Counting the loop factors amounts to counting the explicit factors of \hbar since every loop is proportional to $\hbar/16\pi^2$. Other factors of \hbar are taken care of by our choice of mass unit. We associate Λ in the SMEFT with the mass of some heavy particle that originates from expanding its propagator; thus $[\Lambda] = L^{-1}$. We may then write the generic operator including its coefficient as

$$\left(\frac{\hbar}{16\pi^2} \right)^x \frac{1}{\Lambda^{d_c-4}} \partial^{N_p} \varphi^{N_\varphi} A_\mu^{N_A} \psi^{N_\psi} \kappa^{N_\kappa} \quad (5.85)$$

To find x we just compute the length and energy dimension of the generic operator, which has to be equal to $[\mathcal{L}] = E L^{-3}$, i.e.

$$\left[\left(\frac{\hbar}{16\pi^2} \right)^x \frac{1}{\Lambda^{d_c-4}} \partial^{N_p} \varphi^{N_\varphi} A_\mu^{N_A} \psi^{N_\psi} \kappa^{N_\kappa} \right] = (EL)^x E^{(d_c-d_\chi)/2} L^{(d_c-d_\chi)/2-4} \stackrel{!}{=} E L^{-3} \quad (5.86)$$

where we used the relations

$$\begin{aligned} \left[\partial^{N_p} \varphi^{N_\varphi} A_\mu^{N_A} \psi^{N_\psi} \kappa^{N_\kappa} \right] &= E^{(N_\varphi+N_A+N_\psi-N_\kappa)/2} L^{-(2N_p+2N_\psi+N_\varphi+N_A+N_\kappa)/2} \\ &= E^{(d_c-d_\chi)/2} L^{-(d_\chi+d_c)/2} \end{aligned} \quad (5.87)$$

$$\left[\frac{1}{\Lambda^{d_c-4}} \right] = L^{d_c-4} \quad (5.88)$$

It is now easy to see that

$$x = \frac{d_\chi - d_c}{2} + 1 \quad (5.89)$$

In conclusion, we have rederived the known power counting formula for the SMEFT, which estimates the coefficient of an EFT operator $C(d_c, d_\chi)$ with canonical dimension d_c and chiral dimension d_χ

$$C(d_c, d_\chi) = \frac{1}{\Lambda^{d_c-4}} \left(\frac{1}{16\pi^2} \right)^{(d_\chi-d_c)/2+1} \quad (5.90)$$

5.4. Example for SMEFT in a UV Model: $u\bar{u} \rightarrow t\bar{t}$ via gluon exchange in the 2HDM

As discussed in the introductory chapters, it is well motivated to consider the SM Higgs sector as an effective description only and thus consider extensions of the scalar sector. See e.g. [170] for a comprehensive review of extended scalar sectors. Therefore, we employ a Two-Higgs-doublet model (2HDM) [170–172] as the UV completion of SMEFT. In contrast to the SM, this model (2HDM) contains not one, but two independent scalar SU(2) doublets. In this discussion we will not consider a general 2HDM model; for simplicity we consider a model where the scalar sector is CP-conserving and most importantly the model contains a CP-even neutral scalar h that is considerably lighter than a new physics scale $v \ll \Lambda_{2\text{HDM}}$ characterizing the masses of the additional 2HDM states. In other words, the model has a well-defined decoupling limit [172] and it is therefore possible to integrate out the states with masses of $\mathcal{O}(\Lambda_{2\text{HDM}})$. As is characteristic for a decoupling EFT all new physics effects vanish in the limit $\Lambda \rightarrow \infty$ and the SM Higgs sector is recovered.

5.4.1. 2HDM in the decoupling limit

Integrating out the scalars in this limit we match the 2HDM to SMEFT at the electroweak scale in terms of dimension six SMEFT operators.

The 2HDM scalar sector consists of two complex doublets Φ_1, Φ_2 in the fundamental representation of the weak gauge group $SU(2)$ with hypercharge $Y = 1/2$. The Lagrangian reads

$$\mathcal{L}_{2HDM} = D_\mu \Phi_n^\dagger D^\mu \Phi_n - V_{2HDM} \quad (5.91)$$

The potential for a generic 2HDM model is the most general potential consistent with the symmetries

$$\begin{aligned} V_{2HDM} = & m_{11}^2 \Phi_1^\dagger \Phi_1 + m_{22}^2 \Phi_2^\dagger \Phi_2 - \left[m_{12}^2 \Phi_1^\dagger \Phi_2 + \text{h.c.} \right] + \frac{1}{2} \lambda_1 \left(\Phi_1^\dagger \Phi_1 \right)^2 + \frac{1}{2} \lambda_2 \left(\Phi_2^\dagger \Phi_2 \right)^2 \\ & + \lambda_3 \left(\Phi_1^\dagger \Phi_1 \right) \left(\Phi_2^\dagger \Phi_2 \right) + \lambda_4 \left(\Phi_1^\dagger \Phi_2 \right) \left(\Phi_2^\dagger \Phi_1 \right) \\ & + \left\{ \frac{1}{2} \lambda_5 \left(\Phi_1^\dagger \Phi_2 \right)^2 + \left[\lambda_6 \left(\Phi_1^\dagger \Phi_1 \right) + \lambda_7 \left(\Phi_2^\dagger \Phi_2 \right) \right] \left(\Phi_1^\dagger \Phi_2 \right) + \text{h.c.} \right\} \end{aligned} \quad (5.92)$$

The coefficients λ_5, λ_6 and λ_7 can be complex in principle. However, we take all coefficients λ_i to be real to exclude any explicit CP violating effects in the Higgs sector. In addition, the λ_i have to satisfy several conditions for the potential to be bounded from below, see e.g. [172]. Furthermore, we assume that the mass matrix m_{ij}^2 has at least one negative eigenvalue so that spontaneous symmetry breaking occurs. Hence, the two Higgs doublets obtain vacuum expectation values

$$\langle \Phi_1 \rangle = \frac{1}{\sqrt{2}} \begin{pmatrix} 0 \\ v_1 \end{pmatrix}, \quad \langle \Phi_2 \rangle = \frac{1}{\sqrt{2}} \begin{pmatrix} 0 \\ v_2 \end{pmatrix}, \quad (5.93)$$

where we can always choose the phases of the doublets such that v_1 and v_2 are positive.

Determining the spectrum and masses

Minimizing the potential we arrive at the following conditions

$$m_{11}^2 = m_{12}^2 t_\beta - \frac{1}{2} v^2 \left[\lambda_1 c_\beta^2 + \lambda_{345} s_\beta^2 + 3 \lambda_6 s_\beta c_\beta + \lambda_7 s_\beta^2 t_\beta \right] \quad (5.94)$$

$$m_{22}^2 = m_{12}^2 t_\beta^{-1} - \frac{1}{2} v^2 \left[\lambda_2 s_\beta^2 + \lambda_{345} c_\beta^2 + \lambda_6 c_\beta^2 t_\beta^{-1} + 3 \lambda_7 s_\beta c_\beta \right], \quad (5.95)$$

allowing us to eliminate the parameters m_{11}^2 and Here we defined

$$\lambda_{345} = \lambda_3 + \lambda_4 + \lambda_5, \quad v^2 = v_1^2 + v_2^2 = (246 \text{ GeV})^2 \quad (5.96)$$

and the mixing angle β

$$t_\beta \equiv \tan \beta \equiv \frac{v_2}{v_1}, \quad s_\beta \equiv \sin \beta \equiv \frac{v_2}{\sqrt{v_1^2 + v_2^2}}, \quad c_\beta \equiv \cos \beta \equiv \frac{v_1}{\sqrt{v_1^2 + v_2^2}} \quad (5.97)$$

The mixing angle β is one of the most important realizations of any 2HDM model. Expanding around the expectation values, it becomes clear that a rotation by β diagonalizes the mass matrices of two neutral pseudoscalar degrees of freedom and the two charged scalar fields. The two Higgs doublets contain in total eight degrees of freedom. Out of those eight, three are identified as Goldstone bosons (G^\pm and G^0) which are absorbed by

the W^\pm and Z bosons. The five remaining particles are two neutral scalars h and H^0 with $m_h \leq M_{H^0} \equiv M_0$. There remains a pseudoscalar A and a charged scalar H^\pm . Expanding around the vacuum expectation values, a rotation by the mixing angle β diagonalizes the mass matrix of the pseudoscalar and charged scalar degrees of freedom. Their masses are given by

$$M_A^2 = \frac{m_{12}^2}{s_\beta c_\beta} - \frac{v^2}{2} (2\lambda_5 + t_\beta^{-1}\lambda_6 + t_\beta\lambda_7) \quad (5.98)$$

$$M_{H^\pm}^2 \equiv M_H^2 = M_A^2 + \frac{v^2}{2} (\lambda_5 - \lambda_4) \quad (5.99)$$

The remaining two neutral scalar degrees of freedom mix according to the following mass matrix

$$\mathcal{M}^2 \equiv M_A^2 \begin{pmatrix} s_\beta^2 & -s_\beta c_\beta \\ -s_\beta c_\beta & c_\beta^2 \end{pmatrix} + \mathcal{B}^2 \quad (5.100)$$

with

$$\mathcal{B}^2 \equiv v^2 \begin{pmatrix} \lambda_1 c_\beta^2 + 2\lambda_6 s_\beta c_\beta + \lambda_5 s_\beta^2 & (\lambda_3 + \lambda_4)s_\beta c_\beta + \lambda_6 c_\beta^2 + \lambda_7 s_\beta^2 \\ (\lambda_3 + \lambda_4)s_\beta c_\beta + \lambda_6 c_\beta^2 + \lambda_7 s_\beta^2 & \lambda_2 s_\beta^2 + 2\lambda_7 s_\beta c_\beta + \lambda_5 c_\beta^2 \end{pmatrix}. \quad (5.101)$$

To diagonalize \mathcal{M}^2 a second mixing angle is introduced. It is defined via the relation

$$\begin{pmatrix} M_0^2 & 0 \\ 0 & m_h^2 \end{pmatrix} = \begin{pmatrix} c_\alpha & s_\alpha \\ -s_\alpha & c_\alpha \end{pmatrix} \begin{pmatrix} \mathcal{M}_{11}^2 & \mathcal{M}_{12}^2 \\ \mathcal{M}_{12}^2 & \mathcal{M}_{22}^2 \end{pmatrix} \begin{pmatrix} c_\alpha & -s_\alpha \\ s_\alpha & c_\alpha \end{pmatrix} \quad (5.102)$$

and demanding $M_0 \geq m_h$. The explicit expression for α and the masses M_0, m_h are given in Appendix B.

The two Higgs doublets written in terms of physical states and Goldstone bosons take the form

$$\Phi_1 = \begin{pmatrix} c_\beta G^+ - s_\beta H^+ \\ \frac{1}{\sqrt{2}} [v_1 + c_\alpha H - s_\alpha h + i c_\beta G - i s_\beta A] \end{pmatrix} \quad (5.103)$$

$$\Phi_2 = \begin{pmatrix} s_\beta G^+ + c_\beta H^+ \\ \frac{1}{\sqrt{2}} [v_2 + s_\alpha H + c_\alpha h + i s_\beta G + i c_\beta A] \end{pmatrix} \quad (5.104)$$

Higgs basis

For matching calculations to SMEFT, it is more convenient to work with a different basis of Higgs doublets where only one doublet picks up a vacuum expectation value and all the heavy fields are contained in one doublet in the alignment limit. This is realized in the *Higgs basis* [173], which is just a rotation by the mixing angle β

$$\begin{pmatrix} H_1 \\ H_2 \end{pmatrix} = \begin{pmatrix} c_\beta & s_\beta \\ -s_\beta & c_\beta \end{pmatrix} \begin{pmatrix} \Phi_1 \\ \Phi_2 \end{pmatrix}. \quad (5.105)$$

H_1 and H_2 have the explicit form

$$H_1 = \begin{pmatrix} G^+ \\ \frac{1}{\sqrt{2}} [v + c_{\beta-\alpha}H + s_{\beta-\alpha}h + iG^0] \end{pmatrix} \quad (5.106)$$

$$H_2 = \begin{pmatrix} H^+ \\ \frac{1}{\sqrt{2}} [-s_{\beta-\alpha}H + c_{\beta-\alpha}h + iA] \end{pmatrix}. \quad (5.107)$$

We see explicitly that only H_1 has a non-zero vacuum expectation value. Taking the limit $c_{\beta-\alpha} \rightarrow 0$ and $s_{\beta-\alpha} \rightarrow 1$ H_1 is identical to the SM Higgs-doublet whereas all the heavy degrees of freedom are contained in H_2 .

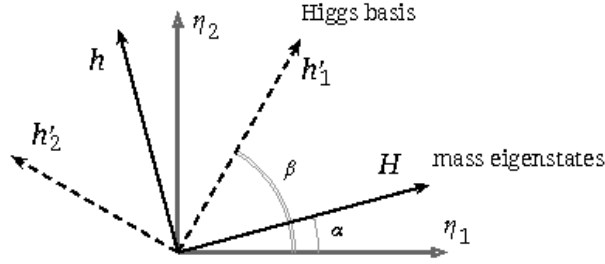


Figure 5.5.: Three bases for the neutral scalar degrees of freedom taken from [170]

Scalar quark couplings

The 2HDM Higgs couplings to fermions are model dependent. The most general Yukawa Lagrangian (this is usually referred to as type III) reads

$$-\mathcal{L}_Y = \bar{q}_L \tilde{\Phi}_1 Y_{u,1} u_R + \bar{q}_L \Phi_1 Y_{d,1} d_R + \bar{q}_L \tilde{\Phi}_2 Y_{u,2} u_R + \bar{q}_L \Phi_2 Y_{d,2} d_R + \text{h.c.} \quad (5.108)$$

with $\tilde{\Phi}_i \equiv i\sigma_2 \Phi_i^*$. Here $Y_{u,1}, Y_{u,2}, Y_{d,1}, Y_{d,2}$ are the Yukawa couplings in flavor space. We will not work with the most general type-III model. Rather, we restrict ourselves to a type II model, where $Y_{u,1} = Y_{d,2} = 0$, i.e.

$$-\mathcal{L}_Y = \bar{q}_L \Phi_1 Y_{d,1} d_R + \bar{q}_L \tilde{\Phi}_2 Y_{u,2} u_R + \text{h.c.} \quad (5.109)$$

In a type-II model, the neutral member of one Higgs doublet couples the up-type quarks, whereas the neutral member of the other Higgs doublet couples to down-type quarks. This has the advantage that flavor-changing neutral currents (FCNCs) mediated by Higgs bosons are automatically absent [174, 175]. For instance, a type-II 2HDM model is realized in the Higgs sector of the MSSM [176]. Rewriting (5.109) in the Higgs basis, we arrive at

$$-\mathcal{L}_Y = c_\beta \bar{q}_L H_1 Y_{d,1} d_R - s_\beta \bar{q}_L H_2 Y_{d,1} d_R + s_\beta \bar{q}_L \tilde{H}_1 Y_{u,2} u_R + c_\beta \bar{q}_L \tilde{H}_2 Y_{u,2} u_R + \text{h.c.} \quad (5.110)$$

The terms proportional to H_1 and \tilde{H}_1 are the usual SM Higgs couplings, which include the fermion mass terms if we replace H_1 by the Higgs vacuum expectation value v .

$$\eta_i^U \equiv V_L^U \eta_i^{U,0} V_R^{U\dagger}, \quad \eta_i^D \equiv V_L^D \eta_i^{D,0} V_R^{D\dagger} \quad (5.111)$$

$$M_D = \frac{1}{\sqrt{2}}v_1\eta_1^D, \quad M_U = \frac{1}{\sqrt{2}}v_2\eta_2^D \quad (5.112)$$

Integrating out the heavy Higgs doublet H_2 at tree-level produces the effective operators

$$\mathcal{L}_{4ferm} = \frac{t_\beta^{-2}}{M_S^2} \bar{u}_R Y_{u,2} q_L \bar{q}_L Y_{u,2} u_R + \frac{t_\beta^2}{M_S^2} \bar{d}_R Y_{d,1} q_L \bar{q}_L Y_{d,1} d_R \quad (5.113)$$

Using the Fierz identity

$$\bar{A}_R D_L \bar{C}_L B_R = -\frac{1}{2} \bar{A}_R \gamma^\mu B_R \bar{C}_L \gamma_\mu D_L \quad (5.114)$$

we arrive at

$$\mathcal{L}_{4ferm} = -\frac{1}{2} \frac{t_\beta^{-2} m_u^2}{M_S^2 v^2} \bar{u}_R \gamma_\mu u_R \bar{q}_L \gamma^\mu q_L - \frac{1}{2} \frac{t_\beta^2 m_d^2}{M_S^2 v^2} \bar{d}_R \gamma_\mu d_R \bar{q}_L \gamma^\mu q_L \quad (5.115)$$

Alignment and decoupling limit

Since our goal is to write down a low-energy EFT consisting of the Warsaw basis dimension six operators, we have to investigate the proper limits in which the light Higgs h has identical couplings to the SM Higgs h_{SM} and the heavy 2HDM degrees of freedom (H^0, A, H^\pm) become infinitely heavy and thus decouple.

The first condition can be achieved by taking the *alignment limit*, which is defined by $c_{\beta-\alpha} \rightarrow 0$ resp. $s_{\beta-\alpha} \rightarrow 1$. Since the couplings of h to vector boson pairs are identical to those of h_{SM} times $s_{\beta-\alpha}$, h has the same couplings as h_{SM} . Closely related to the alignment limit is the *decoupling limit*.

Taking the decoupling limit amounts to integrating out one of the Higgs doublets so that the resulting low-energy effective theory is the SM Higgs sector with one weak hypercharge $Y = 1/2$ scalar doublet. The limit is formally defined as the limit in which $M_A^2 \gg |\lambda_i|v^2$. At the same time the coupling constants λ_i in (5.92) are held fixed so that $|\lambda_i| \lesssim \mathcal{O}(1)$ and the λ_i stay small enough so that the theory remains weakly coupled, i.e. $|\alpha_i| = \frac{|\lambda_i|}{4\pi} \lesssim 1$. The parameters defined in (B.22) help us to define the relevant mass scales. It is easy to see that the masses of the H, A and H^\pm are of $\mathcal{O}(M_S)$. More precisely [172]

$$m_h = \mathcal{O}(v) \quad (5.116)$$

$$M_0, M_A, M_H = M_S + \mathcal{O}\left(\frac{v^2}{M_S}\right). \quad (5.117)$$

The hierarchy of energy scales is easily seen as $v \ll M_S$ and we integrate out all the particles of $\mathcal{O}(M_S)$. The connection to the alignment limit is given by the relation

$$\cos(\beta - \alpha) = \mathcal{O}\left(\frac{v^2}{M_S^2}\right) \quad (5.118)$$

Therefore, the decoupling limit automatically implies the alignment limit. It should be stressed, however, that the converse is not true in general. If $|\lambda_i|v^2 \geq M_A^2$, then we speak of *alignment without decoupling*.

5.4.2. Top-Down EFT

Similar to the toy model of Sec. 5.1, we analyze the process $u(k_1)\bar{u}(k_2) \rightarrow t(p_1)\bar{t}(p_2)$ via s-channel gluon exchange. The relevant diagrams are the same as in the toy model in Fig. 5.1 with the internal photon replaced by a gluon. We take only the top quark as massive, which implies that $Y_t = \sqrt{2}m_t \csc \beta/v$ is the only non-vanishing Yukawa coupling matrix element and that the heavy states couple exclusively to third-generation quarks. Defining $g \equiv m_t \cot \beta/v$, the relevant interaction Lagrangian is given by

$$\mathcal{L}_{int} = g\bar{t}tH + g\bar{t}i\gamma_5 tA + \sqrt{2}g\bar{t}_L b_R H^+ + \text{h.c.} \quad (5.119)$$

where t and b are the Dirac fields of the top- and bottom quarks with $t_{R/L} = P_{R/L}t$, etc. and $P_{R/L}$ the right- or left-handed projector, respectively. With the notation of Sec. 5.1, the correction to the amplitude can be written as

$$\delta\mathcal{A} = i\frac{g_s^2}{q^2}\bar{v}(k_2)\gamma_\mu T^A u(k_1)\bar{u}(p_1)\delta\Gamma^\mu T^A v(p_2) \quad (5.120)$$

where $T^A = \lambda^A/2$ are the generators of SU(3) with λ^A the Gell-Mann matrices and g_s is the QCD coupling constant. Here and in the following, we strictly work at order g_s^2 and subsequently drop terms of higher order without further comments.

The relevant diagrams are displayed in Fig. 5.6. Summing up all three contributions, we

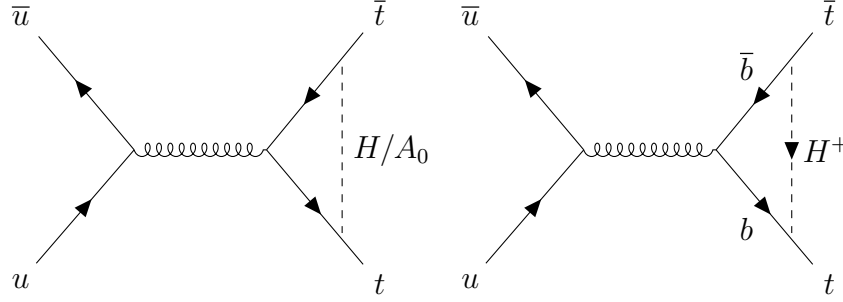


Figure 5.6.: One loop diagram for $u(k_1)\bar{u}(k_2) \rightarrow t(p_1)\bar{t}(p_2)$ with one loop correction due to heavy 2HDM states to the top quark vertex function

end up with

$$\delta\Gamma^\mu = \frac{g^2}{16\pi^2} \frac{1}{M_S^2} \left[m_t i\sigma^{\mu\nu} q_\nu + \left(\frac{2}{9} - \frac{2}{3} \ln \frac{q^2}{M_S^2} + i\frac{2\pi}{3} \right) q^2 \gamma^\mu P_R - \left(\frac{2}{3} \ln \frac{m_t^2}{M_S^2} + \frac{8}{9} + 2h_1(z) \right) q^2 \gamma^\mu \right] \quad (5.121)$$

where on-shell renormalization of the t -quark has been employed as in [177] and we expanded to first order in $1/M_S^2$. Pure gauge terms proportional to q^μ have been dropped as they cannot be represented by gauge invariant local operators and do not contribute to physical processes.

Expression (5.121) can be reproduced by an effective field theory specified by the Lagrangian

$$\mathcal{L}_{eff} = \mathcal{L}_{eff}^{tree} + \mathcal{L}_{eff}^{loop} = \sum_{i=1}^4 \frac{C_i}{M_S^2} Q_i \quad (5.122)$$

where

$$\mathcal{L}_{eff}^{tree} = \frac{C_1}{M_S^2} \bar{t}_R q_L \bar{q}_L t_R \quad (5.123)$$

arises when the heavy fields are integrated out at tree level with $C_1 = 2g^2$ and

$$\mathcal{L}_{eff}^{loop} = \frac{C_2}{M_S^2} D^\mu G_{\mu\nu}^A \bar{t} T^A \gamma^\nu P_R t + \frac{C_3}{M_S^2} D^\mu G_{\mu\nu}^A \bar{t} T^A \gamma^\nu t + \frac{C_4}{M_S^2} m_t G_{\mu\nu}^A \bar{t} T^A \sigma^{\mu\nu} t \quad (5.124)$$

is generated at one loop, where $G_{\mu\nu}^A$ is the gluonic field strength tensor and q_L the left-handed third generation quark doublet. The loop diagram associated with \mathcal{L}_{eff}^{tree} is displayed in Fig. 5.1 (e) and gives

$$\delta\Gamma_{Q_1}^\mu = \frac{C_1}{16\pi^2 M_S^2} \left[\left(\frac{5}{9} - \frac{1}{3} \ln \frac{q^2}{\mu^2} + i\frac{\pi}{3} \right) q^2 \gamma^\mu P_R - \left(\frac{1}{3} \ln \frac{m_t^2}{\mu^2} + h_1(z) \right) q^2 \gamma^\mu \right] \quad (5.125)$$

and the tree-contributions from \mathcal{L}_{eff}^{loop} in Fig. 5.1 (d) read

$$\delta\Gamma_{Q_{2-4}}^\mu = \frac{1}{g_s} \left[\frac{C_2}{M_S^2} q^2 \gamma^\mu P_R + \frac{C_3}{M_S^2} q^2 \gamma^\mu - \frac{2C_4}{M_S^2} m_t i \sigma^{\mu\nu} q_\nu \right] \quad (5.126)$$

Performing the matching procedure reveals that the coefficients are given by

$$C_1 = 2g^2, \quad C_2 = C_3 = -\frac{g_s g^2}{16\pi^2} \left(\frac{2}{3} \ln \frac{\mu^2}{M_S^2} + \frac{8}{9} \right), \quad C_4 = -\frac{g_s g^2}{16\pi^2} \frac{1}{2} \quad (5.127)$$

As before, the artificial dependence on μ cancels when both contributions are added and the full result is restored.

Note that the four effective operators we found in (5.122) - (5.124) can be matched to the Warsaw basis [24] by virtue of Fierz identities and the equations of motion for the gluons. Dropping terms that do not contribute to the process at hand, the relevant expressions are given by

$$Q_1 \longrightarrow - \left(Q_{qu}^{(8)3333} + \frac{1}{6} Q_{qu}^{(1)3333} \right) \quad (5.128)$$

$$Q_2 \longrightarrow g_s \left(Q_{qu}^{(8)1133} + \frac{1}{2} Q_{uu}^{1331} - \frac{1}{6} Q_{uu}^{1133} \right) \quad (5.129)$$

$$Q_3 \longrightarrow g_s \left(Q_{qu}^{(8)3311} + Q_{qu}^{(8)1133} + \frac{1}{2} Q_{uu}^{1331} - \frac{1}{6} Q_{uu}^{1133} + \frac{1}{4} Q_{qq}^{(3)1331} + \frac{1}{4} Q_{qq}^{(1)1331} - \frac{1}{6} Q_{qq}^{(1)1133} \right) \quad (5.130)$$

$$Q_4 \longrightarrow \frac{\sqrt{2}m_t}{v} (Q_{uG}^{33} + Q_{uG}^{*33}) \quad (5.131)$$

Note that in the Warsaw basis, the operators Q_2 and Q_3 introduce an extra factor of g_s . This has to be so, as treating the four-fermion operators introduced in this manner on the same footing as Q_1 would spoil the underlying systematic expansion in g_s . This is analogous to (5.28) in the toy model. It is now straight forward to identify the relevant Wilson coefficients of the Warsaw basis operators to order g_s^2 for the process at hand. The explicit expressions are given below.

5.4.3. Bottom-Up SMEFT calculation

Without referring to the UV model, we could have started with a new-physics scale Λ and the complete set of Warsaw basis operators that are relevant for the process under consideration. We have to distinguish between four-fermion contributions entering at tree or one-loop level, respectively. We display the contributions in Fig. 5.7.

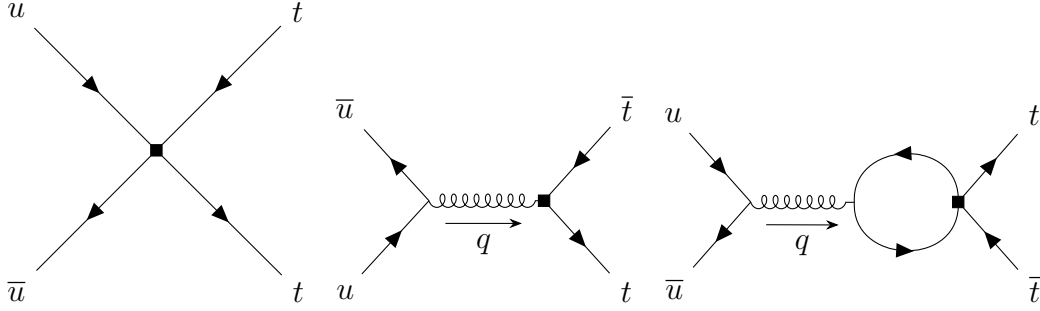


Figure 5.7.: Contributions needed to reproduce the $1/M^2$ correction to the full theory within the EFT. The black square represents the insertion of a SMEFT dimension 6 operator.

The tree contribution is given by the plain four-fermion vertex (here $\bar{v} = \bar{v}(k_2), u = u(k_1), \bar{u} = \bar{u}(p_1)$ and $v = v(p_2)$)

$$\begin{aligned} \delta\mathcal{A}_{tree} = & \frac{i}{\Lambda^2} \left(2 \left(C_{(qq)}^{(1)1133} + C_{(qq)}^{(3)1133} \right) \bar{v}\gamma_\mu P_L u \bar{u}\gamma^\mu P_L v \right. \\ & - 2 \left(C_{qq}^{(1)1331} + C_{qq}^{(3)1331} \right) \bar{v}\gamma_\mu P_L v \bar{u}\gamma^\mu P_L u \\ & + 2C_{uu}^{1133} \bar{v}\gamma_\mu P_R u \bar{u}\gamma^\mu P_R v - 2C_{uu}^{1331} \bar{v}\gamma_\mu P_R v \bar{u}\gamma^\mu P_R u \\ & + C_{qu}^{(1)1133} \bar{v}\gamma_\mu P_L u \bar{u}\gamma^\mu P_R v + C_{qu}^{(1)3311} \bar{v}\gamma_\mu P_R u \bar{u}\gamma^\mu P_L v \\ & - C_{qu}^{(1)1331} \bar{v}\gamma_\mu P_L v \bar{u}\gamma^\mu P_R u - C_{qu}^{(1)3113} \bar{v}\gamma_\mu P_R v \bar{u}\gamma^\mu P_L u \\ & + C_{qu}^{(8)1133} \bar{v}T^A \gamma_\mu P_L u \bar{u}T^A \gamma^\mu P_R v + C_{qu}^{(8)3311} \bar{v}T^A \gamma_\mu P_R u \bar{u}T^A \gamma^\mu P_L v \\ & \left. - C_{qu}^{(8)1331} \bar{v}T^A \gamma_\mu P_L v \bar{u}T^A \gamma^\mu P_R u - C_{qu}^{(8)3113} \bar{v}T^A \gamma_\mu P_R v \bar{u}T^A \gamma^\mu P_L u \right) \end{aligned}$$

whereas the one-loop contribution yields

$$\delta\Gamma_{loop}^\mu = -\frac{1}{16\pi^2\Lambda^2} (q^2 \gamma^\mu F_1 + m_t i \sigma^{\mu\nu} q_\nu F_2) \quad (5.132)$$

with

$$\begin{aligned} F_1 = & \left(\frac{5}{9} - \frac{1}{3} \ln \frac{q^2}{\mu^2} + i \frac{\pi}{3} \right) \left(\left(C_{ud}^{(8)3333} + C_{qu}^{(8)3333} \right) P_R + \left(C_{qd}^{(8)3333} + 8C_{qq}^{(3)3333} \right) P_L \right) \\ & - \left(\frac{1}{3} \ln \frac{m_t^2}{\mu^2} + h_1(z) \right) \left(C_{qu}^{(8)3333} + 4 \left(C_{qq}^{(1)3333} + C_{qq}^{(3)3333} \right) P_L + 4C_{uu}^{3333} P_R \right) \\ & - \frac{4}{3} \left(\left(C_{qq}^{(1)3333} + 3C_{qq}^{(3)3333} \right) P_L + C_{uu}^{3333} P_R \right) \end{aligned}$$

$$F_2 = 2 \left(C_{qu}^{(1)3333} - \frac{1}{6} C_{qu}^{(8)3333} \right) \quad (5.133)$$

In addition, the chromomagnetic operator enters at tree-level as before. Its contribution is given by

$$\delta\Gamma_{uG}^\mu = -\frac{\sqrt{2}v}{g_s\Lambda^2} i\sigma^{\mu\nu} q_\nu (C_{uG}^{*33} P_L + C_{uG}^{33} P_R) \quad (5.134)$$

Note that we have implicitly assumed the new physics sector to couple to the third particle generation only as we neglected generation mixing four-fermion operators in the one-loop contribution. For a comparison to the previous section, it is advantageous to rewrite the four-fermion tree contribution by virtue of Fierz identities like $\bar{v}(k_2)\gamma_\mu P_L v(p_2)\bar{u}(p_1)\gamma^\mu P_L u(k_1) = -\bar{v}(k_2)\gamma_\mu P_L u(k_1)\bar{u}(p_1)\gamma^\mu P_L v(p_2)$ and $2T_{ab}^A T_{cd}^A = \delta_{ad}\delta_{bc} - \delta_{ab}\delta_{cd}/3$.

Comparing (5.132) - (5.134) with the top-down result in Sec. 5.4.2 reveals that when identifying Λ with M_S , the non-vanishing SMEFT Wilson coefficients are given by

$$C_{qu}^{(8)3333} = 6C_{qu}^{(1)3333} = -2g^2 \quad (5.135)$$

$$\begin{aligned} C_{uu}^{1331} &= -3C_{uu}^{1133} = C_{qu}^{(8)3311} = \frac{1}{2}C_{qu}^{(8)1133} = 4C_{qq}^{(3)1331} = -6C_{qq}^{(1)1133} = 4C_{qq}^{(1)1331} \\ &= -\frac{g_s^2 g^2}{16\pi^2} \left(\frac{2}{3} \ln \frac{\mu^2}{M_S^2} + \frac{8}{9} \right) \end{aligned} \quad (5.136)$$

$$C_{uG}^{33} = C_{uG}^{*33} = -\frac{g_s g^2 m_t}{16\pi^2 v} \frac{1}{\sqrt{2}} \quad (5.137)$$

The μ -dependence matches the known results for the renormalization-group equations in SMEFT [94–98].

5.5. Discussion

A consistent power-counting scheme is indispensable when working with an EFT to control the EFT expansion. While EFT methods for physics beyond the SM aim to be as general as possible, a set of minimal assumptions about the relationship between low- and high-energy physics needs to be specified. The coupling strength between heavy and light fields directly influences the power counting. For the SMEFT, assuming a weakly coupled heavy sector, this implies counting both canonical dimensions and loop orders.

In this chapter, we discussed several examples to illustrate the drawbacks of considering only canonical dimensions. First, we illustrated this thesis by using a toy model involving a heavy scalar singlet. Here, we compared by explicit calculation the full theory with a bottom-up and top-down EFT treatment. We saw there that treating the EFT operator coefficients as $\mathcal{O}(1)$ numbers fails to reproduce the full theory result. As the new physics effects of the toy model are fairly generic, a bottom-up EFT should be able to reproduce such a scenario. Furthermore, we have discussed general power-counting rules and showed how the notion of chiral dimensions can be used to count loop orders. We provide explicit examples for SMEFT corrections to Higgs production in gluon fusion and a calculation matching a two-Higgs doublet to the SMEFT as applications of the proposed power-counting scheme.

Weakening the assumption of a weakly coupled UV sector, it is, of course, possible to construct alternative power-counting schemes. However, the underlying presumptions and counting rules must, in any case, be stated and consistently applied. For example, in the case of a strongly coupled Higgs sector, SMEFT may be replaced by HEFT, which follows a different power counting (see Sec 3.4.2). Finally, assumptions about the flavor structures, such as Minimal Flavor Violation (MFV), are, of course, permissible but should not be considered power-counting assumptions and should thus be treated as separate topics.

6. Linear Sigma Model: Nondecoupling EFT

Our aim in this chapter is to illustrate features of nonlinear EFTs and, in particular, to investigate the relation between the EFT expansion in inverse mass powers and the loop expansion. To that end, we take a simple $SO(4)$ symmetric linear σ -model and integrate out the massive degree of freedom. The Higgs Lagrangian in the SM is a realization of a $SU(2) \times U(1)$ gauged linear σ -model. This toy model serves as a simple yet instructive example for illustrating the transition from a linear to a nonlinear EFT description. This structure is closely mirrored in the relation between SMEFT and HEFT when considering the decoupling or nondecoupling of heavy degrees of freedom in realistic scenarios such as extended Higgs sectors.

We integrate out the massive scalar at tree level and compare the resulting EFT with the nondecoupling terms in the one-loop effective action. For a strongly coupled scalar with mass $M \sim 4\pi v$, the respective contributions are of comparable size, and both are needed to get a renormalization-scheme-independent result. The authors of [178] have derived nondecoupling effects in the $SU(2)$ gauged linear σ -model using functional methods. In comparison with [178], we make the underlying EFT assumptions more explicit. In this chapter, we rederive parts of their results using the more modern methods outlined in Chapter 4, which makes the calculations more efficient and transparent. In addition, we discuss the renormalization scheme dependence and analyze the resulting low-energy EFT, the nonlinear σ -model, in the strongly and weakly coupled regions of its parameter space.

The chapter is organized as follows. In Sec. 6.1 we discuss basic features of the linear σ -model and introduce the exponential parametrization of the Goldstone fields as the adequate parametrization to integrate out the heavy scalar. In addition, we show how the nonlinear σ -model emerges after decoupling the heavy degree of freedom from the spectrum. This sets the stage to integrate out the massive scalar at tree level in Sec. 6.2, which takes the form of a chiral Lagrangian. In Sec. 6.3, we then derive the one-loop effective action. The renormalization of the one-loop effective action and the elimination of the background scalar to obtain the nondecoupling $\mathcal{O}(1/16\pi^2)$ effects is discussed in Sec. 6.4. We explicitly show that the combination of tree-level and one-loop-level effects gives a result that does not depend on the scalar mass renormalization scheme. In Sec. 6.5, we consider Goldstone scattering at one loop and verify that the previously obtained Wilson coefficients provide the necessary counterterms to give a finite result. Finally, in Sec. 6.6, we discuss the results and conclude the chapter.

6.1. The model

We consider the Lagrangian of an $SO(N)$ -invariant linear σ -model containing N scalar fields ϕ_i :

$$\mathcal{L} = \frac{1}{2} \partial_\mu \phi_n \partial^\mu \phi_n - \frac{\lambda}{8} (\phi_n \phi_n - v^2)^2, \quad n = 1, \dots, N \quad (6.1)$$

The model is invariant under a global $SO(N)$ symmetry acting on the scalar fields. However, the minimum of the potential that corresponds to the ground state of the theory lies at

$$|\phi_{\text{vac}}|^2 = v^2 \quad (6.2)$$

As is well known, the model exhibits spontaneous symmetry breaking $SO(N) \rightarrow SO(N-1)$, which gives rise to $N-1$ Nambu-Goldstone bosons [179–182], along with one massive scalar degree of freedom. Using the parametrization

$$\phi_i = \pi_i(x), \quad (i = 1, \dots, N-1), \quad \phi_N = v + \sigma(x) \quad (6.3)$$

this structure becomes explicit in the Lagrangian:

$$\mathcal{L} = \frac{1}{2} (\partial_\mu \pi_i \partial^\mu \pi_i + \partial_\mu \sigma \partial^\mu \sigma - \lambda v^2 \sigma^2) - \frac{\lambda}{2} v \sigma (\sigma^2 + \pi_i \pi_i) - \frac{\lambda}{8} (\sigma^2 + \pi_i \pi_i)^2 \quad (6.4)$$

Here, the fields π_i represent the $N-1$ massless Goldstone bosons, while σ is the massive scalar with mass $m_\sigma^2 = \lambda v^2$. In (6.4), the full $SO(N)$ symmetry is no longer manifest, though it remains encoded in the structure of the interaction terms. The unbroken $SO(N-1)$ symmetry, acting on the Goldstone fields, remains explicit.

According to Goldstone's theorem, there is one massless Goldstone boson for each spontaneously broken generator. In this case, $SO(N)$ has $N(N-1)/2$ generators. Of these, $(N-1)(N-2)/2$ generators remain unbroken in the vacuum, leaving $N-1$ spontaneously broken generators, corresponding to the $N-1$ Goldstone bosons.

For simplicity, we now specialize to the case $N = 4$, making use of the isomorphism $SO(4) \simeq SU(2)_L \times SU(2)_R$. The symmetry-breaking pattern is

$$SU(2)_L \times SU(2)_R \rightarrow SU(2)_V \quad (6.5)$$

To make the $SU(2)_L \times SU(2)_R$ symmetry manifest, we use the exponential parametrization and write the complex scalar doublet as

$$\phi = \frac{v + S}{\sqrt{2}} U \begin{pmatrix} 0 \\ 1 \end{pmatrix} \quad (6.6)$$

where S is the massive scalar and the matrix U encodes the Goldstone fields φ^a through

$$U = \exp \left(\frac{2i\Phi}{v} \right), \quad \Phi = \varphi^a T^a. \quad (6.7)$$

Here, σ^a denote the Pauli matrices, and $T^a = \sigma^a/2$ are the $SU(2)$ generators. With this parametrization, the Lagrangian in (6.4) becomes

$$\mathcal{L} = \frac{v^2}{4} \langle \partial^\mu U^\dagger \partial_\mu U \rangle \left(1 + \frac{S}{v} \right)^2 + \frac{1}{2} \partial_\mu S \partial^\mu S - V(S) \quad (6.8)$$

where $M^2 = \lambda v^2$, and the potential is

$$V(S) = M^2 v^2 \left[\frac{1}{2} \left(\frac{S}{v} \right)^2 + \frac{1}{2} \left(\frac{S}{v} \right)^3 + \frac{1}{8} \left(\frac{S}{v} \right)^4 \right] \quad (6.9)$$

Although (6.8) contains interaction vertices of arbitrarily high mass dimension, the theory remains renormalizable since it is related to (6.4) via a field redefinition. Our toy model is equivalent to the Higgs sector of the SM in the gaugeless limit, i.e. with gauge couplings set to zero and no fermions present.

Nonlinear σ -model

After integrating out the heavy scalar S , the resulting EFT takes the form of a nonlinear σ -model. The nonlinear σ -model can be formally derived from the linear model by taking the decoupling limit $m_\sigma \rightarrow \infty$ while keeping v fixed [183]. In this limit, the dynamics of the Goldstone bosons are constrained to lie on the $SO(N-1)$ vacuum manifold. The corresponding constraint reads:

$$|\phi|^2 = v^2 \quad \Leftrightarrow \quad \pi^2 + 2v\sigma + \sigma^2 = 0 \quad (6.10)$$

The Lagrangian of the nonlinear σ -model then becomes [184]

$$\mathcal{L} = \frac{1}{2} \partial_\mu \pi_i \partial^\mu \pi_i + \frac{1}{2} \frac{(\pi_i \partial^\mu \pi_i)(\pi_j \partial_\mu \pi_j)}{v^2 - \pi^2} \quad (6.11)$$

In the following, however, we will use the exponential parametrization, which is more suitable for our matching calculation. From (6.8), it is clear that taking the limit $S \rightarrow 0$ yields

$$\mathcal{L} = \frac{v^2}{4} \langle \partial^\mu U^\dagger \partial_\mu U \rangle \quad (6.12)$$

as the effective theory. The two parameterizations of the Goldstone fields (6.11) and (6.12) are related by a field redefinition [29, 185, 186].

6.2. EFT

After integrating out the heavy scalar at one loop, the resulting EFT takes the form of a chiral Lagrangian. The most general chiral Lagrangian up to chiral dimension $d_\chi = 4$ (corresponding to loop order $L = 1$) is given by

$$\mathcal{L}_{\text{EFT}} = \frac{v^2}{4} \langle \partial^\mu U^\dagger \partial_\mu U \rangle + C_1 \langle \partial^\mu U^\dagger \partial_\mu U \rangle^2 + C_2 \langle \partial_\mu U^\dagger \partial_\nu U \rangle \langle \partial^\mu U^\dagger \partial^\nu U \rangle \quad (6.13)$$

The Lagrangian exhibits a manifest global $SU(2)_L \times SU(2)_R$ symmetry acting linearly on the Goldstone matrix:

$$U \rightarrow g_L U g_R^\dagger, \quad g_{L,R} \in SU(2)_{L,R} \quad (6.14)$$

In the following, we compute the coefficients C_1 and C_2 by performing a matching calculation using functional methods. Specifically, we focus on the $\mathcal{O}(1/16\pi^2)$ nondecoupling

one-loop effects, neglecting terms of order $\mathcal{O}(1/M^2 16\pi^2)$. We compare these nondecoupling contributions with the tree-level terms of order $\mathcal{O}(v^2/M^2)$. For a strongly coupled theory with $M \sim 4\pi v$, both contributions are of comparable size. For a consistent EFT treatment, both $\mathcal{O}(v^2/M^2)$ and $\mathcal{O}(1/16\pi^2)$ terms must be included, as only their sum is renormalization-scheme independent with respect to the mass parameter M . We introduce the following shorthand notation for the NLO operators:

$$\mathcal{O}_1 = \langle \partial^\mu U^\dagger \partial_\mu U \rangle^2, \quad \mathcal{O}_2 = \langle \partial_\mu U^\dagger \partial_\nu U \rangle \langle \partial^\mu U^\dagger \partial^\nu U \rangle \quad (6.15)$$

6.2.1. Tree-Level EFT

We now proceed to integrate out the heavy degree of freedom at tree level. The Lagrangian can be written in the form:

$$\mathcal{L}_S = \frac{1}{2} S (-\partial^2 - M^2) S + J_1 S + J_2 S^2 + J_3 S^3 + J_4 S^4 \quad (6.16)$$

with the currents J_i given by

$$\begin{aligned} J_1 &= \frac{v}{2} \langle \partial^\mu U^\dagger \partial_\mu U \rangle, & J_2 &= \frac{1}{4} \langle \partial^\mu U^\dagger \partial_\mu U \rangle, \\ J_3 &= -\frac{M^2}{2v}, & J_4 &= -\frac{M^2}{8v^2} \end{aligned} \quad (6.17)$$

The equation of motion for S then reads:

$$(-\partial^2 - M^2 + 2J_2) S + J_1 + 3J_3 S^2 + 4J_4 S^3 = 0 \quad (6.18)$$

We solve this equation iteratively as an expansion in powers of $1/M^2$:

$$S = S_1 + S_2 + S_3 + \dots, \quad S_l = \mathcal{O}(1/M^{2l}) \quad (6.19)$$

The first two terms in the expansion are given by:

$$S_1 = \frac{J_1}{M^2} = \frac{v}{2M^2} \langle \partial^\mu U^\dagger \partial_\mu U \rangle, \quad (6.20)$$

$$S_2 = \frac{1}{M^2} [-\partial^2 S_1 + 2J_2 S_1 + 3J_3 S_1^2] = -\frac{v}{M^4} \left(\partial^2 \langle \partial^\mu U^\dagger \partial_\mu U \rangle + \frac{1}{8} \langle \partial^\mu U^\dagger \partial_\mu U \rangle^2 \right) \quad (6.21)$$

The effective Lagrangian can be systematically expanded in terms of chiral dimensions, which correspond to the number of derivatives acting on the Goldstone fields:

$$\mathcal{L}_{\text{EFT}} = \mathcal{L}^{(2)} + \mathcal{L}^{(4)} + \mathcal{L}^{(6)} + \dots \quad (6.22)$$

The first two terms read:

$$\mathcal{L}^{(2)} = \frac{v^2}{4} \langle \partial^\mu U^\dagger \partial_\mu U \rangle, \quad (6.23)$$

$$\mathcal{L}^{(4)} = -\frac{M^2}{2} S_1^2 + J_1 S_1 = \frac{v^2}{8M^2} \langle \partial^\mu U^\dagger \partial_\mu U \rangle^2 \quad (6.24)$$

Calculating the effective tree-level Lagrangian at chiral dimension 6 requires a bit more work. The relevant terms are schematically given by:

$$\mathcal{L}^{(6)} = \frac{1}{2}S_1(-\partial^2)S_1 - M^2S_1S_2 + J_1S_2 + J_2S_1^2 + J_3S_1^3 \quad (6.25)$$

Since $J_1 = M^2S_1$, the contributions involving S_2 cancel, leaving:

$$\mathcal{L}^{(6)} = \frac{v^2}{8M^4} (\partial_\alpha \langle \partial^\mu U^\dagger \partial_\mu U \rangle)^2 \quad (6.26)$$

Note that the terms $J_2S_1^2 + J_3S_1^3$ vanish identically. Thus, the resulting tree-level EFT up to chiral dimension four is given by:

$$\mathcal{L} = \frac{v^2}{4} \langle \partial^\mu U^\dagger \partial_\mu U \rangle + \frac{v^2}{8M^2} \langle \partial^\mu U^\dagger \partial_\mu U \rangle^2 \quad (6.27)$$

6.2.2. SMEFT-like EFT

We now investigate (6.27) for a weakly coupled ($\lambda = \mathcal{O}(1)$) scenario in which M and v are of comparable size, i.e. $v/M = \mathcal{O}(1)$. Although this example is of a more academic nature, it nicely illustrates the relation between linear and nonlinear EFTs. The resulting EFT will be organized in terms of mass dimensions. We take (6.27) and expand up to terms of mass dimension eight

$$\begin{aligned} \mathcal{L} = & \frac{1}{2} \partial_\mu \varphi^a \partial^\mu \varphi^a + \frac{1}{6v^2} (\varphi^a \partial_\mu \varphi^a \varphi^b \partial_\mu \varphi^b - \partial^\mu \varphi^a \partial_\mu \varphi^a \varphi^b \varphi^b) + \frac{1}{2v^2 M^2} (\partial_\mu \varphi^a \partial^\mu \varphi^a)^2 \\ & + \frac{1}{45v^4} (\partial^\mu \varphi^a \partial_\mu \varphi^a \varphi^b \varphi^b \varphi^c \varphi^c - \varphi^a \partial_\mu \varphi^a \varphi^b \partial_\mu \varphi^b \varphi^c \varphi^c) + \mathcal{O}\left(\frac{1}{v^6}, \frac{1}{v^4 M^2}, \frac{1}{v^2 M^4}\right) \end{aligned} \quad (6.28)$$

A striking feature of this limit is that all the interaction vertices are power-suppressed. The first four-Goldstone interaction term is here a dimension six operator suppressed by a factor $1/v^2$ and expanding \mathcal{O}_1 produces a mass dimension eight operator as a first term. Taking the decoupling limit here ($v, M \rightarrow \infty$) would yield a free theory. To further illustrate the differences between the linear and nonlinear EFT consider the s-channel amplitude for Goldstone scattering via scalar exchange

$$\mathcal{M} = \frac{i}{v^2} \frac{s}{1 - \frac{s}{M^2}} = i \frac{x}{1 - \frac{x}{\lambda}} \quad (6.29)$$

where we defined $x = s/v^2$. An EFT description is valid for $x \ll \lambda$ where the denominator can be expanded. Depending on the size of λ we can discern two scenarios

- $\lambda \sim 1$: weak coupling, SMEFT-like scenario
- $16\pi^2 \gg \lambda \gg 1$: strong coupling, HEFT-like scenario

The size of λ is constrained by perturbative unitarity bounds [187]. Similar to the Lee-Quigg-Thacker bound [188, 189] for the Higgs mass in the SM, one can derive through a coupled channel analysis

$$\lambda \leq \frac{8\pi}{3} \approx 8.38 \quad (6.30)$$

6.3. Integrating the scalar out at the one-loop level

To integrate the heavy scalar out at the one-loop-level we compute the one-loop effective action using the method outlined in Chapter 4 based on [47]. First of all, we split the fields into classical background fields and quantum fluctuations and retain then only terms up to quadratic order in the fluctuation fields, i.e.

$$S \longrightarrow S + \tilde{S} \quad (6.31)$$

$$U \longrightarrow U\tilde{U} \quad (6.32)$$

where we defined

$$\tilde{U} = \exp(i\tilde{\varphi}^a \sigma^a / v) \quad (6.33)$$

and the fluctuation fields are $\tilde{\eta} = (\tilde{S}, \tilde{\varphi}^a)^T$. We expand here the Goldstone kinetic term to quadratic order in the fluctuation fields $\tilde{\varphi}^a$. Under $U \rightarrow U\tilde{U}$ the derivative terms transform as follows

$$\partial_\mu U \rightarrow \partial_\mu U\tilde{U} + U\partial_\mu \tilde{U} \quad (6.34)$$

$$\partial_\mu U^\dagger \rightarrow \partial_\mu \tilde{U}^\dagger U^\dagger + \tilde{U}^\dagger \partial_\mu U^\dagger \quad (6.35)$$

Then the Goldstone kinetic term becomes

$$\langle \partial^\mu U^\dagger \partial_\mu U \rangle \rightarrow \langle \partial^\mu U^\dagger \partial_\mu U \rangle + \langle \partial^\mu \tilde{U}^\dagger \partial_\mu \tilde{U} \rangle + \langle \partial_\mu \tilde{U}^\dagger U^\dagger \partial^\mu U \tilde{U} \rangle + \langle \tilde{U}^\dagger \partial_\mu U^\dagger U \partial^\mu \tilde{U} \rangle \quad (6.36)$$

Expanding the Goldstone kinetic term to quadratic order in the fluctuation fields yields

$$\langle \partial^\mu U^\dagger \partial_\mu U \rangle \rightarrow \langle \partial^\mu U^\dagger \partial_\mu U \rangle + 2\partial_\mu \tilde{\varphi}^a \partial^\mu \tilde{\varphi}^a - i\partial_\mu \tilde{\varphi}^a \langle \sigma_a (U^\dagger \partial^\mu U - \partial^\mu U^\dagger U) \rangle \quad (6.37)$$

Plugging this parameterization into (6.8) we get the following expression

$$\begin{aligned} \mathcal{L}(\varphi^a, \tilde{\varphi}^a, S, \tilde{S}) &= \mathcal{L}(\varphi^a, S) \\ &+ \tilde{S} \left[-\partial^2 S + \frac{v}{2} \left(1 + \frac{S}{v} \right) \langle \partial^\mu U^\dagger \partial_\mu U \rangle - M^2 v \left(\frac{S}{v} + \frac{3}{2} \left(\frac{S}{v} \right)^2 + \frac{1}{2} \left(\frac{S}{v} \right)^3 \right) \right] \\ &+ \tilde{\varphi}^a \left[-\frac{v}{2} \left(1 + \frac{S}{v} \right)^2 \partial_\mu J_a^\mu - \left(1 + \frac{S}{v} \right) \partial_\mu S J_a^\mu \right] \\ &+ \frac{1}{2} \tilde{S} \left[-\partial^2 - M^2 \left(1 + 3\frac{S}{v} + \frac{3}{2} \left(\frac{S}{v} \right)^2 \right) + \frac{1}{2} \langle \partial^\mu U^\dagger \partial_\mu U \rangle \right] \tilde{S} \\ &+ \tilde{S} \partial_\mu \tilde{\varphi}^a J_a^\mu \left(1 + \frac{S}{v} \right) + \frac{1}{2} \tilde{\varphi}^a \left[-\partial^\mu \left(1 + \frac{S}{v} \right)^2 \partial_\mu \delta^{ab} - \left(1 + \frac{S}{v} \right)^2 \epsilon^{abc} J^{\mu c} \partial_\mu \right] \tilde{\varphi}^b \\ &+ \mathcal{O}(\tilde{\varphi}^3, \tilde{S}^3, \tilde{\varphi}^2 \tilde{S}, \tilde{\varphi} \tilde{S}^2) \end{aligned} \quad (6.38)$$

where we defined the current

$$J_\mu^a = \frac{i}{2} \langle \sigma_a (\partial_\mu U^\dagger U - U^\dagger \partial_\mu U) \rangle = -i \langle \sigma_a (U^\dagger \partial_\mu U) \rangle = \frac{2}{v} \partial_\mu \varphi^a + \dots \quad (6.39)$$

Here the terms linear in the fluctuation fields are just the classical equations of motion for the background fields. Therefore, they vanish, since the (classical) background fields satisfy the classical equations of motion. In the next step, we identify the corresponding expressions for the fluctuation operator \mathcal{O}

$$\mathcal{L}^{(\eta^2)} = \frac{1}{2} \bar{\eta}^\dagger \mathcal{O} \bar{\eta} \quad (6.40)$$

with

$$\mathcal{O} = \begin{pmatrix} \Delta_H & X_{LH}^\dagger \\ X_{LH} & \Delta_L \end{pmatrix} \quad (6.41)$$

The entries of \mathcal{O} are given by

$$\Delta_H = -\partial^2 - M^2 \left(1 + 3\frac{S}{v} + \frac{3}{2} \left(\frac{S}{v} \right)^2 \right) + \frac{1}{2} \langle \partial^\mu U^\dagger \partial_\mu U \rangle \quad (6.42)$$

$$\Delta_L = -\partial^\mu \left(1 + \frac{S}{v} \right)^2 \partial_\mu \delta^{ab} - \left(1 + \frac{S}{v} \right)^2 \epsilon^{abc} J^{\mu c} \partial_\mu \quad (6.43)$$

$$X_{LH}^\dagger = \left(1 + \frac{S}{v} \right) J_a^\mu \partial_\mu \quad (6.44)$$

$$X_{LH} = -\partial_\mu \left(1 + \frac{S}{v} \right) J_a^\mu \quad (6.45)$$

In the following, we proceed to diagonalize the fluctuation operator in order to perform the functional integration. Concretely, we need to compute the inverse of Δ_L to obtain the shifted fluctuation operator in the hard region

$$\tilde{\Delta}_H = \Delta_H - X_{LH}^\dagger \Delta_L^{-1} X_{LH} = -\partial^2 - M^2 - U \quad (6.46)$$

In our case, the general formula for the one-loop effective action reads

$$S_H = -\frac{i}{2} \int d^d x \sum_{n=1}^{\infty} \frac{1}{n} \int \frac{d^d p}{(2\pi)^d} \text{tr} \left\{ \left(\frac{2ip\partial + \partial^2 + U(x, \partial_x + ip)}{p^2 - M^2} \right)^n \mathbf{1} \right\} \quad (6.47)$$

It remains to determine U up to the required order in perturbation theory.

6.3.1. Inverting Δ_L

Our Δ_L is a 3x3 matrix in isospin space and has the form

$$(\Delta_L(x, \partial_x + ip))^{ab} = \alpha \delta^{ab} + \epsilon^{abc} \beta^c \quad (6.48)$$

with

$$\alpha = \left(1 + \frac{S}{v} \right)^2 p^2 \left(1 - \frac{\partial^2}{p^2} - 2i \frac{p_\mu \partial^\mu}{p^2} \right) - 2\partial^\mu \left(\frac{S}{v} \right) \left(1 + \frac{S}{v} \right) (\partial_\mu + ip_\mu) \quad (6.49)$$

and

$$\beta^c = - \left(1 + \frac{S}{v} \right)^2 J^{\mu c} (\partial_\mu + ip_\mu) \quad (6.50)$$

To find the inverse of this matrix we first write down the most general form the inverse can have

$$(\Delta_L^{-1})^{ab} = A\delta^{ab} + B\epsilon^{abc}\beta^c + C\beta^a\beta^b \quad (6.51)$$

The coefficients can be determined from the condition $(\Delta_L)^{ac}(\Delta_L^{-1})^{cb} = \delta^{ab}$:

$$A = \frac{1}{\alpha + \frac{\beta^c\beta^c}{\alpha}}, \quad B = \frac{-1}{\alpha^2 + \beta^c\beta^c}, \quad C = \frac{1}{\alpha^3 + \alpha\beta^c\beta^c} \quad (6.52)$$

Expanding the coefficients up to $\mathcal{O}(p^{-6})$ we get

$$A = \frac{1}{\alpha} - \frac{\beta^c\beta^c}{p^6} = \frac{1}{p^2} \left(1 + \frac{\partial^2}{p^2} + 2i\frac{p_\lambda\partial^\lambda}{p^2} - 4\frac{p_\alpha p_\beta \partial^\alpha \partial^\beta}{p^4} \right) - \frac{\beta^c\beta^c}{p^6} \quad (6.53)$$

$$B = -\frac{1}{p^4}, \quad C = \frac{1}{p^6} \quad (6.54)$$

6.3.2. Calculation of \mathcal{L}_H

In order to compute $\tilde{\Delta}_H(x, \partial_x + ip)$ we need to shift X_{LH} as well

$$X_{LH}(x, \partial_x + ip) = -(\partial_\mu + ip_\mu) \left(1 + \frac{S}{v} \right) J_a^\mu \quad (6.55)$$

$$X_{LH}^\dagger(x, \partial_x + ip) = \left(1 + \frac{S}{v} \right) J_a^\mu (\partial_\mu + ip_\mu) \quad (6.56)$$

We employ the counting $p_\mu, v \sim \zeta$ where ζ is the hard scale. Keep in mind that $S/v \sim \zeta^{-2}$. We neglect operators that are suppressed by $1/16\pi^2 M^2$. The effective Lagrangian in our case is given by

$$\mathcal{L}_H = \underbrace{-\frac{i}{2} \int \frac{d^d p}{(2\pi)^d} \frac{U(x, \partial_x + ip)}{p^2 - M^2}}_{\mathcal{L}_H^{(1)}} \underbrace{-\frac{i}{4} \int \frac{d^d p}{(2\pi)^d} \frac{U(x, \partial_x + ip)^2}{(p^2 - M^2)^2}}_{\mathcal{L}_H^{(2)}} \quad (6.57)$$

It remains to determine $U(x, \partial_x + ip)$ up to the desired order. First of all, in our case

$$U(x, \partial_x + ip) = W + X_{LH}^\dagger \Delta_L^{-1} X_{LH} \quad (6.58)$$

where

$$W = M^2 \left(3\frac{S}{v} + \frac{3}{2} \left(\frac{S}{v} \right)^2 \right) - \frac{1}{2} \langle \partial^\mu U^\dagger \partial_\mu U \rangle \quad (6.59)$$

To compute $\mathcal{L}_H^{(1)}$ we need to expand $U(x, \partial_x + ip)$ up to order ζ^{-2} :

$$U(x, \partial_x + ip) = W - J_a^\mu (\partial_\mu + ip_\mu) \frac{1}{p^2} \left(1 + \frac{\partial^2}{p^2} + 2i \frac{p_\lambda \partial^\lambda}{p^2} - 4 \frac{p_\alpha p_\beta \partial^\alpha \partial^\beta}{p^4} \right) (\partial_\nu + ip_\nu) J_a^\nu + \epsilon^{abc} J^{\mu a} (\partial_\lambda J_\nu^b) \frac{J^{\lambda c} p_\mu p_\nu}{p^4} \quad (6.60)$$

$$= W + J^{\mu a} \frac{p_\mu p_\nu}{p^2} J^{\nu a} + J^{\mu a} \frac{p_\mu p_\nu}{p^4} \partial^2 J^{\nu a} - 4 J^{\mu a} \frac{p_\mu p_\alpha p_\beta p_\nu}{p^6} \partial^\alpha \partial^\beta J^{\nu a} + \epsilon^{abc} J^{\mu a} (\partial_\lambda J_\nu^b) \frac{J^{\lambda c} p_\mu p_\nu}{p^4} \quad (6.61)$$

$$= W + J^{\mu a} J_{\mu a} \frac{1}{d} - \frac{(\partial_\mu J_\nu^a)(\partial^\mu J^{\nu a})}{p^2} \left(\frac{1}{d} - \frac{4}{d(d+2)} \right) + \epsilon^{abc} J^{\mu a} (\partial_\nu J_\mu^b) J^{\nu c} \frac{1}{d} \quad (6.62)$$

Here we made use of $\partial_\mu J^{\mu a} = 0$. Performing the momentum integral we get for $\mathcal{L}_H^{(1)}$

$$\mathcal{L}_H^{(1)} = \left(W + J^{\mu a} J_{\mu a} \frac{1}{d} \right) \frac{M^2}{32\pi^2} (N_\epsilon + 1) - \frac{1}{32\pi^2} (\partial_\mu J_\nu^a)(\partial^\mu J^{\nu a}) \left(\frac{1}{d} - \frac{4}{d(d+2)} \right) (N_\epsilon + 1) + \epsilon^{abc} J^{\mu a} (\partial_\nu J_\mu^b) J^{\nu c} \frac{1}{32\pi^2} \frac{1}{d} (N_\epsilon + 1) \quad (6.63)$$

$$= W \frac{M^2}{32\pi^2} (N_\epsilon + 1) + J^{\mu a} J_{\mu a} \frac{M^2}{128\pi^2} \left(N_\epsilon + \frac{3}{2} \right) - \frac{1}{384\pi^2} (\partial_\mu J_\nu^a)(\partial^\mu J^{\nu a}) \left(N_\epsilon + \frac{5}{6} \right) + \epsilon^{abc} J^{\mu a} (\partial_\nu J_\mu^b) J^{\nu c} \frac{1}{32\pi^2} \frac{1}{4} \left(N_\epsilon + \frac{3}{2} \right) \quad (6.64)$$

Here we defined

$$N_\epsilon = \frac{1}{\epsilon} + \ln \frac{\bar{\mu}^2}{M^2} \quad (6.65)$$

The expression involving the current J_μ^a can be reduced to the basis operators $\mathcal{O}_{1,2}$ using $SU(2)$ identities. All the necessary calculational steps can be found in Appendix D. Here we just state the final result

$$\mathcal{L}_H^{(1)} = \langle \partial^\mu U^\dagger \partial_\mu U \rangle \frac{M^2}{16\pi^2} \frac{1}{8} + \left(\frac{3}{2} \frac{S}{v} + \frac{3}{4} \left(\frac{S}{v} \right)^2 \right) \frac{M^4}{16\pi^2} (N_\epsilon + 1) + \frac{1}{16\pi^2} \frac{1}{6} (\mathcal{O}_1 - \mathcal{O}_2) \left(N_\epsilon + \frac{11}{6} \right) \quad (6.66)$$

For $\mathcal{L}_H^{(2)}$ it is enough to use U up to order ζ^0 , i.e.

$$U(x, \partial_x + ip) = W + J^{\mu a} \frac{p_\mu p_\nu}{p^2} J^{\nu a}. \quad (6.67)$$

Squaring this expression gives

$$U^2 = W^2 + 2W J^{\mu a} \frac{p_\mu p_\nu}{p^2} J^{\nu a} + J^{\mu a} \frac{p_\mu p_\nu}{p^2} J^{\nu a} J^{\alpha b} \frac{p_\alpha p_\beta}{p^2} J^{\beta b} = W^2 + \frac{2}{d} W J^{\mu a} J_{\mu a} + \frac{(J^{\mu a} J_{\mu a})^2}{d(d+2)} + 2 \frac{(J_{\mu a} J_{\nu a})(J^{\mu b} J^{\nu b})}{d(d+2)} \quad (6.68)$$

After performing the momentum integrals we have

$$\begin{aligned}\mathcal{L}_H^{(2)} = & W^2 \frac{1}{64\pi^2} N_\epsilon + W J^{\mu a} J_{\mu a} \frac{1}{128\pi^2} \left(N_\epsilon + \frac{1}{2} \right) \\ & + \frac{1}{16\pi^2} \frac{1}{96} (J^{\mu a} J_{\mu a})^2 \left(N_\epsilon + \frac{5}{6} \right) + \frac{1}{16\pi^2} \frac{1}{48} (J_{\mu a} J_{\nu a}) (J^{\mu b} J^{\nu b}) \left(N_\epsilon + \frac{5}{6} \right)\end{aligned}\quad (6.69)$$

Again using the identities in Appendix D this can be reduced to basis operators

$$\begin{aligned}\mathcal{L}_H^{(2)} = & \frac{1}{16\pi^2} \frac{9}{4} \frac{S^2}{v^2} N_\epsilon + \frac{1}{16\pi^2} \frac{3}{8} M^2 \frac{S}{v} \langle \partial^\mu U^\dagger \partial_\mu U \rangle \\ & - \frac{1}{16\pi^2} \frac{1}{48} \mathcal{O}_1 \left(N_\epsilon + \frac{4}{3} \right) + \frac{1}{16\pi^2} \frac{1}{12} \mathcal{O}_2 \left(N_\epsilon + \frac{5}{6} \right)\end{aligned}\quad (6.70)$$

The full effective Lagrangian is then given by

$$\begin{aligned}\mathcal{L}_{eff} = & \langle \partial^\mu U^\dagger \partial_\mu U \rangle \frac{M^2}{16\pi^2} \frac{1}{8} + \frac{1}{16\pi^2} \frac{3}{8} M^2 \frac{S}{v} \langle \partial^\mu U^\dagger \partial_\mu U \rangle \\ & + \frac{3}{2} \frac{S}{v} \frac{M^4}{16\pi^2} (N_\epsilon + 1) + 3 \frac{S^2}{v^2} \frac{M^4}{16\pi^2} \left(N_\epsilon + \frac{1}{4} \right) \\ & + \frac{1}{16\pi^2} \mathcal{O}_1 \left(\frac{7}{48} N_\epsilon + \frac{5}{18} \right) - \frac{1}{16\pi^2} \frac{1}{12} \mathcal{O}_2 \left(N_\epsilon + \frac{17}{6} \right)\end{aligned}\quad (6.71)$$

Our result agrees with [178]. The result still contains the background scalar S . Before S can be eliminated via the equation of motion, the effective Lagrangian needs to be renormalized. That is the subject of the next section.

6.4. Renormalization

To understand the renormalization of the linear σ -model, we start with the bare Lagrangian

$$\mathcal{L} = \partial^\mu \phi_b^\dagger \partial_\mu \phi_b + m_b^2 \phi_b^\dagger \phi_b - \frac{\lambda_b}{2} \left(\phi_b^\dagger \phi_b \right)^2 \quad (6.72)$$

where we use the subscript b to denote the bare fields and couplings. Introducing the renormalized parameters

$$\phi_b = \sqrt{Z_\phi} \phi, \quad m_b^2 = Z_{m^2} m^2, \quad \lambda_b = \mu^{2\epsilon} Z_\lambda \lambda \quad (6.73)$$

we write the renormalized Lagrangian

$$\mathcal{L} = \partial^\mu \phi^\dagger \partial_\mu \phi + m^2 \phi^\dagger \phi - \frac{\lambda}{2} \left(\phi^\dagger \phi \right)^2 \quad (6.74)$$

$$+ (Z_\phi - 1) \partial^\mu \phi^\dagger \partial_\mu \phi + (Z_\phi Z_{m^2} - 1) m^2 \phi^\dagger \phi - (Z_\phi^2 Z_\lambda - 1) \frac{\lambda}{2} \left(\phi^\dagger \phi \right)^2 \quad (6.75)$$

Using the parametrization (6.6) we observe

$$Z_\phi = Z_v = Z_S \quad (6.76)$$

Since the scalar S is integrated out we can set $Z_S = 1$ and instead perform a finite field shift after renormalizing the other quantities. Plugging in the exponential parameterization

$$\begin{aligned} \mathcal{L} = & \frac{v^2}{4} \langle \partial^\mu U^\dagger \partial_\mu U \rangle \left(1 + \frac{S}{v} \right)^2 + \frac{1}{2} \partial_\mu S \partial^\mu S + \frac{m^2}{2} (v + S)^2 - \frac{\lambda}{8} (v + S)^4 \\ & + \delta_{m^2} \frac{m^2}{2} (v + S)^2 - \delta_\lambda \frac{\lambda}{8} (v + S)^4 \end{aligned} \quad (6.77)$$

where

$$\delta_\lambda = Z_\lambda - 1, \quad \delta_{m^2} = Z_{m^2} - 1 \quad (6.78)$$

From here, we can read off the counterterm Lagrangian, keeping in mind that we only need terms up to S^2

$$\mathcal{L}_{c.t.} = (\delta_{m^2} - \delta_\lambda) \frac{M^2 v}{2} S - \frac{1}{2} \frac{M^2}{2} (3\delta_\lambda - \delta_{m^2}) S^2 \quad (6.79)$$

The divergent part of the renormalization constant can be found in the literature e.g., in [98] and are given by

$$\delta_\lambda = \frac{3}{8\pi^2} \lambda \frac{1}{\epsilon}, \quad \delta_{m^2} = \frac{3}{16\pi^2} \lambda \frac{1}{\epsilon} \quad (6.80)$$

so that the counterterm Lagrangian is given by

$$\mathcal{L}_{c.t.} = -\frac{3}{32\pi^2} \frac{M^4}{v} \frac{1}{\epsilon} S + \frac{5}{32\pi^2} \frac{M^2}{v^2} \frac{1}{\epsilon} \frac{M^2}{2} S^2 + \text{finite} \quad (6.81)$$

We chose a renormalization condition such that the terms linear in S (tadpole) vanish, i.e.

$$\mathcal{L}_{c.t.} = -\frac{3}{32\pi^2} \frac{M^4}{v} \left(\frac{1}{\epsilon} + 1 \right) S + \frac{5}{32\pi^2} \frac{M^2}{v^2} \frac{1}{\epsilon} \frac{M^2}{2} S^2 \quad (6.82)$$

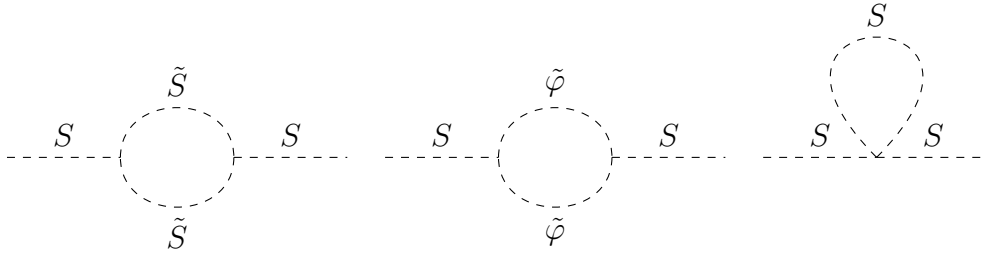
6.4.1. Background scalar self-energy

Before we can eliminate the background scalar S we first need to compute its mass renormalization. Following [178] we calculate the background scalar self-energy. Since in the on-shell scheme, the renormalized mass is identified with the pole mass at $p^2 = M_R^2$, the renormalization constant has to be calculated diagrammatically. As we substitute the background scalar S in the end by the leading term in its equation of motion suppressed by M^2 , we consider only contributions to the self-energy of $\mathcal{O}(M^4)$. The diagrams contributing to the scalar self-energy $\mathcal{O}(M^4)$ are displayed in Fig. 6.1. The background scalar self-energy is given in terms of Passarino-Veltman scalar functions by

$$\Sigma_S(p^2) = \frac{3}{32\pi^2} \frac{M^4}{v^2} [A_0(M^2) + 3B_0(p^2; M^2, M^2)] + \frac{3}{32\pi^2} \frac{p^4}{v^2} B_0(p^2; 0, 0) \quad (6.83)$$

The scalar tadpole function A_0 and bubble function B_0 are defined in (E.1) and (E.4) respectively. Within the EFT's domain of validity for $0 < z = p^2/4M^2 < 1$, the background scalar self-energy takes the explicit form

$$\Sigma_S(p^2) = \frac{3}{32\pi^2} \frac{M^4}{v^2} [4N_\epsilon + 7 - 6\sqrt{z^{-1} - 1} \arcsin \sqrt{z}] + \frac{3}{32\pi^2} \frac{p^4}{v^2} [N_\epsilon + 2 - \ln 4z - i\pi] \quad (6.84)$$


 Figure 6.1.: Background scalar self-energy diagrams of $\mathcal{O}(M^4)$

In the on-shell scheme, the renormalization condition is

$$\delta M^2 = \text{Re}(\Sigma_S(M^2)) \quad (6.85)$$

Evaluating the self-energy at $p^2 = M^2$, we end up with

$$\Sigma_S(M^2) = \frac{3}{32\pi^2} \frac{M^4}{v^2} [5N_\epsilon + 9 - \sqrt{3}\pi - i\pi] \quad (6.86)$$

and thus, the mass counterterm is given by

$$\delta M_{OS}^2 = \frac{3}{32\pi^2} \frac{M^4}{v^2} [5N_\epsilon + 9 - \sqrt{3}\pi] \quad (6.87)$$

This result agrees with [178]. The divergent part of δM^2 is the same in every renormalization scheme, but in each scheme, the finite part is different a priori. In general, we may write

$$\delta M^2 = \frac{3}{32\pi^2} \frac{M^4}{v^2} [5N_\epsilon + \Omega] \quad (6.88)$$

with the constant Ω depending on the renormalization scheme. The renormalized mass is thus given by

$$M_{ren}^2 = M^2 \left(1 - \frac{3}{32\pi^2} \frac{M^2}{v^2} \Omega \right) = M^2 \left(1 - \frac{3\lambda}{32\pi^2} \Omega \right) \quad (6.89)$$

Note that in the $\overline{\text{MS}}$ scheme $\Omega = 0$ and in the on-shell scheme $\Omega = 9 - \sqrt{3}\pi$.

6.4.2. Elimination of the background scalar S

Adding the counterterm Lagrangian (6.81) to the the effective Lagrangian (6.71) we obtain the "renormalized" Lagrangian

$$\begin{aligned} \mathcal{L}_{\text{eff}}^{\text{ren}} &= \mathcal{L}_{\text{eff}} + \mathcal{L}_{c.t.} = \frac{1}{16\pi^2} \frac{M^2}{4} \frac{S}{v} \langle \partial^\mu U^\dagger \partial_\mu U \rangle \\ &+ \frac{1}{16\pi^2} \frac{M^4}{v^2} \left(3N_\epsilon + \frac{3}{4} - 8\pi^2 \frac{v^2}{M^2} \frac{\delta M^2}{M^2} \right) S^2 \\ &+ \frac{1}{16\pi^2} \mathcal{O}_1 \left(\frac{7}{48} N_\epsilon + \frac{5}{18} \right) - \frac{1}{16\pi^2} \frac{1}{12} \mathcal{O}_2 \left(N_\epsilon + \frac{17}{6} \right) \end{aligned} \quad (6.90)$$

This Lagrangian still contains the background scalar S . As we aim to calculate the $\mathcal{O}(1/16\pi^2)$ terms in the effective action, we can integrate out S at tree level. To integrate out S we just substitute the first term in the expansion in $1/M^2$ (6.20):

$$S = \frac{v}{2M^2} \langle \partial^\mu U^\dagger \partial_\mu U \rangle \quad (6.91)$$

We end up with

$$\mathcal{L}_{\text{eff}}^{\text{ren}} = -\frac{1}{16\pi^2} \frac{1}{24} \mathcal{O}_1 \left(N_\epsilon - \frac{85}{6} + \frac{9}{2} \Omega \right) - \frac{1}{16\pi^2} \frac{1}{12} \mathcal{O}_2 \left(N_\epsilon + \frac{17}{6} \right) \quad (6.92)$$

Plugging in $\Omega = 9 - \sqrt{3}\pi$ for the on-shell scheme we reproduce the result of [178]

$$\mathcal{L}_{\text{eff}}^{\text{ren,OS}} = -\frac{1}{16\pi^2} \frac{1}{24} \mathcal{O}_1 \left(N_\epsilon + \frac{79}{3} - \frac{27\pi}{2\sqrt{3}} \right) - \frac{1}{16\pi^2} \frac{1}{12} \mathcal{O}_2 \left(N_\epsilon + \frac{17}{6} \right) \quad (6.93)$$

However, the scheme-dependent parameter drops out of physical predictions since \mathcal{O}_1 is generated at tree level with a coefficient that depends on M . Explicitly, we have

$$C_1 = \frac{v^2}{8M^2} - \frac{1}{16\pi^2} \frac{3}{16} \Omega - \frac{1}{16\pi^2} \frac{1}{24} \left(N_\epsilon - \frac{85}{6} \right) \quad (6.94)$$

Plugging in the renormalized mass (6.89), we see that the scheme-dependent constant drops out

$$C_1 \supset \frac{v^2}{8M_{\text{ren}}^2} - \frac{1}{16\pi^2} \frac{3}{16} \Omega = \frac{v^2}{8M^2} + \frac{1}{16\pi^2} \frac{3}{16} \Omega - \frac{1}{16\pi^2} \frac{3}{16} \Omega = \frac{v^2}{8M^2} \quad (6.95)$$

i.e. the coefficient C_1 is indeed scheme-independent. Finally, the results for the Wilson coefficients are

$$C_1 = \frac{v^2}{8M^2} - \frac{1}{16\pi^2} \frac{1}{24} \left(N_\epsilon - \frac{85}{6} \right), \quad C_2 = -\frac{1}{16\pi^2} \frac{1}{12} \left(N_\epsilon + \frac{17}{6} \right) \quad (6.96)$$

6.5. Goldstone scattering at NLO

We have seen in the previous sections that integrating out the heavy scalar from the linear σ -model generates a nonlinear σ -model which takes the form of a chiral Lagrangian

$$\mathcal{L}_{\text{eff}} = \frac{v^2}{4} \langle \partial_\mu U^\dagger \partial^\mu U \rangle + C_1 \mathcal{O}_1 + C_2 \mathcal{O}_2 \quad (6.97)$$

where the coefficients $C_{1,2}$ are given in (6.96). These coefficients act as counterterms for one-loop amplitudes computed from the first $d_\chi = 2$ term in (6.97). To illustrate this, we examine the 4-Goldstone amplitude $\mathcal{M}(\varphi^a(p_a)\varphi^b(p_b) \rightarrow \varphi^c(p_c)\varphi^d(p_d))$ in this section. We employ the standard Mandelstam variables

$$s = (p_a + p_b)^2, \quad t = (p_a - p_c)^2, \quad u = (p_a - p_d)^2 \quad (6.98)$$

Bose and crossing symmetry imply that the amplitude may be decomposed as [190]

$$\mathcal{M}(\varphi^a\varphi^b \rightarrow \varphi^c\varphi^d) = \delta_{ab}\delta_{cd} A(s, t, u) + \delta_{ac}\delta_{bd} A(t, s, u) + \delta_{ad}\delta_{bc} A(u, t, s) \quad (6.99)$$

where the function A is symmetric in the last two arguments $A(s, t, u) = A(s, u, t)$.

First of all, we have to extract the four-Goldstone vertex from

$$\mathcal{L}_2 = \frac{v^2}{4} \langle \partial^\mu U^\dagger \partial_\mu U \rangle \quad (6.100)$$

Expanding (6.100) to fourth order in φ we obtain

$$\mathcal{L}_{(p^2)} = \frac{1}{2} \partial_\mu \varphi^a \partial^\mu \varphi^a + \frac{1}{6v^2} (\varphi^a \partial_\mu \varphi^a \varphi^b \partial_\mu \varphi^b - \partial^\mu \varphi^a \partial_\mu \varphi^a \varphi^b \varphi^b) + \dots \quad (6.101)$$

It is straightforward to derive the Feynman rule for the four-point vertex (see (F.6)), giving rise to the tree-level amplitude

$$\mathcal{M} = \delta_{ab} \delta_{cd} \frac{s}{v^2} + \delta_{ac} \delta_{bd} \frac{t}{v^2} + \delta_{ad} \delta_{bc} \frac{u}{v^2} \quad (6.102)$$

Thus, the function A at leading order is given by

$$A_{LO}(s, t, u) = \frac{s}{v^2} \quad (6.103)$$

Working up to $\mathcal{O}(p^4)$ requires the calculation of the Goldstone amplitude at one loop

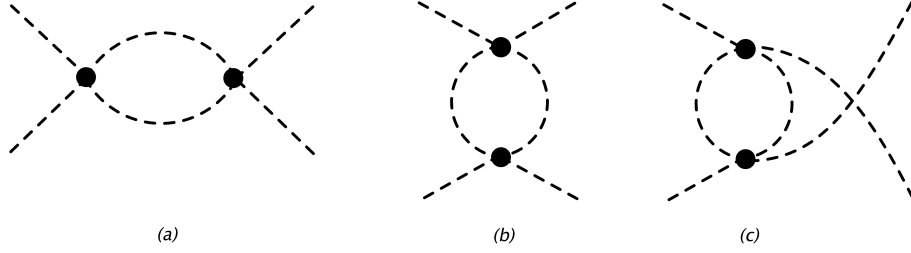


Figure 6.2.: One-loop diagrams for $\varphi\varphi \rightarrow \varphi\varphi$ scattering. Black circles denote vertices from the LO Lagrangian.

using (6.100). The three one-loop diagrams are depicted in Fig. 6.2, and evaluating them gives

$$A_{(p^2)}^{1loop}(s, t, u) = \frac{1}{32\pi^2} \frac{1}{v^4} \left[\frac{2}{3} (s^2 + t^2 + u^2) \left(\frac{1}{\epsilon} + \frac{4}{3} \right) + t^2 + u^2 - s^2 \ln \frac{-s}{\mu^2} - \frac{1}{6} (3t^2 - s^2 + u^2) \ln \frac{-t}{\mu^2} - \frac{1}{6} (3u^2 - s^2 + t^2) \ln \frac{-u}{\mu^2} \right] \quad (6.104)$$

and therefore, the full one-loop amplitude reads [53]

$$\begin{aligned} \mathcal{M}_{abcd} = & \frac{1}{32\pi^2} \frac{1}{v^4} \delta_{ab} \delta_{cd} \left[\frac{2}{3} (s^2 + t^2 + u^2) \left(\frac{1}{\epsilon} + \frac{4}{3} \right) + t^2 + u^2 - s^2 \ln \frac{-s}{\mu^2} - \frac{1}{6} (3t^2 - s^2 + u^2) \ln \frac{-t}{\mu^2} - \frac{1}{6} (3u^2 - s^2 + t^2) \ln \frac{-u}{\mu^2} \right] \\ & + \frac{1}{32\pi^2} \frac{1}{v^4} \delta_{ac} \delta_{bd} \left[\frac{2}{3} (s^2 + t^2 + u^2) \left(\frac{1}{\epsilon} + \frac{4}{3} \right) + s^2 + u^2 - t^2 \ln \frac{-t}{\mu^2} - \frac{1}{6} (3s^2 - t^2 + u^2) \ln \frac{-s}{\mu^2} - \frac{1}{6} (3u^2 - s^2 + t^2) \ln \frac{-u}{\mu^2} \right] \\ & + \frac{1}{32\pi^2} \frac{1}{v^4} \delta_{ad} \delta_{bc} \left[\frac{2}{3} (s^2 + t^2 + u^2) \left(\frac{1}{\epsilon} + \frac{4}{3} \right) + s^2 + t^2 - u^2 \ln \frac{-u}{\mu^2} - \frac{1}{6} (3s^2 - t^2 + u^2) \ln \frac{-s}{\mu^2} - \frac{1}{6} (3t^2 - s^2 + u^2) \ln \frac{-t}{\mu^2} \right] \end{aligned}$$

$$\begin{aligned}
 & -\frac{1}{6} (3s^2 - t^2 + u^2) \ln \frac{-s}{\mu^2} - \frac{1}{6} (3u^2 - t^2 + s^2) \ln \frac{-u}{\mu^2} \Big] \\
 & + \frac{1}{32\pi^2} \frac{1}{v^4} \delta_{ad} \delta_{bc} \left[\frac{2}{3} (s^2 + t^2 + u^2) \left(\frac{1}{\epsilon} + \frac{4}{3} \right) + t^2 + s^2 - u^2 \ln \frac{-u}{\mu^2} \right. \\
 & \left. - \frac{1}{6} (3s^2 - u^2 + t^2) \ln \frac{-s}{\mu^2} - \frac{1}{6} (3t^2 - u^2 + s^2) \ln \frac{-t}{\mu^2} \right] \quad (6.105)
 \end{aligned}$$

The amplitude is divergent and contains $1/\epsilon$ poles, which need to be removed by counterterms. The coefficients of the $d_\chi = 4$ operators

$$\mathcal{L}_{(p^4)} = C_1 \langle \partial^\mu U^\dagger \partial_\mu U \rangle^2 + C_2 \langle \partial_\mu U^\dagger \partial_\nu U \rangle \langle \partial^\mu U^\dagger \partial^\nu U \rangle \quad (6.106)$$

that we calculated in a top-down matching calculation are precisely those counterterms. They absorb the divergences coming from one-loop graphs with vertices $\mathcal{L}_{(p^2)}$. The operators $\mathcal{O}_{1,2}$ give rise to a four-point contact vertex, and their contribution to the A function is

$$A_{(p^4)}^{tree}(s, t, u) = \left[8C_1 \frac{s^2}{v^4} + 4C_2 \frac{t^2 + u^2}{v^4} \right] \quad (6.107)$$

The full amplitude is

$$\begin{aligned}
 \mathcal{M}_{NLO} = & \delta_{ab} \delta_{cd} \left[8C_1 \frac{s^2}{v^4} + 4C_2 \frac{t^2 + u^2}{v^4} \right] + \delta_{ac} \delta_{bd} \left[8C_1 \frac{t^2}{v^4} + 4C_2 \frac{s^2 + u^2}{v^4} \right] \\
 & + \delta_{ad} \delta_{bc} \left[8C_1 \frac{u^2}{v^4} + 4C_2 \frac{t^2 + s^2}{v^4} \right] \quad (6.108)
 \end{aligned}$$

Plugging in our explicit results (6.96) yields

$$A_{(p^4)}^{tree}(s, t, u) = \frac{s^2}{v^2 M^2} - \frac{1}{16\pi^2} \frac{1}{3} \left[\frac{s^2 + t^2 + u^2}{v^4} \left(\frac{1}{\epsilon} + \ln \frac{\bar{\mu}^2}{M^2} \right) - \frac{85}{5} \frac{s^2}{v^4} + \frac{17}{6} \frac{t^2 + u^2}{v^4} \right] \quad (6.109)$$

and adding this result to (6.104)

$$\begin{aligned}
 A_{(p^4)}^{1loop}(s, t, u) = & \frac{s^2}{v^2 M^2} + \frac{1}{16\pi^2} \frac{1}{v^4} \left[s^2 \frac{31}{6} - \frac{s^2}{2} \ln \frac{-s}{M^2} \right. \\
 & \left. - \frac{1}{12} (3t^2 - s^2 + u^2) \ln \frac{-t}{M^2} - \frac{1}{12} (3u^2 - s^2 + t^2) \ln \frac{-u}{M^2} \right] \quad (6.110)
 \end{aligned}$$

cancel all $1/\epsilon$ poles, and the result is finite as required. The matrix elements for Goldstone scattering can be decomposed according to their isospin ($I = 0, 1, 2$)

$$\langle I', I'_3 | \mathcal{M} | I, I_3 \rangle = \mathcal{M}^I \delta_{II'} \delta_{I_3 I'_3} \quad (6.111)$$

The isospin amplitudes [57, 190] are given by

$$\begin{aligned}
 \mathcal{M}^{I=0} &= 3A(s, t, u) + A(t, u, s) + A(u, s, t) \\
 \mathcal{M}^{I=1} &= A(t, u, s) - A(u, s, t) \\
 \mathcal{M}^{I=2} &= A(t, u, s) + A(u, s, t)
 \end{aligned} \quad (6.112)$$

For example $\varphi^+ \varphi^- \rightarrow \varphi^+ \varphi^-$ scattering corresponds to the $\mathcal{M}^{I=0}$ amplitude.

6.6. Discussion

In this chapter, we used the $SO(4)$ linear σ -model as a prototype to showcase the emergence of a nondecoupling EFT. We integrated out the massive degree of freedom and performed the matching to the resulting low-energy EFT, the nonlinear σ -model or chiral Lagrangian. At the one-loop order, we calculated the one-loop nondecoupling effects of $\mathcal{O}(1/16\pi^2)$ (i.e., those that survive in the limit $M \rightarrow \infty$) using functional methods. Here, we found that both the tree-level and one-loop contributions are necessary for a renormalization-scheme independent result (6.95). That fact can also be understood by considering that in a strongly coupled theory with $M \sim 4\pi v$, the tree-level Wilson coefficients of $\mathcal{O}(v^2/M^2)$ and the nondecoupling contributions at one loop of $\mathcal{O}(1/16\pi^2)$ are parametrically of the same size. From this example, a general lesson can be drawn. When constructing a top-down EFT framework, it is vital to take the underlying assumptions seriously, particularly the parameter space of the UV theory, which will have direct implications for the organizing principle of the EFT. The conclusions from Chapter 5 also hold in this case.

7. 2HDM: Nonlinear EFT

After discussing the Two-Higgs Doublet Model (2HDM) [171] in Chapter 7 as a well-known extension of the SM, we return to it in this chapter. Recently, there has been renewed interest in the 2HDM, particularly in the context of EFT approaches around the electroweak scale [191–194]. The motivation for this section is twofold. First, we investigate the 2HDM in a particularly interesting region of its parameter space, the nondecoupling limit, which corresponds to a strongly coupled scenario. In addition, we demonstrate how the Higgs-Electroweak Chiral Lagrangian (Higgs-EwChL) naturally emerges as the low-energy effective description after integrating out the heavy scalar degrees of freedom in this regime.

We employ functional matching techniques, which streamline the calculation and enhance transparency. The functional approach allows us to go beyond existing results in the literature [194] by computing higher-order terms in the Higgs function and deriving certain all-order expressions in powers of the Higgs field h . The technique we use was originally developed in [119] in the context of matching the Standard Model singlet extension to the Higgs Effective Field Theory (HEFT).

We include a brief analysis of the decoupling limit, where the heavy scalar fields are integrated out in a weakly coupled regime. We compare the resulting linear EFT with the previously obtained nonlinear EFT and point out the key differences. This chapter is organized as follows. In Section 7.1, we introduce a convenient parametrization of the 2HDM scalar sector that is tailored for matching onto the Higgs–Electroweak Chiral Lagrangian (HEFT). In Section 7.2, we perform the tree-level functional matching of the nondecoupling 2HDM to the leading-order electroweak chiral Lagrangian. Section 7.3 extends this analysis to the one-loop–induced local EFT operators for $h \rightarrow \gamma\gamma$ and $h \rightarrow \gamma Z$. We rederive parts of the results diagrammatically to highlight the efficiency of the functional approach. In Sec. 7.4, we compute the one-loop coefficient of the custodial-symmetry–violating operator Q_{β_1} . Sec. 7.5 discusses the viable 2HDM parameter space for TeV-scale heavy scalars, covering the decoupling, nondecoupling, and alignment regimes. Sec. 7.6 then briefly explores the phenomenological implications of our EFT results. In Sec. 7.7, we take a look at the decoupling limit and perform the matching to SMEFT at canonical dimension six, where we briefly comment on the differences to the nonlinear EFT. In Sec. 7.8, we conclude. Finally, the Appendix 7.9 to this chapter presents the all-orders solution $H_0(h)$ to the leading-order equation of motion for the heavy scalar field.

This chapter draws in part on the results of [2], to which the author of this thesis contributed as a co-author.

7.1. Nondecoupling Regime - Higgs-EWChL

We have already introduced the 2HDM in Section 5.4 and discussed the potential (5.92) and the mass eigenstates. In this chapter, we shall work with the same model but perform a convenient field redefinition in the scalar sector. Instead of working with the doublets

Φ_n , it is useful to employ a non-linear parametrization for the matching to HEFT. To this end, we define the conjugate doublets $\tilde{\Phi}_n \equiv i\sigma_2 \Phi_n^*$, with $n = 1, 2$ and the matrix fields

$$S_n \equiv (\tilde{\Phi}_n, \Phi_n) \quad (7.1)$$

Using these matrix fields we may write the Lagrangian of the scalar sector as

$$\mathcal{L}_S = \frac{1}{2} \langle D_\mu S_n^\dagger D^\mu S_n \rangle - V \quad (7.2)$$

where $\langle \dots \rangle$ denotes the trace, a sum over n is understood, and V is the 2HDM potential (5.92) (with $\lambda_6 = \lambda_7 = 0$) expressed in terms of the matrix fields S_n . Following the discussion in [195] we write the S_n in polar coordinates as

$$S_n \equiv U R_n, \quad R_n = \frac{1}{\sqrt{2}} [(v_n + h_n) \mathbf{1} + i C_n \sigma_a \rho_a] \quad (7.3)$$

Here $\sigma_a = 2T_a$, $a = 1, 2, 3$ are the Pauli matrices and $U = \exp(2i\varphi_a T_a/v)$ is the matrix of the electroweak Goldstone bosons. The v_n are, as before, the respective vevs of the two Higgs doublet fields (5.93) and

$$C_1 = -\sin \beta, \quad C_2 = \cos \beta \quad (7.4)$$

where the mixing angle β was defined in (5.97). As before in the doublet representation the non-linear parametrization (7.3) comprises eight real degrees of freedom expressed through the real fields φ_a, ρ_a and h_n . From the electroweak quantum numbers of S_n and U we can deduce that the covariant derivatives are given by

$$D_\mu \Phi = \partial_\mu \Phi + ig W_\mu \Phi - ig' B_\mu \Phi T_3 \quad \text{for } \Phi = S_n, U \quad (7.5)$$

where $W^\mu = W_a^\mu T_a$ and B^μ are the gauge fields of $SU(2)_L$ and $U(1)_Y$. From these expressions, we can derive the covariant derivatives for the physical fields. Using (7.3) it follows

$$D_\mu R_n = \partial_\mu R_n + ig' B_\mu [T_3, R_n] \quad (7.6)$$

As a result, $h_{1,2}$ and ρ_3 are electroweak singlets, whereas $\rho_{1,2}$ are $SU(2)_L$ singlets yet charged under $U(1)_Y$. Therefore,

$$D_\mu h_n = \partial_\mu h_n \quad \text{and} \quad D_\mu \rho_a = \partial_\mu \rho_a + g' B_\mu \varepsilon_{ab3} \rho_b \quad (7.7)$$

It is convenient to trade $\rho_{1,2}$ for the eigenstates ρ^\pm of charge and hypercharge (with $Q = Y = \pm 1$)

$$D_\mu \rho^\pm = \partial_\mu \rho^\pm \pm ig' B_\mu \rho^\pm, \quad \rho^\pm = \frac{1}{\sqrt{2}} (\rho_1 \mp i \rho_2) \quad (7.8)$$

Inserting (7.3) into (7.2), the kinetic term takes the form

$$\begin{aligned} \mathcal{L}_{S,kin} &= \frac{1}{2} \langle D_\mu S_n^\dagger D^\mu S \rangle = \\ &= \frac{1}{4} \langle D_\mu U^\dagger D^\mu U \rangle [(v_n + h_n)^2 + \rho_a \rho_a] + \frac{1}{2} D_\mu \rho_a D^\mu \rho_a \end{aligned}$$

$$+ \langle iU^\dagger D_\mu U T_a \rangle [\varepsilon_{abc} \rho_b D^\mu \rho_c + C_n (\rho_a \partial^\mu h_n - D^\mu \rho_a h_n)] \quad (7.9)$$

Expressed in terms of the matrix fields S_n the potential reads [195]

$$\begin{aligned} V = & \frac{m_{11}^2}{2} \langle S_1^\dagger S_1 \rangle + \frac{m_{22}^2}{2} \langle S_2^\dagger S_2 \rangle - m_{12}^2 \langle S_1^\dagger S_2 \rangle \\ & + \frac{\lambda_1}{8} \langle S_1^\dagger S_1 \rangle^2 + \frac{\lambda_2}{8} \langle S_2^\dagger S_2 \rangle^2 + \frac{\lambda_3}{4} \langle S_1^\dagger S_1 \rangle \langle S_2^\dagger S_2 \rangle \\ & + \lambda_4 \langle S_1^\dagger S_2 P_+ \rangle \langle S_1^\dagger S_2 P_+ \rangle + \frac{\lambda_5}{2} \left(\langle S_1^\dagger S_2 P_+ \rangle^2 + \langle S_1^\dagger S_2 P_- \rangle^2 \right) \end{aligned} \quad (7.10)$$

Here $P_\pm = (1 \pm \sigma_3)/2$ are projection operators. Note that we have set $\lambda_6 = \lambda_7 = 0$ with respect to the most general potential (5.92) thereby assuming invariance under the discrete symmetry $S_1 \rightarrow -S_1, S_2 \rightarrow S_2$ only softly broken by the dimension 2 operator m_{12}^2 . This choice prevents flavor-changing neutral currents (FCNCs) at tree-level. Choosing $\lambda_6 = \lambda_7 = 0$ and $m_{12}^2 \neq 0$ generates finite Higgs-mediated FCNCs at one loop [172].

As before, we assume CP invariance, such that all parameters are real. It is now obvious that the polar coordinate parametrization (7.3) has the advantage that the Goldstone matrix U disappears from the potential, which is entirely a function of the h_n and ρ_a . The Goldstone fields only enter the kinetic term. The terms in the potential linear in the fields vanish due to the definition of $v_{1,2}$. The mass terms quadratic in the fields ρ_a are already diagonalized by ρ_\pm, ρ_3 , for the h_n mass terms a further rotation in fieldspace is necessary

$$\begin{pmatrix} H_0 \\ h \end{pmatrix} = \begin{pmatrix} c_\alpha & s_\alpha \\ -s_\alpha & c_\alpha \end{pmatrix} \begin{pmatrix} h_1 \\ h_2 \end{pmatrix} \quad (7.11)$$

Thus, the mass eigenstates in the scalar sector are given by h , which we identify as the observed Higgs boson at $m_h = 125\text{GeV}$, and the additional scalars $H \equiv H_0, H^\pm \equiv \pm i\rho^\pm$ and the pseudoscalar $A_0 \equiv -\rho_3$. We trade in the eight potential parameters $m_{11}^2, m_{22}^2, m_{12}^2, \lambda_1, \dots, \lambda_5$ for the vevs, particle masses and soft breaking term

$$v_1, \quad v_2, \quad m_h, \quad M_0 \equiv M_{H_0}, \quad M_H \equiv M_{H^\pm}, \quad M_A \equiv M_{A_0}, \quad s_\alpha, \quad m_{12}^2 \quad (7.12)$$

or equivalently

$$v, \quad t_\beta, \quad m_h, \quad M_0, \quad M_H, \quad M_A, \quad c_{\beta-\alpha}, \quad \bar{m}^2 \equiv \frac{m_{12}^2}{s_\beta c_\beta} \quad (7.13)$$

It is instructive to display the 2HDM scalar Lagrangian in terms of the physical fields h, H, A_0, H^\pm

$$\begin{aligned} \mathcal{L} = & \frac{1}{2} \partial_\mu h \partial^\mu h + \frac{1}{2} \partial_\mu H \partial^\mu H + \frac{1}{2} \partial_\mu A_0 \partial^\mu A_0 + D^\mu H^- D_\mu H^+ - V(h, H, A_0, H^\pm) + \mathcal{L}_Y \\ & + \frac{v^2}{4} \left(1 + 2s_{\beta-\alpha} \frac{h}{v} + 2c_{\beta-\alpha} \frac{H}{v} + \frac{h^2}{v^2} + \frac{H^2}{v^2} \right) \langle D^\mu U^\dagger D_\mu U \rangle \\ & + J_3^\mu [iH^- \partial_\mu H^+ - iH^+ \partial_\mu H^- + c_{\beta-\alpha} (h \partial_\mu A_0 - A_0 \partial_\mu h) + s_{\beta-\alpha} (A_0 \partial_\mu H - H \partial_\mu A_0)] \\ & + J_+^\mu [A_0 \partial_\mu H^+ - H^+ \partial_\mu A_0 - i c_{\beta-\alpha} (H^+ \partial_\mu h - h \partial_\mu H^+) + i s_{\beta-\alpha} (H^+ \partial_\mu H - H \partial_\mu H^+)] \end{aligned}$$

$$+ J_-^\mu [A_0 \partial_\mu H^- - H^- \partial_\mu A_0 + i c_{\beta-\alpha} (H^- \partial_\mu h - h \partial_\mu H^-) - i s_{\beta-\alpha} (H^- \partial_\mu H - H \partial_\mu H^-)] \quad (7.14)$$

where \mathcal{L}_Y denotes the Yukawa Lagrangian, which we discuss below. Here we introduced the currents

$$J_3^\mu = \langle i U^\dagger D_\mu U T_3 \rangle, \quad J_\pm^\mu = \langle i U^\dagger D_\mu U T_\pm \rangle \quad (7.15)$$

where $T_\pm = 1/\sqrt{2} (T_1 \pm iT_2)$. The full scalar potential in terms of the physical fields reads

$$\begin{aligned} V = & \frac{1}{2} m_h^2 h^2 + \frac{1}{2} M_0^2 H^2 + M_H^2 H^+ H^- + \frac{1}{2} M_A^2 A_0^2 \\ & - d_1 h^3 - d_2 h^2 H - d_3 h H^2 - d_4 H^3 - d_5 h H^+ H^- - d_6 h A_0^2 - d_7 H^+ H^- H - d_8 H A_0^2 \\ & - z_1 h^4 - z_2 h^3 H - z_3 h^2 H^2 - z_4 h H^3 - z_5 H^4 \\ & - z_6 h^2 H^+ H^- - z_7 h H H^+ H^- - z_8 H^2 H^+ H^- - z_9 (H^+ H^-)^2 - z_{10} A_0^2 h^2 \\ & - z_{11} A_0^2 h H - z_{12} H^2 A_0^2 - z_{13} A_0^2 H^+ H^- - z_{14} A_0^4 \end{aligned} \quad (7.16)$$

The explicit expression for the d_i, z_i in terms of the input parameters (7.13) can be found in appendix A.

Yukawa couplings

The scalar sector couples to the fermions through Yukawa terms. There exist several possible Yukawa sectors. Here we choose for definiteness a type II Yukawa sector which is given by the Lagrangian [171]

$$\mathcal{L}_Y = -\bar{q}_L \Phi_1 Y_d P_- q_R - \bar{q}_L \tilde{\Phi}_2 Y_u P_+ q_R - \bar{l}_L \Phi_1 Y_e P_- l_R + \text{h.c.} \quad (7.17)$$

In terms of the matrix fields S_n it can be written as

$$\mathcal{L}_Y = -\bar{q}_L Y_d S_1 P_- q_R - \bar{q}_L Y_u S_2 P_+ q_R - \bar{l}_L Y_L S_1 P_- l_R + \text{h.c.} \quad (7.18)$$

It is useful to express the Yukawa Lagrangian in terms of the physical fields

$$\begin{aligned} \mathcal{L}_Y = & - \left(1 + \frac{c_\alpha}{c_\beta} \frac{H}{v} - \frac{s_\alpha}{c_\beta} \frac{h}{v} - i t_\beta \frac{A_0}{v} \right) J_{f1} - \left(1 + \frac{s_\alpha}{s_\beta} \frac{H}{v} + \frac{c_\alpha}{s_\beta} \frac{h}{v} - i t_\beta^{-1} \frac{A_0}{v} \right) J_{f2} \\ & + \sqrt{2} t_\beta \frac{H^+}{v} J_{c1} + \sqrt{2} t_\beta^{-1} \frac{H^-}{v} J_{c2} + \text{h.c.} \end{aligned} \quad (7.19)$$

Here we defined the fermion currents

$$J_{f1} = \bar{q}_L \mathcal{M}_d U P_- q_R + \bar{l}_L \mathcal{M}_e U P_- l_R, \quad J_{f2} = \bar{q}_L \mathcal{M}_u U P_+ q_R \quad (7.20)$$

$$J_{c1} = \bar{q}_L \mathcal{M}_d U P_{12} q_R + \bar{l}_L \mathcal{M}_e U P_{12} l_R, \quad J_{c2} = \bar{q}_L \mathcal{M}_u U P_{21} q_R \quad (7.21)$$

where we employed the projectors

$$P_{12} \equiv T_1 + iT_2, \quad P_{21} \equiv T_1 - iT_2 \quad (7.22)$$

The fermion mass matrices \mathcal{M}_q can be expressed through the Yukawa matrices

$$\mathcal{M}_u = \frac{v}{\sqrt{2}} Y_u s_\beta, \quad \mathcal{M}_d = \frac{v}{\sqrt{2}} Y_d c_\beta, \quad \mathcal{M}_e = \frac{v}{\sqrt{2}} Y_e c_\beta \quad (7.23)$$

The generalization to other types of Yukawa sectors follows easily and will be discussed below.

7.2. Tree-level matching in the nondecoupling regime

We write the full Lagrangian of the 2HDM as

$$\mathcal{L}_{2HDM} = \mathcal{L}_0 + \mathcal{L}_{S,kin} - V + \mathcal{L}_Y \quad (7.24)$$

where \mathcal{L}_0 denotes the unbroken SM

$$\begin{aligned} \mathcal{L}_0 = & -\frac{1}{2}\langle G_{\mu\nu}G^{\mu\nu} \rangle - \frac{1}{2}\langle W_{\mu\nu}W^{\mu\nu} \rangle - \frac{1}{4}B_{\mu\nu}B^{\mu\nu} \\ & + \bar{q}_L i \not{D} q_L + \bar{l}_L i \not{D} l_L + \bar{u}_R i \not{D} u_R + \bar{d}_R i \not{D} d_R + \bar{e}_R i \not{D} e_R \end{aligned} \quad (7.25)$$

We now proceed to integrate out the heavy scalars at tree level and compute the $\mathcal{O}(1)$ effective Lagrangian. The procedure of integrating out a heavy scalar in the nondecoupling has been described in detail in [40, 119]. We shall follow this procedure and adapt it accordingly.

7.2.1. Algorithm for tree-level matching

First of all, we notice that the potential (7.16) contains the heavy fields A_0 and H^\pm only at the quadratic order and higher, as they can appear exclusively as the uncharged and CP-even combinations H^+H^- and A_0^2 , respectively. As a result, there can be no tree diagrams with only internal lines from those fields. Integrating out these fields at tree level and to LO ($\mathcal{O}(M_S^0)$) therefore implies $A_0 = H^\pm = 0$. This constitutes an important simplification. Even though the 2HDM contains more scalar degrees of freedom than the singlet extension, in both cases just one real scalar needs to be considered to obtain the leading order effective Lagrangian in the nondecoupling regime. The part of the Lagrangian that depends on H is given by

$$\mathcal{L}_{H_0} = \frac{1}{2}H(-\partial^2 - M_0^2)H + J_1H + J_2H^2 + J_3H^3 + J_4H^4 \quad (7.26)$$

where the J_i are given by

$$\begin{aligned} J_1 &= d_2h^2 + z_2h^3 + \frac{v}{2}c_{\beta-\alpha}\langle D^\mu U^\dagger D_\mu U \rangle - \frac{c_\alpha}{c_\beta}\frac{J_{f1} + J_{f1}^*}{v} - \frac{s_\alpha}{s_\beta}\frac{J_{f2} + J_{f2}^*}{v} \\ J_2 &= d_3h + z_3h^2 + \frac{1}{4}\langle D^\mu U^\dagger D_\mu U \rangle \\ J_3 &= d_4 + z_4h, \quad J_4 = z_5 \end{aligned} \quad (7.27)$$

Making the dependence of the J_i and the potential parameters d_i, z_i on the heavy mass M_0 explicit to consistently perform the EFT expansion we write

$$J_i \equiv M_0^2 J_i^0 + \bar{J}_i, \quad d_i \equiv M_0^2 d_{i0} + \bar{d}_i, \quad z_i \equiv M_0^2 z_{i0} + \bar{z}_i \quad (7.28)$$

Note that z_1, \dots, z_5 and d_2, \dots, d_4 do not depend on M_A, M_H . Integrating out the field H at tree level amounts to solving its equation of motion

$$(-\partial^2 - M_0^2 + 2J_2)H + J_1 + 3J_3H^2 + 4J_4H^3 = 0 \quad (7.29)$$

and inserting the solution $H_0(h)$ back into the Lagrangian. The equation of motion (7.29) can be solved iteratively in inverse powers of M_0

$$H = H_0 + H_1 + H_2 + \dots, \quad H_l = \mathcal{O}(1/M_0^{2l}) \quad (7.30)$$

We insert the ansatz (7.30) into (7.29) to obtain algebraic equations for the H_i . Retaining only terms of $\mathcal{O}(M_0^2)$ gives an equation for H_0

$$J_1^0 + (-1 + 2J_2^0)H_0 + 3J_3^0H_0^2 + 4J_4H_0^3 = 0 \quad (7.31)$$

Keeping only the terms of $\mathcal{O}(1)$ gives an equation for H_1 in terms of H_0

$$H_1 = \frac{(-\partial^2 + 2\bar{J}_2)H_0 + \bar{J}_1 + 3\bar{J}_3H_0^2 + 4\bar{J}_4H_0^3}{M_0^2(1 - J_2^0 - 6J_3^0H_0 - 12J_4^0H_0^2)} \quad (7.32)$$

Similarly, equations for the $H_{l \geq 2}$ may be derived.

The coefficients J_i^0 in (7.31) are functions of h only and therefore we compute the solution $H_0(h)$. Although (7.31) can be solved analytically it is convenient to expand $H_0(h)$ in an infinite power series in h

$$H_0(h) = \sum_{k=2}^{\infty} r_k h^k \quad (7.33)$$

where all the coefficients are of $\mathcal{O}(1)$. For our matching calculation we only need the first few coefficients

$$\begin{aligned} r_2 &= d_{20} \\ r_3 &= d_{20}d_{30} \\ r_4 &= d_{20}d_{30}^2 + d_{20}^2d_{40} \\ r_5 &= d_{20}d_{30}^3 + 3d_{20}^2d_{30}d_{40} \end{aligned} \quad (7.34)$$

For the reader's convenience we display the relevant potential parameters

$$vd_{20} = -\frac{c_{\beta-\alpha}}{2} \frac{s_{2\alpha}}{s_{2\beta}} \quad (7.35)$$

$$vd_{30} = s_{\beta-\alpha} \frac{s_{2\alpha}}{s_{2\beta}} \quad (7.36)$$

$$vd_{40} = -\frac{c_{\beta-\alpha}}{2} - s_{\beta-\alpha}^2 \frac{s_{\alpha+\beta}}{s_{2\beta}} \quad (7.37)$$

Inserting $H = H_0 + H_1$ into (7.14) and retaining only the $\mathcal{O}(M_0^2)$ and $\mathcal{O}(1)$ terms we get the leading order effective Lagrangian. The terms with H_1 vanish due to the equation of motion for H_0 . In addition, we will show in the appendix to this chapter that all $\mathcal{O}(M_0^2)$ cancel up to an irrelevant constant

$$\begin{aligned} \mathcal{L}_{hH_0,LO} &= \frac{1}{2} (\partial_\mu h)^2 - \frac{m^2}{2} h^2 + d_1 h^3 + \bar{z}_1 h^4 + \frac{1}{2} (\partial_\mu H_0)^2 + \bar{J}_1 H_0 + \bar{J}_2 H_0^2 + \bar{J}_3 H_0^3 + \bar{J}_4 H_0^4 \\ &\quad + \frac{v^2}{4} \langle D^\mu U^\dagger D_\mu U \rangle \left(1 + 2s_{\beta-\alpha} \frac{h}{v} + \frac{h^2}{v^2} \right) - v(J_{f1} + J_{f1}^*) \left(1 - \frac{s_\alpha}{c_\beta} \frac{h}{v} \right) \end{aligned}$$

$$-v(J_{f_2} + J_{f_2}^*) \left(1 + \frac{c_\alpha h}{s_\beta v}\right) \quad (7.38)$$

where $H_0 = H_0(h)$. The kinetic term for h takes the form

$$\mathcal{L}_{h,kin} = \frac{1}{2} (\partial_\mu h)^2 + \frac{1}{2} (\partial_\mu H_0)^2 = \frac{1}{2} (\partial_\mu h)^2 (1 + F_h(h)) \quad (7.39)$$

where

$$F_h(h) = \left(\frac{dH_0(h)}{dh}\right)^2 \quad (7.40)$$

To bring the kinetic term to its canonical form $(\partial\tilde{h})^2/2$ the field redefinition

$$\tilde{h} = \int_0^h \sqrt{1 + F_h(s)} ds = h \left(1 + \frac{2}{3} r_2^2 h^2 + \frac{3}{2} r_2 r_3 h^3 + \mathcal{O}(h^4)\right) \quad (7.41)$$

is required. Inverting this we arrive at

$$h(\tilde{h}) = \tilde{h} \left(1 - \frac{2}{3} r_2^2 \tilde{h}^2 - \frac{3}{2} r_2 r_3 \tilde{h}^3 + \mathcal{O}(\tilde{h}^4)\right) \quad (7.42)$$

After eliminating h in favor of \tilde{h} and dropping the tilde in the end, the result takes the form of an electroweak chiral Lagrangian with a light Higgs (3.23) and we can calculate the general functions in (3.23) up to the desired order in h .

The parameters of the Higgs potential (3.24) are given by

$$V_3 = -\frac{2d_1 v}{m_h^2} \quad (7.43)$$

$$V_4 = -\frac{16}{3} (vd_{20})^2 - 8\frac{v^2}{m_h^2} \bar{z}_1 - 8\frac{(v\bar{d}_2)(vd_{20})}{m_h^2} \quad (7.44)$$

$$V_5 = \frac{2v^3}{m_h^2} (2d_{20}^2 d_1 - \bar{d}_3 d_{20}^2 - \bar{z}_2 d_{20} - \bar{d}_2 d_{20} d_{30}) - 3d_{20}^2 d_{30} v^3 \quad (7.45)$$

The cubic coefficient is not affected by the field redefinition (7.42). Moreover, the coefficients of the Flare function $F_U(h)$ (3.24) can be written as

$$F_1 = 2s_{\beta-\alpha}, \quad F_2 = 1 + 2c_{\beta-\alpha} v d_{20}, \quad F_3 = 2c_{\beta-\alpha} v^2 d_{20} d_{30} - \frac{4}{3} s_{\beta-\alpha} v^2 d_{20}^2 \quad (7.46)$$

$$F_4 = -\frac{(vd_{20})^3}{3} + 2c_{\beta-\alpha} v^3 \left(d_{20} d_{30}^2 + d_{20}^2 d_{40} - \frac{4}{3} d_{20}^3\right) - 3v^3 d_{20}^3 d_{30} s_{\beta-\alpha} \quad (7.47)$$

Here, the field redefinition (7.42) plays no role for the coefficients $f_{U,1}$ and $f_{U,2}$. Making use of (7.35) - (7.37) and trigonometric identities the potential and the Flare function take the form

$$\begin{aligned} F_U(h) = & 2s_{\beta-\alpha} \frac{h}{v} + \left(1 - \frac{s_{2\alpha}}{s_{2\beta}} c_{\beta-\alpha}^2\right) \left(\frac{h}{v}\right)^2 - \frac{4}{3} \frac{s_{2\alpha}^2}{s_{2\beta}^2} s_{\beta-\alpha} c_{\beta-\alpha}^2 \left(\frac{h}{v}\right)^3 \\ & - \frac{c_{\beta-\alpha}^2}{12} \frac{s_{2\alpha}^2}{s_{2\beta}^3} (10s_{2\alpha} - 3s_{2\beta} - 7s_{4\alpha-2\beta}) \left(\frac{h}{v}\right)^4 + \mathcal{O}(h^5) \end{aligned} \quad (7.48)$$

$$\begin{aligned}
 V(h) = & \frac{m_h^2 v^2}{2} \left\{ \left(\frac{h}{v} \right)^2 + \left[s_{\beta-\alpha} + \frac{2c_{\beta-\alpha}^2 c_{\beta+\alpha}}{s_{2\beta}} \left(1 - \frac{\bar{m}^2}{m_h^2} \right) \right] \left(\frac{h}{v} \right)^3 \right. \\
 & + \left[\frac{1}{4} - \frac{c_{\beta-\alpha}^2}{4s_{2\beta}^2} \left(\frac{1}{6}(7 - 12c_{2(\beta+\alpha)} - 19c_{4\alpha}) - (1 - 2c_{2\alpha}c_{2\beta} - 3c_{4\alpha}) \frac{\bar{m}^2}{m_h^2} \right) \right] \left(\frac{h}{v} \right)^4 \\
 & \left. - \frac{c_{\beta-\alpha}^2 s_{2\alpha}^2}{2s_{2\beta}^3} \left[c_{\beta+\alpha} + 3c_{\beta-3\alpha} - (2c_{\beta+\alpha} + 3c_{3\beta-\alpha} + 11c_{\beta-3\alpha}) \frac{\bar{m}^2}{4m_h^2} \right] \left(\frac{h}{v} \right)^5 + \mathcal{O}(h^6) \right\}
 \end{aligned} \tag{7.49}$$

It is easy to see that the SM is recovered in the alignment limit $c_{\beta-\alpha} \rightarrow 0$. It remains to calculate the Yukawa Higgs function

$$\mathcal{F}_{Y_i}(h) = \mathcal{M}_i + \sum_{n=1}^{\infty} \mathcal{M}_i^{(n)} \left(\frac{h}{v} \right)^n = \mathcal{M}_i \left(1 + \sum_{n=1}^{\infty} \mu_i^{(n)} \left(\frac{h}{v} \right)^n \right) \tag{7.50}$$

$$\mu_d^{(1)} = -\frac{s_\alpha}{c_\beta}, \quad \mu_d^{(2)} = \frac{c_\alpha}{c_\beta}(vd_{20}), \quad \mu_d^{(3)} = \frac{2}{3} \frac{s_\alpha}{c_\beta}(vd_{20})^2 + \frac{c_\alpha}{c_\beta}(vd_{20})(vd_{30}) \tag{7.51}$$

and

$$\mu_u^{(1)} = \frac{c_\alpha}{s_\beta}, \quad \mu_u^{(2)} = \frac{s_\alpha}{s_\beta}(vd_{20}), \quad \mu_u^{(3)} = -\frac{2}{3} \frac{c_\alpha}{s_\beta}(vd_{20})^2 + \frac{s_\alpha}{s_\beta}(vd_{20})(vd_{30}) \tag{7.52}$$

The Higgs-fermion couplings for a type II Yukawa sector are given by the following expressions

$$\begin{aligned}
 \mathcal{M}_u + \sum_{n=1}^{\infty} \mathcal{M}_u^{(n)} \left(\frac{h}{v} \right)^n = \\
 \mathcal{M}_u \left[1 + \frac{c_\alpha}{s_\beta} \frac{h}{v} - \frac{c_{\beta-\alpha}}{2} \frac{s_\alpha^2 c_\alpha}{s_\beta^2 c_\beta} \left(\frac{h}{v} \right)^2 - \frac{c_{\beta-\alpha}}{6} \frac{s_{2\alpha}^2}{s_{2\beta}^2} (2s_{2\alpha} - (1 - 2c_{2\alpha})t_\beta^{-1}) \left(\frac{h}{v} \right)^3 + \dots \right]
 \end{aligned} \tag{7.53}$$

$$\begin{aligned}
 \mathcal{M}_d + \sum_{n=1}^{\infty} \mathcal{M}_d^{(n)} \left(\frac{h}{v} \right)^n = \\
 \mathcal{M}_d \left[1 - \frac{s_\alpha}{c_\beta} \frac{h}{v} - \frac{c_{\beta-\alpha}}{2} \frac{s_\alpha c_\alpha^2}{s_\beta c_\beta^2} \left(\frac{h}{v} \right)^2 + \frac{c_{\beta-\alpha}}{6} \frac{s_{2\alpha}^2}{s_{2\beta}^2} (2s_{2\alpha} - (1 + 2c_{2\alpha})t_\beta) \left(\frac{h}{v} \right)^3 + \dots \right]
 \end{aligned} \tag{7.54}$$

Using functional methods we have reproduced the results of [194] and obtained several new expressions, the cubic and quartic coefficients of $F_U(h)$, the coefficient of h^5 in $V(h)$ and the fermionic couplings. Higher orders may be easily calculated following the procedure in this section and making use of the all-orders expression $H_0(h)$ derived in Section 7.9. This defines an algorithm to extend the tree-level matching to all orders in h .

Our discussion may be extended to include the NLO terms of $\mathcal{O}(1/M_S^2)$ in the effective Lagrangian

$$\mathcal{L}_{eff} = \mathcal{L}_{LO} + \Delta\mathcal{L}_{NLO} + \mathcal{O}(M_S^{-4}), \quad \mathcal{L}_{LO} = \mathcal{L}_0 + \mathcal{L}_{Uh,LO} \tag{7.55}$$

At this order also the pseudoscalar A_0 and charged scalar H^\pm generate four-fermion operators (see Section (7.2.3) for further details)

$$\begin{aligned} \Delta\mathcal{L}_{NLO} = & \frac{[(-\partial^2 + 2\bar{J}_2)H_0 + \bar{J}_1 + 3\bar{J}_3H_0^2 + 4\bar{J}_4H_0^3]^2}{2M_0^2(1 - J_2^0 - 6J_3^0H_0 - 12J_4^0H_0^2)} \\ & - \frac{1}{2M_A^2v^2} [t_\beta^2(J_{f1}^2 + J_{f1}^{*2} - 2J_{f1}J_{f1}^*) + t_\beta^{-2}(J_{f2}^2 + J_{f2}^{*2} - 2J_{f2}J_{f2}^*) \\ & + 2(J_{f1} - J_{f1}^*)(J_{f2} - J_{f2}^*)] + \frac{2}{M_H^2v^2}(t_\beta^2J_{c1}J_{c1}^* + t_\beta^{-2}J_{c2}J_{c2}^* + J_{c1}J_{c2} + J_{c1}^*J_{c2}^*) \end{aligned} \quad (7.56)$$

We end the discussion in this section with some general remarks:

- We have shown that upon integrating out the heavy scalars in the nondecoupling limit the resulting EFT takes the form of a nonlinear EFT. Characteristic for a nonlinear EFT are all-order Higgs function $F(h)$ which arise here due to the contributions of the function $H_0(h)$.
- Although the LO Lagrangian is of $\mathcal{O}(1)$ in the $1/M_S$ expansion, it contains terms of arbitrary canonical dimensions because the nonlinear EFT is organized by chiral dimensions. It is easy to check that every term in the LO Lagrangian has chiral dimension 2 where m_h comes with one unit of chiral dimension.
- The NLO terms in (7.56) all have chiral dimension four and are suppressed by v^2/M_S^2 . To cover all NLO terms, the contributions from one-loop diagrams in the full model would need to be included. They are suppressed by a loop factor $1/16\pi^2$ that is of similar size as v^2/M_S^2 in the nondecoupling limit ($M_S \sim 4\pi v$).

7.2.2. Other Yukawa interactions

Apart from the type II Yukawa sector there are three other possibilities without FCNCs at the tree level. We have

(a) Type I

$$\mathcal{L}_Y = -\bar{q}_L Y_d S_2 P_{-qR} - \bar{q}_L Y_u S_2 P_{+qR} - \bar{l}_L Y_l S_2 P_{-lR} + \text{h.c.} \quad (7.57)$$

(b) Type-X (lepton specific)

$$\mathcal{L}_Y = -\bar{q}_L Y_d S_2 P_{-qR} - \bar{q}_L Y_u S_2 P_{+qR} - \bar{l}_L Y_l S_1 P_{-lR} + \text{h.c.} \quad (7.58)$$

(c) Type-Y (flipped)

$$\mathcal{L}_Y = -\bar{q}_L Y_d S_1 P_{-qR} - \bar{q}_L Y_u S_2 P_{+qR} - \bar{l}_L Y_l S_2 P_{-lR} + \text{h.c.} \quad (7.59)$$

The matching for the other Yukawa structures can be easily inferred from our matching results. For example, in a type I 2HDM all fermions couple exclusively to S_2 such that the matching will have the same form as the up-type terms

$$\mathcal{M}_{u,d,e} + \sum_{n=1}^{\infty} \mathcal{M}_{u,d,e}^{(n)} \left(\frac{h}{v}\right)^n =$$

$$\mathcal{M}_{u,d,e} \left[1 + \frac{c_\alpha h}{s_\beta v} - \frac{c_{\beta-\alpha}}{2} \frac{s_\alpha^2 c_\alpha}{s_\beta^2 c_\beta} \left(\frac{h}{v} \right)^2 - \frac{c_{\beta-\alpha}}{6} \frac{s_{2\alpha}^2}{s_{2\beta}^2} (2s_{2\alpha} - (1 - 2c_{2\alpha})t_\beta^{-1}) \left(\frac{h}{v} \right)^3 + \dots \right] \quad (7.60)$$

7.2.3. Four-fermion operators in the alignment limit

We have already seen that the NLO Lagrangian at $\mathcal{O}(M_S^{-2})$ contains four-fermion operators. From the explicit solution to the leading-order equation of motion (see Section 7.9) we know that $H_0(h)$ vanishes in the alignment limit ($c_{\beta-\alpha} = 0$). In that case the leading EFT effects are four-fermions operators of canonical dimension 6 and chiral dimension 4 that arise from integrating out the heavy scalars at tree level. We can use (7.32) and set $H_0(h) = 0$ and get

$$H_1 = \frac{\bar{J}_1}{M_0^2(1 - 2J_2^0)} \supset \frac{1}{v^2 M_0^2} (-t_\beta (J_{f1} + J_{f1}^*) + t_\beta^{-1} (J_{f2} + J_{f2}^*)) \quad (7.61)$$

where we retain only the fermion currents in the following. Since we are working at $\mathcal{O}(M_S^{-2})$ the pseudoscalar A_0 and the charged scalar H^\pm also contribute. Their equations of motions can be solved iteratively as well and we find

$$A_0 = \frac{i}{v^2 M_A^2} (t_\beta (J_{f1} - J_{f1}^*) + t_\beta^{-1} (J_{f2} - J_{f2}^*)) + \mathcal{O}(M_A^{-4}) \quad (7.62)$$

and

$$H^- = \frac{\sqrt{2}}{v M_H^2} (t_\beta J_{c1} + t_\beta^{-1} J_{c2}^*) + \mathcal{O}(M_H^{-4}) \quad (7.63)$$

The fermion currents were defined in (7.20).

Plugging these solutions back into the Lagrangian and keeping only four-fermion operators we get

$$\begin{aligned} \mathcal{L}_{4fermion} = & \frac{1}{2M_0^2 v^2} [t_\beta^2 (J_{f1}^2 + J_{f1}^{*2} + 2J_{f1} J_{f1}^*) + t_\beta^{-2} (J_{f2}^2 + J_{f2}^{*2} + 2J_{f2} J_{f2}^*) \\ & - 2(J_{f1} + J_{f1}^*)(J_{f2} + J_{f2}^*)] - \frac{1}{2M_A^2 v^2} [t_\beta^2 (J_{f1}^2 + J_{f1}^{*2} - 2J_{f1} J_{f1}^*) \\ & + t_\beta^{-2} (J_{f2}^2 + J_{f2}^{*2} - 2J_{f2} J_{f2}^*) + 2(J_{f1} - J_{f1}^*)(J_{f2} - J_{f2}^*)] \\ & + \frac{2}{M_H^2 v^2} (t_\beta^2 J_{c1} J_{c1}^* + t_\beta^{-2} J_{c2} J_{c2}^* + J_{c1} J_{c2} + J_{c1}^* J_{c2}^*) \end{aligned} \quad (7.64)$$

To see which independent four-fermion operators appear we evaluate the various terms and reduce them to the basis operators in [37].

$$J_{f1}^2 = \mathcal{M}_d \otimes \mathcal{M}_d \mathcal{O}_{FY3} + \mathcal{M}_e \otimes \mathcal{M}_e \mathcal{O}_{FY10} + 2\mathcal{M}_d \otimes \mathcal{M}_e \mathcal{O}_{FY9} \quad (7.65)$$

$$J_{f2}^2 = \mathcal{M}_u \otimes \mathcal{M}_u \mathcal{O}_{FY1} \quad (7.66)$$

$$\begin{aligned} J_{f1} J_{f1}^* = & -\mathcal{M}_d \tilde{\otimes} \mathcal{M}_d \left[\frac{1}{12} \mathcal{O}_{LR3} + \frac{1}{2} \mathcal{O}_{LR4} - \frac{1}{6} \mathcal{O}_{LR12} - \mathcal{O}_{LR13} \right] \\ & - \mathcal{M}_e \tilde{\otimes} \mathcal{M}_e \left[\frac{1}{4} \mathcal{O}_{LR8} - \frac{1}{2} \mathcal{O}_{LR17} \right] - \mathcal{M}_d \tilde{\otimes} \mathcal{M}_e \left[\frac{1}{4} \mathcal{O}_{LR9} - \frac{1}{2} \mathcal{O}_{LR18} + \text{h.c.} \right] \end{aligned} \quad (7.67)$$

$$J_{f2}J_{f2}^* = -\mathcal{M}_u\tilde{\otimes}\mathcal{M}_u\left[\frac{1}{12}\mathcal{O}_{LR1} + \frac{1}{2}\mathcal{O}_{LR2} + \frac{1}{6}\mathcal{O}_{LR10} + \mathcal{O}_{LR11}\right] \quad (7.68)$$

$$J_{f1}J_{f2}^* = \mathcal{M}_d\otimes\mathcal{M}_u\mathcal{O}_{FY5} + \mathcal{M}_e\otimes\mathcal{M}_u\mathcal{O}_{FY7} \quad (7.69)$$

$$J_{f1}J_{f2} = \mathcal{M}_d\otimes\mathcal{M}_u\mathcal{O}_{ST5} + \mathcal{M}_e\otimes\mathcal{M}_u\mathcal{O}_{ST9} \quad (7.70)$$

$$\begin{aligned} |J_{c1}|^2 = & -\mathcal{M}_d\tilde{\otimes}\mathcal{M}_d\left[\frac{1}{12}\mathcal{O}_{LR3} + \frac{1}{2}\mathcal{O}_{LR4} + \frac{1}{6}\mathcal{O}_{LR12} + \mathcal{O}_{LR13}\right] \\ & -\mathcal{M}_e\tilde{\otimes}\mathcal{M}_e\left[\frac{1}{4}\mathcal{O}_{LR8} + \frac{1}{2}\mathcal{O}_{LR17}\right] -\mathcal{M}_d\tilde{\otimes}\mathcal{M}_e\left[\frac{1}{4}\mathcal{O}_{LR9} + \frac{1}{2}\mathcal{O}_{LR18} + \text{h.c.}\right] \end{aligned} \quad (7.71)$$

$$|J_{c2}|^2 = -\mathcal{M}_u\tilde{\otimes}\mathcal{M}_u\left[\frac{1}{12}\mathcal{O}_{LR1} + \frac{1}{2}\mathcal{O}_{LR2} - \frac{1}{6}\mathcal{O}_{LR10} - \mathcal{O}_{LR11}\right] \quad (7.72)$$

$$J_{c1}J_{c2} = \mathcal{M}_d\otimes\mathcal{M}_u\mathcal{O}_{ST6} + \mathcal{M}_e\otimes\mathcal{M}_u\mathcal{O}_{ST10} \quad (7.73)$$

where we employ the notation of Ref. [196]

$$\begin{aligned} \mathcal{F}^{(1)}\otimes\mathcal{F}^{(2)}\mathcal{O} &= \mathcal{F}_{ij}^{(1)}\mathcal{F}_{kl}^{(2)}\bar{\psi}_i\dots\psi_j\bar{\psi}_k\dots\psi_l \\ \mathcal{F}^{(1)}\tilde{\otimes}\mathcal{F}^{(2)}\mathcal{O} &= \mathcal{F}_{il}^{(1)}\mathcal{F}_{kj}^{(2)}\bar{\psi}_i\dots\psi_j\bar{\psi}_k\dots\psi_l \end{aligned} \quad (7.74)$$

for a four-fermion operator $\mathcal{O} \equiv \bar{\psi}_i\dots\psi_j\bar{\psi}_k\dots\psi_l$ and i, j, k, l are generation indices. In addition, we took the fermion mass matrices as hermitean. Summarizing we can conclude that the following operators (and their hermitean conjugates) are generated at tree level

$$\begin{aligned} & \mathcal{O}_{LR1}, \mathcal{O}_{LR2}, \mathcal{O}_{LR3}, \mathcal{O}_{LR4}, \mathcal{O}_{LR8}, \mathcal{O}_{LR9}, \mathcal{O}_{LR10}, \mathcal{O}_{LR11}, \mathcal{O}_{LR12}, \mathcal{O}_{LR13}, \mathcal{O}_{LR17}, \mathcal{O}_{LR18}, \\ & \mathcal{O}_{ST5}, \mathcal{O}_{ST6}, \mathcal{O}_{ST9}, \mathcal{O}_{ST10}, \mathcal{O}_{FY1}, \mathcal{O}_{FY3}, \mathcal{O}_{FY5}, \mathcal{O}_{FY7}, \mathcal{O}_{FY9}, \mathcal{O}_{FY10} \end{aligned} \quad (7.75)$$

In addition to the operators generated in the heavy Higgs model [40] and the singlet extension [119], there are two additional operators with explicit factors of P_{12} and P_{21} due to charged scalar exchange

$$\mathcal{O}_{ST6} = \bar{q}_L U P_{21} q_R \bar{q}_L U P_{12} q_R, \quad \mathcal{O}_{ST10} = \bar{q}_L U P_{21} q_R \bar{l}_L U P_{12} l_R \quad (7.76)$$

Moreover, the result will serve as a cross check for our matching result from Section 5.4.2. In the decoupling limit we can treat the heavy scalar masses as degenerate when working up to the canonical dimension 6 as $M_0, M_A, M_H = \bar{m} + \mathcal{O}(v)$. As a result several terms cancel between the three contributions and we obtain the compact expression

$$\mathcal{L}_{4fermion} = \frac{2}{\bar{m}^2 v^2} (t_\beta^2 (|J_{f1}|^2 + |J_{c1}|^2) + t_\beta^{-2} (|J_{f2}|^2 + |J_{c2}|^2) + J_{f1}J_{f2} + J_{c1}J_{c2} + \text{h.c.}) \quad (7.77)$$

Plugging in our results from (7.65) to (7.73) we end up with

$$\begin{aligned} \mathcal{L}_{4fermion} = & -\frac{t_\beta^2}{\bar{m}^2 v^2} \left\{ \mathcal{M}_d\tilde{\otimes}\mathcal{M}_d\left[\frac{1}{3}\mathcal{O}_{LR3} + 2\mathcal{O}_{LR4}\right] + \mathcal{M}_e\tilde{\otimes}\mathcal{M}_e\mathcal{O}_{LR8} \right. \\ & \left. + \mathcal{M}_d\tilde{\otimes}\mathcal{M}_e[\mathcal{O}_{LR9} + \text{h.c.}] \right\} - \frac{t_\beta^{-2}}{\bar{m}^2 v^2} \mathcal{M}_u\tilde{\otimes}\mathcal{M}_u\left[\frac{1}{3}\mathcal{O}_{LR1} + 2\mathcal{O}_{LR2}\right] \end{aligned}$$

$$+ \mathcal{M}_d \otimes \mathcal{M}_u [\mathcal{O}_{ST5} + \mathcal{O}_{ST6} + \text{h.c.}] + \mathcal{M}_e \otimes \mathcal{M}_u [\mathcal{O}_{ST9} + \mathcal{O}_{ST10} + \text{h.c.}] \quad (7.78)$$

Picking out the term $\propto t_\beta^{-2}$ and focusing only on third generation quark reproduces our result from (5.127)

$$\mathcal{L}_{4\text{fermion}} \supset -\frac{t_\beta^{-2} m_t^2}{v^2 \bar{m}^2} \left(\frac{1}{3} \bar{q}_L \gamma^\mu q_L \bar{t}_R \gamma^\mu t_R + 2 \bar{q}_L \gamma^\mu T^A q_L \bar{t}_R \gamma^\mu T^A t_R \right) \quad (7.79)$$

7.3. Nondecoupling effects at one loop

While the calculation of the complete one-loop effective Lagrangian resulting from integrating out the heavy scalars is beyond the scope of this work, we calculate in the following a particularly important class of one-loop effects. Integrating out the heavy charged scalar H^\pm at one-loop generates local operators inducing $h \rightarrow \gamma\gamma$ and $h \rightarrow \gamma Z$ transitions. Since these processes are loop-suppressed in the SM, the EFT corrections appear at the same chiral order as the leading contributions.

7.3.1. Functional matching

To perform the functional integration over the \tilde{H}^\pm fluctuations we use the methods discussed in chapter 4. Expanding the Lagrangian up to quadratic order in \tilde{H}^\pm gives us

$$\mathcal{L}_{\tilde{H}^\pm}^{(2)} = \tilde{H}^+ \Delta \tilde{H}^-, \quad \Delta = -D^2 - M_H^2 - U \quad (7.80)$$

where $D_\mu = \partial_\mu + X_\mu$ and

$$X_\mu = ieA_\mu + i\frac{g}{2c_W}(1 - 2s_W^2)Z_\mu \quad (7.81)$$

$$-U = d_5 h + d_7 H + z_6 h^2 + z_7 h H + z_8 H^2 \quad (7.82)$$

Here e is the electromagnetic coupling, $s_W = \sin \theta_W$, $c_W = \cos \theta_W$ with the Weinberg angle θ_W , A the photon and Z the Z-boson field. We have seen in Chapter (4) that the Gaussian integration results in the following expression

$$\mathcal{L}_{eff} = -ic_s \sum_{n=1}^{\infty} \frac{1}{n} \int \frac{d^4 p}{(2\pi^4)} \left\langle \left(\frac{2ip \cdot D + D^2 + U}{p^2 - M_H^2} \right)^n \right\rangle \quad (7.83)$$

It is important to realize that for a strongly-coupled scenario the series in (7.83) does not converge in the sense that only a finite number of terms will contribute at any given order in the $1/M_H$ expansion. Since $U \sim M_H^2$ in our case, which is of the same order as the denominator $p^2 - M_H^2$, an infinite number of terms in the sum over n contributes at a given order in the $1/M_H$ expansion. However, there are only finitely many terms at any given order in the Higgs field h , since $U^n = \mathcal{O}(h^n)$. As a result, every EFT operator Q is accompanied by a Higgs-function $F_Q(h)$ as is characteristic for the Higgs-electroweak chiral Lagrangian. At any given order in h^n the operator coefficient is well-defined and calculable.

In a weakly-coupled model of the heavy sector, on the contrary, a generic matrix U scales

as $\mathcal{O}(M_S)$ such that only a finite number of terms contribute at a given order in the $1/M_H$ expansion.

The relevant terms of the UOLEA contain two field strengths and, a priori, arbitrary powers of h . Here we neglect, however, contributions with four or more powers of h and thus need to retain only terms of order \hat{U} and \hat{U}^2 . The corresponding terms of the UOLEA are [129]

$$\begin{aligned} \mathcal{L}_{eff} = \frac{c_s}{(4\pi)^2} \left[-\frac{1}{12M_H^2} \langle \hat{U} \hat{X}_{\mu\nu} \hat{X}^{\mu\nu} \rangle + \frac{1}{24M_H^4} \left(\frac{4}{5} \langle \hat{U}^2 \hat{X}_{\mu\nu} \hat{X}^{\mu\nu} \rangle + \frac{1}{5} \langle (\hat{U} \hat{X}_{\mu\nu})^2 \rangle \right) \right. \\ \left. - \frac{1}{60M_H^6} \left(\frac{2}{3} \langle \hat{U}^2 \hat{X}_{\mu\nu} \hat{U} \hat{X}^{\mu\nu} \rangle + \langle \hat{U}^3 (\hat{X}_{\mu\nu})^2 \rangle \right) \right] \end{aligned} \quad (7.84)$$

We can specialize to our case with $c_s = 1$ for a complex scalar and $\hat{U}, \hat{X}_{\mu\nu} \propto \mathbb{1}$

$$\mathcal{L}_{eff} = -\frac{X_{\mu\nu} X^{\mu\nu}}{192\pi^2} \left[\frac{U}{M_H^2} - \frac{U^2}{2M_H^4} + \frac{U^3}{3M_H^6} + \mathcal{O}(h^4) \right] \quad (7.85)$$

To capture the nondecoupling effects we only need the part of $U \sim M_H^2$ and express H_0 through h via the LO equation of motion

$$\frac{U}{M_H^2} = -d_{5H}h - d_{7H}H_0(h) - z_{6H}h^2 - z_{7H}hH_0(h) - z_{8H}H_0(h)^2 \quad (7.86)$$

Here we introduced the notation

$$d_i = M_H^2 d_{iH} + M_0^2 d_{i0} + \bar{d}_i, \quad z_i = M_H^2 z_{iH} + M_0^2 z_{i0} + \bar{z}_i \quad (7.87)$$

where

$$\begin{aligned} d_{5H} &= -2s_{\beta-\alpha}, & d_{7H} &= -2c_{\beta-\alpha}, & z_{6H} &= -s_{\beta-\alpha}^2, \\ z_{7H} &= -2s_{\beta-\alpha}c_{\beta-\alpha}, & z_{8H} &= -c_{\beta-\alpha}^2 \end{aligned} \quad (7.88)$$

Note that the dependence of d_5, d_7 and z_6, z_7, z_8 on M_0 cancels at every order of h in U . In addition, h needs to be expressed in terms of the canonically normalized Higgs field \tilde{h} using $h(\tilde{h})$ (7.42). However, for the first two terms of $F_X(h)$ through order h^2 the field redefinition plays no role. Inserting $H_0(h)$ and retaining terms up to $\mathcal{O}(h^3)$ we get

$$\begin{aligned} \frac{U(h)}{M_H^2} &= -vd_{5H}\frac{h}{v} - v^2(z_{6H} + d_{7H}d_{20})\frac{h^2}{v^2} \\ &+ v^3 \left(\frac{2}{3}d_{20}^2d_{5H} - d_{20}d_{30}d_{7H} - d_{20}z_{7H} \right) \frac{h^3}{v^3} + \mathcal{O}(h^4) \end{aligned} \quad (7.89)$$

which gives the effective Lagrangian

$$\mathcal{L}_{eff} = -\frac{X_{\mu\nu} X^{\mu\nu}}{192\pi^2} \left[-vd_{50}\frac{h}{v} - v^2 \left(\frac{d_{5H}^2}{2} + z_{6H} + d_{7H}d_{20} \right) \frac{h^2}{v^2} \right. \quad (7.90)$$

$$\left. + v^3 \left(\frac{2}{3}d_{20}^2d_{5H} - d_{20}d_{30}d_{7H} - d_{20}z_{7H} \right) \frac{h^3}{v^3} + \mathcal{O}(h^4) \right] \quad (7.91)$$

Finally, plugging in the explicit expressions and using trigonometric identities

$$\mathcal{L}_{X,4} = \frac{e^2}{16\pi^2} \left(A_{\mu\nu} A^{\mu\nu} + \frac{1-2s_W^2}{s_W c_W} A_{\mu\nu} Z^{\mu\nu} \right) F_X(h) \quad (7.92)$$

$$\begin{aligned} F_X(h) &= \frac{s_{\beta-\alpha}}{6} \frac{h}{v} - \frac{1}{12} \left(s_{\beta-\alpha}^2 + \frac{s_{2\alpha}}{c_{2\beta}} c_{\beta-\alpha}^2 \right) \left(\frac{h}{v} \right)^2 \\ &\quad - \frac{1}{36} \left[2s_{\beta-\alpha}^2 + c_{\beta-\alpha}^2 s_{\beta-\alpha} \frac{s_{2\alpha}}{s_{2\beta}} \left(-3 + 4 \frac{s_{2\alpha}}{s_{2\beta}} \right) \right] \left(\frac{h}{v} \right)^3 + \mathcal{O}(h^4) \end{aligned} \quad (7.93)$$

where $A_{\mu\nu} = \partial_\mu A_\nu - \partial_\nu A_\mu$, $Z_{\mu\nu} = \partial_\mu Z_\nu - \partial_\nu Z_\mu$. We have shown in (4.23) that the terms of the form $X^2 U^n$ can be calculated for arbitrary n in the case $\hat{U} \propto \mathbb{1}$ and the sum can be performed

$$\mathcal{L}_{eff} = \frac{1}{16\pi^2} \sum_{n=1}^{\infty} \frac{(-1)^n}{12nM_H^{2n}} \langle U^n X_{\mu\nu} X^{\mu\nu} \rangle = \frac{-X_{\mu\nu} X^{\mu\nu}}{192\pi^2} \ln \left(1 + \frac{U(h)}{M_H^2} \right) \quad (7.94)$$

In the alignment limit, this permits us to give a closed form expression of (7.94) to all orders in h . We show in the appendix to this chapter (Sec. 7.9) that $H_0(h)$ vanishes in the alignment limit and U , therefore, reduces to $U/M_H^2 = 2h/v + (h/v)^2$ since $vd_{5H} = -2$ and $v^2 z_{6H} = -1$. Then (7.94) takes the form of (7.92) with the function $F_X(h)$ given by

$$F_X(h) = \frac{1}{6} \ln \left(1 + \frac{h}{v} \right) \quad (7.95)$$

which corresponds to the well-known low-energy theorems [197]. In contrast to the tree-level nondecoupling effects, the loop induced $h \rightarrow \gamma\gamma$ and $h \rightarrow \gamma Z$ terms survive in this limit, which makes them phenomenologically interesting [194, 198] (see Sec. 7.6).

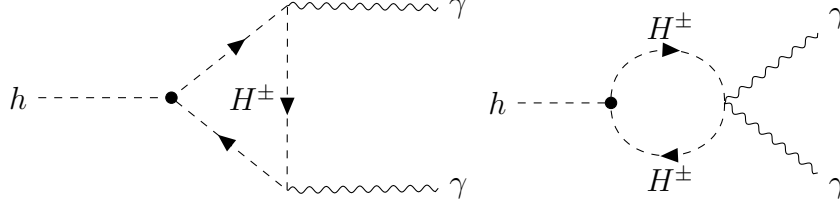
7.3.2. Diagrammatic matching

We now briefly reflect on the preceding calculation. We employed the functional approach to integrate out the charged scalar H^\pm at one loop and presented an algorithm to calculate the coefficients of $F_X(h)$ to arbitrary order in h . All the necessary information came from performing the path integral. Diagrammatic matching on the other hand is much more cumbersome, especially for couplings of the form $h^n A_\mu A^{\mu\nu}$ for large n , since many diagrams and combinatoric factors need to be taken into account. To illustrate this fact, we calculate the coefficient $c_{\gamma\gamma h}$ using the diagrammatic approach. This will serve as a cross check for our result and showcase the elegance and relative simplicity of the functional approach in comparison. A similar matching calculation can be found in [194].

$h \rightarrow \gamma\gamma$

Let us therefore compute the amplitude for the decay $h(q) \rightarrow \gamma(\mu, p_1) + \gamma(\nu, p_2)$ in the full 2HDM and in the EFT. At the one-loop order in the 2HDM we have to consider two

types of diagrams¹



where second triangle graph with reversed momentum flow is understood. The expression for the triangle graph is

$$\begin{aligned}
 & \text{Triangle diagram with momentum } k \text{ in the loop} \\
 & = i\mathcal{M}_{h\gamma\gamma}^{(1)} = -\frac{i}{4\pi^2} e^2 d_5 I_1^{\mu\nu} \quad (7.96)
 \end{aligned}$$

where the loop integral is given by

$$I_1^{\mu\nu} = \int \frac{d^d k}{i\pi^{d/2}} \frac{k^\mu k^\nu}{[k^2 - M_H^2][(k+p_1)^2 - M_H^2][(k-p_2)^2 - M_H^2]} \quad (7.97)$$

The tensor integral can be reduced to Passarino-Veltman scalar integrals, e.g. using **Package-X** [200, 201]

$$I^{\mu\nu} = \left(\frac{M_H^2}{2} C_0(0, 0, q^2; M_H^2, M_H^2, M_H^2) + \frac{1}{4} \right) \left(g^{\mu\nu} - \frac{p_1^\nu p_2^\mu}{p_1 \cdot p_2} \right) + B_0(q^2; M_H^2, M_H^2) \frac{g^{\mu\nu}}{4} \quad (7.98)$$

where we made use of the Ward identities ($\epsilon_\mu^*(p_1)p_1^\mu = \epsilon_\mu^*(p_2)p_2^\mu = 0$). The scalar functions are defined in appendix E. The diagram with reversed momentum flow gives the same result due to charge conjugation invariance. The divergent part of $\mathcal{M}_{h\gamma\gamma}^{(1)}$ is canceled by the bubble diagram so that the final amplitude is finite as required

$$\begin{aligned}
 & \text{Bubble diagram} \\
 & = i\mathcal{M}_{h\gamma\gamma}^{(3)} = \frac{i}{8\pi^2} e^2 d_5 g^{\mu\nu} B_0(q^2; M_H^2, M_H^2) \quad (7.99)
 \end{aligned}$$

In total, we have

$$\mathcal{M}^{\mu\nu} = 2\mathcal{M}_{h\gamma\gamma}^{(1)\mu\nu} + \mathcal{M}_{h\gamma\gamma}^{(3)\mu\nu} = -\frac{\alpha}{2\pi} d_5 F_{H^\pm}(\tau) \left(g^{\mu\nu} - \frac{p_2^\mu p_1^\nu}{p_1 \cdot p_2} \right) \quad (7.100)$$

where the form factor is given by

$$F_{H^\pm}(\tau) = 1 + \frac{1}{4} \frac{f(\tau)}{\tau} = 1 - \frac{\arcsin^2 \sqrt{\tau}}{\tau} \quad (7.101)$$

¹The diagrams in this section of been drawn with **TikZ-Feynman** [199].

The loop function $f(\tau)$ is defined in (E.10) and $\tau = m_h^2/4M_H^2$. For $\tau \ll 1$ we expand

$$F_{H^\pm}(s) = -\frac{\tau}{3} - \frac{8}{45}\tau^2 + \mathcal{O}(\tau^3) \quad (7.102)$$

which yields

$$\mathcal{M}^{\mu\nu} = \frac{\alpha}{2\pi} d_5 \frac{m_h^2}{12M_H^2} \left(g^{\mu\nu} - \frac{p_2^\mu p_1^\nu}{p_1 \cdot p_2} \right) \quad (7.103)$$

To capture the nondecoupling effects we need to take the limit $M_H \rightarrow \infty$

$$\lim_{M_H \rightarrow \infty} \frac{d_5}{M_H^2} = d_{5H} = -2 \frac{s_{\beta-\alpha}}{v} \quad (7.104)$$

such that the 2HDM $h \rightarrow \gamma\gamma$ amplitude in the nondecoupling limit reads

$$\mathcal{M}^{\mu\nu} = -\frac{\alpha}{2\pi} \frac{s_{\beta-\alpha}}{6} \frac{m_h^2}{v} \left(g^{\mu\nu} - \frac{p_2^\mu p_1^\nu}{p_1 \cdot p_2} \right) \quad (7.105)$$

This result has to be equated with the corresponding EwChL amplitude. There the process is given by the local operator at $d_\chi = 4$

$$\mathcal{L}_{h\gamma\gamma} = \frac{\alpha}{4\pi} c_{\gamma\gamma h} \frac{h}{v} A_{\mu\nu} A^{\mu\nu} \quad (7.106)$$

giving rise to the amplitude

$$\mathcal{M}^{\mu\nu} = -\frac{\alpha}{2\pi} c_{\gamma\gamma h} \frac{m_h^2}{v} \left(g^{\mu\nu} - \frac{p_2^\mu p_1^\nu}{p_1 \cdot p_2} \right) \quad (7.107)$$

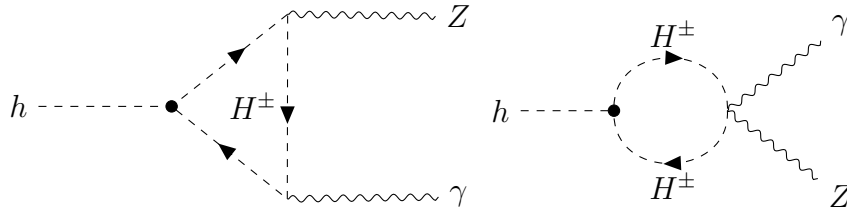
Comparing (7.105) and (7.107), we can read off

$$c_{\gamma\gamma h} = \frac{s_{\beta-\alpha}}{6} \quad (7.108)$$

which gives the same result as before (7.92).

$h \rightarrow \gamma Z$

For the process $h \rightarrow \gamma Z$ we can proceed in a similar way but now one of the bosons in the final state is massive. We have to consider the diagrams



Again a triangle graph with reversed momentum flow is understood. The expression for the triangle graph is

$$h \text{ --- } \bullet \begin{cases} \nearrow \text{---} Z \\ \searrow \text{---} \gamma \end{cases} \quad \begin{matrix} \text{---} k \text{---} \\ \text{---} H^\pm \text{---} \end{matrix} \quad = i\mathcal{M}_{h \rightarrow \gamma Z}^{(1)} = -\frac{i}{16\pi^2} e^2 \frac{1-2s_W^2}{s_W c_W} d_5 I_2^{\mu\nu} \quad (7.109)$$

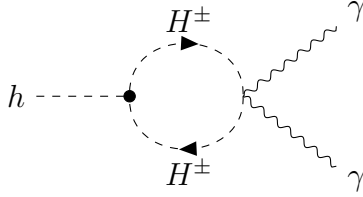
where now the triangle diagram gives rise to the tensor integral

$$I_2^{\mu\nu} = \int \frac{d^d k}{i\pi^{d/2}} \frac{4k^\mu k^\nu - 2k^\mu p_2^\nu}{[k^2 - M_H^2][(k+p_1)^2 - M_H^2][(k-p_2)^2 - M_H^2]} \quad (7.110)$$

Reducing the tensor integral to Passarino-Veltman scalar integral using **Package-X** we get

$$\begin{aligned} I_2^{\mu\nu} = & \left(1 - \frac{m_Z^2}{m_h^2 - m_Z^2} (B_0(m_h^2, M_H^2, M_H^2) - B_0(m_Z^2, M_H^2, M_H^2)) \right. \\ & + 2M_H^2 C_0(0, m_Z^2, m_h^2, M_H^2, M_H^2, M_H^2) \left(g^{\mu\nu} - 2 \frac{p_1^\nu p_2^\mu}{m_h^2 - m_Z^2} \right) \\ & \left. + g^{\mu\nu} B_0(m_h^2, M_H^2, M_H^2) \right) \end{aligned} \quad (7.111)$$

As before the bubble diagram cancels the divergent part of the amplitude such that the final result is finite as required



$$= i\mathcal{M}_{h \rightarrow \gamma Z}^{(3)} = \frac{i}{8\pi^2} e^2 \frac{1 - 2s_W^2}{s_W c_W} d_5 g^{\mu\nu} B_0(m_h^2; M_H^2, M_H^2)$$

(7.112)

The amplitude for the decay process $h(q) \rightarrow \gamma(\mu, p_1) + Z(\nu, p_2)$ for on-shell Higgs is given by

$$\mathcal{M}_{h \rightarrow \gamma Z}^{2HDM} = \epsilon_\mu^*(p_1) \epsilon_\nu^*(p_2) \mathcal{M}^{\mu\nu} \quad (7.113)$$

$$\mathcal{M}^{\mu\nu} = \mathcal{F}_{h\gamma Z}^{H^\pm}(\tau, \sigma) \mathcal{T}^{\mu\nu} \quad (7.114)$$

Here $\epsilon_\mu, \epsilon_\nu$ are the photon and Z polarization vectors respectively, $\tau = m_h^2/4M_H^2$, $\sigma = m_Z^2/4M_H^2$ and we define the tensor

$$\mathcal{T}^{\mu\nu} = g^{\mu\nu} - \frac{2p_1^\nu p_2^\mu}{m_h^2 - m_Z^2} \quad (7.115)$$

The form factor $\mathcal{F}_{h\gamma Z}^{H^\pm}(\tau, \sigma)$ is given by

$$\begin{aligned} \mathcal{F}_{h\gamma Z}^{H^\pm}(\tau, \sigma) = & -\frac{\alpha d_5}{2\pi} \frac{1 - 2s_W^2}{s_W c_W} \left[1 - \frac{m_Z^2}{m_h^2 - m_Z^2} (h(\tau) - h(\sigma)) \right. \\ & \left. + \frac{M_H^2}{m_h^2 - m_Z^2} (f(\tau) - f(\sigma)) \right] \end{aligned} \quad (7.116)$$

where the loop-functions $f(\tau)$ and $h(\tau)$ are defined in the appendix in eqs. (E.10) and (E.6). Expanding the formfactor up to $\mathcal{O}(M_H^{-2})$ we get

$$\mathcal{F}_{h\gamma Z}^{H^\pm} = \frac{\alpha d_5}{2\pi} \frac{1 - 2s_W^2}{s_W c_W} \frac{1}{12} \frac{m_h^2 - m_Z^2}{M_H^2} \quad (7.117)$$

Taking the nondecoupling limit (7.104) we end up with

$$\mathcal{F}_{h\gamma Z}^{H^\pm} = -\frac{\alpha}{2\pi} \frac{1 - 2s_W^2}{s_W c_W} \frac{s_{\beta-\alpha}}{6} \frac{m_h^2 - m_Z^2}{v} \quad (7.118)$$

To perform the matching in the EwCHL we have the $d_\chi = 4$ operator

$$\mathcal{L}_{h\gamma Z} = \frac{\alpha}{4\pi} \frac{1 - 2s_W^2}{s_W c_W} c_{\gamma Zh} \frac{h}{v} A_{\mu\nu} Z^{\mu\nu} \quad (7.119)$$

giving rise to the amplitude

$$\mathcal{M}^{\mu\nu} = -\frac{\alpha}{2\pi} \frac{1 - 2s_W^2}{s_W c_W} c_{\gamma Zh} \frac{m_h^2 - m_Z^2}{v} \left(g^{\mu\nu} - 2 \frac{p_2^\mu p_1^\nu}{m_h^2 - m_Z^2} \right) \quad (7.120)$$

Comparing we get

$$c_{\gamma Zh} = \frac{s_{\beta-\alpha}}{6} \quad (7.121)$$

Let us recap what we just did; we rederived our matching result for the linear coefficient of $F_X(h)$ (7.92) this time using the diagrammatic approach which turned out be much more cumbersome since we had to calculate the full amplitude in each case and then expand in inverse powers of the heavy mass. In the functional approach no such complications are necessary and moreover it provides an algorithm to compute $F_X(h)$ up to arbitrary orders in h

7.4. Custodial symmetry breaking

The scalar potential (7.10) violates custodial symmetry since it contains the term

$$\Delta V_{CSB} = (\lambda_5 - \lambda_4) \langle S_1^\dagger S_2 T_3 \rangle^2 \quad (7.122)$$

Recall that the custodial symmetry group acts on the matrix fields as

$$S_{1,2} \longrightarrow L S_{1,2} L^\dagger, \quad L \in SU(2) \quad (7.123)$$

When the heavy scalars are integrated out, the two-derivative operator

$$\mathcal{L}_{\beta_1} = \beta_1 v^2 \langle U^\dagger D_\mu U T_3 \rangle^2 \quad (7.124)$$

is generated.

The parameter β_1 is related to the parameter T of oblique electroweak corrections [202, 203], $\beta_1 = \alpha T/2$ where α is the Sommerfeld fine structure constant. This can be most easily seen in unitary gauge ($U = 1$) where it takes the form

$$\mathcal{L}_{\beta_1} = -\beta_1 \frac{g^2 v^2}{4c_W^2} Z_\mu Z^\mu \quad (7.125)$$

which is effectively a correction to the Z -mass of $\delta m_Z^2 = -2\beta_1 m_Z^2$. Thus, the ρ -parameter gets a correction

$$\rho = \frac{m_W^2}{c_W^2(m_Z^2 + \delta m_Z^2)} = 1 + 2\beta_1 \quad (7.126)$$

The parameter T of oblique electroweak corrections is defined as

$$T = \frac{\rho - 1}{\alpha} \quad (7.127)$$

which gives the desired result.

Naively it would seem that \mathcal{L}_{β_1} is a LO effect since it has chiral dimension 2. However, it would produce $\mathcal{O}(1)$ corrections to the electroweak T -parameter. Therefore, it cannot be a leading order effect, since empirically such corrections do not exist. Accordingly \mathcal{L}_{β_1} is counted as a NLO operator with chiral dimension 4 [40].

In the following, we compute β_1 explicitly and show that it is generated at the one-loop level. To compute β_1 we employ the functional matching procedure [47] that was discussed in Chapter 4. The relevant part of the 2HDM Lagrangian for our matching calculation is given by

$$\begin{aligned} \mathcal{L} = & \frac{1}{2}\partial_\mu h\partial^\mu h + \frac{1}{2}\partial_\mu H\partial^\mu H + \frac{1}{2}\partial_\mu A_0\partial^\mu A_0 + \partial_\mu H^+\partial^\mu H^- \\ & + J_3^\mu [iH^-\partial_\mu H^+ - iH^+\partial_\mu H^- + c_{\beta-\alpha}(h\partial_\mu A_0 - A_0\partial_\mu h) + s_{\beta-\alpha}(A_0\partial_\mu H - H\partial_\mu A_0)] \\ & + J_+^\mu [A_0\partial_\mu H^+ - H^+\partial_\mu A_0 - ic_{\beta-\alpha}(H^+\partial_\mu h - h\partial_\mu H^+) + is_{\beta-\alpha}(H^+\partial_\mu H - H\partial_\mu H^+)] \\ & + J_-^\mu [A_0\partial_\mu H^- - H^-\partial_\mu A_0 + ic_{\beta-\alpha}(H^-\partial_\mu h - h\partial_\mu H^-) - is_{\beta-\alpha}(H^-\partial_\mu H - H\partial_\mu H^-)] \end{aligned} \quad (7.128)$$

Now we expand the scalar fields into classical background fields and quantum fluctuations

$$\phi \rightarrow \phi + \tilde{\phi} \quad (7.129)$$

Expanding (7.128) up to quadratic order in the fluctuations we arrive at

$$\mathcal{L}^{(2)} = \frac{1}{2} \begin{pmatrix} \tilde{h} & \tilde{H} & \tilde{A}_0 & \tilde{H}^+ & \tilde{H}^- \end{pmatrix} \begin{pmatrix} \Delta_{hh} & 0 & -X_{Ah} & -X_{+h}^\dagger & -X_{-h}^\dagger \\ 0 & \Delta_{HH} & -X_{AH} & -X_{+H}^\dagger & -X_{-H}^\dagger \\ X_{Ah} & X_{AH} & \Delta_{AA} & X_{A-} & X_{A+} \\ X_{+h} & X_{+H} & -X_{A-} & \Delta_{+-} & 0 \\ X_{-h} & X_{-H} & -X_{A+} & 0 & \Delta_{+-}^\dagger \end{pmatrix} \begin{pmatrix} \tilde{h} \\ \tilde{H} \\ \tilde{A}_0 \\ \tilde{H}^- \\ \tilde{H}^+ \end{pmatrix} \quad (7.130)$$

The entries of the fluctuation operator are given by

$$\Delta_{hh} = -\partial^2 - m_h^2 \quad (7.131)$$

$$\Delta_{HH} = -\partial^2 - M_0^2 \quad (7.132)$$

$$\Delta_{AA} = -\partial^2 - M_A^2 \quad (7.133)$$

$$\Delta_{+-} = -\partial^2 - M_h^2 + 2iJ_3^\mu\partial_\mu \quad (7.134)$$

$$X_{Ah} = -2c_{\beta-\alpha}J_3^\mu\partial_\mu \quad (7.135)$$

$$X_{AH} = 2s_{\beta-\alpha}J_3^\mu\partial_\mu \quad (7.136)$$

$$X_{\pm h} = \mp i2c_{\beta-\alpha}J_\pm^\mu\partial_\mu \quad (7.137)$$

$$X_{\pm H} = \pm i2s_{\beta-\alpha}J_\pm^\mu\partial_\mu \quad (7.138)$$

$$X_{\pm A} = -2J_\pm^\mu\partial_\mu \quad (7.139)$$

The fluctuation operator has the schematic form

$$\mathcal{O} = \begin{pmatrix} \Delta_L & -X_{L\mathcal{H}}^\dagger \\ X_{L\mathcal{H}} & \Delta_{\mathcal{H}} \end{pmatrix} \quad (7.140)$$

Following [47] the fluctuation operator can be brought into block-diagonal form

$$\tilde{\mathcal{O}} = \begin{pmatrix} \Delta_L & 0 \\ 0 & \tilde{\Delta}_{\mathcal{H}} \end{pmatrix} \quad (7.141)$$

with $\tilde{\Delta}_{\mathcal{H}} = \Delta_{\mathcal{H}} - (-X_{L\mathcal{H}}^\dagger)\Delta_L^{-1}X_{L\mathcal{H}}$. In our case the modified fluctuation operator for the heavy fields reads

$$\tilde{\Delta}_{\mathcal{H}} = \begin{pmatrix} \Delta_{HH} & -X_{AH} & -X_{+H}^\dagger & -X_{-H}^\dagger \\ X_{AH} & \tilde{\Delta}_{AA} & X_{A-} & X_{A+} \\ X_{+H} & -X_{A-} & \tilde{\Delta}_{+-} & 0 \\ X_{-H} & -X_{A+} & 0 & \tilde{\Delta}_{+-}^\dagger \end{pmatrix} \quad (7.142)$$

with

$$\tilde{\Delta}_{AA} = \Delta_{AA} + X_{Ah}\Delta_{hh}^{-1}X_{Ah} \quad (7.143)$$

$$\tilde{\Delta}_{+-} = \Delta_{+-} + X_{+h}^\dagger\Delta_{hh}^{-1}X_{+h} \quad (7.144)$$

Here Δ_{hh}^{-1} is given by

$$\Delta_{hh}^{-1} = \frac{1}{p^2 - m_h^2} \quad (7.145)$$

It is easy to see that $\tilde{\Delta}_{\mathcal{H}}$ has the generic form

$$\tilde{\Delta}_{\mathcal{H}} = -\partial^2 \mathbb{1} - M^2 - U \quad (7.146)$$

with

$$M^2 = \begin{pmatrix} M_0^2 & 0 & 0 & 0 \\ 0 & M_A^2 & 0 & 0 \\ 0 & 0 & M_H^2 & 0 \\ 0 & 0 & 0 & M_H^2 \end{pmatrix} \quad (7.147)$$

It remains to perform the shift $\partial_x \rightarrow \partial_x + ip$. We will drop henceforth all partial derivatives in U after the shift, since we only need terms of the form J_3^2 . Since the heavy masses are not degenerate the master formula for the EFT Lagrangian in [47] needs to be modified slightly

$$\mathcal{L}_{1loop} = -\frac{i}{2} \sum_{n=1}^{\infty} \frac{1}{n} \int \frac{d^d p}{(2\pi)^d} \text{tr} \left\{ \left((p^2 - M^2)^{-1} U(x, \partial_x + ip) \right)^n \mathbb{1} \right\} \quad (7.148)$$

where

$$(p^2 - M^2)^{-1} = \begin{pmatrix} \frac{1}{p^2 - M_0^2} & 0 & 0 & 0 \\ 0 & \frac{1}{p^2 - M_A^2} & 0 & 0 \\ 0 & 0 & \frac{1}{p^2 - M_H^2} & 0 \\ 0 & 0 & 0 & \frac{1}{p^2 - M_H^2} \end{pmatrix} \quad (7.149)$$

To perform the calculation we need the relations

$$J_3^\mu J_{3\mu} = -\langle U^\dagger D_\mu U T_3 \rangle^2, \quad J_+^\mu J_{-\mu} = \frac{1}{2} \langle U^\dagger D_\mu U T_3 \rangle^2 \quad (7.150)$$

For the contributions arising from heavy-heavy loops we need the integral [204]

$$\begin{aligned} I^{\mu\nu}(A, B) &= \int \frac{d^d p}{(2\pi)^d} \frac{4p^\mu p^\nu}{(p^2 - A)(p^2 - B)} \\ &= \frac{ig^{\mu\nu}}{16\pi^2} \left[A \left(\frac{1}{\epsilon} + \log \frac{\bar{\mu}^2}{A} + 1 \right) + B \left(\frac{1}{\epsilon} + \log \frac{\bar{\mu}^2}{B} + 1 \right) + F(A, B) \right] \end{aligned} \quad (7.151)$$

where the function F is given by

$$F(x, y) = \frac{x+y}{2} - \frac{xy}{x-y} \log \frac{x}{y} \quad (7.152)$$

On the contrary for the heavy-light loop contribution we need

$$\int \frac{d^d p}{(2\pi)^d} \frac{p^\mu p^\nu}{p^2 (p^2 - M^2)} = M^2 \int \frac{d^d p}{(2\pi)^d} \frac{p^\mu p^\nu}{p^4 (p^2 - M^2)} = \frac{iM^2}{(4\pi)^2} \frac{g^{\mu\nu}}{4} \left(\frac{1}{\epsilon} + \log \frac{\bar{\mu}^2}{M^2} + \frac{3}{2} \right) \quad (7.153)$$

We will get contributions to \mathcal{O}_{β_1} from the $n = 1$ and $n = 2$ terms in the sum. The first term is

$$\begin{aligned} \mathcal{L}_{1loop}^{(n=1)} &= \frac{i}{2} \int \frac{d^d p}{(2\pi)^d} \frac{X_{Ah} \Delta_{hh}^{-1} X_{Ah}}{p^2 - M_A^2} + 2 \frac{X_{+h}^\dagger \Delta_{hh}^{-1} X_{+h}}{p^2 - M_H^2} \\ &= \frac{c_{\beta-\alpha}^2}{32\pi^2} \langle U^\dagger D_\mu U T_3 \rangle^2 \\ &\quad \left[(M_H^2 - M_A^2) \left(\frac{1}{\epsilon} + 1 \right) + M_H^2 \log \frac{\bar{\mu}^2}{M_H^2} - M_A^2 \log \frac{\bar{\mu}^2}{M_A^2} + F(m_h^2, M_H^2) - F(m_h^2, M_A^2) \right] \end{aligned} \quad (7.154)$$

The $n = 2$ contribution is given by

$$\begin{aligned} \mathcal{L}^{(n=2)} &= \frac{-i}{4} \left[2s_{\beta-\alpha}^2 J_3^\mu J_3^\nu I_{\mu\nu}(M_A^2, M_0^2) + 4J_+^\mu J_-^\nu I_{\mu\nu}(M_H^2, M_A^2) \right. \\ &\quad \left. + 4s_{\beta-\alpha}^2 J_+^\mu J_-^\nu I_{\mu\nu}(M_H^2, M_0^2) + 2J_3^\mu J_3^\nu I_{\mu\nu}(M_H^2, M_H^2) \right] \end{aligned} \quad (7.155)$$

Inserting the integrals we end up with

$$\begin{aligned} \mathcal{L}^{(n=2)} &= \frac{1}{32\pi^2} \langle U^\dagger D_\mu U T_3 \rangle^2 \left[s_{\beta-\alpha}^2 \left\{ F(M_0^2, M_H^2) - F(M_A^2, M_0^2) \right\} + F(M_A^2, M_H^2) \right. \\ &\quad \left. - c_{\beta-\alpha}^2 \left\{ (M_H^2 - M_A^2) \left(\frac{1}{\epsilon} + 1 \right) + M_H^2 \log \frac{\bar{\mu}^2}{M_H^2} - M_A^2 \log \frac{\bar{\mu}^2}{M_A^2} \right\} \right] \end{aligned} \quad (7.156)$$

We see that the divergent parts cancel precisely between the $n = 1$ and $n = 2$ terms so that the final result reads

$$\mathcal{L}_{\beta_1} = \frac{1}{32\pi^2} \langle U^\dagger D_\mu U T_3 \rangle^2 \left[c_{\beta-\alpha}^2 \left\{ F(m_h^2, M_H^2) - F(m_h^2, M_A^2) \right\} \right]$$

$$+s_{\beta-\alpha}^2 \left\{ F(M_0^2, M_H^2) - F(M_A^2, M_0^2) \right\} + F(M_A^2, M_H^2) \right] \quad (7.157)$$

Our result agrees with the previously obtained expressions in the literature [204, 205]. The phenomenological requirement of approximate custodial symmetry indicates the treatment of the mass difference $M_H^2 - M_A^2 = (v^2/2)(\lambda_5 - \lambda_4)$ as a small coupling with chiral dimension 2. Expand the coefficient of \mathcal{O}_{β_1} to first order in $M_H^2 - M_A^2$ we end up with

$$\mathcal{L}_{\beta_1} = v^2 \frac{\lambda_5 - \lambda_4}{64\pi^2} \langle U^\dagger D_\mu U T_3 \rangle^2 \left[\frac{c_{\beta-\alpha}^2}{2} + s_{\beta-\alpha}^2 \left\{ \frac{1}{2} - \frac{M_0^4}{(M_0^2 - M_H^2)^2} \log \frac{M_0^2}{M_H^2} - \frac{M_0^2 M_H^2}{(M_0^2 - M_H^2)^2} \right\} \right] \quad (7.158)$$

7.5. Parameter Range - Decoupling vs. Nondecoupling Limit

After making use of the decoupling limit various times in this chapter we now offer a detailed discussion of the 2HDM parameter range carefully distinguishing the decoupling and nondecoupling limits.

For the construction of a low-energy EFT, we consider the phenomenologically viable scenario where the masses of the BSM scalar degrees of freedom in the 2HDM are taken to be much larger than the electroweak scale, i.e.

$$M_S \sim M_0, M_H, M_A \gg m_h \sim v \quad (7.159)$$

Depending on the numerical values of the parameters, we can discern two basic scenarios, corresponding to weak and strong coupling, respectively. They are given by

(I) *Nondecoupling regime*² (strong coupling, nonlinear EFT)

$$1 \ll |\lambda_i| \lesssim 16\pi^2, \quad m_h \sim v \sim \bar{m} \ll M_S \quad \implies \quad c_{\beta-\alpha} = \mathcal{O}(1) \quad (7.160)$$

While $c_{\beta-\alpha}$ is a priori unconstrained in this regime, we will also consider the case $c_{\beta-\alpha} \ll 1$, referred to as the *nondecoupling regime with (quasi-)alignment*. We note that calculating the leading EFT effects in this limit is equivalent to setting $\bar{m} = 0$, recovering the \mathbb{Z}_2 symmetric 2HDM without soft breaking. It is well known that this model has no decoupling limit [206, 207].

(II) *Decoupling regime*³ (weak coupling, linear EFT)

$$\lambda_i = \mathcal{O}(1), \quad m_h \sim v \ll \bar{m} \sim M_S \quad \implies \quad c_{\beta-\alpha} \ll 1 \quad (7.161)$$

In the strong-coupling case, we require the λ_i to be somewhat below the nominal strong-coupling limit $M_S \approx 4\pi v$ corresponding to $|\lambda_i| \approx 16\pi^2$. Otherwise a description of the heavy scalar dynamics in terms of resonances would no longer be valid. To be more precise, the magnitude of the couplings is constrained by perturbative unitarity [209–215]. For loop corrections to the constraints, see [216, 217]. Generally speaking, these

²Although not stated explicitly, this limit was used to derive nondecoupling effects in [194].

³This limit has been studied extensively in [208]. The model we consider in this work is simpler because of the additional, softly broken, \mathbb{Z}_2 symmetry $S_1 \rightarrow -S_1$ we imposed.

give much stronger bounds, namely $|\lambda_i| \lesssim 4\pi$. Furthermore, the couplings are constrained such that the potential is bounded from below and that the symmetry breaking vacuum is the global minimum of the potential. For the 2HDM with (softly broken) \mathbb{Z}_2 symmetry, the necessary and sufficient conditions on the couplings read [218–222]

$$\lambda_1 \geq 0, \quad \lambda_2 \geq 0, \quad \lambda_3 \geq -\sqrt{\lambda_1 \lambda_2}, \quad \lambda_3 + \lambda_4 - |\lambda_5| \geq -\sqrt{\lambda_1 \lambda_2} \quad (7.162)$$

To satisfy these bounds, the absolute values of the couplings have to be taken large uniformly, which limits the possible mass splitting between the heavy scalars. Especially the perturbative unitarity constraints severely restrict the possible parameter space of the nondecoupling regime. Nevertheless, masses of $M_S \lesssim 1$ TeV are still possible for $\bar{m} \sim v$, which clearly fulfills the power counting of the nondecoupling regime.

In the decoupling regime, all new physics effects are suppressed by powers of the heavy mass scale M_S as formalized by the Appelquist-Carazzone decoupling theorem [85]. A decoupling regime automatically implies the alignment limit $c_{\beta-\alpha} = 0$. In this limit, the h -couplings approach their SM values [208]. An explicit calculation then gives

$$c_{\beta-\alpha}^2 = \frac{v^4}{16\bar{m}^4} s_{2\beta}^2 [\lambda_1 - \lambda_2 + c_{2\beta}(\lambda_1 + \lambda_2 - 2\lambda_{345})]^2 + \mathcal{O}(v^6/\bar{m}^6) \quad (7.163)$$

with $\lambda_{345} \equiv \lambda_3 + \lambda_4 + \lambda_5$. When $\bar{m} \gg v$, this indeed approaches zero. As mentioned above, there is no similar relation in the nondecoupling regime, and thus, $c_{\beta-\alpha}$ is unconstrained a priori.

There exist various matching calculations in the decoupling limit, see e.g. [193, 223, 224]. In [193], the authors performed matching calculations in the 2HDM to SMEFT and HEFT and reported that they found agreement in the predictions of both EFTs. This is, however, unsurprising since they assumed a decoupling scenario for both the SMEFT and HEFT calculation. In such a weakly coupled scenario, SMEFT and the HEFT are guaranteed to give identical predictions as they differ only by a field redefinition. In particular, SMEFT and HEFT can not be distinguished by whether the heavy degrees of freedom are integrated out before or after spontaneous symmetry breaking.

To illustrate the the two regimes discussed above, we take the hH_0^2 -coupling d_3 as an example. It reads

$$d_3 = -\frac{s_{\beta-\alpha}}{2v} [(m_h^2 + 2M_0^2 - 3\bar{m}^2)(1 - 2c_{\beta-\alpha}^2 + 2s_{\beta-\alpha}c_{\beta-\alpha} \cot 2\beta) + \bar{m}^2] \quad (7.164)$$

In the nondecoupling regime $M_0 \sim M_S \gg m_h, \bar{m}$, so $d_3 = \mathcal{O}(M_S^2)$, whereas in the decoupling regime, the masses and parameters of the model scale as

$$M_0^2, M_H^2, M_A^2 = \bar{m}^2 + \mathcal{O}(v^2), \quad m_h^2 = \mathcal{O}(v^2), \quad c_{\beta-\alpha} = \mathcal{O}(v^2/\bar{m}^2) \quad (7.165)$$

so d_3 reduces to

$$d_3 = -\frac{m_h^2}{2v} - v s_{\beta}^2 c_{\beta}^2 (\lambda_1 + \lambda_2 - 2\lambda_{345}) + \mathcal{O}(v^3/\bar{m}^2) \quad (7.166)$$

Evidently, all heavy mass dependence has canceled. Similar calculations show that this cancellation works for all d_i and z_i . It is now straightforward to see that all nondecoupling effects vanish in the decoupling-regime. Obviously, all tree-level nondecoupling effects vanish in the decoupling limit, since they are all proportional to $c_{\beta-\alpha}$. Also the anomalous $h\gamma\gamma$ - and hZZ -couplings disappear as the ratio d_i as z_i/M_S^2 goes to zero in the limit $M_S \rightarrow \infty$.

Tree Level		Loop Level	
c_V	$s_{\beta-\alpha}$	c_γ	$\frac{s_{\beta-\alpha}}{6}$
c_u	$s_{\beta-\alpha} + c_{\beta-\alpha} t_\beta^{-1}$	$c_{\gamma Z}$	$\frac{1-2s_W^2}{s_W c_W} \frac{s_{\beta-\alpha}}{6}$
c_d	$s_{\beta-\alpha} - c_{\beta-\alpha} t_\beta$	c_g	0

Table 7.1.: LO matching results for the type II 2HDM.

7.6. Phenomenological considerations

To gain insight into the experimental validity of the nondecoupling limit, it is convenient to compare our matching results with a global HEFT fit. Using LHC run I and II data the authors of [225] performed such a fit to constrain the following effective HEFT couplings

$$\begin{aligned} \mathcal{L}_{fit} = & 2c_V \left(m_W W_\mu^+ W_\mu^- + \frac{1}{2} m_Z^2 Z_\mu Z^\mu \right) \frac{h}{v} - \sum_f c_f m_f \bar{\psi} \psi \\ & + \frac{\alpha}{4\pi} c_\gamma A_{\mu\nu} A^{\mu\nu} \frac{h}{v} + \frac{\alpha}{4\pi} c_{\gamma Z} A_{\mu\nu} Z^{\mu\nu} \frac{h}{v} + \frac{\alpha_s}{4\pi} c_g \langle G_{\mu\nu} G^{\mu\nu} \rangle \frac{h}{v} \end{aligned} \quad (7.167)$$

with $\psi \in \{t, b, c, \tau, \mu\}$. We summarize our matching results in table 7.1. From [225] several conclusions can be drawn. First of all, the (quasi-) alignment limit appears to be valid, since the fit result for the Higgs-vector boson coupling c_V gives a constraint for $s_{\beta-\alpha}$

$$c_V = 1.01 \pm 0.06 \implies s_{\beta-\alpha} \gtrsim 0.95 \quad (7.168)$$

where the error is given in the 68% probability interval. Thus, we can infer $c_{\beta-\alpha} \ll 1$ and see that the (quasi-)alignment limit is phenomenologically realized. Using our matching result for the anomalous Higgs-photon coupling and the constraint for $s_{\beta-\alpha}$, we find

$$c_\gamma \in [0.16, 0.17] \quad (7.169)$$

This coupling is bounded from below in the alignment limit ($c_\gamma = 1/6$) and as such particularly important. The global HEFT fit cites the following bound for c_γ

$$c_\gamma = 0.05 \pm 0.20 \quad (7.170)$$

We see that our matching result lies within the error bounds and, thus, consistent. If the constraints on c_γ could be further narrowed, e.g. with more data from the LHC, the nondecoupling regime could be excluded experimentally. In principle, a photon collider could probe local couplings of the form $h^2 A_{\mu\nu} A^{\mu\nu}$ through processes such as $\gamma\gamma \rightarrow hh$. Much stronger bounds for $s_{\beta-\alpha}$ can be obtained by using global fits for the 2HDM [226, 227] instead of using an EFT approach. However, a detailed analysis lies beyond the scope of this work.

7.7. Linear EFT

After tackling the nondecoupling limit, let us now consider the decoupling limit. Here it is convenient to work in the Higgs basis (5.105), since to leading order in the EFT

expansion the heavy states are all contained in the doublet H_2 while the doublet H_1 can be identified with the SM Higgs doublet. Thus, to obtain the low-energy EFT we can easily integrate out H_2 at tree level, i.e. solve its (classical) equation of motion and plug it back into the Lagrangian. The resulting linear EFT is SMEFT and we can thus compute the matching to the Warsaw basis [24]. The dominant EFT effects arise from canonical dimension 6 terms. This has already been discussed in [193, 224, 228].

In the Higgs basis the potential takes the following form

$$\begin{aligned} V = & Y_1 H_1^\dagger H_1 + Y_2 H_2^\dagger H_2 + Y_3 \left(H_1^\dagger H_2 + H_2^\dagger H_1 \right) \\ & + \frac{Z_1}{2} (H_1^\dagger H_1)^2 + \frac{Z_2}{2} (H_2^\dagger H_2)^2 + Z_3 (H_1^\dagger H_1) (H_2^\dagger H_2) + Z_4 (H_1^\dagger H_2) (H_2^\dagger H_1) \\ & + \left[\frac{Z_5}{2} (H_1^\dagger H_2)^2 + \left(Z_6 (H_1^\dagger H_1) + Z_7 (H_2^\dagger H_2) \right) (H_1^\dagger H_2) + \text{h.c.} \right] \end{aligned} \quad (7.171)$$

where the coefficients are given by

$$Y_1 = -\frac{m_h^2}{2} + \frac{c_{\beta-\alpha}^2}{2} (m_h^2 - M_0^2) \quad (7.172)$$

$$Y_2 = \bar{m}^2 - \frac{m_h^2}{2} - \frac{1}{2} (M_0^2 - m_h^2) c_{\beta-\alpha} (c_{\beta-\alpha} - 2s_{\beta-\alpha} \cot(2\beta)) \quad (7.173)$$

$$Y_3 = \frac{1}{2} s_{\beta-\alpha} c_{\beta-\alpha} (M_0^2 - m_h^2) \quad (7.174)$$

$$Z_1 = \frac{s_{\beta-\alpha}^2 m_h^2 + c_{\beta-\alpha}^2 M_0^2}{v^2} \quad (7.175)$$

$$Z_3 = \frac{2}{v^2} (M_H^2 - Y_2) \quad (7.176)$$

$$Z_4 = \frac{M_0^2 s_{\beta-\alpha}^2 + m_h^2 c_{\beta-\alpha}^2 + M_A^2 - 2M_H^2}{v^2} \quad (7.177)$$

$$Z_5 = \frac{M_0^2 s_{\beta-\alpha}^2 + m_h^2 c_{\beta-\alpha}^2 - M_A^2}{v^2} \quad (7.178)$$

$$Z_6 = \frac{(m_h^2 - M_0^2) s_{\beta-\alpha} c_{\beta-\alpha}}{v^2} \quad (7.179)$$

The potential stability conditions imply

$$Y_1 = -\frac{1}{2} v^2 Z_1, \quad Y_3 = -\frac{1}{2} v^2 Z_6 \quad (7.180)$$

which can be verified by the explicit expressions. Working in the decoupling limit implies $c_{\beta-\alpha} \ll 1$ and from (7.163) we know

$$c_{\beta-\alpha} = \mathcal{O} \left(\frac{v^2}{\bar{m}^2} \right) \quad (7.181)$$

Identifying $\Lambda = \bar{m}$ as the heavy scale we can trade Y_2 for \bar{m}^2 since $Y_2 = \bar{m}^2 + \mathcal{O}(v^2)$. Now we can integrate out H_2 at tree level following the usual steps. The solution to the tree-level equation of motion is given by

$$H_2 = -\frac{Z_6}{\bar{m}^2} H_1 \left(H_1^\dagger H_1 - \frac{v^2}{2} \right) + \mathcal{O} \left(\frac{1}{\bar{m}^4} \right) \quad (7.182)$$

Plugging this back into the Lagrangian (assuming as before a type II Yukawa sector)

$$\begin{aligned}\mathcal{L} = & D_\mu H_1^\dagger D^\mu H_1 - \left(Y_1 - v^4 \frac{Z_6^2}{4Y_2} \right) (H_1^\dagger H_1) - \frac{1}{2} \left(Z_1 + 2v^2 \frac{Z_6^2}{Y_2} \right) (H_1^\dagger H_1)^2 + \frac{Z_6^2}{Y_2} (H_1^\dagger H_1)^3 \\ & - (\bar{q}_L c_\beta H_1 Y_d P_- q_R + \bar{l}_L c_\beta H_1 Y_e P_- l_R + \text{h.c.}) \left[1 + t_\beta \frac{Z_6}{\bar{m}^2} \left(H_1^\dagger H_1 - \frac{v^2}{2} \right) \right] \\ & - (\bar{q}_L s_\beta \tilde{H}_1 Y_u P_- q_R + \text{h.c.}) \left[1 - t_\beta^{-1} \frac{Z_6}{\bar{m}^2} \left(H_1^\dagger H_1 - \frac{v^2}{2} \right) \right]\end{aligned}\quad (7.183)$$

At the order we are working we can identify H_1 with the SM Higgs doublet ϕ . Comparing with the Warsaw basis it is easy to see that the following dimension six operators are generated

$$\begin{aligned}\mathcal{L} = & \frac{C_H}{\Lambda^2} (\phi^\dagger \phi)^3 + \left[\frac{C_{Hu}}{\Lambda^2} (\phi^\dagger \phi) (\bar{q}_L u_R \tilde{\phi}) + \frac{C_{Hd}}{\Lambda^2} (\phi^\dagger \phi) (\bar{q}_L d_R \phi) \right. \\ & \left. + \frac{C_{He}}{\Lambda^2} (\phi^\dagger \phi) (\bar{l}_L e_R \phi) + \text{h.c.} \right]\end{aligned}\quad (7.184)$$

Note that the operators $Q_{H\Box}$ and Q_{HD} are absent. Therefore, it is not necessary to perform a field redefinition to canonically renormalize the kinetic term. The Wilson coefficients for the SMEFT operators are

$$\frac{C_H}{\Lambda^2} = \frac{Z_6^2}{Y_2} = c_{\beta-\alpha}^2 \frac{\bar{m}^2}{v^4} + \mathcal{O}\left(\frac{1}{\Lambda^4}\right) \quad (7.185)$$

$$\frac{C_{Hd}}{\Lambda^2} = -\sqrt{2} \frac{\mathcal{M}_d}{v} t_\beta \frac{Z_6}{Y_2} = \sqrt{2} \frac{\mathcal{M}_d}{v} t_\beta \frac{c_{\beta-\alpha}}{v^2} + \mathcal{O}\left(\frac{1}{\Lambda^4}\right) \quad (7.186)$$

$$\frac{C_{He}}{\Lambda^2} = -\sqrt{2} \frac{\mathcal{M}_e}{v} t_\beta \frac{Z_6}{Y_2} = \sqrt{2} \frac{\mathcal{M}_e}{v} t_\beta \frac{c_{\beta-\alpha}}{v^2} + \mathcal{O}\left(\frac{1}{\Lambda^4}\right) \quad (7.187)$$

$$\frac{C_{Hu}}{\Lambda^2} = \sqrt{2} \frac{\mathcal{M}_u}{v} t_\beta^{-1} \frac{Z_6}{Y_2} = -\sqrt{2} \frac{\mathcal{M}_u}{v} t_\beta^{-1} \frac{c_{\beta-\alpha}}{v^2} + \mathcal{O}\left(\frac{1}{\Lambda^4}\right) \quad (7.188)$$

To bring the Lagrangian to a HEFT-like form we use the exponential parameterization

$$H_1 = \frac{v+h}{\sqrt{2}} U \begin{pmatrix} 0 \\ 1 \end{pmatrix} \quad (7.189)$$

The complete EFT Lagrangian up to terms of order $1/M_S^2$ is given by

$$\begin{aligned}\mathcal{L} = & \mathcal{L}_0 + \frac{1}{2} \partial_\mu h \partial^\mu h - \frac{m_h^2}{2} h^2 + \frac{v^2}{4} \langle D_\mu U^\dagger D^\mu U \rangle \left(1 + 2 \frac{h}{v} + \frac{h^2}{v^2} \right) \\ & - \frac{m_h^2 v^2}{2} \left[(1 - 2\xi^2) \left(\frac{h}{v} \right)^3 + \left(\frac{1}{4} - 3\xi^2 \right) \left(\frac{h}{v} \right)^4 - \frac{3}{2} \xi^2 \left(\frac{h}{v} \right)^5 - \frac{1}{4} \xi^2 \left(\frac{h}{v} \right)^6 \right] \\ & - (J_{f1} + J_{f1}^*) \left[1 + (1 - t_\beta c_{\beta-\alpha}) \left(\frac{h}{v} \right) - \frac{3}{2} t_\beta c_{\beta-\alpha} \left(\frac{h}{v} \right)^2 - \frac{1}{2} t_\beta c_{\beta-\alpha} \left(\frac{h}{v} \right)^3 \right] \\ & - (J_{f2} + J_{f2}^*) \left[1 + (1 + t_\beta^{-1} c_{\beta-\alpha}) \left(\frac{h}{v} \right) + \frac{3}{2} t_\beta^{-1} c_{\beta-\alpha} \left(\frac{h}{v} \right)^2 + \frac{1}{2} t_\beta^{-1} c_{\beta-\alpha} \left(\frac{h}{v} \right)^3 \right]\end{aligned}\quad (7.190)$$

where we defined

$$\xi = c_{\beta-\alpha} \frac{\bar{m}}{m_h} \quad (7.191)$$

Tree level corrections to this Lagrangian are of $\mathcal{O}(M_S^{-4})$. We observe that the Higgs coupling in are reduced with respect to their SM values. In contrast to SM singlet extension the coefficients of the Flare function does not receive corrections since no field redefinition is necessary ($C_{H,kin} = 0$). Also now the Higgs self-couplings are correlated which was not the case before in the nonlinear EFT. In addition, the linear EFT only contains terms up to h^6 in the potential, since it is organized by canonical dimensions and we work up to dimension six. We can further illustrate the difference between linear and nonlinear EFT by looking at the $hh \rightarrow hh$ amplitude [119] at tree level. In the full 2HDM the amplitude is $\mathcal{M} = \mathcal{M}_1 + \mathcal{M}_2$, where

$$\mathcal{M}_1 = 24z_1 - 4d_2^2 \left[\frac{1}{s - M_0^2} + \frac{1}{t - M_0^2} + \frac{1}{u - M_0^2} \right] \quad (7.192)$$

consists of the local, quartic h self-coupling and H_0 boson exchange. Here s, t, u denote the usual Mandelstam variables. The nonlocal contribution from h -exchange is given by

$$\mathcal{M}_2 = -36d_1^2 \left[\frac{1}{s - m_h^2} + \frac{1}{t - m_h^2} + \frac{1}{u - m_h^2} \right] \quad (7.193)$$

\mathcal{M}_2 is the same in the full theory and in the EFT, which is why we concentrate on \mathcal{M}_1 in the following. Integrating out a heavy resonance in the diagrammatic picture implies expanding the propagator

$$\frac{1}{s - M_0^2} = -\frac{1}{M_0^2} \sum_{n=0}^{\infty} \frac{s^n}{M_0^n} \quad (7.194)$$

Making use of the property $s+t+u = 4m_h^2$ and keeping in mind that in the nondecoupling limit $vd_2 \sim M_0^2$ we find

$$\mathcal{M}_1 = 24z_1 + 12 \frac{d_2^2}{M_0^2} + 16 \frac{d_2^2 m_h^2}{M_0^4} \quad (7.195)$$

Inserting the parametrization $d_2 = M_0^2 d_{20} + \bar{d}_2$, $z_1 = M_0^2 z_{10} + \bar{z}_1$

$$\mathcal{M}_1 = 12 \frac{M_0^2}{v^2} (2z_{10} + v^2 d_{20}^2) + 24 \left(\bar{z}_1 + d_{20} \bar{d}_2 + \frac{2}{3} d_{20}^2 m_h^2 \right) + \mathcal{O} \left(\frac{1}{M_0^2} \right) \quad (7.196)$$

The term $\propto M_0^2$ vanishes and taking the limit $M_0 \rightarrow \infty$ gives

$$\mathcal{M}_1 = -12 \frac{m_h^2}{v^2} \left[\frac{1}{4} - \frac{c_{\beta-\alpha}^2}{4s_{2\beta}^2} \left(\frac{1}{6} (7 - 12c_{2(\beta+\alpha)} - 19c_{4\alpha}) - (1 - 2c_{2\alpha}c_{2\beta} - 3c_{4\alpha}) \frac{\bar{m}^2}{m_h^2} \right) \right] \quad (7.197)$$

which reproduces the amplitude from the local h^4 -amplitude coming from (7.44). In the linear EFT on the other hand the couplings scale as

$$d_2 = -\frac{3}{2} c_{\beta-\alpha} \frac{\bar{m}^2}{v}, \quad z_1 = -\frac{1}{8} \frac{m_h^2}{v^2} \left(1 - 3\xi^2 + \mathcal{O} \left(\frac{1}{\Lambda^4} \right) \right) \quad (7.198)$$

Here $v d_2$ is of $\mathcal{O}(1)$ and z_1 includes dimension six corrections such that the expression for the amplitude becomes

$$\mathcal{M}_1 = 24z_1 + 12 \frac{d_2^2}{M_0^2} = -12 \frac{m_h^2}{v^2} \left(\frac{1}{4} - 3\xi^2 \right) \quad (7.199)$$

which reproduces the amplitude from the local, quartic h -vertex in the nonlinear theory (7.190).

7.8. Discussion

In this chapter, we have derived the low-energy EFT at the electroweak scale for the 2HDM in the nondecoupling regime. In this strongly coupled region of parameter space, the resulting EFT takes the form of an electroweak chiral Lagrangian, also known as HEFT or nonlinear EFT. Employing functional methods throughout the matching procedure, we present an algorithm to compute the Higgs-dependent functions characteristic of a nonlinear EFT to arbitrary orders in the Higgs field h . In addition to the results of [2], we include a discussion of tree-level generated four-fermion operators and explicitly compute the coefficient of the custodial symmetry-violating operator Q_{β_1} . To highlight the advantages of the functional approach, we contrast it with the diagrammatic matching procedure by deriving the loop-induced local operators contributing to $h \rightarrow \gamma\gamma$ and $h \rightarrow \gamma Z$ using both methods. These anomalous Higgs-gauge boson couplings exhibit nondecoupling behavior that persists even in the alignment limit, making them promising targets for future experimental tests.

7.9. Appendix: Exact solution for $H_0(h)$

In this appendix, we integrate out the heavy scalar field H by solving its equation of motion. We present an exact analytic solution for the leading-order term $H_0(h)$ of $\mathcal{O}(1)$, that arises from solving the equation of motion at $\mathcal{O}(M_S^2)$. This implies that we can set $A = H^\pm = 0$ in this approximation. The calculation is analogous to the one presented in the Appendix of [119]. To calculate H_0 only terms of $\mathcal{O}(M_S^2)$ need to be retained in the Lagrangian. In this limit (7.2) reads

$$\mathcal{L}_M = -m_{11}^2 \phi_1^2 - m_{22}^2 \phi_2^2 - \frac{\lambda_1}{2} \phi_1^4 - \frac{\lambda_2}{2} \phi_2^4 - \lambda_{345} \phi_1^2 \phi_2^2 \quad (7.200)$$

while $\phi_n^2 \equiv (v_n + h_n)^2/2$ and

$$\begin{aligned} \lambda_1 &= \frac{M_0^2}{v^2} \frac{c_\alpha^2}{c_\beta^2}, \quad \lambda_2 = \frac{M_0^2}{v^2} \frac{s_\alpha^2}{s_\beta^2}, \quad \lambda_{345} \equiv \lambda_3 + \lambda_4 + \lambda_5 = \frac{M_0^2}{v^2} \frac{s_\alpha c_\alpha}{s_\beta c_\beta} \\ m_{11}^2 &= -\frac{M_0^2}{2} \left(c_\alpha^2 + \frac{s_\alpha c_\alpha c_\beta}{s_\beta} \right), \quad m_{22}^2 = -\frac{M_0^2}{2} \left(s_\alpha^2 + \frac{s_\alpha c_\alpha c_\beta}{s_\beta} \right) \end{aligned} \quad (7.201)$$

Expressing the ϕ_n through h and H we obtain

$$\phi_1 = \frac{1}{\sqrt{2}} (c_\beta v + c_\alpha H - s_\alpha h)$$

$$\phi_2 = \frac{1}{\sqrt{2}} (s_\beta v + s_\alpha H + c_\alpha h) \quad (7.202)$$

For convenience we define the combination

$$R^2 = \frac{c_\alpha}{c_\beta} \phi_1^2 + \frac{s_\alpha}{s_\beta} \phi_2^2 \quad (7.203)$$

The Lagrangian (7.200) then takes the form

$$\mathcal{L}_M = \frac{M_0^2}{2} (s_\alpha s_\beta + c_\alpha c_\beta) R^2 - \frac{M_0^2}{2v^2} R^4 \quad (7.204)$$

The equation of motion for H reads

$$\frac{\partial \mathcal{L}}{\partial H} = \frac{\partial \mathcal{L}}{\partial R^2} \frac{\partial R^2}{\partial H} = 0 \quad (7.205)$$

The question is now to determine which factor of the product $\frac{\partial \mathcal{L}}{\partial R^2} \frac{\partial R^2}{\partial H}$ contains the relevant solution $H_0(h)$. Here we are integrating out H at tree level using functional methods, i.e. we solve the equation of motion and reinsert the solution $H_0(h)$ back into the Lagrangian to obtain an effective Lagrangian. This is equivalent to matching all possible tree level diagrams with internal H lines to an effective, low-energy Lagrangian for h . Let us therefore consider a general diagram with H lines only. Recalling the form of the H Lagrangian (7.26), such a general diagram contains a number V_n of vertices $J_n H^n$ ($n = 1, \dots, 4$), P H -field propagators, and L Loops. From the standard topological identities

$$\begin{aligned} 2P &= V_1 + 2V_2 + 3V_3 + 4V_4 \\ L &= P - (V_1 + V_2 + V_3 + V_4) + 1 \end{aligned} \quad (7.206)$$

we can deduce

$$L = V_4 + \frac{V_3 - V_1}{2} + 1 \quad (7.207)$$

As we are working at tree level we may set $L = 0$ and obtain

$$V_1 = V_3 + 2V_4 + 2 \quad (7.208)$$

This relation tells us that $V_1 \geq 2$ since $V_3, V_4 \geq 0$. As a result, the tree-level effective Lagrangian has to start at $\mathcal{O}(J_1^2)$ and H_0 accordingly at $\mathcal{O}(J_1)$. Since $J_1 = \mathcal{O}(h^2)$ we know that $H_0(h) = \mathcal{O}(h^2)$.

Following these considerations we can discard the solution for $H_0(h)$ of the form

$$0 = \frac{\partial R^2}{\partial H} = v + \left(\frac{s_\alpha^2 c_\alpha}{s_\beta} - \frac{s_\alpha c_\alpha^2}{c_\beta} \right) h + \left(\frac{s_\alpha^3}{s_\beta} + \frac{c_\alpha^3}{c_\beta} \right) H \quad (7.209)$$

since it is linear in h .

The relevant solution to the equation of motion, therefore, follows from $\partial \mathcal{L} / \partial R^2 = 0$, which is quadratic in H . It can be written as

$$R^2 = \frac{v^2}{2} (s_\alpha s_\beta + c_\alpha c_\beta) = \frac{v^2}{2} c_{\beta-\alpha} \quad (7.210)$$

This result confirms that the absence of any non-trivial terms of $\mathcal{O}(M_S^2)$ in the effective Lagrangian. From (7.210) it follows that the $H_0(h)$ satisfies $R^2(h, H_0(h)) = \text{const.}$, which, reinserted into (7.204), gives a field-independent, irrelevant constant. From (7.210) we can finally deduce

$$H_0(h) = \frac{v + \left(\frac{s_\alpha^2 c_\alpha}{s_\beta} - \frac{s_\alpha c_\alpha^2}{c_\beta} \right) h}{\frac{s_\alpha^3}{s_\beta} + \frac{c_\alpha^3}{c_\beta}} \left[\sqrt{1 - \frac{\left(\frac{s_\alpha^3}{s_\beta} + \frac{c_\alpha^3}{c_\beta} \right) \left(\frac{s_\alpha c_\alpha^2}{s_\beta} + \frac{s_\alpha^2 c_\alpha}{c_\beta} \right) h^2}{\left(v + \left(\frac{s_\alpha^2 c_\alpha}{s_\beta} - \frac{s_\alpha c_\alpha^2}{c_\beta} \right) h \right)^2}} - 1 \right] \quad (7.211)$$

Furthermore, we note that the combination

$$\frac{s_\alpha c_\alpha^2}{s_\beta} + \frac{s_\alpha^2 c_\alpha}{c_\beta} = -c_{\beta-\alpha} \left[1 - 2c_{\beta-\alpha}^2 + 2c_{\beta-\alpha} s_{\beta-\alpha} \cot(2\beta) \right] \quad (7.212)$$

vanishes in the alignment limit. The square root in (7.211) then reduces to 1 and as a result $H_0(h) = 0$. In conclusion, all tree-level nondecoupling effects vanish in the alignment limit.

8. Anomalous HEFT couplings for Off-shell Higgs in $gg \rightarrow Z_L Z_L$

In the last chapter, we performed a top-down matching calculation and matched the 2HDM in the nondecoupling limit to the Electroweak Chiral Lagrangian. Now, we turn to an example where the HEFT is used as a bottom-up EFT in a high-energy process to parametrize the effects of an unknown UV sector. In this chapter, we analyze (longitudinal) Z -boson production via gluon fusion $gg \rightarrow Z_L Z_L$ with anomalous couplings from the EwChL. Using this process, we illustrate how the EwChL is systematically applied, emphasizing the role of loop orders and chiral dimensions in the selection of operators. In our analysis, we focus especially on the kinematic region where the virtual Higgs boson in the s -channel is highly off-shell. This kinematic region is of particular interest since the effects of some new physics operators grow sharply with increasing center-of-mass energy. We will demonstrate, however, that this behavior should not be taken at face value since EFT corrections should remain small for the effective description to be valid.

Vector boson production via gluon fusion has been widely discussed in the literature. It was suggested to use off-shell Higgs events in $pp \rightarrow ZZ$ to constrain the Higgs decay width [229]. The process $pp \rightarrow ZZ$ has also been studied in a SMEFT context [230]. Recently, there has been renewed interest in HEFT treatments for $gg \rightarrow ZZ$ where the Higgs boson is off-shell [231]. To our knowledge, however, there are no studies in the literature where the HEFT is applied systematically with a non-redundant operator basis. Therefore, our motivation in this chapter is to showcase the consistent application of the Higgs-EwChL rather than providing a detailed phenomenological study. While we do not provide a complete next-to-leading order (NLO) calculation in the EFT, we explain which contributions would be required for such an undertaking.

We calculate the corresponding Goldstone process $gg \rightarrow \varphi^0 \varphi^0$ in this chapter and find that at leading order in the EFT, only three anomalous couplings are needed.

The chapter is organized as follows. In Sec. 8.1, we introduce the anomalous couplings from the electroweak chiral Lagrangian relevant for the process $gg \rightarrow ZZ$ and classify them by their order in the EFT expansion, distinguishing leading from subleading contributions. In Sec. 8.2, we present a warm-up analysis of the $t\bar{t} \rightarrow ZZ$ amplitude, which gives insight into the full $gg \rightarrow ZZ$ amplitude and exposes potential unitarity-violating effects in the EFT. Sec. 8.3 is devoted to the computation of the $gg \rightarrow Z_L Z_L$ amplitude: we include the anomalous couplings, study its asymptotic behavior at large s , and provide a quantitative estimate of the next-to-leading order effects. We discuss phenomenological implications in Sec. 8.4, and Sec. 8.6 collects additional technical details of the calculation as an appendix. This chapter is based on the publication [3], where the author of this thesis is a co-author.

8.1. Effective field theory framework for $gg \rightarrow ZZ$

8.1.1. Electroweak chiral Lagrangian

We employ the Electroweak chiral Lagrangian (HEFT) in this chapter. The HEFT Lagrangian at leading order is defined in (3.21) and (3.23). At next-to-leading order in the chiral counting several new operators enter the process. A basis of NLO operators with chiral dimension four has been compiled in [40], where the operators are divided into seven classes: UhD^2 , UhD^4 , X^2h , $XUhD^2$, ψ^2UhD , ψ^2UhD^2 , and ψ^4Uh . Out of these we list all the operators that can contribute to the process $gg \rightarrow ZZ$ at leading and next-to-leading order in the chiral counting

$$UhD^2 : \quad Q_{\beta_1} = \langle T_3 U^\dagger D_\mu U \rangle^2 \eta \quad (8.1)$$

$$\begin{aligned} UhD^2 : \quad Q_{D1} &= \langle D^\mu U^\dagger D_\mu U \rangle^2, \quad Q_{D2} = \langle D_\mu U^\dagger D_\nu U \rangle \langle D^\mu U^\dagger D^\nu U \rangle \\ Q_{D7} &= \langle D^\mu U^\dagger D_\mu U \rangle \partial_\nu \eta \partial^\nu \eta, \quad Q_{D8} = \langle D_\mu U^\dagger D_\nu U \rangle \partial^\mu \eta \partial^\nu \eta \\ Q_{D11} &= (\partial_\mu \eta \partial^\mu \eta)^2 \end{aligned} \quad (8.2)$$

$$\begin{aligned} X^2h : \quad Q_{Xh1} &= g'^2 B_{\mu\nu} B^{\mu\nu} \eta, \quad Q_{Xh2} = g^2 \langle W_{\mu\nu} W^{\mu\nu} \rangle \eta \\ Q_{Xh3} &= g_s^2 \langle G_{\mu\nu} G^{\mu\nu} \rangle \eta \end{aligned} \quad (8.3)$$

$$\begin{aligned} XUhD^2 : \quad Q_{XU1} &= g' g B_{\mu\nu} \langle W^{\mu\nu} U T_3 U^\dagger \rangle \eta, \quad Q_{XU7} = 2ig' B_{\mu\nu} \langle T_3 D^\mu U^\dagger D^\nu U \rangle \eta \\ Q_{XU7} &= 2ig \langle W_{\mu\nu} D^\mu U D^\nu U^\dagger \rangle \eta \end{aligned} \quad (8.4)$$

$$\begin{aligned} \psi^2UhD : \quad Q_{\psi V1} &= \bar{q}_L \gamma^\mu q_L i \langle T_3 U^\dagger D_\mu U \rangle, \quad Q_{\psi V2} = \bar{q}_L \gamma^\mu U T_3 U^\dagger q_L i \langle T_3 U^\dagger D_\mu U \rangle \\ Q_{\psi V4} &= \bar{u}_R \gamma^\mu u_R i \langle T_3 U^\dagger D_\mu U \rangle, \quad Q_{\psi V5} = \bar{d}_R \gamma^\mu d_R i \langle T_3 U^\dagger D_\mu U \rangle \end{aligned} \quad (8.5)$$

$$\psi^2UhD : \quad Q_{\psi S1} = \bar{q}_L U P_+ q_R \langle D_\mu U^\dagger D^\mu U \rangle, \quad Q_{\psi S2} = \bar{q}_L U P_- q_R \langle D_\mu U^\dagger D^\mu U \rangle \quad (8.6)$$

where we used the notation $\eta \equiv h/v$.

We have omitted to write down the four-fermion operators of class ψ^4Uh , since they contribute only at NNLO. Our operator selection is based on the premise of CP conservation and we have selected the terms with powers of the Higgs field h^n relevant for the process under consideration. In addition, we need to include two NNLO operators at chiral dimension 6 in our analysis

$$Q_{GU1} = g_s^2 \langle G_{\mu\nu} G^{\mu\nu} \rangle \langle D_\lambda U^\dagger D^\lambda U \rangle, \quad Q_{GU2} = g_s^2 \langle G_\mu^\lambda G_{\lambda\nu} \rangle \langle D^\mu U^\dagger D^\nu U \rangle \quad (8.7)$$

which give rise to local $ggZZ$ interactions.

The authors of Ref. [231] use a different set of (redundant) HEFT operators to parametrize new-physics effects in ZZ production. We have explicitly checked that their set can be reduced to our selection of operators using integration by parts and the equation of motion. In addition, they have included $d_\chi = 4$ operators with the explicit custodial-symmetry breaking factor τ_L . Since those factors are accompanied with additional weak coupling factors, we take them as subleading and do not consider them in our analysis.

In the following, we discuss at which order in the EFT the operators listed above enter the amplitude for $gg \rightarrow ZZ$.

8.1.2. EFT applied to $gg \rightarrow ZZ$ - overview

To define the leading order in the EFT expansion it is important to keep in mind that the process is induced at the one-loop order, which therefore constitutes the LO in the EFT. At LO we have to consider all one-loop topologies with any number of LO vertices and all tree diagrams with a single insertion of a NLO vertex. The corresponding diagrams for $gg \rightarrow ZZ$ at LO in the EFT are shown in Figure 8.1. There are the one-loop topologies (a),(b) whereas diagram (c) is a tree graph with a single insertion of a NLO vertex. In

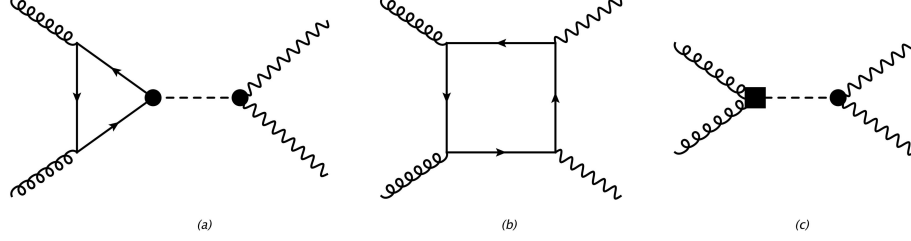


Figure 8.1.: Diagrams for $gg \rightarrow ZZ$ at leading order in the chiral counting. Black circles and black squares denote vertices from the LO and NLO Lagrangian, respectively. Additional diagrams with permutations of the external legs are not explicitly shown.

all diagrams any number of vertices from the LO $d_\chi = 2$ Lagrangian is allowed, but note that diagram (b) does not contain any anomalous couplings, since the gluon-quark and Z -boson-quark interactions are SM-like at LO. It obvious to see from Fig. 8.1 that new physics in $gg \rightarrow ZZ$ is described by three parameters.

Although we will not attempt to provide a complete calculation of EFT corrections at next-to-leading order for $gg \rightarrow ZZ$ we still would like to present an overview over all contributions that would be required in such an analysis. Here next-to-leading order is equivalent to two-loop order in the chiral counting. Representative contributions can be found in Fig. 8.2. The NLO contributions can be divided into three classes: (I) two-loop topologies with an arbitrary number of LO vertices (diagrams (f) and (g)), (II) one-loop topologies with one insertion of a NLO vertex and any number of LO vertices (diagram (a),(b),(c)) and (III) tree graphs with either two insertions of NLO vertices (diagram (d)) or one NNLO vertex (diagram (e)). The operators listed in (8.1)-(8.6) and (8.7) enter the various graphs in Fig. 8.2 as follows

$$\begin{aligned}
 (a) : & Q_{Xh1}, Q_{Xh2}, Q_{XU1} & (d) : & Q_{Xh3}, Q_{Xh1}, Q_{Xh2}, Q_{XU1} \\
 (b) : & Q_{\psi S1}, Q_{\psi S2} & (e) : & Q_{GU1}, Q_{GU2} \\
 (c) : & Q_{\psi V1}, Q_{\psi V2}, Q_{\psi V4}, Q_{\psi V5}
 \end{aligned} \tag{8.8}$$

We have omitted the NLO effect coming from Q_{β_1} since the corresponding vertex has the same form as the hZZ coupling c_Z at leading order and can, therefore, the coefficient C_{β_1} can be absorbed into c_Z as a NLO correction.

Some $d_\chi = 4$ operators contribute to the $gg \rightarrow ZZ$ amplitude only beyond next-to-leading (2-loop) order and, as a result, should be dropped at our level of approximation. Representative example of such cases have been compiled in Fig. 8.3. They come from operators in the class UhD^4 (a), from Q_{XU7} and Q_{XU8} of class $XUhD^2$ (b), and from the 4-fermion interactions of class ψ^4Uh (c). In the chiral counting, these graphs are all of

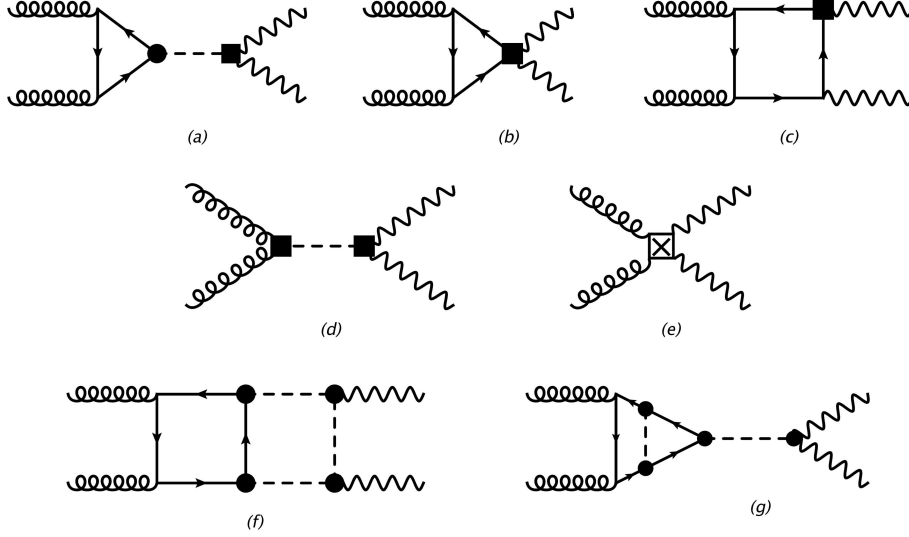


Figure 8.2.: Representative diagrams for $gg \rightarrow ZZ$ at next-to-leading order in the chiral counting. Black circles, black squares and crossed squares denote vertices from the LO, NLO and NNLO Lagrangian, respectively.

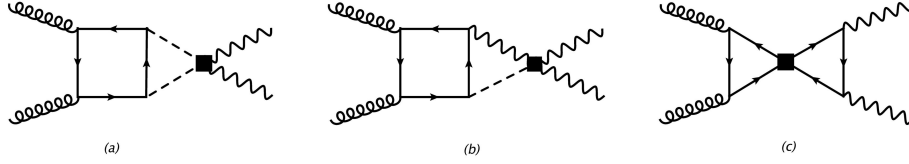


Figure 8.3.: Sample diagrams for $gg \rightarrow ZZ$ with operators from the Lagrangian at chiral dimension 4, which would only contribute at next-to-next-to-leading (3-loop) order to this process. Black squares denote vertices from the NLO Lagrangian, respectively.

three-loop order since a NLO operator is inserted in a two-loop topology diagram. In principle, higher-order QCD corrections [232, 233] could be included. QCD corrections are based on an expansion in the strong coupling g_s and can be discussed independently of the EFT loop expansion. However, this is beyond the scope of this work, which is based on the systematics of the EFT expansion.

The relevant terms from \mathcal{L}_2 and \mathcal{L}_4 entering the $gg \rightarrow ZZ$ amplitude at leading order are

$$\mathcal{L}_{LO,int} = c_V \frac{h}{v} m_Z^2 Z_\mu Z^\mu - \sum_f c_f m_f \bar{f} f \frac{h}{v} + \frac{\alpha_s}{8\pi} c_{ggh} \frac{h}{v} G_{\mu\nu}^A G^{A\mu\nu} \quad (8.9)$$

And next-to-leading order terms from $\mathcal{L}_4 + \mathcal{L}_6$,

$$\begin{aligned} \mathcal{L}_{int,NLO} = & C_{\beta_1} Q_{\beta_1} + C_{Xh1} Q_{Xh1} + C_{Xh2} Q_{Xh2} + C_{XU1} Q_{XU1} \\ & + C_{\psi V1} Q_{\psi V1} + C_{\psi V2} Q_{\psi V2} + C_{\psi V4} Q_{\psi V4} + C_{\psi V5} Q_{\psi V5} \\ & + C_{\psi S1} (Q_{\psi S1} + \text{h.c.}) + C_{\psi S2} (Q_{\psi S2} + \text{h.c.}) + C_{GU1} Q_{GU1} + C_{GU2} Q_{GU2} \quad (8.10) \\ \supset & -C_{\beta_1} m_Z^2 \frac{h}{v} Z_\mu Z^\mu + \frac{\alpha}{8\pi} C_{ZZh} \frac{h}{v} Z_{\mu\nu} Z^{\mu\nu} \\ & - \frac{g}{2c_W} Z_\mu (C_{\psi VL} \bar{t}_L \gamma^\mu t_L + C_{\psi VR} \bar{t}_R \gamma^\mu t_R) + \frac{g^2}{2c_W^2} C_{\psi S1} Z_\mu Z^\mu \bar{t} t \end{aligned}$$

$$+ \frac{g_s^2}{4} \frac{g^2}{c_W^2} C_{GU1} G_{\mu\nu}^A G^{A\mu\nu} Z_\lambda Z^\lambda + \frac{g_s^2}{4} \frac{g^2}{c_W^2} C_{GU2} G_\mu^{A\lambda} G_{\lambda\nu}^A Z^\mu Z^\nu \quad (8.11)$$

where the terms with $C_{GU1,2}$ have $d_\chi = 6$, the others $d_\chi = 4$, and

$$\frac{\alpha}{8\pi} C_{ZZh} \equiv g'^2 s_W^2 C_{Xh1} + \frac{g^2}{2} c_W^2 C_{Xh2} - \frac{gg'}{2} s_W c_W C_{XU1} \quad (8.12)$$

$$C_{\psi VL} \equiv C_{\psi V1} + \frac{1}{2} C_{\psi V2}, \quad C_{\psi VR} \equiv C_{\psi V4} \quad (8.13)$$

In (8.11) we have only retained the top-quark contributions from the operators with fermions since those dominate for longitudinal Z -bosons at high energy. The anomalous Z -fermion gauge couplings, parameterized by $C_{\psi Vi}$ are constrained by electroweak precision LEP measurements [234].

8.2. Anomalous Higgs couplings in $t\bar{t} \rightarrow ZZ$

It is instructive to first investigate the subprocess $t\bar{t} \rightarrow ZZ$ to study perturbative unitarity violation in the full process. The relevant diagrams are displayed in Fig. 8.4. The matrix element for the process $t(k_1)\bar{t}(k_2) \rightarrow Z(p_1, \mu)Z(p_2, \nu)$ is given by

$$\mathcal{M} = g_Z^2 \epsilon_\mu^* \epsilon_\nu^* \mathcal{M}^{\mu\nu} \quad (8.14)$$

Here $\epsilon_\mu, \epsilon_\nu$ are the Z -polarization vectors and

$$\begin{aligned} \mathcal{M}^{\mu\nu} = & - \frac{\bar{v}(k_2) (v_t + a_t \gamma_5) \gamma^\nu (\not{k}_1 - \not{p}_1 + m_t) (v_t + a_t \gamma_5) \gamma^\mu u(k_1)}{t - m_t^2} \\ & - \frac{\bar{v}(k_2) (v_t + a_t \gamma_5) \gamma^\mu (\not{k}_1 - \not{p}_2 + m_t) (v_t + a_t \gamma_5) \gamma^\nu u(k_1)}{u - m_t^2} \\ & + \frac{m_t}{2} c_V c_t \frac{g^{\mu\nu}}{s - m_h^2} \bar{v}(k_2) u(k_1) \end{aligned} \quad (8.15)$$

Here we defined [235]

$$g_Z = \frac{g}{c_W} = 2 \frac{m_Z}{v}, \quad v_t = \frac{1}{4} - \frac{2}{3} s_W^2, \quad a_t = \frac{1}{4} \quad (8.16)$$

In the limit $m_t \rightarrow 0$ the amplitude satisfies the Ward identities $p_{1\mu} \mathcal{M}^{\mu\nu} = p_{2\nu} \mathcal{M}^{\mu\nu} = 0$

The leading contribution to the squared spin-averaged matrix element that is proportional to s is given by

$$\frac{1}{4} \sum_{spins} |\mathcal{M}|^2 = \frac{1}{2} \frac{m_t^2}{v^2} \frac{s}{v^2} (1 - c_t c_V)^2 + \mathcal{O}(s^0) \quad (8.17)$$

It is obvious that this perturbative unitarity violating contribution vanishes in the SM ($c_t = c_V = 1$). In the SM the leading term is the $\mathcal{O}(s^0)$ contribution

$$\frac{1}{4} \sum_{spins} |\mathcal{M}_{SM}|^2 = \frac{1}{162} \frac{m_t^4}{v^4} \frac{1}{ut} [16x_Z^4 (t^2 + u^2) (64s_W^8 - 96s_W^6 + 108s_W^4 - 54s_W^2)]$$

$$+144x_Z^2 s_W^2 (4s_W^2 - 3) s^2 + 162 (x_Z^4 + x_Z^2 + 1) (t^2 + u^2) - 81s^2] + \mathcal{O}(s^{-1}) \quad (8.18)$$

where we used the notation $x_i = m_i/m_t$. We may use Goldstone equivalence to study the behavior of the amplitude for large values of s . In the Goldstone limit the amplitude is given by

$$\begin{aligned} \mathcal{M} = & \frac{m_t}{v^2} \bar{v}(k_2) u(k_1) \left(1 - c_t c_V \frac{s}{s - m_h^2} \right) \\ & + \frac{m_t^2}{v^2} \left(\frac{\bar{v}(k_2) \gamma_5 (\not{k}_1 - \not{p}_1 + m_t) \gamma_5 u(k_1)}{t - m_t^2} + \frac{\bar{v}(k_2) \gamma_5 (\not{k}_1 - \not{p}_2 + m_t) \gamma_5 u(k_1)}{u - m_t^2} \right) \end{aligned} \quad (8.19)$$

Here the the unitarity violating part of the amplitude is directly visible.

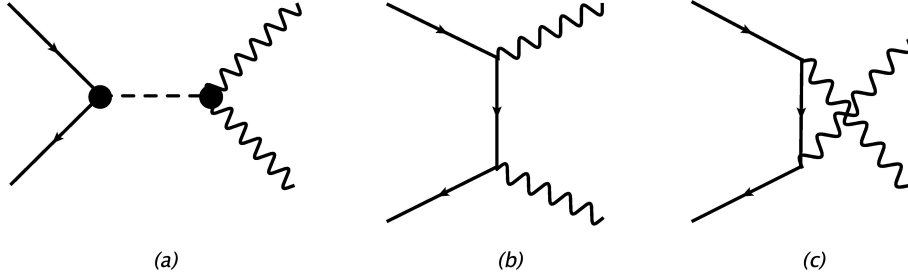


Figure 8.4.: Diagrams for $t\bar{t} \rightarrow ZZ$ at leading order in the chiral counting. Black circles denote vertices from the LO Lagrangian.

8.3. Anomalous Higgs couplings in $gg \rightarrow Z_L Z_L$

In this section, we investigate the process $gg \rightarrow \varphi^0 \varphi^0$, which is by the Goldstone equivalence theorem [188, 236] equivalent to the original process in the high energy limit. We show the diagrams for $gg \rightarrow \varphi^0 \varphi^0$ at leading order in Figs. 8.5 and 8.6. Note the additional topology in diagram (b) of Fig. 8.5 that is not present in the process $gg \rightarrow ZZ$. It reproduces the large s behavior of the box diagrams (b) of Fig. 8.1 and is vital to cancel the unitarity violating part $\propto \ln^2 s$ of the amplitude in the SM.

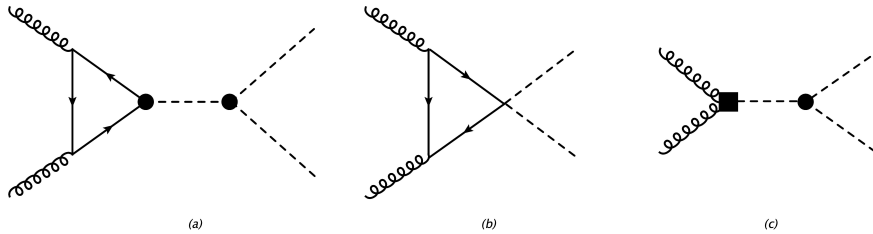


Figure 8.5.: Tree-level and triangle graphs. Black circles and black squares denote vertices from the LO and NLO Lagrangian, respectively. Additional diagrams with permutations of the external legs are not explicitly shown.

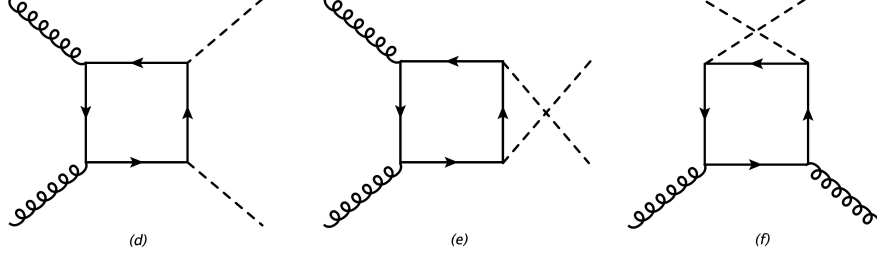


Figure 8.6.: Box graphs, Background

We have collected the relevant couplings entering the leading order Goldstone amplitude in the form of an interaction Lagrangian.

$$\mathcal{L}_{int,LO} = i \frac{m_t}{v} \bar{t} \gamma_5 t \varphi^0 + \frac{m_t}{2v^2} \bar{t} t (\varphi^0)^2 + c_V \partial_\mu \varphi^0 \partial^\mu \varphi^0 \frac{h}{v} - c_t m_t \frac{h}{v} \bar{t} t + \frac{\alpha_s}{8\pi} c_{ggh} \frac{h}{v} G_{\mu\nu}^A G^{A\mu\nu} \quad (8.20)$$

8.3.1. General Structure

The amplitude for the process $g(k_1, \epsilon_1) g(k_2, \epsilon_2) \rightarrow \varphi^0(p_1) \varphi^0(p_2)$ can be decomposed as

$$\mathcal{M}^{AB} = \delta^{AB} \mathcal{M}^{\mu\nu} \epsilon_{1\mu} \epsilon_{2\nu} \quad (8.21)$$

$$\mathcal{M}^{\mu\nu} = \frac{\alpha_s m_t^2}{\pi v^2} (A_1(s, t, u) T_1^{\mu\nu} + A_2(s, t, u) T_2^{\mu\nu}) \quad (8.22)$$

Here k_1, k_2 are the gluon momenta and p_1, p_2 the Goldstone momenta, where

$$k_1^2 = k_2^2 = p_1^2 = p_2^2 = 0 \quad (8.23)$$

and we introduced the usual Mandelstam variables

$$s = (k_1 + k_2)^2, \quad t = (k_1 - p_1)^2, \quad u = (k_2 - p_1)^2 \quad (8.24)$$

The amplitudes with longitudinal polarization $\epsilon_L(p)$ of the Z boson at high energy are related to the Goldstone limit through the replacement $\epsilon_L^\mu(p) \rightarrow ip^\mu/m_Z$. A, B are the color indices and $\epsilon_{1\mu}, \epsilon_{2\nu}$ are the polarization vectors of the gluons. We define the two linearly independent tensor structures

$$T_1^{\mu\nu} = g^{\mu\nu} - \frac{k_1^\nu k_2^\mu}{k_1 \cdot k_2} \quad (8.25)$$

$$T_2^{\mu\nu} = g^{\mu\nu} + \frac{k_1 \cdot k_2}{(k_1 \cdot p_1)(k_2 \cdot p_1)} p_1^\mu p_1^\nu - \frac{k_2^\mu p_1^\nu}{k_2 \cdot p_1} - \frac{p_1^\mu k_1^\nu}{k_1 \cdot p_1} \quad (8.26)$$

They satisfy

$$T_1 \cdot T_2 = 0, \quad T_1 \cdot T_1 = T_2 \cdot T_2 = 2, \quad k_1^\mu T_{\mu\nu}^{1,2} = k_2^\nu T_{\mu\nu}^{1,2} = 0 \quad (8.27)$$

The two factors correspond to two independent helicity configurations. The part proportional A_1 corresponds to the case where the gluon helicities have the same sign, that is, $++$ or $--$, and A_2 encodes the opposite helicity amplitude, i.e. $+-$ and $-+$. This can

be seen by considering an explicit representation of the momenta in the center-of-mass frame

$$k_1^\mu = \frac{\sqrt{s}}{2}(1, 0, 0, 1)^T, \quad k_2^\mu = \frac{\sqrt{s}}{2}(1, 0, 0, -1)^T, \quad p_1^\mu = \frac{\sqrt{s}}{2}(1, 0, \sin \theta, \cos \theta)^T \quad (8.28)$$

Here θ is the scattering angle. The gluon polarization vectors with positive and negative helicity

$$\epsilon_+^\mu(k_1) = \epsilon_-^\mu(k_2) = \frac{1}{\sqrt{2}}(0, 1, i, 0)^T, \quad \epsilon_-^\mu(k_1) = \epsilon_+^\mu(k_2) = \frac{1}{\sqrt{2}}(0, 1, -i, 0)^T \quad (8.29)$$

Thus,

$$\epsilon_\pm^\mu(k_1)\epsilon_\pm^\nu(k_2)T_{1\mu\nu} = -1, \quad \epsilon_\pm^\mu(k_1)\epsilon_\pm^\nu(k_2)T_{2\mu\nu} = 0 \quad (8.30)$$

and

$$\epsilon_\pm^\mu(k_1)\epsilon_\mp^\nu(k_2)T_{2\mu\nu} = -1, \quad \epsilon_\pm^\mu(k_1)\epsilon_\mp^\nu(k_2)T_{1\mu\nu} = 0 \quad (8.31)$$

The helicity amplitudes do not interfere and the spin- and color averaged matrix element squared reads

$$|\overline{\mathcal{M}}|^2 = \frac{\alpha_s^2}{16\pi^2} \frac{m_t^4}{v^4} (|A_1|^2 + |A_2|^2) \quad (8.32)$$

The differential cross section is then given by

$$\frac{d\sigma}{d\cos\theta} = \frac{1}{32\pi s} |\overline{\mathcal{M}}|^2 \quad (8.33)$$

8.3.2. Form factors at leading order

The two form factors at LO in the EFT are given by

$$\begin{aligned} A_1(s, t, u) = & \frac{1}{s - m_h^2} \left(\left[1 - \frac{1}{2} C(s) s \left(1 - \frac{4m_t^2}{s} \right) \right] \left[s(1 - c_t c_V) - m_h^2 \right] - \frac{c_{ggh} c_V}{4m_t^2} s^2 \right) \\ & - \frac{1}{2} [2 + 4m_t^2 C(s) + sm_t^2 (D(s, t) + D(s, u) + D(t, u))] \end{aligned} \quad (8.34)$$

$$\begin{aligned} A_2(s, t, u) = & -\frac{1}{4} \frac{1}{tu} [2s(t^2 + u^2) C(s) + 2t^3 C(t) + 2u^3 C(u) - st^3 D(s, t) - su^3 D(s, u) \\ & + 2stu m_t^2 (D(s, t) + D(s, u) + D(t, u))] \end{aligned} \quad (8.35)$$

Our results are consistent with [235] in the limit $m_Z \rightarrow 0$. For parts of the calculation and cross-checks `FeynCalc` [237–240] and `Package-X` [200, 201] proved useful. The precise definitions of the loop functions C, D are given in the Appendix (E.9), (E.16). The first line of (8.34) comes from the diagrams in Fig. 8.5 while the second line stems from the box diagrams of Fig. 8.6. Only the box diagrams of Fig. 8.6 contribute to A_2 . Details of the calculation are given at the end of this chapter in Sec. 8.6. The impact of the anomalous couplings is most clearly seen in the asymptotic behavior of the form factors for large s . Keeping the scattering angle θ fixed, the variables t and u scale with s for $s \rightarrow \infty$. In this limit one finds

$$A_1(s) = -1 + \left[-\frac{1}{4} \log^2 \frac{-s}{m_t^2} + 1 \right] (1 - c_t c_V) - c_{ggh} c_V \frac{s + m_h^2}{4m_t^2} + \mathcal{O}\left(\frac{1}{s}\right) \quad (8.36)$$

Note that the first term leading to a $\log^2 s$ growth of the amplitude is absent in the SM ($c_t = c_V = 1$), since it will lead to unitarity violation. In the SM the leading term decays like $\frac{\log^2 s}{s}$. The asymptotic expression of A_2 is given by

$$A_2(s, t, u) = -\frac{1}{4} \frac{t}{u} \log^2 \frac{s}{-t} + i\pi \left(\frac{t}{2u} \log \frac{s}{-t} \right) + \{t \leftrightarrow u\} + \mathcal{O}\left(\frac{1}{s}\right) \quad (8.37)$$

This expression is of order unity and takes the special values

$$\begin{aligned} A_2(s \rightarrow \infty)|_{t \rightarrow 0} &= i\frac{\pi}{2} \\ A_2(s \rightarrow \infty)|_{u=t=-s/2} &= -\frac{1}{2} \ln^2 2 + i\pi \ln 2 = -0.240 + 2.18i \end{aligned} \quad (8.38)$$

8.3.3. Subleading EFT corrections

Having discussed the various local operators entering $gg \rightarrow Z_L Z_L$ at next-to-leading order, we analyze how they enter the amplitude. We reiterate that we do not attempt a full NLO calculation, but rather take the corrections from these operators as representative for the other terms. To remain within the range of validity of the EFT these effects need to be subdominant. Typical next-to-leading order terms carry a parametric suppression of

$$\frac{v^2}{M^2} = \frac{v^2}{16\pi^2 f^2} = \frac{\xi}{16\pi^2} \quad (8.39)$$

where f is the scale of the (strongly-coupled) Higgs sector, $M = 4\pi f$ a typical resonance mass acting as the EFT cut-off, and the vacuum tilting parameter $\xi = v^2/f^2$. For numerical estimates we will assume $f \approx 0.7 \text{ TeV}$ and $M \approx 8 \text{ TeV}$ as representative values. We emphasize that these values should be understood as rough order-of-magnitude estimates. The nonlinear EFT is valid for energies sufficiently below the cut-off scale, i.e. $s \sim f^2 \ll M^2$.

In the following we discuss how the different operators enter the amplitude.

$$d_\chi = 4 \text{ **operator** } g^2 y_t Z_\mu Z^\mu \bar{t} t : C_{\psi S1}$$

In the Goldstone limit, this operator gives a contribution to the Lagrangian of the form

$$\mathcal{L}_{\psi S1} = C_{\psi S1} \frac{2}{v^2} \partial_\mu \varphi^0 \partial^\mu \varphi^0 \bar{t} t \quad (8.40)$$

The insertion of this operator in diagram (b) of Fig. 8.5 gives rise to a correction of the form factor A_1 (8.34) by

$$\begin{aligned} \Delta A_1^{\psi S1} &= \left[1 - \frac{1}{2} s C(s) \left(1 - \frac{4m_t^2}{s} \right) \right] (-2s) \frac{C_{\psi S1}}{m_t} \\ &= \left[\frac{1}{4} \ln^2 \frac{-s}{m_t^2} + 1 \right] (-2s) \frac{C_{\psi S1}}{m_t} + \mathcal{O}(s^0) \end{aligned} \quad (8.41)$$

where the second line is the leading term in the asymptotic expansion for large s . The typical size of the coefficient $C_{\psi S1}$ can be estimated by considering a toy model with a heavy scalar H with Higgs-like couplings of the form

$$\mathcal{L}_H = -\frac{1}{2} M^2 H^2 + \frac{v}{2} \langle \partial^\mu U^\dagger \partial_\mu U \rangle H - \frac{m_t}{v} H \bar{t} t \quad (8.42)$$

Integrating out H at tree level, generates the operator $Q_{\psi S1} + \text{h.c.}$ with a coefficient

$$\frac{C_{\psi S1}}{m_t} = -\frac{1}{2M^2} \sim \frac{\xi}{16\pi^2} \frac{1}{v^2} \quad (8.43)$$

where $\xi = v^2/f^2$ and $M = 4\pi f$, in agreement with the power counting expectation. In the 2HDM (see Chapter 7) the corresponding Wilson coefficient is given by

$$\frac{C_{\psi S1}}{m_t} = -\frac{c_{\beta-\alpha}}{2M_0^2} (c_{\beta-\alpha} - s_{\beta-\alpha} \cot \beta) \sim -\frac{1}{2M_0^2} \quad (8.44)$$

which follows the same power counting.

$$d_\chi = 4 \text{ operators } g^3 Z_\mu \bar{t} \gamma^\mu t_{L/R} : C_{\psi VL,R}$$

The operators in this class modify the coupling of the Z boson to top-quarks and enter the box diagrams as shown in Fig. 8.2 (c). In the Goldstone limit these operators lead to an interaction Lagrangian of the form

$$\mathcal{L}_{\psi VL/R} = -C_{\psi VL} \bar{t}_L \gamma^\mu t_L \partial_\mu \varphi^0 - C_{\psi VR} \bar{t}_R \gamma^\mu t_R \partial_\mu \varphi^0 \quad (8.45)$$

Using integration by parts to shift the partial derivative and using the equation of motion

$$i \not{\partial} t_L = m_t (1 + i\varphi^0) t_R, \quad i \not{\partial} t_R = m_t (1 - i\varphi^0) t_L \quad (8.46)$$

leads to

$$\mathcal{L}_{\psi VL/R} = -i \frac{m_t}{v} \frac{\delta_V}{2} \varphi^0 \bar{t} \gamma_5 t + \frac{m_t}{2v^2} \delta_V (\varphi^0)^2 \bar{t} t \quad (8.47)$$

where

$$\delta_V = 2(C_{\psi VL} - C_{\psi VR}) \quad (8.48)$$

In the Goldstone limit these couplings enter the box diagrams (d)-(f) in Fig. 8.6 and the triangle diagram (b) in Fig. 8.5, which reproduces the high-energy behavior of the box diagram (b) for the full Z case in Fig. 8.1 and give a correction factor of

$$1 + \delta_V \quad (8.49)$$

for the entire box contribution (the contributions to $A_{1/2}$ in (8.34) and (8.35)). The correction from δ_V has an impact on the terms that grow with s in A_1 , entering the asymptotic amplitude as

$$A_1(s, t, u) = -\frac{1}{4} \ln^2 \frac{-s}{m_t^2} [1 + \delta_V - c_t c_V] - c_t c_V - c_{ggh} c_V \frac{s + m_h^2}{4m_t^2} + \mathcal{O}\left(\frac{1}{s}\right) \quad (8.50)$$

δ_V thus contributes to the logarithmic growth of A_1 in addition to $1 - c_t c_V$. Parametrically, $\delta_V \sim \xi/(16\pi^2)$, which is subleading to $1 - c_t c_V \sim \xi$ and numerically negligible.

Z prime

The operators in this class are generated within a model featuring a heavy Z' boson. We consider a general framework in which the Standard Model (SM) is extended by a $U(1)'$ symmetry, and the associated Z' boson is a singlet under the SM gauge group. Different classes of Z' models are distinguished by the $U(1)'$ charges assigned to the SM fields. The mass of the Z' boson can arise either via spontaneous breaking of the $U(1)'$ symmetry or through the Stückelberg mechanism [241–243]. A summary of the various model realizations is provided in [244]. To account for the coupling of the Z' to the Goldstone matrix U , we extend its covariant derivative as follows:

$$D_\mu U \rightarrow D_\mu U - 2ig_D Q_U Z'_\mu U T_3 \quad (8.51)$$

where g_D denotes the $U(1)'$ gauge coupling, and $Q_i = \mathcal{O}(1)$ represent the $U(1)'$ charges of the SM fields. Following [244], we consider the general Lagrangian:

$$\mathcal{L} = -\frac{1}{4} Z'_\mu Z'^{\mu\nu} + \frac{M_{Z'}^2}{2} Z'_\mu Z'^\mu - Z'_\mu J^\mu \quad (8.52)$$

and integrate out the Z' boson at tree level. For simplicity, we neglect kinetic mixing effects. The current J_μ is defined as:

$$J_\mu = -ig_D v^2 \langle U^\dagger D_\mu U T_3 \rangle + g_D (Q_{t_L} \bar{t}_L \gamma_\mu t_L + Q_{t_R} \bar{t}_R \gamma_\mu t_R) \quad (8.53)$$

where we retain only the Z' couplings to the Goldstone bosons and the top quark. Integrating out the Z' yields the effective Lagrangian:

$$\mathcal{L}_{\text{eff}} = -\frac{J_\mu J^\mu}{2M_{Z'}^2} \quad (8.54)$$

which generates the operators $Q_{\psi V1/4}$ with coefficients:

$$C_{\psi V1/4} = \frac{v^2}{M_{Z'}^2} g_D^2 Q_U Q_{t_{L/R}} \sim \frac{\xi}{16\pi^2} \quad (8.55)$$

in agreement with our power counting expectations. Here, $g_D = \mathcal{O}(1)$ reflects the assumption that SM fermions couple weakly to the heavy sector.

$d_\chi = 6$ **operator** $g^2 g^2 (G^A)^2 Z^2 : C_{GU1/2}$

The $d_\chi = 6$ operators lead to a NLO contribution in the form of a purely local interaction as illustrated in Fig. 8.1 (e). To compute the relevant matrix elements we expand

$$Q_{GU1} \supset \frac{2g_s^2}{v^2} (\partial_\mu A_\nu^A \partial^\mu A^{A\nu} - \partial_\mu A_\nu^A \partial^\nu A^{A\mu}) \partial_\lambda \varphi^0 \partial^\lambda \varphi^0 \quad (8.56)$$

$$Q_{GU2} \supset \frac{g_s^2}{v^2} (2\partial_\mu A^{A\lambda} \partial_\lambda A_\nu^A - \partial_\lambda A_\mu^A \partial^\lambda A_\nu^A - \partial_\mu A^{A\lambda} \partial_\nu A_\lambda^A) \partial^\mu \varphi^0 \partial^\nu \varphi^0 \quad (8.57)$$

The matrix elements can then be computed

$$\langle \varphi^0 \varphi^0 | Q_{GU1} | gg \rangle = \frac{g_s^2}{2} \delta^{AB} \frac{4s^2}{v^2} T_1^{\mu\nu} \epsilon_{1\mu} \epsilon_{2\nu} \quad (8.58)$$

$$\langle \varphi^0 \varphi^0 | Q_{GU2} | gg \rangle = \frac{g_s^2}{2} \delta^{AB} \frac{1}{v^2} [-s^2 T_1^{\mu\nu} + 2ut T_2^\mu] \epsilon_{1\mu} \epsilon_{2\nu} \quad (8.59)$$

The formfactors including our specific NLO and NNLO effects reads

$$A_1^{NLO}(s) = -2m_t C_{\psi S1} \frac{s}{m_t^2} \left[1 - \frac{1}{2} s C(s) \left(1 - \frac{4m_t^2}{s} \right) \right] \quad (8.60)$$

Their coefficients can be estimated following the above considerations yielding

$$C_{GU1/2} \sim \frac{1}{v^2} \frac{1}{(16\pi^2)^2} \xi \quad (8.61)$$

This leads to a form factor correction of

$$\Delta A_1^{GU}(s) = 8\pi^2 \frac{s^2}{m_t^2} \left[C_{GU1} - \frac{1}{4} C_{GU2} \right], \quad \Delta A_2^{GU}(s) = 4\pi^2 \frac{tu}{m_t^2} C_{GU2} \quad (8.62)$$

Again we estimate the typical size of the coefficients from a toy model with a heavy scalar H

$$\mathcal{L}_H = -\frac{1}{2} M^2 H^2 + \frac{v}{2} \langle \partial^\mu U^\dagger \partial_\mu U \rangle H + \frac{\alpha_s}{8\pi} c_{ggH} \frac{H}{v} G_{\mu\nu}^A G^{A\mu\nu} \quad (8.63)$$

which gives

$$C_{GU1} = \frac{c_{ggH}}{32\pi^2 M^2} \sim \frac{1}{16\pi^2 M^2}, \quad C_{GU2} = 0 \quad (8.64)$$

This shifts A_1 by

$$\Delta A_1^{GU,H} = \frac{s}{4m_t^2} \frac{s}{M^2} c_{ggH} \quad (8.65)$$

which can be interpreted as a correction to the $c_{ggH} c_V$ term in A_1

$$c_{ggH} c_V \rightarrow c_{ggH} c_V - c_{ggH} \frac{s}{M^2} \quad (8.66)$$

The relative correction is of order $s/M^2 \sim f^2/M^2$ and again small. Naively, the contact interactions in Fig. 8.2 (e) leading to a quadratic s -dependence (8.62) would seem to dominate over the leading-order results. However, our discussion of the toy model reveals that these contributions remain subleading for large s , as long as we stay within the range of validity of the EFT, i.e. $\sqrt{s} \ll M$. For smaller values of s , on the other hand, the quadratic s dependence implies a particularly strong suppression.

8.3.4. Toy models for c_{ggH}

To get an idea of the typical size of the coefficient c_{ggH} we investigate two toy models where c_{ggH} is generated from the exchange of heavy resonances.

First of all, we consider a heavy, vector-like Dirac fermion Q that can couple directly to the Higgs singlet

$$\mathcal{L}_Q = \bar{Q}(i\not{D} - M_Q)Q - y h \bar{Q}Q \quad (8.67)$$

where $M_Q \approx 4\pi f$ is the resonance mass, and $y \approx 4\pi$ is the (strong) coupling of the Higgs boson to the vector-quark. Similarly to the top quark, a vector-like quark gives rise to triangle diagrams at one loop, generating the local coupling c_{ggh} as a first approximation. Integrating out Q at one loop gives a contribution to A_1 that we implement by replacing

$$c_{ggh} \rightarrow c_{ggh}(s) = \frac{y v}{M_Q} F_Q(s) \quad (8.68)$$

where the function F_Q is given by

$$F_Q(s) = \frac{1}{\tau} [1 + (1 - \tau^{-1}) \arcsin^2 \sqrt{\tau}] = \frac{2}{3} + \frac{7}{45} \tau + \frac{4}{63} \tau^2 + \dots \quad (8.69)$$

and $\tau = s/4M_Q^2$. The matching result for c_{ggh} is therefore

$$c_{ggh} = \frac{2 y_Q v}{3 M_Q} \sim \sqrt{\xi} \quad (8.70)$$

in accordance with our power counting expectation. For values of s well below the production threshold $\sqrt{s} = 2M_Q$ the local approximation of $c_{ggh}(s)$, corresponding to the $\tau = 0$ limit, is rather reliable even for sizable values of τ [230]. This is analogous to the well-known fact in the SM that the Higgs-gluon coupling mediated by a top-quark-loop is well approximated by a local coupling for energies below $2m_t$ [245]. For instance, even for a large energy $\sqrt{s} = M_Q$ already outside the range of validity of the EFT, $F_Q(0) = 0.6667$ is changed only to $F_Q(1/4) = 0.7101$. For lower energies where the EFT is valid the difference between the local approximation and the full s -dependence become almost negligible. Specifically for $\sqrt{s} = 1$ TeV and $M_Q = 8$ TeV, we have $F_Q(\tau) = 0.6673$ which is basically unchanged compared to the $s = 0$ limit. Treating the Higgs-gluon coupling from new physics as a local operator with coefficient c_{ggh} should, therefore, be an excellent approximation throughout the range of validity of the EFT. As a second example, we consider a model with a heavy, colored scalar S in a representation R of $SU(3)$ coupled to the Higgs singlet h

$$\mathcal{L}_S = D_\mu S^\dagger D^\mu S - M_S^2 S^\dagger S - \kappa h S^\dagger S \quad (8.71)$$

where the color indices have been suppressed. We allow $\kappa \sim 4\pi M_S$ in the strong-coupling case. The covariant derivative here is given by

$$D_\mu S = (\partial_\mu + i g_s T_R^A G_\mu^A) S \quad (8.72)$$

where T_R^A are the $SU(3)$ generators in the representation R . The effects of integrating out S at the one-loop level on the leading order form factor A_1 are taken into account by replacing

$$c_{ggh} \rightarrow \frac{\kappa v}{M_S^2} T(R) F_S(s) \quad (8.73)$$

Here $T(R)$ is the index of the representation R and the loop function

$$F_S(s) = \frac{1}{2\tau} \left(\frac{\arcsin^2 \sqrt{\tau}}{\tau} - 1 \right) = \frac{1}{6} + \frac{4\tau}{45} + \frac{2\tau^2}{35} + \mathcal{O}(\tau^3) \quad (8.74)$$

where $\tau = s/4M_S^2$. To obtain the matching result for the local operator c_{ggh} , only the leading term in the expansion in τ is relevant. For a scalar octet ($T(\mathbf{8}) = 3$) we get

$$c_{ggh} = \frac{\kappa v}{M_S^2} \frac{1}{2} \sim \sqrt{\xi} \quad (8.75)$$

which agrees with our power counting expectation. Again for $\sqrt{s} = 1 \text{ TeV}$ and $M_S = 8 \text{ TeV}$, we have $F_S(\tau) = 0.1670$, which is very close to $F_S(0) = 0.1667$.

8.3.5. RGE effects

Another class of NLO contributions arises from the renormalization-group (RG) running of the leading-order anomalous couplings. The one-loop renormalization of the Higgs–Electroweak Chiral Lagrangian was computed in [196, 246] (see also [247]). At this order, the beta function for c_{ggh} vanishes, so we only need to consider the RG evolution of c_V and c_t . The beta-function of the coefficient c_i is defined by

$$\beta_{c_i} = 16\pi^2 \frac{dc_i}{d \ln \mu} \quad (8.76)$$

At one loop β_{c_V} and β_{c_t} read (retaining only the top-quark contribution from the Yukawa sector)

$$\begin{aligned} \beta_{c_V} = & \frac{3}{8} \frac{v^2}{m_h^2} c_V (c_V^2 - c_{2V}) (3g^4 + 2g^2 g'^2 + g'^4) + \frac{g^2}{12} c_V [37(c_{2V} - c_V^2) + 17(1 - c_{2V})] \\ & + \frac{3}{4} g'^2 c_V (1 - c_V^2) + \frac{m_h^2}{2v^2} [c_V (10(c_V^2 - c_{2V}) + 4(c_{2V} - 1)) + 6c_{3V}] \\ & + 24 \frac{m_t^4}{m_h^2 v^2} c_t (c_{2V} - c_V^2) + 6 \frac{m_t^2}{v^2} [(c_V - 1)(c_t^2 + 1) + (c_t - 1)^2] \end{aligned} \quad (8.77)$$

and

$$\begin{aligned} \beta_{c_t} = & \frac{3}{8} \frac{v^2}{m_h^2} c_V [c_t (c_t - c_V) - 2c_{2t}] (3g^4 + 2g^2 g'^2 + g'^4) + \frac{17g^2 + 9g'^2}{12} c_t (1 - c_V^2) \\ & + \frac{m_h^2}{v^2} [c_t (3\kappa_3 (c_t - c_V) + 2c_V^2 + c_{2V} - 2c_{2t}) - 3c_V + 6c_{3t}] \\ & + 24 \frac{m_t^4}{m_h^2 v^2} c_t [2c_{2t} + c_t (c_V - c_t)] + 6 \frac{m_t^2}{v^2} c_t (c_t^2 - 1 + 2c_{2t}) \end{aligned} \quad (8.78)$$

Note that all three couplings, c_V , c_t and c_{ggh} , are scale invariant under QCD. This simplifies their interpretations in the presence of QCD radiative corrections. We employ the definitions

$$F_1 = 2c_V, \quad F_2 = c_{2V}, \quad F_3 = c_{3V} \quad V_3 = \kappa_3 \quad (8.79)$$

$$\mathcal{M}_t = m_t, \quad \mathcal{M}_t^{(1)} = m_t c_t, \quad \mathcal{M}_t^{(2)} = m_t c_{2t}, \quad \mathcal{M}_t^{(3)} = m_t c_{3t} \quad (8.80)$$

which relate the parameters of the Lagrangian in (3.24) to the phenomenological couplings. Both β_{c_V} and β_{c_t} vanish in the SM-limit

$$c_V = c_{2V} = c_t = \kappa_3 = 1, \quad c_{3V} = c_{2t} = c_{3t} = 0 \quad (8.81)$$

With numerical values for the parameters, the beta functions in (8.77) and (8.78) become

$$\begin{aligned} \beta_{c_V} = & 22.69 c_t (c_{2V} - c_V^2) - 5.92 c_t + 3.14 c_V + 2.96 c_t^2 c_V \\ & - 1.03 c_{2V} c_V + 0.849 c_V^3 + 0.773 c_{3V} \end{aligned} \quad (8.82)$$

and

$$\begin{aligned} \beta_{c_t} = & 50.78 c_t c_{2t} + 23.65 c_t^2 c_V - 19.73 c_t^3 - 2.27 c_t + 0.258 c_t c_{2V} - 1.93 c_V c_{2t} \\ & - 1.15 c_t c_V^2 + 1.55 c_{3t} + 0.773 (c_t (c_t - c_V) \kappa_3 - c_V) \end{aligned} \quad (8.83)$$

The large numerical coefficients are dominated by the terms carrying a m_t^4 dependence in (8.77) and (8.78), which are formally leading in the limit of large top-quark masses.

Solving the RG equation (8.76) to linear order in the beta functions, we have

$$c_i(\mu_1) \approx c_i(\mu_2) + \frac{\beta_{c_i}}{16\pi^2} \ln \frac{\mu_1}{\mu_2} \quad (8.84)$$

We imagine a scenario where the new physics resides at a scale of $\mu_1 = 8 \text{ TeV}$ (the EFT cut-off), whereas the coefficients c_V and c_t are determined in experiments at a scale $\mu_2 = 1 \text{ TeV}$.

Numerically, retaining only the m_t^4 terms in the beta functions (8.77), (8.78), we find for the evolution in (8.84)

$$c_V(\mu_1) \approx c_V(\mu_2) + 0.30 c_t (c_{2V} - c_V^2) \quad (8.85)$$

$$c_t(\mu_1) \approx c_t(\mu_2) + 0.30 c_t [c_t (c_V - c_t) + 2c_{2t}] \quad (8.86)$$

These results indicate that RGE running effects could have a sizable impact on the anomalous couplings, when comparing their values at the scale of LHC measurements with those at the EFT cut-off. Experimentally c_t and c_V are close to 1 (within 10%) [225] but c_{2t} and c_{2V} could still deviate from their SM values ($c_{2V} = 1, c_{2t} = 0$).

8.4. Phenomenological considerations

m_t	m_Z	m_h	$\alpha_s(m_Z)$	$G_F = 1/\sqrt{2}v^2$
173 GeV	91.19 GeV	125 GeV	0.1179	$1.166 \cdot 10^{-5} \text{ GeV}^{-2}$

Table 8.1.: Input parameter used in the analysis taken from [59]

This section contains an exploratory analysis of the corrections to the SM cross section due to anomalous couplings. Our input parameters are collected in Table 8.1. Although our primary goal is to elucidate the EFT systematics rather than perform a detailed phenomenological study, we nonetheless provide rough numerical estimates of new-physics effects. Concretely, we plot the partonic differential cross section

$$\left. \frac{d\sigma}{d\cos\theta} \right|_{\theta=\pi/2} \quad (8.87)$$

as a function of the partonic center-of-mass energy \sqrt{s} , varying one anomalous coupling at a time and setting all others to their SM values. While a complete phenomenological analysis would require convolution with the gluon parton-distribution functions, the partonic cross section alone already captures the leading dependence on \sqrt{s} and thus offers a useful first estimate of the size of new-physics corrections. The numerical evaluation of the loop functions in our analysis was performed using the **LoopTools** package [248]. While the NLO operators remain largely unconstrained we can be more specific about the LO anomalous couplings, which have been constrained in a global fit [225]

$$c_V = 1.01 \pm 0.06, \quad c_t = 1.01^{+0.09}_{-0.10}, \quad c_{ggh} = -0.01^{+0.08}_{-0.07} \quad (8.88)$$

where the error bars correspond to the 68 % probability interval. Therefore, the combination $c_{tV} = c_t c_V$ can still deviate from unity by roughly 10 %. For the NLO operators we use our power counting expectations for the analysis

$$C_{\psi S1} \sim -\frac{\xi}{16\pi^2} \frac{m_t}{v^2}, \quad C_{GU1} \sim \frac{c_{ggh}}{32\pi^2 M^2} \quad (8.89)$$

The results are given in Figs. 8.7-8.10. We make several comments:

- In Fig. 8.7a we analyze the effect of the LO coupling $c_{tV} = c_t c_V$. These couplings impact the cross-section most strongly for small $\sqrt{s} \sim 500\text{GeV}$. The relative $\ln^2 s$ growth with respect to the SM amplitude only becomes noticeable for center-of-mass energies far outside the range of validity of the EFT.
- The leading new-physics effect at larger \sqrt{s} is due to c_{ggh} as can be seen in Fig. 8.7b. For values of c_{ggh} close to central values of the global fit, we remain within the range of validity of the EFT and the deviations from the SM increase for large \sqrt{s} .
- The corrections to the cross-section coming from $Q_{\psi S1}$ are rather small as is characteristic for a NLO effect. Although the $Q_{\psi S1}$ corrections exhibit the same large- s behavior as those from c_{ggh} , they are numerically much smaller due to the additional loop factor.
- The corrections from C_{GU1} (Fig. 8.9) are enhanced by a factor s^2 with respect to the SM amplitude. As we discussed this behavior should not be taken at face value if the EFT is to remain applicable. For energies below the EFT cutoff $M \sim 8\text{TeV}$ and typical values of the coefficient $c_{ggh} \sim 0.1$ the correction due to C_{GU1} to the cross-section is characteristic for a NLO correction. The behavior of C_{GU2} is expected to be similar.
- In Fig. 8.10 we compare the SM amplitudes for $gg \rightarrow \varphi^0 \varphi^0$ and $gg \rightarrow Z_L Z_L$ using the formulae in [235]. We find excellent agreement between the two; the deviation for $\sqrt{s} = 500\text{GeV}$ is already below 1%. This is not surprising since the deviations from the Goldstone limit scale as $\sim m_Z^2/s$ and thus become negligible for large \sqrt{s} .

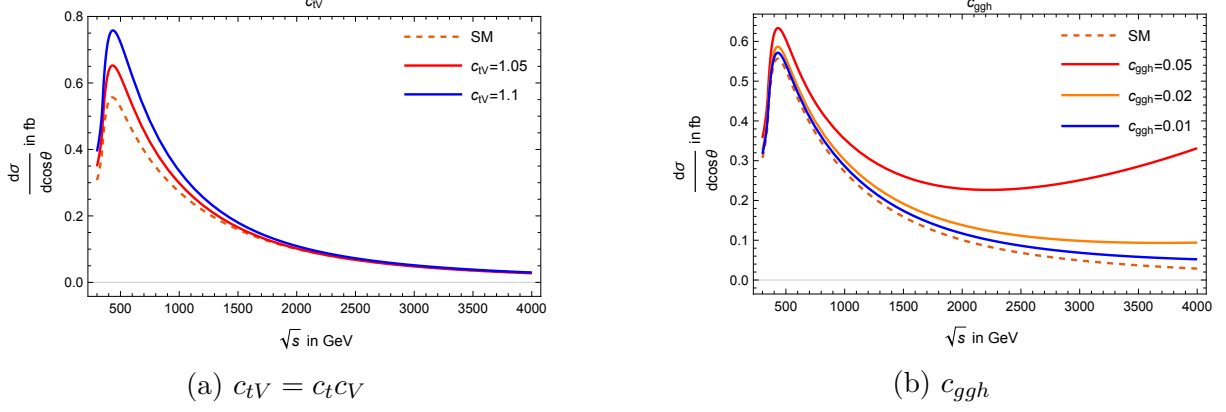


Figure 8.7.: Energy dependence of the scattering cross section at $\cos \theta = 0$ in units of fb. Here only the LO anomalous couplings are varied while all other coefficients are set to their SM values.

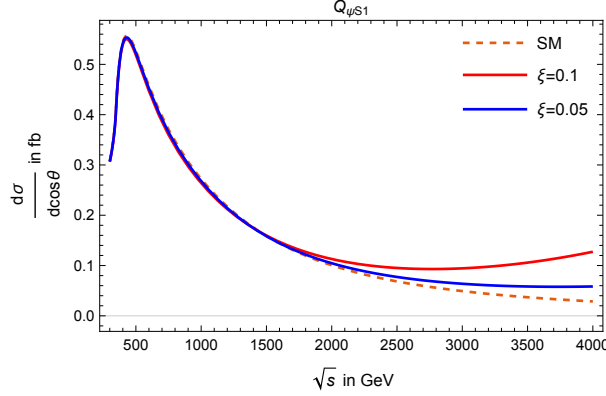


Figure 8.8.: Energy dependence of the scattering cross section at $\cos \theta = 0$ in units of fb. Here only the HEFT coefficient $C_{\psi S1} = -\xi m_t / 16\pi^2 v^2$ is varied while all other coefficients are set to their SM values.

8.5. Discussion

We presented a systematic discussion of EFT corrections to longitudinal Z -boson pair production via gluon fusion. We focus the kinematic region in which the Higgs boson is highly off-shell. The most appropriate EFT for this process is the electroweak chiral Lagrangian (nonlinear EFT), whose power counting is organized as a loop expansion captured by counting chiral dimensions. We show that the leading EFT effects arise at one loop and depend on three anomalous couplings, which reduce to two independent parameters. We then identify the NLO operators contributing at two-loop order in the chiral counting and outline the additional terms that a complete NLO calculation would require. In the Goldstone limit, the LO amplitude can be compactly written in terms of two form factors. We present explicit expressions for these form factors and derive subleading corrections induced by local NLO operators. To validate our power-counting assumptions, we study several illustrative new-physics scenarios that generate specific anomalous couplings. Although some NLO contributions exhibit a pronounced growth with the partonic center-of-mass energy s , we demonstrate that they remain subdominant throughout the domain of validity of the EFT. Furthermore, we find that the local

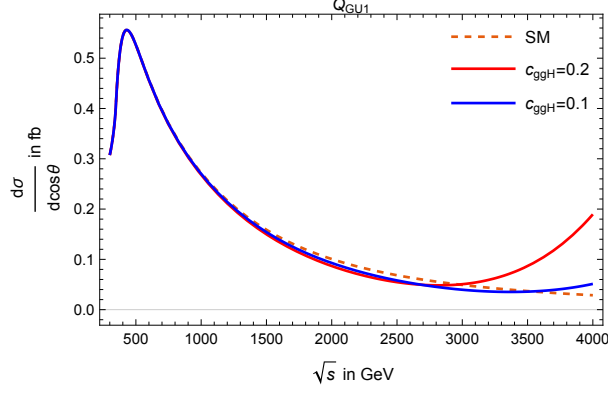


Figure 8.9.: Energy dependence of the scattering cross section at $\cos \theta = 0$ in units of fb. Here only the NLO anomalous couplings $C_{GU1} = c_{ggH}/32\pi^2 M^2$ varied while all other coefficients are set to their SM values.

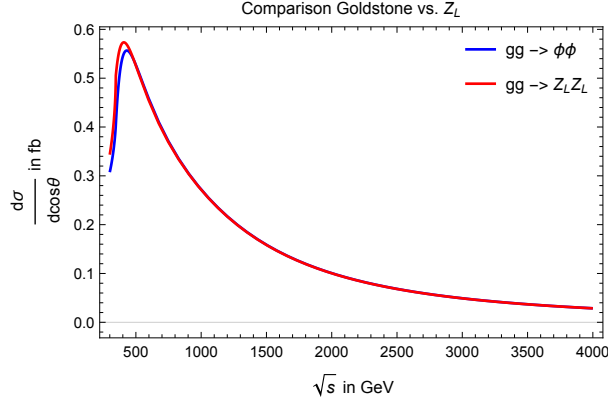


Figure 8.10.: Energy dependence of the scattering cross section at $\cos \theta = 0$ in units of fb. Here we plot the SM scattering cross section for the processes $gg \rightarrow \varphi^0 \varphi^0$ and $gg \rightarrow Z_L Z_L$. For large \sqrt{s} we find good agreement between the two processes validating our choice to use the Goldstone limit.

anomalous Higgs–gluon coupling c_{ggh} , which enters at leading order in the chiral counting, provides an excellent approximation for heavy-resonance-mediated new physics. A brief phenomenological study confirms that c_{ggh} dominates the new-physics effects at large center-of-mass energies.

8.6. Appendix: Details of the calculation

In this section we provide the detailed expressions for the diagrams in Figs. 8.5 and 8.6. For diagrams (a) and (b) in Fig. 8.5 we need the following loop integral

$$\begin{aligned}
 I^{\mu\nu} &= \int \frac{d^4 k}{(2\pi)^4} \frac{\text{Tr} [\gamma^\mu (\not{k} + m) \gamma^\nu (\not{k} - \not{k}_2 + m) (\not{k} + \not{k}_1 - m)]}{[k^2 - m^2] [(k + k_1)^2 - m^2] [(k - k_2)^2 - m^2]} \\
 &= \frac{i}{4\pi^2} m \left(g^{\mu\nu} - \frac{k_1^\nu k_2^\mu}{k_1 \cdot k_2} \right) \left[1 - \frac{1}{2} \left(1 - \frac{4m_t^2}{s} \right) C(s) s \right]
 \end{aligned} \tag{8.90}$$

where we dropped terms proportional to k_1^μ and k_2^ν that vanish due to the Ward identities and the loop function $C(s)$ is defined in (E.9). The explicit expressions for the different diagrams in Fig. 8.5

$$\begin{aligned} i\mathcal{M}_a^{\mu\nu} &= -g_s^2 \frac{m_t}{v^2} c_t c_V \frac{s}{s - m_h^2} I^{\mu\nu} \\ &= -i \frac{\alpha_s}{\pi} \frac{m_t^2}{v^2} c_t c_V \frac{s}{s - m_h^2} \left[1 - \frac{1}{2} \left(1 - \frac{4m_t^2}{s} \right) C(s) s \right] \end{aligned} \quad (8.91)$$

$$i\mathcal{M}_b^{\mu\nu} = g_s^2 \frac{m_t}{v^2} I^{\mu\nu} = i \frac{\alpha_s}{\pi} \frac{m_t^2}{v^2} \left[1 - \frac{1}{2} \left(1 - \frac{4m_t^2}{s} \right) C(s) s \right] \quad (8.92)$$

$$i\mathcal{M}_c^{\mu\nu} = i \frac{\alpha_s}{4\pi} c_V c_{ggh} \frac{s}{s - m_h^2} \frac{s}{v^2} \quad (8.93)$$

Next we provide expressions for the box diagrams in Fig. 8.6. The diagrams with reversed momentum flow give the same result due to charge conjugation invariance. We start with the s -channel box diagram (omitting the prefactors)

$$\mathcal{M}_d = \int \frac{d^d q}{(2\pi)^d} \frac{\text{tr}[\gamma^\mu(\not{q} + m_t)\gamma^\nu(\not{q} - \not{k}_2 + m_t)\gamma_5(\not{q} + \not{k}_1 - \not{p}_1 + m_t)\gamma_5(\not{q} + \not{k}_1 + m_t)]}{(q^2 - m_t^2)((q + k_1)^2 - m_t^2)((q - k_2)^2 - m_t^2)((q + k_1 - p_1)^2 - m_t^2)} \quad (8.94)$$

The t -channel graph is given by

$$\mathcal{M}_e = \int \frac{d^d q}{(2\pi)^d} \frac{\text{tr}[\gamma^\mu(\not{q} + m_t)\gamma^\nu(\not{q} - \not{k}_2 + m_t)\gamma_5(\not{q} + \not{k}_1 - \not{p}_2 + m_t)\gamma_5(\not{q} + \not{k}_1 + m_t)]}{(q^2 - m_t^2)((q + k_1)^2 - m_t^2)((q - k_2)^2 - m_t^2)((q + k_1 - p_2)^2 - m_t^2)} \quad (8.95)$$

The u -channel graph is given by

$$\mathcal{M}_f = \int \frac{d^d q}{(2\pi)^d} \frac{\text{tr}[\gamma_5(\not{q} + m_t)\gamma^\nu(\not{q} - \not{k}_2 + m_t)\gamma_5(\not{q} + \not{k}_1 - \not{p}_1 + m_t)\gamma^\mu(\not{q} - \not{p}_1 + m_t)]}{(q^2 - m_t^2)((q - p_1)^2 - m_t^2)((q - k_2)^2 - m_t^2)((q + k_1 - p_1)^2 - m_t^2)} \quad (8.96)$$

Part III.

Conclusion

9. Conclusion and Outlook

In this work, we investigated the systematic application of effective field theories at the electroweak scale. Given the lack of new resonances after the Higgs discovery in 2012, i.e., direct observations of new physics, one must settle for the indirect effects of new physics. Therefore, EFT frameworks are vital since they permit the description of those indirect effects of new physics in a model-independent way. Two such frameworks are widely used for that purpose. The Standard Model Effective Field Theory (SMEFT) comprises the Standard Model (SM) degrees of freedom as building blocks for higher-dimensional operators suppressed by powers of the new physics scale Λ , according to their mass dimensions. As a result, the SMEFT has the physical Higgs boson h as part of an $SU(2)$ doublet as in the SM. The h self-couplings are, thus, correlated and close to their SM values.

The Electroweak Chiral Lagrangian (EwChL, also known as HEFT), on the other hand, is the most general EFT that parametrizes electroweak symmetry breaking $SU(2)_L \times U(1)_Y \rightarrow U(1)_{em}$ and contains the physical Higgs as a gauge singlet. As a nondecoupling EFT based on an expansion in loop orders, its organizing principle differs from SMEFT. It also allows for $\mathcal{O}(1)$ deviations from the SM in the couplings in the Higgs sector. This thesis presents illustrative examples demonstrating the systematic and consistent use of both EFT frameworks, alongside general insights applicable to all EFTs.

First, we took a closer look at the power-counting prescription for SMEFT. Commonly, only the expansion in inverse powers of Λ is made explicit, and, as a result, in many applications, all Wilson coefficients C_i are assumed to be $\mathcal{O}(1)$ numbers. We showed, however, that such an approach may lead to inconsistencies and is incomplete. What is missing is information about the other EFT expansion parameter $1/16\pi^2$, the loop factor. The number of implicit loop factors, the loop order L , associated with a SMEFT operator can be conveniently grasped using the notion of chiral dimensions $d_\chi = 2L + 2$. To assign chiral dimensions to operators, it is necessary to determine the minimum number of weak couplings that are associated with this operator. We determine the assignment of weak couplings to dimension-six operators and rederive the familiar result that operators with field strength tensors are suppressed by a loop factor. Naturally, variations of the proposed power counting scheme are permissible. However, the underlying assumptions must be clearly specified, and the resulting consequences for the power counting must be consistently applied. This statement holds for general EFTs.

As a second application, we moved away from the realm of decoupling EFTs and turned to the $SO(4)$ linear σ -model. We integrated out the massive degree of freedom at one loop and derived the nondecoupling contributions ($\mathcal{O}(1/16\pi^2)$) to the effective Lagrangian, which takes the form of a nonlinear σ -model. However, the tree-level contributions of $\mathcal{O}(1/M^2)$ are also needed to obtain a renormalization-scheme independent result, a direct consequence of the strongly coupled region of parameter space.

In Chapter 7, we illustrate how the EwChL emerges as the natural low-energy EFT after integrating out the heavy scalars in the nondecoupling regime of a Two-Higgs-Doublet Model (2HDM). Using functional methods throughout enables us to derive the matching

to the leading order EwChL in a transparent manner. We also derived the loop induced $h \rightarrow \gamma\gamma$ and $h \rightarrow \gamma Z$ local terms. Our algorithm allows for the computation of the coefficient functions up to arbitrary orders in h , which are, however, of less phenomenological relevance. Furthermore, our calculation could be extended to a full NLO matching calculation with tree-level effects of $\mathcal{O}(1/M_S^2)$ and loop-level effects of $\mathcal{O}(1/16\pi^2)$. The dominant new physics effects are nevertheless expected to be found in the leading-order (LO) couplings. We found that the predictions for an anomalous $h\gamma\gamma$ coupling in the nondecoupling regime are still compatible with experiments and could be confirmed or ruled out experimentally.

As a final exercise, we considered the production of (longitudinal) Z -bosons via gluon fusion $gg \rightarrow Z_L Z_L$ with anomalous HEFT couplings to showcase the systematic application of the EwChL. We pointed out that at LO, the new-physics effects are given by three anomalous couplings, which reduce to two independent parameters. Subsequently, we discussed in detail which $d_\chi = 4$ operators would be required for a complete NLO calculation, emphasizing the interplay of loop topologies and implicit loop factors. These general considerations are also helpful for the HEFT treatment of other processes. Our study lays the groundwork for a future comprehensive phenomenological analysis, including a full NLO calculation. To achieve collider-level predictions for $pp \rightarrow Z_L Z_L$, other partonic channels and convolution with parton distribution functions will be required. With current computational tools, such a project is a promising direction for future research.

Part IV.

Appendix

A. Parameters of the 2HDM potential

The appendix of [2] presents expressions of the coefficients of the scalar potential (7.16) in terms of the input parameters

$$v, \quad m_h, \quad M_0, \quad M_A, \quad M_H, \quad \bar{m}, \quad t_\beta, \quad c_{\beta-\alpha} \quad (\text{A.1})$$

where $\bar{m}^2 = m_{12}^2/s_\beta c_\beta$. The cubic couplings read

$$v d_1 = c_{\beta-\alpha}^2 (\bar{m}^2 - m_h^2) (s_{\beta-\alpha} + c_{\beta-\alpha} \cot(2\beta)) - \frac{m_h^2}{2} s_{\beta-\alpha} \quad (\text{A.2})$$

$$v d_2 = \frac{c_{\beta-\alpha}}{2} [(2m_h^2 + M_0^2 - 3\bar{m}^2) (1 - 2c_{\beta-\alpha}^2 + 2s_{\beta-\alpha}c_{\beta-\alpha} \cot(2\beta)) - \bar{m}^2] \quad (\text{A.3})$$

$$v d_3 = -\frac{s_{\beta-\alpha}}{2} [(2M_0^2 + m_h^2 - 3\bar{m}^2) (1 - 2c_{\beta-\alpha}^2 + 2s_{\beta-\alpha}c_{\beta-\alpha} \cot(2\beta)) + \bar{m}^2] \quad (\text{A.4})$$

$$v d_4 = s_{\beta-\alpha}^2 (\bar{m}^2 - M_0^2) (c_{\beta-\alpha} - s_{\beta-\alpha} \cot(2\beta)) - \frac{M_0^2}{2} c_{\beta-\alpha} \quad (\text{A.5})$$

$$v d_5 = 2s_{\beta-\alpha} \left(\bar{m}^2 - M_H^2 - \frac{m_h^2}{2} \right) + 2c_{\beta-\alpha} \cot(2\beta) (\bar{m}^2 - m_h^2) \quad (\text{A.6})$$

$$v d_6 = s_{\beta-\alpha} \left(\bar{m}^2 - M_A^2 - \frac{m_h^2}{2} \right) + c_{\beta-\alpha} \cot(2\beta) (\bar{m}^2 - m_h^2) \quad (\text{A.7})$$

$$v d_7 = 2c_{\beta-\alpha} \left(\bar{m}^2 - M_H^2 - \frac{M_0^2}{2} \right) + 2s_{\beta-\alpha} \cot(2\beta) (M_0^2 - \bar{m}^2) \quad (\text{A.8})$$

$$v d_8 = c_{\beta-\alpha} \left(\bar{m}^2 - M_A^2 - \frac{M_0^2}{2} \right) + s_{\beta-\alpha} \cot(2\beta) (M_0^2 - \bar{m}^2) \quad (\text{A.9})$$

The expression $\cot(2\beta)$ can be expressed in terms of t_β via the trigonometric identity

$$\cot 2\beta = \frac{1 - t_\beta^2}{2t_\beta} \quad (\text{A.10})$$

The quartic couplings are given by

$$\begin{aligned} v^2 z_1 = & -\frac{m_h^2}{8} + \frac{c_{\beta-\alpha}^2}{8} \left[4s_{\beta-\alpha}^2 \bar{m}^2 + (-3 + 4c_{\beta-\alpha}^4) m_h^2 - (1 - 2c_{\beta-\alpha}^2)^2 M_0^2 \right. \\ & + 4c_{\beta-\alpha} s_{\beta-\alpha} \cot(2\beta) (2\bar{m}^2 - (1 + 2c_{\beta-\alpha}^2) m_h^2 - (1 - 2c_{\beta-\alpha}^2) M_0^2) \\ & \left. + 4c_{\beta-\alpha}^2 \cot^2(2\beta) (\bar{m}^2 - c_{\beta-\alpha}^2 m_h^2 - s_{\beta-\alpha}^2 M_0^2) \right] \end{aligned} \quad (\text{A.11})$$

$$\begin{aligned} v^2 z_2 = & \frac{s_{\beta-\alpha} c_{\beta-\alpha}}{2} (1 - 2c_{\beta-\alpha}^2) [m_h^2 + M_0^2 - 2c_{\beta-\alpha}^2 (M_0^2 - m_h^2) - 2\bar{m}^2] \\ & + c_{\beta-\alpha}^2 \cot(2\beta) [m_h^2 (1 + 2c_{\beta-\alpha}^2 - 4c_{\beta-\alpha}^4) \\ & + 2M_0^2 (1 - 3c_{\beta-\alpha}^2 + 2c_{\beta-\alpha}^4) + \bar{m}^2 (-3 + 4c_{\beta-\alpha}^2)] \\ & + 2c_{\beta-\alpha}^3 s_{\beta-\alpha} \cot^2(2\beta) [M_0^2 - \bar{m}^2 - c_{\beta-\alpha}^2 (M_0^2 - m_h^2)] \end{aligned} \quad (\text{A.12})$$

$$\begin{aligned}
v^2 z_3 = & \frac{1}{4} \left[(2 - 12c_{\beta-\alpha}^2 + 12c_{\beta-\alpha}^4) \bar{m}^2 \right. \\
& + (1 - 2c_{\beta-\alpha}^2) \left((-1 - 3c_{\beta-\alpha}^2 + 6c_{\beta-\alpha}^4) m_h^2 + (-2 + 9c_{\beta-\alpha}^2 - 6c_{\beta-\alpha}^4) M_0^2 \right) \\
& + 2c_{\beta-\alpha}s_{\beta-\alpha} \cot(2\beta) \left((6 - 12c_{\beta-\alpha}^2) \bar{m}^2 + (-1 - 6c_{\beta-\alpha}^2 + 12c_{\beta-\alpha}^4) m_h^2 \right) \\
& + (-5 + 18c_{\beta-\alpha}^2 - 12c_{\beta-\alpha}^4) M_0^2 \\
& \left. + 12c_{\beta-\alpha}^2 s_{\beta-\alpha}^2 \cot^2(2\beta) (\bar{m}^2 - s_{\beta-\alpha}^2 M_0^2 - c_{\beta-\alpha}^2 m_h^2) \right] \quad (A.13)
\end{aligned}$$

$$\begin{aligned}
v^2 z_4 = & \frac{s_{\beta-\alpha}c_{\beta-\alpha}}{2} (1 - 2c_{\beta-\alpha}^2) [m_h^2 - 3M_0^2 + 2c_{\beta-\alpha}^2 (M_0^2 - m_h^2) + 2\bar{m}^2] \\
& + s_{\beta-\alpha}^2 \cot(2\beta) [m_h^2 (2c_{\beta-\alpha}^2 - 4c_{\beta-\alpha}^4) \\
& + M_0^2 (1 - 6c_{\beta-\alpha}^2 + 4c_{\beta-\alpha}^4) + \bar{m}^2 (-1 + 4c_{\beta-\alpha}^2)] \\
& + 2c_{\beta-\alpha}s_{\beta-\alpha}^3 \cot^2(2\beta) [M_0^2 - \bar{m}^2 - c_{\beta-\alpha}^2 (M_0^2 - m_h^2)] \quad (A.14)
\end{aligned}$$

$$\begin{aligned}
v^2 z_5 = & \frac{1}{8} \left[4s_{\beta-\alpha}^2 c_{\beta-\alpha}^2 \bar{m}^2 - s_{\beta-\alpha}^2 (1 - 2c_{\beta-\alpha}^2)^2 m_h^2 - c_{\beta-\alpha}^2 (3 - 2c_{\beta-\alpha}^2)^2 M_0^2 \right. \\
& + 4c_{\beta-\alpha}s_{\beta-\alpha}^3 \cot(2\beta) (-2\bar{m}^2 + (-1 + 2c_{\beta-\alpha}^2) m_h^2 + (3 - 2c_{\beta-\alpha}^2) M_0^2) \\
& \left. + 4s_{\beta-\alpha}^4 \cot^2(2\beta) (\bar{m}^2 - M_0^2 + c_{\beta-\alpha}^2 (M_0^2 - m_h^2)) \right] \quad (A.15)
\end{aligned}$$

$$\begin{aligned}
v^2 z_6 = & \frac{1}{2} [2s_{\beta-\alpha}^2 (\bar{m}^2 - M_H^2) - m_h^2 + c_{\beta-\alpha}^2 (1 - 2c_{\beta-\alpha}^2) (M_0^2 - m_h^2) \\
& + 2c_{\beta-\alpha}s_{\beta-\alpha} \cot(2\beta) (2\bar{m}^2 - m_h^2 - M_0^2 + 3c_{\beta-\alpha}^2 (M_0^2 - m_h^2)) \\
& + 4c_{\beta-\alpha}^2 \cot^2(2\beta) (\bar{m}^2 - s_{\beta-\alpha}^2 M_0^2 - c_{\beta-\alpha}^2 m_h^2)] \quad (A.16)
\end{aligned}$$

$$\begin{aligned}
v^2 z_7 = & c_{\beta-\alpha}s_{\beta-\alpha} (2\bar{m}^2 - 2M_H^2 - (1 - 2c_{\beta-\alpha}^2) (M_0^2 - m_h^2)) \\
& + 2 \cot(2\beta) (M_0^2 - \bar{m}^2 + 2c_{\beta-\alpha}^2 \bar{m}^2 + c_{\beta-\alpha}^2 M_0^2 (-4 + 3c_{\beta-\alpha}^2) \\
& + c_{\beta-\alpha}^2 m_h^2 (2 - 3c_{\beta-\alpha}^2)) \\
& + 4c_{\beta-\alpha}s_{\beta-\alpha} \cot^2(2\beta) (M_0^2 - \bar{m}^2 - c_{\beta-\alpha}^2 (M_0^2 - m_h^2)) \quad (A.17)
\end{aligned}$$

$$\begin{aligned}
v^2 z_8 = & \frac{1}{2} [-m_h^2 + c_{\beta-\alpha}^2 (2(\bar{m}^2 - M_H^2) + (M_0^2 - m_h^2) (-3 + 2c_{\beta-\alpha}^2)) \\
& + 2c_{\beta-\alpha}s_{\beta-\alpha} \cot(2\beta) (-2\bar{m}^2 - 2m_h^2 + 4M_0^2 - 3c_{\beta-\alpha}^2 (M_0^2 - m_h^2)) \\
& + 4s_{\beta-\alpha}^2 \cot^2(2\beta) (\bar{m}^2 - s_{\beta-\alpha}^2 M_0^2 - c_{\beta-\alpha}^2 m_h^2)] \quad (A.18)
\end{aligned}$$

$$\begin{aligned}
v^2 z_9 = & \frac{1}{2} [-s_{\beta-\alpha}^2 m_h^2 - c_{\beta-\alpha}^2 M_0^2 + 4 \cot(2\beta) c_{\beta-\alpha}s_{\beta-\alpha} (M_0^2 - m_h^2) \\
& + 4 \cot^2(2\beta) (\bar{m}^2 - M_0^2 + c_{\beta-\alpha}^2 (M_0^2 - m_h^2))] \quad (A.19)
\end{aligned}$$

$$\begin{aligned}
v^2 z_{10} = & \frac{1}{4} [2s_{\beta-\alpha}^2 (\bar{m}^2 - M_A^2) - m_h^2 (1 + c_{\beta-\alpha}^2 - 2c_{\beta-\alpha}^4) + c_{\beta-\alpha}^2 M_0^2 (1 - 2c_{\beta-\alpha}^2) \\
& + 2c_{\beta-\alpha}s_{\beta-\alpha} \cot(2\beta) (2\bar{m}^2 - m_h^2 - M_0^2 + 3c_{\beta-\alpha}^2 (M_0^2 - m_h^2)) \\
& + 4c_{\beta-\alpha}^2 \cot^2(2\beta) (\bar{m}^2 - s_{\beta-\alpha}^2 M_0^2 - c_{\beta-\alpha}^2 m_h^2)] \quad (A.20)
\end{aligned}$$

$$\begin{aligned}
v^2 z_{11} = & \frac{1}{2} [c_{\beta-\alpha}s_{\beta-\alpha} (2\bar{m}^2 - 2M_A^2 + (2c_{\beta-\alpha}^2 - 1) (M_0^2 - m_h^2)) \\
& + 2 \cot(2\beta) (M_0^2 - \bar{m}^2 + 2c_{\beta-\alpha}^2 \bar{m}^2 + c_{\beta-\alpha}^2 M_0^2 (-4 + 3c_{\beta-\alpha}^2) \\
& + c_{\beta-\alpha}^2 m_h^2 (2 - 3c_{\beta-\alpha}^2)) \\
& + 4c_{\beta-\alpha}s_{\beta-\alpha} \cot^2(2\beta) (M_0^2 - \bar{m}^2 - c_{\beta-\alpha}^2 (M_0^2 - m_h^2))] \quad (A.21)
\end{aligned}$$

$$v^2 z_{12} = \frac{1}{4} [-m_h^2 + c_{\beta-\alpha}^2 (2\bar{m}^2 + 3m_h^2 - 2M_A^2 - 3M_0^2) + 2c_{\beta-\alpha}^4 (M_0^2 - m_h^2)]$$

$$\begin{aligned}
 & + 2c_{\beta-\alpha}s_{\beta-\alpha}\cot(2\beta)\left(4M_0^2 - 2m_h^2 - 2\bar{m}^2 - 3c_{\beta-\alpha}^2(M_0^2 - m_h^2)\right) \\
 & + 4s_{\beta-\alpha}^2\cot^2(2\beta)\left(\bar{m}^2 - M_0^2 + c_{\beta-\alpha}^2(M_0^2 - m_h^2)\right)
 \end{aligned} \tag{A.22}$$

$$\begin{aligned}
 v^2 z_{13} = 4v^2 z_{14} = \frac{1}{2} \left[-s_{\beta-\alpha}^2 m_h^2 - c_{\beta-\alpha}^2 M_0^2 + 4\cot(2\beta)c_{\beta-\alpha}s_{\beta-\alpha}(M_0^2 - m_h^2) \right. \\
 \left. + 4\cot^2(2\beta)(\bar{m}^2 - M_0^2 + c_{\beta-\alpha}^2(M_0^2 - m_h^2)) \right]
 \end{aligned} \tag{A.23}$$

In the alignment limit ($c_{\beta-\alpha} \rightarrow 0$) the coupling constants simplify to

$$\begin{aligned}
 vd_1 &= -\frac{m_h^2}{2}, \quad vd_2 = 0, \quad vd_3 = \bar{m}^2 - M_0^2 - \frac{m_h^2}{2} \\
 vd_5 &= 2\bar{m}^2 - 2M_H^2 - m_h^2, \quad vd_6 = \bar{m}^2 - M_A^2 - \frac{m_h^2}{2}, \\
 d_4 &= \frac{1}{2}d_7 = d_8 = \cot(2\beta)\frac{(M_0^2 - \bar{m}^2)}{v}
 \end{aligned} \tag{A.24}$$

$$\begin{aligned}
 v^2 z_1 &= -\frac{m_h^2}{8}, \quad v^2 z_2 = 0, \quad v^2 z_3 = \frac{1}{2}\left(\bar{m}^2 - M_0^2 - \frac{m_h^2}{2}\right), \quad v^2 z_6 = \bar{m}^2 - M_H^2 - \frac{m_h^2}{2} \\
 z_4 &= \frac{z_7}{2} = z_{11} = \cot(2\beta)\frac{(M_0^2 - \bar{m}^2)}{v^2}, \quad v^2 z_{10} = -\frac{1}{2}(M_A^2 - \bar{m}^2) - \frac{m_h^2}{4} \\
 4z_5 &= z_8 = z_9 = 2z_{12} = z_{13} = 4z_{14} = -\frac{m_h^2}{2v^2} - 2\cot^2(2\beta)\frac{(M_0^2 - \bar{m}^2)}{v^2}
 \end{aligned} \tag{A.25}$$

It is convenient to express the original potential parameters in (7.10) in terms of the scalar masses and the mixing angles. The relations read

$$m_{11}^2 = s_\beta^2 \bar{m}^2 - \frac{1}{2}(c_\alpha^2 M_0^2 + s_\alpha^2 m_h^2) - \frac{s_\beta^2 s_{2\alpha}}{2 s_{2\beta}}(M_0^2 - m_h^2) \tag{A.26}$$

$$m_{22}^2 = c_\beta^2 \bar{m}^2 - \frac{1}{2}(s_\alpha^2 M_0^2 + c_\alpha^2 m_h^2) - \frac{c_\beta^2 s_{2\alpha}}{2 s_{2\beta}}(M_0^2 - m_h^2) \tag{A.27}$$

$$\lambda_1 = \frac{1}{c_\beta^2 v^2}(c_\alpha^2 M_0^2 + s_\alpha^2 m_h^2 - s_\beta^2 \bar{m}^2) \tag{A.28}$$

$$\lambda_2 = \frac{1}{s_\beta^2 v^2}(s_\alpha^2 M_0^2 + c_\alpha^2 m_h^2 - c_\beta^2 \bar{m}^2) \tag{A.29}$$

$$\lambda_3 = \frac{1}{v^2}\left(2M_H^2 - \bar{m}^2 + \frac{s_{2\alpha}}{s_{2\beta}}(M_0^2 - m_h^2)\right) \tag{A.30}$$

$$\lambda_4 = \frac{1}{v^2}(M_A^2 - 2M_H^2 + \bar{m}^2) \tag{A.31}$$

The absence of a decoupling limit for $\bar{m} = 0$ follows immediately from these equations. In that case the λ_i cannot be of $\mathcal{O}(1)$ which corresponds to the weak coupling regime.

B. Explicit computation of the scalar masses in the 2HDM

Here we give an explicit computation of the scalar masses in the 2HDM following [172]. To that end we parametrize the Higgs doublets Φ_i as follows

$$\Phi_i = \begin{pmatrix} \phi_i^+ \\ \frac{1}{\sqrt{2}}[v_i + \rho_i + i\eta_i] \end{pmatrix} \quad (\text{B.1})$$

Plugging in the parametrization in the potential and collecting the quadratic terms we derive the mass matrices for the various fluctuations. The mass term for the pseudoscalars reads

$$\mathcal{V}_\eta = \frac{1}{2}v^2 \left(\frac{m_{12}^2}{v^2} - \frac{\lambda_6 c_\beta^2}{2} - \lambda_5 s_\beta c_\beta - \frac{\lambda_7 s_\beta^2}{2} \right) \begin{pmatrix} \eta_1 & \eta_2 \end{pmatrix} \begin{pmatrix} t_\beta & -1 \\ -1 & t_\beta^{-1} \end{pmatrix} \begin{pmatrix} \eta_1 \\ \eta_2 \end{pmatrix} \quad (\text{B.2})$$

The mass matrix is easily diagonalized. A rotation by the angle β does the job.

$$\begin{pmatrix} \eta_1 \\ \eta_2 \end{pmatrix} = \begin{pmatrix} c_\beta & -s_\beta \\ s_\beta & c_\beta \end{pmatrix} \begin{pmatrix} G^0 \\ A \end{pmatrix} \quad (\text{B.3})$$

The eigenvalues, i.e. masses, are

$$m_{G^0}^2 = 0, \quad M_A^2 = \bar{m}^2 - \frac{1}{2}v^2 (2\lambda_5 + \lambda_6 t_\beta^{-1} + \lambda_7 t_\beta) \quad (\text{B.4})$$

so that the mass term reads in terms of the physical state A and the Goldstone G^0

$$\mathcal{V}_\eta = \frac{1}{2}M_A^2 \begin{pmatrix} G^0 & A \end{pmatrix} \begin{pmatrix} 0 & 0 \\ 0 & 1 \end{pmatrix} \begin{pmatrix} G^0 \\ A \end{pmatrix} \quad (\text{B.5})$$

The mass term for the charged scalars reads

$$\mathcal{V}_{\phi^\pm} = v^2 \left(\frac{m_{12}^2}{v^2} - s_\beta c_\beta (\lambda_4 + \lambda_5) - \frac{\lambda_6 c_\beta^2}{2} - \frac{\lambda_7 s_\beta^2}{2} \right) \begin{pmatrix} \phi_1^- & \phi_2^- \end{pmatrix} \begin{pmatrix} t_\beta & -1 \\ -1 & t_\beta^{-1} \end{pmatrix} \begin{pmatrix} \phi_1^+ \\ \phi_2^+ \end{pmatrix} \quad (\text{B.6})$$

The mass matrix is diagonalized as before.

$$\begin{pmatrix} \phi_1^+ \\ \phi_2^+ \end{pmatrix} = \begin{pmatrix} c_\beta & -s_\beta \\ s_\beta & c_\beta \end{pmatrix} \begin{pmatrix} G^+ \\ H^+ \end{pmatrix} \quad (\text{B.7})$$

The eigenvalues, i.e. masses, are

$$m_{G^+}^2 = 0, \quad M_H^2 = \bar{m}^2 - \frac{1}{2}v^2 \left((\lambda_4 + \lambda_5) + \lambda_6 t_\beta^{-1} + \lambda_7 t_\beta \right) = M_A^2 + \frac{v^2}{2}(\lambda_5 - \lambda_4). \quad (\text{B.8})$$

Again there is a massless eigenstate G^+ which is just the Goldstone corresponding to the W^+ boson. The other massive state is heavy scalar H^+ . Thus, the quadratic term in the potential in terms of mass eigenstates reads

$$\mathcal{V}_{\phi^\pm} = M_H^2 \begin{pmatrix} G^- & H^- \end{pmatrix} \begin{pmatrix} 0 & 0 \\ 0 & 1 \end{pmatrix} \begin{pmatrix} G^+ \\ H^+ \end{pmatrix} \quad (\text{B.9})$$

The mass term for the neutral scalars reads

$$\mathcal{V}_\eta = \frac{1}{2} \begin{pmatrix} \rho_1 & \rho_2 \end{pmatrix} \begin{pmatrix} \mathcal{M}_{11}^2 & \mathcal{M}_{12}^2 \\ \mathcal{M}_{12}^2 & \mathcal{M}_{22}^2 \end{pmatrix} \begin{pmatrix} \rho_1 \\ \rho_2 \end{pmatrix} \quad (\text{B.10})$$

$$\mathcal{M}_{11}^2 = m_{12}^2 t_\beta + v^2 \left(c_\beta^2 \lambda_1 + \frac{3}{2} s_\beta c_\beta \lambda_6 - \frac{1}{2} t_\beta s_\beta^2 \lambda_7 \right) \quad (\text{B.11})$$

$$\mathcal{M}_{22}^2 = m_{12}^2 t_\beta^{-1} + v^2 \left(s_\beta^2 \lambda_2 + \frac{3}{2} s_\beta c_\beta \lambda_7 - \frac{1}{2} t_\beta^{-1} c_\beta^2 \lambda_7 \right) \quad (\text{B.12})$$

$$\mathcal{M}_{12}^2 = -m_{12}^2 + v^2 \left(s_\beta c_\beta \lambda_{345} + \frac{3}{2} c_\beta^2 \lambda_6 + \frac{3}{2} s_\beta^2 \lambda_7 \right) \quad (\text{B.13})$$

The mass matrix for the neutral scalar degrees of freedom is more complicated. It can be written in the form

$$\mathcal{M}^2 \equiv M_A^2 \begin{pmatrix} s_\beta^2 & -s_\beta c_\beta \\ -s_\beta c_\beta & c_\beta^2 \end{pmatrix} + \mathcal{B}^2 \quad (\text{B.14})$$

with

$$\mathcal{B}^2 \equiv v^2 \begin{pmatrix} \lambda_1 c_\beta^2 + 2\lambda_6 s_\beta c_\beta + \lambda_5 s_\beta^2 & (\lambda_3 + \lambda_4) s_\beta c_\beta + \lambda_6 c_\beta^2 + \lambda_7 s_\beta^2 \\ (\lambda_3 + \lambda_4) s_\beta c_\beta + \lambda_6 c_\beta^2 + \lambda_7 s_\beta^2 & \lambda_2 s_\beta^2 + 2\lambda_7 s_\beta c_\beta + \lambda_5 c_\beta^2 \end{pmatrix}. \quad (\text{B.15})$$

Similarly as before we introduce a mixing angle α to diagonalize the mass matrix \mathcal{M}^2

$$\begin{aligned} \begin{pmatrix} M_0^2 & 0 \\ 0 & m_h^2 \end{pmatrix} &= \begin{pmatrix} c_\alpha & s_\alpha \\ -s_\alpha & c_\alpha \end{pmatrix} \begin{pmatrix} \mathcal{M}_{11}^2 & \mathcal{M}_{12}^2 \\ \mathcal{M}_{12}^2 & \mathcal{M}_{22}^2 \end{pmatrix} \begin{pmatrix} c_\alpha & -s_\alpha \\ s_\alpha & c_\alpha \end{pmatrix} \\ &= \begin{pmatrix} \mathcal{M}_{11}^2 c_\alpha^2 + 2s_\alpha c_\alpha \mathcal{M}_{12}^2 + \mathcal{M}_{22}^2 s_\alpha^2 & \mathcal{M}_{12}^2 (c_\alpha^2 - s_\alpha^2) + (\mathcal{M}_{22}^2 - \mathcal{M}_{11}^2) s_\alpha c_\alpha \\ \mathcal{M}_{12}^2 (c_\alpha^2 - s_\alpha^2) + (\mathcal{M}_{22}^2 - \mathcal{M}_{11}^2) s_\alpha c_\alpha & \mathcal{M}_{11}^2 s_\alpha^2 + 2s_\alpha c_\alpha \mathcal{M}_{12}^2 - \mathcal{M}_{22}^2 c_\alpha^2 \end{pmatrix}. \end{aligned} \quad (\text{B.16})$$

The angle α is determined by demanding that the off-diagonal matrix elements in (B.16) vanish and that $M_0 \geq m_h$. This lifts the sign ambiguity for α and we arrive at the expressions

$$c_{2\alpha} = \frac{\mathcal{M}_{11}^2 - \mathcal{M}_{22}^2}{\sqrt{(\mathcal{M}_{11}^2 - \mathcal{M}_{22}^2)^2 + 4(\mathcal{M}_{12}^2)^2}}, \quad s_{2\alpha} = \frac{2\mathcal{M}_{12}^2}{\sqrt{(\mathcal{M}_{11}^2 - \mathcal{M}_{22}^2)^2 + 4(\mathcal{M}_{12}^2)^2}}. \quad (\text{B.17})$$

Plugging α back in (B.16) results in an expression for the neutral CP-even scalar masses

$$m_h^2 = \frac{1}{2} \left[\mathcal{M}_{11}^2 + \mathcal{M}_{22}^2 - \sqrt{(\mathcal{M}_{11}^2 - \mathcal{M}_{22}^2)^2 + 4(\mathcal{M}_{12}^2)^2} \right] \quad (\text{B.18})$$

$$M_0^2 = \frac{1}{2} \left[\mathcal{M}_{11}^2 + \mathcal{M}_{22}^2 + \sqrt{(\mathcal{M}_{11}^2 - \mathcal{M}_{22}^2)^2 + 4(\mathcal{M}_{12}^2)^2} \right] \quad (\text{B.19})$$

From these result we can express the original Higgs doublets Φ_i in terms of the physical Higgs states and the Goldstones

$$\phi_1^\pm = c_\beta G^\pm - s_\beta H^\pm \quad (\text{B.20})$$

$$\phi_2^\pm = s_\beta G^\pm + c_\beta H^\pm \quad (\text{B.21})$$

It is convenient to define the following combinations of parameters

$$\begin{aligned} m_D^4 &= \mathcal{B}_{11}^2 \mathcal{B}_{22}^2 - (\mathcal{B}_{12}^2)^2, \\ m_L^2 &= \mathcal{B}_{11}^2 c_\beta^2 + \mathcal{B}_{22}^2 s_\beta^2 + \mathcal{B}_{12}^2 s_{2\beta}, \\ m_T^2 &= \mathcal{B}_{11}^2 + \mathcal{B}_{22}^2, \\ M_S^2 &= M_A^2 + m_T^2 = \mathcal{M}_{11}^2 + \mathcal{M}_{22}^2. \end{aligned} \quad (\text{B.22})$$

The square root term in (B.18) can thus be written as

$$\sqrt{(\mathcal{M}_{11}^2 - \mathcal{M}_{22}^2)^2 + 4(\mathcal{M}_{12}^2)^2} = \sqrt{m_S^4 - 4M_A^2 m_L^2 - 4m_D^4} \quad (\text{B.23})$$

Hence, a more useful expression for the scalar masses reads

$$m_h^2 = \frac{1}{2} \left[M_S^2 - \sqrt{M_S^4 - 4M_A^2 m_L^2 - 4m_D^4} \right] \quad (\text{B.24})$$

$$M_0^2 = \frac{1}{2} \left[M_S^2 + \sqrt{M_S^4 - 4M_A^2 m_L^2 - 4m_D^4} \right] \quad (\text{B.25})$$

Additionally, we have

$$c_{\beta-\alpha}^2 = \frac{m_L^2 - m_h^2}{M_0^2 - m_h^2} = \frac{m_L^2 - m_h^2}{M_0^2} + \mathcal{O}\left(\frac{1}{M_0^4}\right) \quad (\text{B.26})$$

where we used the trigonometric identity $c_{\beta-\alpha}^2 = \frac{1}{2} (1 + c_{2\alpha} c_{2\beta} + s_{2\alpha} s_{2\beta})$.

C. Useful relations for one-loop integrals

Loop Integrals

At various points in this thesis we have to compute one-loop integrals using dimensional regularization. Here we list a compendium of useful formulae for that purpose. Similar collections can be found in every standard QFT book [48–51]. To evaluate one-loop integrals we make use of the master formula

$$\int \frac{d^d k}{(2\pi)^d} \frac{k^{2a}}{(k^2 - \Delta)^b} = i \frac{(-1)^{a-b}}{(4\pi)^{\frac{d}{2}}} \frac{1}{\Delta^{b-a-\frac{d}{2}}} \frac{\Gamma(a + \frac{d}{2}) \Gamma(b - a - \frac{d}{2})}{\Gamma(b) \Gamma(\frac{d}{2})} \quad (\text{C.1})$$

Here the *gamma function* is defined as

$$\Gamma(z) = \int_0^\infty dt e^{-t} t^{z-1} \quad (\text{C.2})$$

Useful gamma function identities are

$$\Gamma(n) = (n-1)!, \quad \Gamma\left(n + \frac{1}{2}\right) = \frac{(2n)!}{4^n n!} \sqrt{\pi} \quad (n \in \mathbb{N}), \quad \Gamma(z+1) = z\Gamma(z) \quad (z \in \mathbb{C}) \quad (\text{C.3})$$

The gamma function has poles at negative integers. Expanding the gamma function around negative integers $-n$ ($n > 0$) gives

$$\Gamma(-n + \varepsilon) = \frac{(-1)^n}{n!} \left(\frac{1}{\varepsilon} + \psi^{(0)}(n+1) + \mathcal{O}(\varepsilon) \right) \quad (\text{C.4})$$

Expanding around positive integers gives

$$\Gamma(n + \varepsilon) = (n-1)! (1 + \psi^{(0)}(n)\varepsilon + \mathcal{O}(\varepsilon^2)) \quad (\text{C.5})$$

Here

$$\psi^{(0)}(z) = \frac{\Gamma'(z)}{\Gamma(z)} \quad (\text{C.6})$$

is the *Digamma function* with the special values

$$\psi^{(0)}(1) = -\gamma_E, \quad \psi^{(0)}(2) = 1 - \gamma_E \quad (\text{C.7})$$

and γ_E is the Euler-Mascheroni constant

$$\gamma_E = \lim_{n \rightarrow \infty} \left(\sum_{k=1}^n \frac{1}{k} - \ln n \right) \approx 0.5772 \quad (\text{C.8})$$

Frequently used special cases of these formulae are

$$\Gamma(\varepsilon) = \frac{1}{\varepsilon} - \gamma_E + \mathcal{O}(\varepsilon), \quad \Gamma(-1 + \varepsilon) = -\frac{1}{\varepsilon} + \gamma_E - 1 + \mathcal{O}(\varepsilon), \quad \Gamma(1 + \varepsilon) = 1 - \gamma_E \varepsilon + \mathcal{O}(\varepsilon^2) \quad (\text{C.9})$$

The Euler *beta function* can be expressed in terms of gamma functions

$$B(z_1, z_2) = \int_0^1 dt t^{z_1-1} (1-t)^{z_2-1} = \frac{\Gamma(z_1)\Gamma(z_2)}{\Gamma(z_1+z_2)} \quad (\text{C.10})$$

The gamma function also appears in the expression for the d -dimensional solid angle Ω_d

$$\Omega_d = \frac{2\pi^{d/2}}{\Gamma(\frac{d}{2})}, \quad d\Omega_d = d\Omega_{d-1} \sin^{d-2} \theta d\theta \quad (\text{C.11})$$

For tensor integrals we may replace tensor structures due to Lorentz invariance as follows

$$k^{\mu_1} k^{\mu_2} \dots k^{\mu_{2n}} = \frac{2^{-n} \Gamma(\frac{d}{2})}{\Gamma(\frac{d}{2} + n)} (k^2)^n S_n^{\mu_1 \dots \mu_{2n}} \quad (\text{C.12})$$

where $S_n^{\mu_1 \dots \mu_{2n}}$ is the totally symmetric tensor with $2n$ indices. For $n = 1, 2$ we have

$$k^\mu k^\nu \longrightarrow \frac{k^2}{d} g^{\mu\nu} \quad (\text{C.13})$$

$$k^\mu k^\nu k^\rho k^\sigma \longrightarrow \frac{(k^2)^2}{d(d+2)} (g^{\mu\nu} g^{\rho\sigma} + g^{\mu\rho} g^{\nu\sigma} + g^{\mu\sigma} g^{\nu\rho}) \quad (\text{C.14})$$

Various frequently used special cases of the master formula are

$$\int \frac{d^d k}{(2\pi)^d} \frac{1}{(k^2 - \Delta)^n} = \frac{i(-1)^n}{(4\pi)^{d/2}} \frac{\Gamma(n - \frac{d}{2})}{\Gamma(n)} \left(\frac{1}{\Delta}\right)^{n - \frac{d}{2}} \quad (\text{C.15})$$

$$\int \frac{d^d k}{(2\pi)^d} \frac{k^2}{(k^2 - \Delta)^n} = \frac{i(-1)^{n-1}}{(4\pi)^{d/2}} \frac{d}{2} \frac{\Gamma(n - \frac{d}{2} - 1)}{\Gamma(n)} \left(\frac{1}{\Delta}\right)^{n - \frac{d}{2} - 1} \quad (\text{C.16})$$

$$\int \frac{d^d k}{(2\pi)^d} \frac{k^4}{(k^2 - \Delta)^n} = \frac{i(-1)^n}{(4\pi)^{d/2}} \frac{d(d+2)}{4} \frac{\Gamma(n - \frac{d}{2} - 2)}{\Gamma(n)} \left(\frac{1}{\Delta}\right)^{n - \frac{d}{2} - 2} \quad (\text{C.17})$$

$$\int \frac{d^d k}{(2\pi)^d} \frac{k^\mu k^\nu}{(k^2 - \Delta)^n} = \frac{i(-1)^{n-1}}{(4\pi)^{d/2}} \frac{g^{\mu\nu}}{2} \frac{\Gamma(n - \frac{d}{2} - 1)}{\Gamma(n)} \left(\frac{1}{\Delta}\right)^{n - \frac{d}{2} - 1} \quad (\text{C.18})$$

$$\int \frac{d^d k}{(2\pi)^d} \frac{k^\mu k^\nu k^\rho k^\sigma}{(k^2 - \Delta)^n} = \frac{i(-1)^n}{(4\pi)^{d/2}} \frac{\Gamma(n - \frac{d}{2} - 2)}{\Gamma(n)} \left(\frac{1}{\Delta}\right)^{n - \frac{d}{2} - 2} \frac{g^{\mu\nu} g^{\rho\sigma} + g^{\mu\rho} g^{\nu\sigma} + g^{\mu\sigma} g^{\nu\rho}}{4} \quad (\text{C.19})$$

and specializing to $d = 4 - 2\varepsilon$ dimensions we have (up to $\mathcal{O}(\varepsilon)$ terms):

$$\int \frac{d^d k}{(2\pi)^d} \frac{1}{(k^2 - \Delta + i\varepsilon)} = \frac{i}{16\pi^2} \Delta \left(\frac{1}{\varepsilon} + \ln \frac{\bar{\mu}^2}{\Delta} + 1 \right) (\bar{\mu}^2 = \mu^2 4\pi e^{-\gamma_E}) \quad (\text{C.20})$$

$$\int \frac{d^d k}{(2\pi)^d} \frac{1}{(k^2 - \Delta + i\varepsilon)^2} = \frac{i}{16\pi^2} \left(\frac{1}{\varepsilon} + \ln \frac{\bar{\mu}^2}{\Delta} \right) \quad (\text{C.21})$$

$$\int \frac{d^d k}{(2\pi)^d} \frac{k^2}{(k^2 - \Delta + i\varepsilon)^2} = \frac{i}{16\pi^2} \Delta \left(\frac{2}{\varepsilon} + 1 + 2 \ln \frac{\bar{\mu}^2}{\Delta} \right) \quad (\text{C.22})$$

$$\int \frac{d^d k}{(2\pi)^d} \frac{k^4}{(k^2 - \Delta + i\varepsilon)^2} = \frac{3i}{16\pi^2} \Delta^2 \left(\frac{1}{\varepsilon} + \ln \frac{\bar{\mu}^2}{\Delta} + \frac{2}{3} \right) \quad (\text{C.23})$$

$$\int \frac{d^d k}{(2\pi)^d} \frac{1}{(k^2 - \Delta + i\varepsilon)^3} = \frac{-i}{32\pi^2} \frac{1}{\Delta} \quad (\text{C.24})$$

$$\int \frac{d^d k}{(2\pi)^d} \frac{k^2}{(k^2 - \Delta + i\varepsilon)^3} = \frac{i}{16\pi^2} \left(\frac{1}{\varepsilon} - \frac{1}{2} + \ln \frac{\bar{\mu}^2}{\Delta} \right) \quad (\text{C.25})$$

Note that scaleless integrals vanish in dimensional regularization

$$\int \frac{d^d k}{(2\pi)^d} \frac{1}{(k^2)^a} = 0 \quad (\text{C.26})$$

Feynman parameters

Denominators in loop integrals may be combined using *Feynman parameters*

$$\frac{1}{A_1^{\alpha_1} \cdots A_n^{\alpha_n}} = \frac{\Gamma(\alpha_1 + \cdots + \alpha_n)}{\Gamma(\alpha_1) \cdots \Gamma(\alpha_n)} \int_0^1 du_1 \cdots \int_0^1 du_n \frac{\delta(1 - \sum_{k=1}^n u_k) u_1^{\alpha_1-1} \cdots u_n^{\alpha_n-1}}{(\sum_{k=1}^n u_k A_k)^{\sum_{k=1}^n \alpha_k}} \quad (\text{C.27})$$

Combining two propagators gives

$$\frac{1}{AB} = \int_0^1 dx \frac{1}{[A + x(B - A)]^2} \quad (\text{C.28})$$

For three and more propagators it is particularly convenient to decouple the parameter integrals. Such expressions are given by

$$\frac{1}{ABC} = \int_0^1 dx \int_0^1 dy \frac{2x}{[A + x(C - A) + xy(B - C)]^3} \quad (\text{C.29})$$

for three propagators and

$$\frac{1}{ABCD} = \int_0^1 dx \int_0^1 dy \int_0^1 dz \frac{6x^2 y}{[A + x(C - A) + xy(B - C) + xyz(D - B)]^4} \quad (\text{C.30})$$

for four propagators.

D. SU(2) identities and operator reduction

In this section we show how various expressions involving

$$J_\mu^a = \frac{i}{2} \langle \sigma_a (\partial_\mu U^\dagger U - U^\dagger \partial_\mu U) \rangle \quad (\text{D.1})$$

in Chapter 6 can be simplified. The Pauli matrices σ_a have the following properties. Traces identities:

$$\langle \sigma_a \sigma_b \rangle = 2\delta_{ab} \quad (\text{D.2})$$

$$\langle \sigma_a \sigma_b \sigma_c \rangle = 2i\epsilon_{abc} \quad (\text{D.3})$$

$$\langle \sigma_a \sigma_b \sigma_c \sigma_d \rangle = 2(\delta_{ab}\delta_{cd} - \delta_{ac}\delta_{bd} + \delta_{ad}\delta_{bc}) \quad (\text{D.4})$$

(Anti-)commutators:

$$[\sigma_a, \sigma_b] = 2i\epsilon_{abc}\sigma_c \quad (\text{D.5})$$

$$\{\sigma_a, \sigma_b\} = 2\delta_{ab} \mathbb{1}_{2 \times 2} \quad (\text{D.6})$$

In addition, we have for arbitrary 2x2 matrices A, B the following useful identity

$$\langle T_a A \rangle \langle T_a B \rangle = \frac{1}{2} \langle AB \rangle - \frac{1}{4} \langle A \rangle \langle B \rangle \quad (\text{D.7})$$

Here the $T_a = \sigma_a/2$ are the SU(2) generators and we used the $SU(N)$ completeness relation to derive this identity

$$[T^A]_\beta^\alpha [T^A]_\sigma^\lambda = \frac{1}{2} \delta_\sigma^\alpha \delta_\beta^\lambda - \frac{1}{2N} \delta_\beta^\alpha \delta_\sigma^\lambda \quad (\text{D.8})$$

Using the identity we obtain

$$J_\mu^a J_\nu^a = 2 \langle \partial_\mu U^\dagger \partial_\nu U \rangle \quad (\text{D.9})$$

$$(J_\mu^a)^2 = 2 \langle \partial^\mu U^\dagger \partial_\mu U \rangle \quad (\text{D.10})$$

$$(J_\mu^a J_\nu^a) (J^{b\mu} J^{b\nu}) = 4 \langle \partial_\mu U^\dagger \partial_\nu U \rangle \langle \partial^\mu U^\dagger \partial^\nu U \rangle \quad (\text{D.11})$$

In addition, we have for traceless 2x2 matrices A, B, C

$$\epsilon^{abc} \langle \sigma_a A \rangle \langle \sigma_b B \rangle \langle \sigma_c C \rangle = -4i \langle ABC \rangle \quad (\text{D.12})$$

From (D.4) we deduce for traceless 2x2 matrices A, B, C, D

$$\langle ABCD \rangle = \frac{1}{2} (\langle AB \rangle \langle CD \rangle - \langle AC \rangle \langle BD \rangle + \langle AD \rangle \langle BC \rangle) \quad (\text{D.13})$$

In addition, we have for traceless 2x2 matrices A, B, C, D, E, F

$$\begin{aligned}\langle ABC \rangle \langle DEF \rangle &= \frac{1}{2} (\langle AE \rangle \langle BD \rangle \langle CF \rangle + \langle AD \rangle \langle BF \rangle \langle CE \rangle + \langle AF \rangle \langle BE \rangle \langle CD \rangle) \\ &\quad - \frac{1}{2} (\langle AE \rangle \langle BF \rangle \langle CD \rangle + \langle AD \rangle \langle BE \rangle \langle CF \rangle + \langle AF \rangle \langle BD \rangle \langle CE \rangle)\end{aligned}\quad (\text{D.14})$$

Our aim is to reduce the structure $\partial_\mu J_\nu^a \partial^\mu J^{a\nu}$ and write it in terms of the basis operators

$$\mathcal{O}_1 = \langle \partial_\mu U^\dagger \partial^\mu U \rangle^2, \quad \mathcal{O}_2 = \langle \partial_\mu U^\dagger \partial_\nu U \rangle \langle \partial^\mu U^\dagger \partial^\nu U \rangle \quad (\text{D.15})$$

We calculate

$$\begin{aligned}\partial_\mu J_\nu^a \partial^\mu J^{a\nu} &= -4 \langle T_a (\partial_\mu (U^\dagger \partial_\nu U)) \rangle \langle T_a (\partial^\mu (U^\dagger \partial^\nu U)) \rangle = -2 \langle \partial_\mu (U^\dagger \partial_\nu U) \partial^\mu (U^\dagger \partial^\nu U) \rangle \\ &= -2 \langle \partial_\mu U^\dagger \partial_\nu U \partial^\mu U^\dagger \partial^\nu U \rangle - 2 \langle U^\dagger \partial_\mu \partial_\nu U U^\dagger \partial^\mu \partial^\nu U \rangle - 4 \langle \partial_\mu U^\dagger \partial_\nu U U^\dagger \partial^\mu \partial^\nu U \rangle\end{aligned}\quad (\text{D.16})$$

The first term is easily reduced by inserting $UU^\dagger = \mathbb{1}$ twice into the trace and using (D.4)

$$\langle \partial_\mu U^\dagger \partial_\nu U \partial^\mu U^\dagger \partial^\nu U \rangle = \langle (\partial_\mu U^\dagger U) (U^\dagger \partial_\nu U) (\partial^\mu U^\dagger U) (U^\dagger \partial^\nu U) \rangle = \mathcal{O}_2 - \frac{1}{2} \mathcal{O}_1 \quad (\text{D.17})$$

For the second term we integrate by parts and obtain

$$\langle U^\dagger \partial_\mu \partial_\nu U U^\dagger \partial^\mu \partial^\nu U \rangle = -2 \langle \partial_\mu U^\dagger \partial_\nu U U^\dagger \partial^\mu \partial^\nu U \rangle - \langle \partial_\mu U^\dagger \partial^\mu U \partial_\nu U^\dagger \partial^\nu U \rangle \quad (\text{D.18})$$

where the second term can be identified as

$$\langle \partial_\mu U^\dagger \partial^\mu U \partial_\nu U^\dagger \partial^\nu U \rangle = \frac{1}{2} \mathcal{O}_1 \quad (\text{D.19})$$

Thus,

$$\partial_\mu J_\nu^a \partial^\mu J^{a\nu} = 2 (\mathcal{O}_1 - \mathcal{O}_2) \quad (\text{D.20})$$

Additionally, we need to reduce the structure

$$\epsilon^{abc} J^{\mu a} (\partial_\nu J_\mu^b) J^{\nu c} = -4 \langle \partial_\mu U^\dagger \partial_\nu U \partial^\mu U^\dagger \partial^\nu U \rangle - 4 \langle \partial_\mu U^\dagger \partial_\nu U U^\dagger \partial^\mu \partial^\nu U \rangle = 2 (\mathcal{O}_1 - \mathcal{O}_2) \quad (\text{D.21})$$

E. Scalar Integrals

In this appendix we collect relevant Passarino-Veltman scalar integrals [249] where we used the notation of [250]. Parts of this appendix appeared in [3]. The scalar tadpole integral is given by the integral

$$A(m^2) = \frac{\mu^{4-d}}{i\pi^{\frac{d}{2}} r_\Gamma} \int d^d k \frac{1}{[k^2 - m^2 + i\eta]} \quad (\text{E.1})$$

The factor r_Γ was included to remove the overall constant that appears in d -dimensional integrals

$$r_\Gamma \equiv \frac{\Gamma^2(1-\epsilon)\Gamma(1+\epsilon)}{\Gamma(1-2\epsilon)} = 1 - \epsilon\gamma_E + \epsilon^2 \left[\frac{\gamma_E^2}{2} - \frac{\pi^2}{12} \right] + \mathcal{O}(\epsilon^3) \quad (\text{E.2})$$

In $d = 4 - 2\epsilon$ dimensions it is given by

$$A(m^2) = m^2 \left(\frac{\mu^2}{m^2 - i\eta} \right)^\epsilon \left(\frac{1}{\epsilon} + 1 \right) \quad (\text{E.3})$$

The general scalar bubble integral is given by

$$B(q^2; m_1^2, m_2^2) = \frac{\mu^{4-d}}{i\pi^{\frac{d}{2}} r_\Gamma} \int d^d k \frac{1}{[k^2 - m_1^2] [(k+q)^2 - m_2^2]} \quad (\text{E.4})$$

For equal masses we get the expression ($\tau = q^2/4m^2$)

$$B(q^2; m^2, m^2) = \left[\frac{1}{\epsilon} + \ln \frac{\mu^2}{m^2} + 2 - h(\tau) \right] \quad (\text{E.5})$$

where h is defined as

$$h(\tau) = \begin{cases} \sqrt{1-\tau^{-1}} \log \frac{\sqrt{1-\tau^{-1}}+1}{\sqrt{1-\tau^{-1}}-1} & \text{for } \tau < 0 \\ 2\sqrt{\tau^{-1}-1} \arcsin \sqrt{\tau} & \text{for } 0 \leq \tau \leq 1 \\ \sqrt{1-\tau^{-1}} \left[\log \frac{1+\sqrt{1-\tau^{-1}}}{1-\sqrt{1-\tau^{-1}}} - i\pi \right] & \text{for } \tau > 1 \end{cases} \quad (\text{E.6})$$

For vanishing internal masses we have

$$B(q^2; 0, 0) = \left[\frac{1}{\epsilon} + \ln \frac{\mu^2}{-q^2} + 2 \right] \quad (\text{E.7})$$

The general scalar triangle integral is given by

$$C(l_1^2, l_2^2, (l_1 + l_2)^2; m_1^2, m_2^2, m_3^2) = \int \frac{d^4 k}{i\pi^2} \frac{1}{[k^2 - m_1^2] [(k+l_1)^2 - m_2^2] [(k+l_1+l_2)^2 - m_3^2]} \quad (\text{E.8})$$

We need several special cases in this thesis. First of all, we need the case with equal internal masses and two massless external lines

$$C(q^2) = C(0, 0, q^2; m^2, m^2, m^2) = \frac{1}{2q^2} f(\tau) \quad (\text{E.9})$$

where we defined $\tau = q^2/4m^2$ and

$$f(\tau) = \begin{cases} \log^2 \frac{\sqrt{1-\tau^{-1}}+1}{\sqrt{1-\tau^{-1}}-1} & \text{for } \tau < 0 \\ -4 \arcsin^2 \sqrt{\tau} & \text{for } 0 \leq \tau \leq 1 \\ \left[\log \frac{1+\sqrt{1-\tau^{-1}}}{1-\sqrt{1-\tau^{-1}}} - i\pi \right]^2 & \text{for } \tau > 1 \end{cases} \quad (\text{E.10})$$

For $q^2 = 0$ we obtain

$$C(0) = -\frac{1}{2m^2} \quad (\text{E.11})$$

For $0 < \tau \ll 1$ we have

$$C(s) = -\frac{1}{2m^2} - \frac{s}{24m^4} + \mathcal{O}(s^2) \quad (\text{E.12})$$

For $|\tau| \gg 1$ we can expand

$$C(q^2) = \frac{1}{2q^2} \log^2 \frac{-q^2}{m^2} + \mathcal{O}(q^{-3}) \quad (\text{E.13})$$

The other case we need is

$$C(r^2, q^2) = C(0, r^2, q^2; m^2, m^2, m^2) = \frac{1}{2(q^2 - r^2)} (f(\tau) - f(\sigma)) \quad (\text{E.14})$$

where we introduce $\sigma = r^2/4m^2$. The general scalar four-point function is given by

$$\begin{aligned} D(l_1^2, l_2^2, l_3^2, l_4^2, (l_1 + l_2)^2, (l_2 + l_3)^2, m_1^2, m_2^2, m_3^2, m_4^2) = \\ = \int \frac{d^4 q}{i\pi^2} \frac{1}{[q^2 - m_1^2] [(q + l_1)^2 - m_2^2] [(q + l_1 + l_2)^2 - m_3^2] [(q + l_1 + l_2 + l_3)^2 - m_4^2]} \end{aligned} \quad (\text{E.15})$$

Again we need a special case where all external lines are massless and the internal masses are equal

$$D(q^2, r^2) = D(0, 0, 0, 0, q^2, r^2; m^2, m^2, m^2, m^2) = \frac{2}{q^2 r^2} \frac{1}{\beta_2(\tau, \sigma)} g(\tau, \sigma) \quad (\text{E.16})$$

where we defined

$$\beta_1(z) = \sqrt{1 - z^{-1}}, \quad \beta_2(y, z) = \sqrt{1 - y^{-1} - z^{-1}} \quad (\text{E.17})$$

and

$$g(\tau, \sigma) = I_1(\tau, \sigma) + I_1(\sigma, \tau) + I_2(\tau, \sigma) - \frac{\pi^2}{2} \quad (\text{E.18})$$

with

$$I_1(\tau, \sigma) = 2\text{Li}_2(\tau [\beta_1(\sigma) - 1] [\beta_1(\sigma) - \beta_2(\tau, \sigma)]) - 2\text{Li}_2(-\tau [\beta_1(\tau) - 1] [\beta_1(\tau) - \beta_2(\tau, \sigma)]) - \log^2(\tau [\beta_1(\sigma) + 1] [\beta_1(\sigma) - \beta_2(\tau, \sigma)]) \quad (\text{E.19})$$

and

$$I_2(\tau, \sigma) = I_2(\sigma, \tau) = \log(-\sigma [\beta_1(\tau) - \beta_2(\tau, \sigma)]^2) \log(-\tau [\beta_1(\sigma) - \beta_2(\tau, \sigma)]^2) + 2 \log^2(\tau [\beta_1(\tau) + \beta_2(\tau, \sigma)] [\beta_1(\sigma) - \beta_2(\tau, \sigma)]) \quad (\text{E.20})$$

The expression for $g(\tau, \sigma)$ is immediately applicable in the region $\tau, \sigma < 0$. For $\tau, \sigma > 0$ it holds with the prescription $\tau \rightarrow \tau + i\eta$ and $\sigma \rightarrow \sigma + i\eta$ respectively. Setting one of the arguments to zero the box function takes the form

$$D(q^2, 0) = \frac{1}{m^2 q^2} \left(2 + \sqrt{1 - \tau^{-1}} \log \frac{\sqrt{1 - \tau^{-1}} - 1}{\sqrt{1 - \tau^{-1}} + 1} \right) \quad (\text{E.21})$$

Setting both arguments to zero one has

$$D(0, 0) = \frac{1}{6m^4} \quad (\text{E.22})$$

Expanding the box function asymptotically for large $|\tau|, |\sigma| \gg 1$ we have

$$D(q^2, r^2) = \frac{2}{q^2 r^2} \left[\log \left(\frac{-q^2}{m^2} \right) \log \left(\frac{-r^2}{m^2} \right) - \frac{\pi^2}{2} \right] \quad (\text{E.23})$$

Explicit calculation

Let's start by calculating $C(\tau)$ for $\tau < 0$, the result for $\tau > 0$ can be inferred by proper analytical continuation $\tau \rightarrow \tau + i\eta$. Employing the appropriate Feynman parameter identity

$$\frac{1}{ABC} = \int_0^1 dx \int_0^1 dy \frac{2x^2}{[A + x(C - A) + xy(B - C)]^3} \quad (\text{E.24})$$

one has to deal with the double integral

$$C(\tau) = \frac{-1}{m^2} \int_0^1 dx x \int_0^1 dy \frac{1}{1 - 4x\bar{x}y\tau} = \frac{1}{q^2} \int_0^1 dx \frac{\ln 1 - 4x\bar{x}\tau}{x} \quad (\text{E.25})$$

$$= -\frac{1}{q^2} \left(\text{Li}_2 \left(2\tau \left(1 - \sqrt{1 - \tau^{-1}} \right) \right) + \text{Li}_2 \left(2\tau \left(1 + \sqrt{1 - \tau^{-1}} \right) \right) \right) \quad (\text{E.26})$$

At this stage one has to use the dilogarithm identity

$$\text{Li}_2(1 - z) + \text{Li}_2 \left(1 - \frac{1}{z} \right) = -\frac{1}{2} \ln^2 z \quad (\text{E.27})$$

with $z = 1 - 2\tau(1 + \sqrt{1 - \tau^{-1}})$, which yields

$$C(\tau) = \frac{1}{2q^2} \ln^2 \left(1 - 2\tau(1 + \sqrt{1 - \tau^{-1}}) \right) \quad (\text{E.28})$$

or equivalently

$$C(\tau) = \frac{1}{2q^2} \ln^2 \frac{\sqrt{1-\tau^{-1}} + 1}{\sqrt{1-\tau^{-1}} - 1} \quad (\text{E.29})$$

We want to calculate the special case of the scalar box integral with massless legs and all identical internal masses, i.e.

$$\begin{aligned} & D(0, 0, 0, 0, (l_1 + l_2)^2, (l_2 + l_3)^2; m^2, m^2, m^2, m^2) = \\ &= \int \frac{d^4 q}{i\pi^2} \frac{1}{[q^2 - m^2] [(q + l_1)^2 - m^2] [(q + l_1 + l_2)^2 - m^2] [(q + l_1 + l_2 + l_3)^2 - m^2]} \end{aligned} \quad (\text{E.30})$$

We need to discern two cases: (i) $D(s, t)$ or $D(s, u)$ respectively and (ii) $D(u, t)$. For case (i) we have one invariant strictly positive and the other negative whereas in case (ii) there are two negative invariants. To calculate the integral we need the Feynman parameter identity

$$\frac{1}{ABCD} = \int_0^1 dx \int_0^1 dy \int_0^1 dz \frac{6x^2 y}{[A + x(C - A) + xy(B - C) + xyz(D - B)]^4} \quad (\text{E.31})$$

and

$$\int \frac{d^4 q}{i\pi^2} \frac{1}{(k^2 - \Delta + i\epsilon)^4} = \frac{1}{6} \frac{1}{\Delta^2} \quad (\text{E.32})$$

For $\tau, \sigma < 0$ we get

$$D(\tau, \sigma) = \frac{1}{m^4} \int_0^1 dx x^2 \int_0^1 dy \frac{y}{[1 - 4x(1 - x)y\tau][1 - 4y(1 - y)x^2\sigma]} \quad (\text{E.33})$$

F. Feynman Rules

In this appendix we collect the relevant Feynman rules for the models covered in the thesis.

Sigma Model

First of all, we derive the Feynman rule for the quartic Goldstone vertex in $SU(2)$ linear sigma model. To get the Feynman rule we need to expand the U matrices

$$U = 1 + i2\frac{\varphi}{v} - 2\frac{\varphi^2}{v^2} - i\frac{4}{3}\frac{\varphi^3}{v^3} + \dots \quad (\text{F.1})$$

$$U^\dagger = 1 - i2\frac{\varphi}{v} - 2\frac{\varphi^2}{v^2} + i\frac{4}{3}\frac{\varphi^3}{v^3} + \dots \quad (\text{F.2})$$

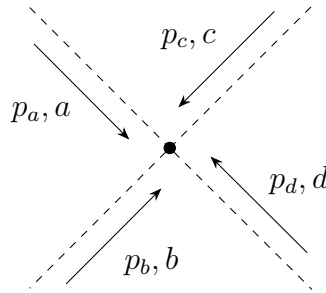
$$\partial_\mu U = 2i\frac{\partial_\mu \varphi}{v} - 2\frac{\partial_\mu \varphi \varphi + \varphi \partial_\mu \varphi}{v^2} - i\frac{4}{3}\frac{\partial_\mu \varphi \varphi^2 + \varphi \partial_\mu \varphi \varphi + \varphi^2 \partial_\mu \varphi}{v^3} + \dots \quad (\text{F.3})$$

$$\partial_\mu U^\dagger = -i2\frac{\partial_\mu \varphi}{v} - 2\frac{\partial_\mu \varphi \varphi + \varphi \partial_\mu \varphi}{v^2} + i\frac{4}{3}\frac{\partial_\mu \varphi \varphi^2 + \varphi \partial_\mu \varphi \varphi + \varphi^2 \partial_\mu \varphi}{v^3} + \dots \quad (\text{F.4})$$

where $\varphi = \varphi^a T^a = \varphi^a \sigma^a / 2$. Using these expansion one can derive the quartic part of the Lagrangian. The contribution quartic in φ can be compactly written as

$$\mathcal{L}_2^{4\varphi} = \frac{1}{3v^2} \langle [\varphi, \partial^\mu \varphi] [\varphi, \partial_\mu \varphi] \rangle = \frac{1}{6v^2} (\varphi^a \partial_\mu \varphi^a \varphi^b \partial_\mu \varphi^b - \partial^\mu \varphi^a \partial_\mu \varphi^a \varphi^b \varphi^b) \quad (\text{F.5})$$

The Feynman rule for the quartic vertex

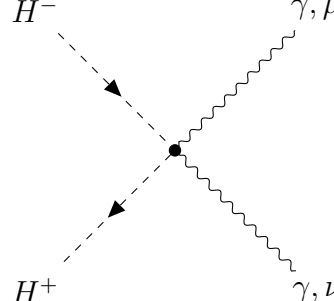


is given by [190]

$$\begin{aligned} i\mathcal{M} = & \frac{i}{v^2} [\delta_{ab}\delta_{cd} (p_a + p_b)^2 + \delta_{ac}\delta_{bd} (p_a + p_c)^2 + \delta_{ad}\delta_{bc} (p_a + p_d)^2] \\ & - \frac{i}{3v^2} (\delta_{ab}\delta_{cd} + \delta_{ac}\delta_{bd} + \delta_{ad}\delta_{bc}) (p_a^2 + p_b^2 + p_c^2 + p_d^2) \end{aligned} \quad (\text{F.6})$$

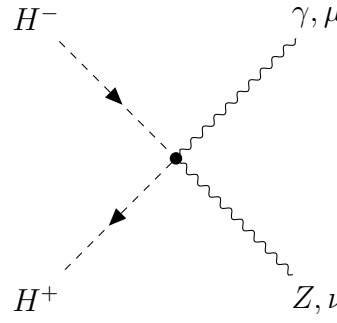
2HDM

The relevant Feynman rules for the $h \rightarrow \gamma\gamma$ and $h \rightarrow \gamma Z$ amplitudes in the 2HDM are [194]



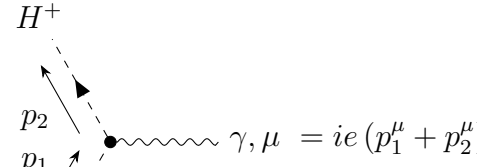
A Feynman diagram showing a loop of charged Higgs bosons (H^\pm) contributing to the $h \rightarrow \gamma\gamma$ amplitude. The external lines are a scalar h (dashed line with a dot) and two photons (γ , wavy lines). The internal lines are H^+ and H^- (dashed lines with arrows). The diagram is labeled with equation (F.7) and the value $= 2ie^2 g_{\mu\nu}$.

$$= 2ie^2 g_{\mu\nu} \quad (\text{F.7})$$



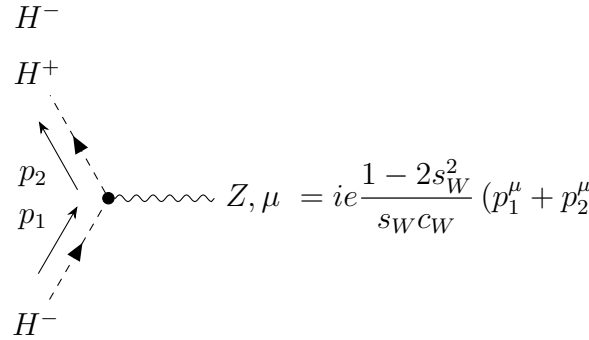
A Feynman diagram showing a loop of charged Higgs bosons (H^\pm) contributing to the $h \rightarrow \gamma Z$ amplitude. The external lines are a scalar h (dashed line with a dot), a photon (γ , wavy line), and a Z boson (Z , wavy line). The internal lines are H^+ and H^- (dashed lines with arrows). The diagram is labeled with equation (F.8) and the value $= 2ie^2 \frac{1 - 2s_W^2}{s_W c_W} g_{\mu\nu}$.

$$= 2ie^2 \frac{1 - 2s_W^2}{s_W c_W} g_{\mu\nu} \quad (\text{F.8})$$



A Feynman diagram showing the tree-level vertex for $h \rightarrow \gamma\gamma$. The external lines are a scalar h (dashed line with a dot) and two photons (γ , wavy lines). The diagram is labeled with equation (F.9) and the value $= ie(p_1^\mu + p_2^\mu)$.

$$= ie(p_1^\mu + p_2^\mu) \quad (\text{F.9})$$



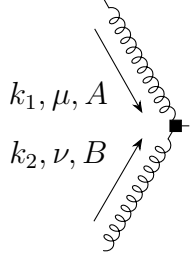
A Feynman diagram showing the tree-level vertex for $h \rightarrow \gamma Z$. The external lines are a scalar h (dashed line with a dot), a photon (γ , wavy line), and a Z boson (Z , wavy line). The diagram is labeled with equation (F.10) and the value $= ie \frac{1 - 2s_W^2}{s_W c_W} (p_1^\mu + p_2^\mu)$.

$$= ie \frac{1 - 2s_W^2}{s_W c_W} (p_1^\mu + p_2^\mu) \quad (\text{F.10})$$

$gg \rightarrow ZZ$

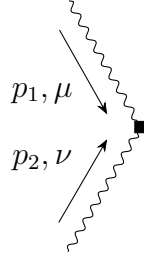
We make use of the following Feynman rules coming from the interaction Lagrangian (8.9,8.10)

Q_{ggh}



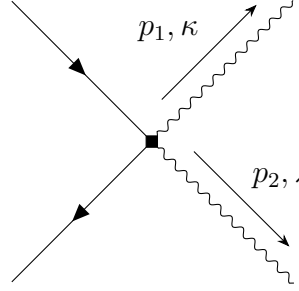
$$= -i \frac{\alpha_s}{4\pi} \delta^{AB} \frac{2k_1 \cdot k_2}{v} \left(g^{\mu\nu} - \frac{k_1^\nu k_2^\mu}{k_1 \cdot k_2} \right) c_{ggh} \quad (\text{F.11})$$

Q_{ZZh}

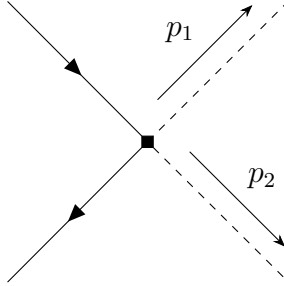


$$= -i \frac{\alpha}{4\pi} \frac{2p_1 \cdot p_2}{v} \left(g^{\mu\nu} - \frac{p_1^\nu p_2^\mu}{p_1 \cdot p_2} \right) c_{ZZh} \quad (\text{F.12})$$

$Q_{\psi S1}$

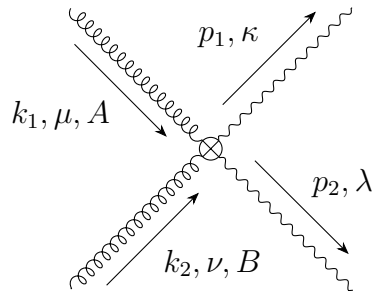


$$= 4i \frac{m_z^2}{v^2} C_{\psi S1} g_{\kappa\lambda} \quad (\text{F.13})$$

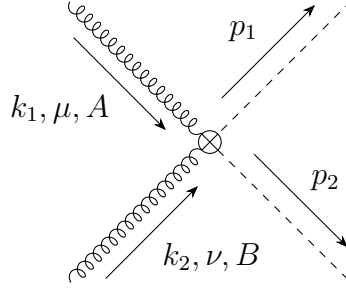


$$= -2i C_{\psi S1} \frac{2p_1 \cdot p_2}{v^2} \quad (\text{F.14})$$

Q_{GU1}

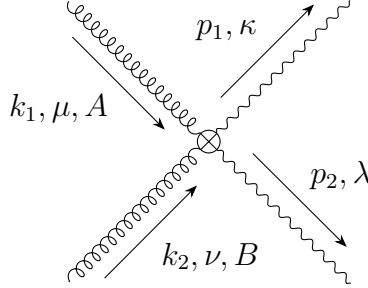


$$= -4ig_s^2\delta^{AB}\frac{m_z^2}{v^2}C_{GU1}(2k_1\cdot k_2)\left(g^{\mu\nu}-\frac{k_1^\nu k_2^\mu}{k_1\cdot k_2}\right)g^{\kappa\lambda} \quad (F.15)$$

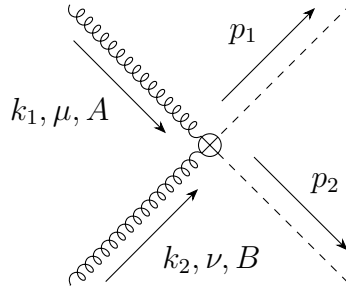


$$= 2ig_s^2\delta^{AB}\frac{1}{v^2}C_{GU1}(2k_1\cdot k_2)(2p_1\cdot p_2)\left(g^{\mu\nu}-\frac{k_1^\nu k_2^\mu}{k_1\cdot k_2}\right) \quad (F.16)$$

Q_{GU2}



$$= -2ig_s^2\delta^{AB}\frac{m_z^2}{v^2}C_{GU2}\left[g^{\mu\lambda}k_1^\nu k_2^\kappa + g^{\mu\kappa}k_1^\nu k_2^\lambda + g^{\nu\lambda}k_1^\kappa k_2^\mu + g^{\nu\kappa}k_1^\lambda k_2^\mu - g^{\mu\nu}(k_1^\kappa k_2^\lambda + k_1^\lambda k_2^\kappa) - (k_1\cdot k_2)(g^{\mu\kappa}g^{\nu\lambda} + g^{\mu\lambda}g^{\nu\kappa})\right] \quad (F.17)$$



$$= 2ig_s^2\delta^{AB}\frac{1}{v^2}C_{GU2}\left[(k_1\cdot p_1)p_2^\nu k_2^\mu + (k_1\cdot p_2)p_1^\nu k_2^\mu + (k_2\cdot p_2)k_1^\nu p_1^\mu + (k_2\cdot p_1)k_1^\nu p_2^\mu - (k_1\cdot k_2)(p_1^\mu p_2^\nu + p_1^\nu p_2^\mu) - g^{\mu\nu}((k_1\cdot p_1)(k_2\cdot p_2) + (k_1\cdot p_2)(k_2\cdot p_1))\right] \quad (F.18)$$

Bibliography

- [1] G. Buchalla et al. “Loop counting matters in SMEFT”. In: *SciPost Phys.* 15.3 (2023), p. 088. DOI: 10.21468/SciPostPhys.15.3.088. arXiv: 2204.11808 [hep-ph].
- [2] G. Buchalla et al. “Two-Higgs-doublet model matched to nonlinear effective theory”. In: *Phys. Rev. D* 110.1 (2024), p. 016015. DOI: 10.1103/PhysRevD.110.016015. arXiv: 2312.13885 [hep-ph].
- [3] Gerhard Buchalla and Florian Pandler. “Anomalous Couplings from the Electroweak Chiral Lagrangian for Off-Shell Higgs in $gg \rightarrow Z_L Z_L$ ”. In: (July 2025). arXiv: 2507.23658 [hep-ph].
- [4] Julian S. Schwinger. “On Quantum electrodynamics and the magnetic moment of the electron”. In: *Phys. Rev.* 73 (1948), pp. 416–417. DOI: 10.1103/PhysRev.73.416.
- [5] S. Tomonaga. “On a relativistically invariant formulation of the quantum theory of wave fields”. In: *Prog. Theor. Phys.* 1 (1946), pp. 27–42. DOI: 10.1143/PTP.1.27.
- [6] R. P. Feynman. “Space - time approach to quantum electrodynamics”. In: *Phys. Rev.* 76 (1949). Ed. by L. M. Brown, pp. 769–789. DOI: 10.1103/PhysRev.76.769.
- [7] X. Fan et al. “Measurement of the Electron Magnetic Moment”. In: *Phys. Rev. Lett.* 130 (7 Feb. 2023), p. 071801. DOI: 10.1103/PhysRevLett.130.071801. URL: <https://link.aps.org/doi/10.1103/PhysRevLett.130.071801>.
- [8] H. Fritzsch, Murray Gell-Mann, and H. Leutwyler. “Advantages of the Color Octet Gluon Picture”. In: *Phys. Lett. B* 47 (1973), pp. 365–368. DOI: 10.1016/0370-2693(73)90625-4.
- [9] H. Fritzsch, Murray Gell-Mann, and P. Minkowski. “Vector - Like Weak Currents and New Elementary Fermions”. In: *Phys. Lett. B* 59 (1975), pp. 256–260. DOI: 10.1016/0370-2693(75)90040-4.
- [10] Gerard 't Hooft. “Renormalizable Lagrangians for Massive Yang-Mills Fields”. In: *Nucl. Phys. B* 35 (1971). Ed. by J. C. Taylor, pp. 167–188. DOI: 10.1016/0550-3213(71)90139-8.
- [11] M. J. G. Veltman. “Perturbation theory of massive Yang-Mills fields”. In: *Nucl. Phys. B* 7 (1968), pp. 637–650. DOI: 10.1016/0550-3213(68)90197-1.
- [12] Steven Weinberg. “A Model of Leptons”. In: *Phys. Rev. Lett.* 19 (1967), pp. 1264–1266. DOI: 10.1103/PhysRevLett.19.1264.
- [13] S. L. Glashow. “Partial Symmetries of Weak Interactions”. In: *Nucl. Phys.* 22 (1961), pp. 579–588. DOI: 10.1016/0029-5582(61)90469-2.
- [14] Abdus Salam. “Weak and Electromagnetic Interactions”. In: *Conf. Proc. C* 680519 (1968), pp. 367–377. DOI: 10.1142/9789812795915_0034.

- [15] Peter W. Higgs. “Broken symmetries, massless particles and gauge fields”. In: *Phys. Lett.* 12 (1964), pp. 132–133. DOI: 10.1016/0031-9163(64)91136-9.
- [16] Peter W. Higgs. “Broken Symmetries and the Masses of Gauge Bosons”. In: *Phys. Rev. Lett.* 13 (1964). Ed. by J. C. Taylor, pp. 508–509. DOI: 10.1103/PhysRevLett.13.508.
- [17] Peter W. Higgs. “Spontaneous Symmetry Breakdown without Massless Bosons”. In: *Phys. Rev.* 145 (1966), pp. 1156–1163. DOI: 10.1103/PhysRev.145.1156.
- [18] F. Englert and R. Brout. “Broken Symmetry and the Mass of Gauge Vector Mesons”. In: *Phys. Rev. Lett.* 13 (1964). Ed. by J. C. Taylor, pp. 321–323. DOI: 10.1103/PhysRevLett.13.321.
- [19] T. W. B. Kibble. “Symmetry breaking in nonAbelian gauge theories”. In: *Phys. Rev.* 155 (1967). Ed. by J. C. Taylor, pp. 1554–1561. DOI: 10.1103/PhysRev.155.1554.
- [20] Georges Aad et al. “Observation of a new particle in the search for the Standard Model Higgs boson with the ATLAS detector at the LHC”. In: *Phys. Lett. B* 716 (2012), pp. 1–29. DOI: 10.1016/j.physletb.2012.08.020. arXiv: 1207.7214 [hep-ex].
- [21] Serguei Chatrchyan et al. “Observation of a New Boson at a Mass of 125 GeV with the CMS Experiment at the LHC”. In: *Phys. Lett. B* 716 (2012), pp. 30–61. DOI: 10.1016/j.physletb.2012.08.021. arXiv: 1207.7235 [hep-ex].
- [22] Steven Weinberg. “Baryon and Lepton Nonconserving Processes”. In: *Phys. Rev. Lett.* 43 (1979), pp. 1566–1570. DOI: 10.1103/PhysRevLett.43.1566.
- [23] W. Buchmuller and D. Wyler. “Effective Lagrangian Analysis of New Interactions and Flavor Conservation”. In: *Nucl. Phys. B* 268 (1986), pp. 621–653. DOI: 10.1016/0550-3213(86)90262-2.
- [24] B. Grzadkowski et al. “Dimension-Six Terms in the Standard Model Lagrangian”. In: *JHEP* 10 (2010), p. 085. DOI: 10.1007/JHEP10(2010)085. arXiv: 1008.4884 [hep-ph].
- [25] Ilaria Brivio and Michael Trott. “The Standard Model as an Effective Field Theory”. In: *Phys. Rept.* 793 (2019), pp. 1–98. DOI: 10.1016/j.physrep.2018.11.002. arXiv: 1706.08945 [hep-ph].
- [26] André David and Giampiero Passarino. “Through precision straits to next standard model heights”. In: *Rev. Phys.* 1 (2016), pp. 13–28. DOI: 10.1016/j.revip.2016.01.001. arXiv: 1510.00414 [hep-ph].
- [27] Michael Trott. “Methodology for theory uncertainties in the standard model effective field theory”. In: *Phys. Rev. D* 104.9 (2021), p. 095023. DOI: 10.1103/PhysRevD.104.095023. arXiv: 2106.13794 [hep-ph].
- [28] Timothy Cohen et al. “Is SMEFT Enough?” In: *JHEP* 03 (2021), p. 237. DOI: 10.1007/JHEP03(2021)237. arXiv: 2008.08597 [hep-ph].
- [29] F. Feruglio. “The Chiral approach to the electroweak interactions”. In: *Int. J. Mod. Phys. A* 8 (1993), pp. 4937–4972. DOI: 10.1142/S0217751X93001946. arXiv: hep-ph/9301281.

- [30] J. Bagger et al. “The Strongly interacting W W system: Gold plated modes”. In: *Phys. Rev. D* 49 (1994), pp. 1246–1264. DOI: 10.1103/PhysRevD.49.1246. arXiv: hep-ph/9306256.
- [31] Vassilis Koulovassilopoulos and R. Sekhar Chivukula. “The Phenomenology of a nonstandard Higgs boson in W(L) W(L) scattering”. In: *Phys. Rev. D* 50 (1994), pp. 3218–3234. DOI: 10.1103/PhysRevD.50.3218. arXiv: hep-ph/9312317.
- [32] C. P. Burgess, J. Matias, and M. Pospelov. “A Higgs or not a Higgs? What to do if you discover a new scalar particle”. In: *Int. J. Mod. Phys. A* 17 (2002), pp. 1841–1918. DOI: 10.1142/S0217751X02009813. arXiv: hep-ph/9912459.
- [33] Li-Ming Wang and Qing Wang. “Nonstandard Higgs in electroweak chiral Lagrangian”. In: (May 2006). arXiv: hep-ph/0605104.
- [34] Benjamin Grinstein and Michael Trott. “A Higgs-Higgs bound state due to new physics at a TeV”. In: *Phys. Rev. D* 76 (2007), p. 073002. DOI: 10.1103/PhysRevD.76.073002. arXiv: 0704.1505 [hep-ph].
- [35] Roberto Contino et al. “Strong Double Higgs Production at the LHC”. In: *JHEP* 05 (2010), p. 089. DOI: 10.1007/JHEP05(2010)089. arXiv: 1002.1011 [hep-ph].
- [36] Roberto Contino. “The Higgs as a Composite Nambu-Goldstone Boson”. In: *Theoretical Advanced Study Institute in Elementary Particle Physics: Physics of the Large and the Small*. 2011, pp. 235–306. DOI: 10.1142/9789814327183_0005. arXiv: 1005.4269 [hep-ph].
- [37] Gerhard Buchalla and Oscar Cata. “Effective Theory of a Dynamically Broken Electroweak Standard Model at NLO”. In: *JHEP* 07 (2012), p. 101. DOI: 10.1007/JHEP07(2012)101. arXiv: 1203.6510 [hep-ph].
- [38] R. Alonso et al. “The Effective Chiral Lagrangian for a Light Dynamical ”Higgs Particle””. In: *Phys. Lett. B* 722 (2013). [Erratum: Phys.Lett.B 726, 926 (2013)], pp. 330–335. DOI: 10.1016/j.physletb.2013.04.037. arXiv: 1212.3305 [hep-ph].
- [39] R. Alonso et al. “Flavor with a light dynamical ”Higgs particle””. In: *Phys. Rev. D* 87.5 (2013), p. 055019. DOI: 10.1103/PhysRevD.87.055019. arXiv: 1212.3307 [hep-ph].
- [40] Gerhard Buchalla, Oscar Catà, and Claudius Krause. “Complete Electroweak Chiral Lagrangian with a Light Higgs at NLO”. In: *Nucl. Phys. B* 880 (2014). [Erratum: Nucl.Phys.B 913, 475–478 (2016)], pp. 552–573. DOI: 10.1016/j.nuclphysb.2014.01.018. arXiv: 1307.5017 [hep-ph].
- [41] R. L. Delgado et al. “One-loop $\gamma\gamma \rightarrow W_L^+ W_L^-$ and $\gamma\gamma \rightarrow Z_L Z_L$ from the Electroweak Chiral Lagrangian with a light Higgs-like scalar”. In: *JHEP* 07 (2014), p. 149. DOI: 10.1007/JHEP07(2014)149. arXiv: 1404.2866 [hep-ph].
- [42] G. Buchalla et al. “Fitting Higgs Data with Nonlinear Effective Theory”. In: *Eur. Phys. J. C* 76.5 (2016), p. 233. DOI: 10.1140/epjc/s10052-016-4086-9. arXiv: 1511.00988 [hep-ph].
- [43] Rodrigo Alonso, Elizabeth E. Jenkins, and Aneesh V. Manohar. “Geometry of the Scalar Sector”. In: *JHEP* 08 (2016), p. 101. DOI: 10.1007/JHEP08(2016)101. arXiv: 1605.03602 [hep-ph].

- [44] Raquel Gómez-Ambrosio et al. “Distinguishing electroweak EFTs with $WLWL \rightarrow n \times h$ ”. In: *Phys. Rev. D* 106.5 (2022), p. 053004. DOI: 10.1103/PhysRevD.106.053004. arXiv: 2204.01763 [hep-ph].
- [45] Raquel Gómez-Ambrosio et al. “SMEFT is falsifiable through multi-Higgs measurements (even in the absence of new light particles)”. In: *Commun. Theor. Phys.* 75.9 (2023), p. 095202. DOI: 10.1088/1572-9494/ace95e. arXiv: 2207.09848 [hep-ph].
- [46] Rafael L. Delgado et al. “Production of two, three, and four Higgs bosons: where SMEFT and HEFT depart”. In: *JHEP* 03 (2024), p. 037. DOI: 10.1007/JHEP03(2024)037. arXiv: 2311.04280 [hep-ph].
- [47] Javier Fuentes-Martin, Jorge Portoles, and Pedro Ruiz-Femenia. “Integrating out heavy particles with functional methods: a simplified framework”. In: *JHEP* 09 (2016), p. 156. DOI: 10.1007/JHEP09(2016)156. arXiv: 1607.02142 [hep-ph].
- [48] Michael E. Peskin and Daniel V. Schroeder. *An Introduction to quantum field theory*. Reading, USA: Addison-Wesley, 1995. ISBN: 978-0-201-50397-5, 978-0-429-50355-9, 978-0-429-49417-8. DOI: 10.1201/9780429503559.
- [49] M. Srednicki. *Quantum field theory*. Cambridge University Press, Jan. 2007. ISBN: 978-0-521-86449-7, 978-0-511-26720-8. DOI: 10.1017/CB09780511813917.
- [50] Matthew D. Schwartz. *Quantum Field Theory and the Standard Model*. Cambridge University Press, Mar. 2014. ISBN: 978-1-107-03473-0, 978-1-107-03473-0.
- [51] A. Zee. *Quantum field theory in a nutshell*. 2003. ISBN: 978-0-691-14034-6.
- [52] Steven Weinberg. *The Quantum theory of fields. Vol. 1: Foundations*. Cambridge University Press, June 2005. ISBN: 978-0-521-67053-1, 978-0-511-25204-4. DOI: 10.1017/CB09781139644167.
- [53] Steven Weinberg. *The quantum theory of fields. Vol. 2: Modern applications*. Cambridge University Press, Aug. 2013. ISBN: 978-1-139-63247-8, 978-0-521-67054-8, 978-0-521-55002-4. DOI: 10.1017/CB09781139644174.
- [54] G. 't Hooft. “Computation of the quantum effects due to a four-dimensional pseudoparticle”. In: *Phys. Rev. D* 14 (12 Dec. 1976), pp. 3432–3450. DOI: 10.1103/PhysRevD.14.3432. URL: <https://link.aps.org/doi/10.1103/PhysRevD.14.3432>.
- [55] David J. Gross and Frank Wilczek. “Ultraviolet Behavior of Nonabelian Gauge Theories”. In: *Phys. Rev. Lett.* 30 (1973). Ed. by J. C. Taylor, pp. 1343–1346. DOI: 10.1103/PhysRevLett.30.1343.
- [56] H. David Politzer. “Reliable Perturbative Results for Strong Interactions?” In: *Phys. Rev. Lett.* 30 (1973). Ed. by J. C. Taylor, pp. 1346–1349. DOI: 10.1103/PhysRevLett.30.1346.
- [57] J. Gasser and H. Leutwyler. “Chiral Perturbation Theory to One Loop”. In: *Annals Phys.* 158 (1984), p. 142. DOI: 10.1016/0003-4916(84)90242-2.
- [58] J. Gasser and H. Leutwyler. “Chiral Perturbation Theory: Expansions in the Mass of the Strange Quark”. In: *Nucl. Phys. B* 250 (1985), pp. 465–516. DOI: 10.1016/0550-3213(85)90492-4.

- [59] S. Navas et al. “Review of particle physics”. In: *Phys. Rev. D* 110.3 (2024), p. 030001. DOI: 10.1103/PhysRevD.110.030001.
- [60] P. Sikivie et al. “Isospin Breaking in Technicolor Models”. In: *Nucl. Phys. B* 173 (1980), pp. 189–207. DOI: 10.1016/0550-3213(80)90214-X.
- [61] Matthew McCullough. “Examining the Higgs”. In: *Higgs Center School*. 2021. URL: <https://higgs.ph.ed.ac.uk/workshops/higgs-centre-school-2021/>.
- [62] J. de Blas et al. “Higgs Boson Studies at Future Particle Colliders”. In: *JHEP* 01 (2020), p. 139. DOI: 10.1007/JHEP01(2020)139. arXiv: 1905.03764 [hep-ph].
- [63] Georges Aad et al. “Constraints on the Higgs boson self-coupling from single- and double-Higgs production with the ATLAS detector using pp collisions at $\sqrt{s}=13$ TeV”. In: *Phys. Lett. B* 843 (2023), p. 137745. DOI: 10.1016/j.physletb.2023.137745. arXiv: 2211.01216 [hep-ex].
- [64] Armen Tumasyan et al. “A portrait of the Higgs boson by the CMS experiment ten years after the discovery.” In: *Nature* 607.7917 (2022). [Erratum: *Nature* 623, (2023)], pp. 60–68. DOI: 10.1038/s41586-022-04892-x. arXiv: 2207.00043 [hep-ex].
- [65] Bartłomiej Zabinski. “Probing the nature of electroweak symmetry breaking with Higgs boson pairs in ATLAS”. In: *30th International Workshop on Deep-Inelastic Scattering and Related Subjects*. July 2023. arXiv: 2307.11467 [hep-ex].
- [66] Georges Aad et al. “A detailed map of Higgs boson interactions by the ATLAS experiment ten years after the discovery”. In: *Nature* 607.7917 (2022). [Erratum: *Nature* 612, E24 (2022)], pp. 52–59. DOI: 10.1038/s41586-022-04893-w. arXiv: 2207.00092 [hep-ex].
- [67] Brando Bellazzini, Csaba Csáki, and Javi Serra. “Composite Higgses”. In: *Eur. Phys. J. C* 74.5 (2014), p. 2766. DOI: 10.1140/epjc/s10052-014-2766-x. arXiv: 1401.2457 [hep-ph].
- [68] Y. Fukuda et al. “Evidence for oscillation of atmospheric neutrinos”. In: *Phys. Rev. Lett.* 81 (1998), pp. 1562–1567. DOI: 10.1103/PhysRevLett.81.1562. arXiv: hep-ex/9807003.
- [69] Q. R. Ahmad et al. “Measurement of the rate of $\nu_e + d \rightarrow p + p + e^-$ interactions produced by ^8B solar neutrinos at the Sudbury Neutrino Observatory”. In: *Phys. Rev. Lett.* 87 (2001), p. 071301. DOI: 10.1103/PhysRevLett.87.071301. arXiv: nucl-ex/0106015.
- [70] K. Eguchi et al. “First results from KamLAND: Evidence for reactor anti-neutrino disappearance”. In: *Phys. Rev. Lett.* 90 (2003), p. 021802. DOI: 10.1103/PhysRevLett.90.021802. arXiv: hep-ex/0212021.
- [71] Vincenzo Cirigliano et al. “Neutrinoless Double-Beta Decay: A Roadmap for Matching Theory to Experiment”. In: (Mar. 2022). arXiv: 2203.12169 [hep-ph].
- [72] A. D. Sakharov. “Violation of CP Invariance, C asymmetry, and baryon asymmetry of the universe”. In: *Pisma Zh. Eksp. Teor. Fiz.* 5 (1967), pp. 32–35. DOI: 10.1070/PU1991v034n05ABEH002497.

- [73] John F. Donoghue, Mikhail M. Ivanov, and Andrey Shkerin. “EPFL Lectures on General Relativity as a Quantum Field Theory”. In: (Feb. 2017). arXiv: 1702.00319 [hep-th].
- [74] Gerard 't Hooft. “Naturalness, chiral symmetry, and spontaneous chiral symmetry breaking”. In: *NATO Sci. Ser. B* 59 (1980). Ed. by Gerard 't Hooft et al., pp. 135–157. DOI: 10.1007/978-1-4684-7571-5_9.
- [75] Christopher T. Hill and Elizabeth H. Simmons. “Strong Dynamics and Electroweak Symmetry Breaking”. In: *Phys. Rept.* 381 (2003). [Erratum: *Phys.Rept.* 390, 553–554 (2004)], pp. 235–402. DOI: 10.1016/S0370-1573(03)00140-6. arXiv: hep-ph/0203079.
- [76] R. D. Peccei. “The Strong CP problem and axions”. In: *Lect. Notes Phys.* 741 (2008). Ed. by Markus Kuster, Georg Raffelt, and Berta Beltran, pp. 3–17. DOI: 10.1007/978-3-540-73518-2_1. arXiv: hep-ph/0607268.
- [77] R. D. Peccei and Helen R. Quinn. “CP Conservation in the Presence of Instantons”. In: *Phys. Rev. Lett.* 38 (1977), pp. 1440–1443. DOI: 10.1103/PhysRevLett.38.1440.
- [78] R. D. Peccei and Helen R. Quinn. “Constraints Imposed by CP Conservation in the Presence of Instantons”. In: *Phys. Rev. D* 16 (1977), pp. 1791–1797. DOI: 10.1103/PhysRevD.16.1791.
- [79] Alexey A. Petrov and Andrew E. Blechman. *Effective Field Theories*. WSP, 2016. ISBN: 978-981-4434-92-8, 978-981-4434-94-2. DOI: 10.1142/8619.
- [80] Aneesh V. Manohar. “Introduction to Effective Field Theories”. In: (Apr. 2018). Ed. by Sacha Davidson et al. DOI: 10.1093/oso/9780198855743.003.0002. arXiv: 1804.05863 [hep-ph].
- [81] Martin Beneke, Matthias König, and Martin Link. “The inverted pendulum as a classical analog of the EFT paradigm”. In: *Phys. Scripta* 99.6 (2024), p. 065240. DOI: 10.1088/1402-4896/ad4184. arXiv: 2308.14441 [hep-ph].
- [82] Steven Weinberg. “Phenomenological Lagrangians”. In: *Physica A* 96.1-2 (1979). Ed. by S. Deser, pp. 327–340. DOI: 10.1016/0378-4371(79)90223-1.
- [83] Aneesh V. Manohar and Mark B. Wise. *Heavy quark physics*. Vol. 10. 2000. ISBN: 978-0-521-03757-0, 978-1-009-40212-5. DOI: 10.1017/9781009402125.
- [84] Thomas Becher, Alessandro Broggio, and Andrea Ferroglia. *Introduction to Soft-Collinear Effective Theory*. Vol. 896. Springer, 2015. DOI: 10.1007/978-3-319-14848-9. arXiv: 1410.1892 [hep-ph].
- [85] Thomas Appelquist and J. Carazzone. “Infrared Singularities and Massive Fields”. In: *Phys. Rev. D* 11 (1975), p. 2856. DOI: 10.1103/PhysRevD.11.2856.
- [86] Rabindra N. Mohapatra and Goran Senjanovic. “Neutrino Mass and Spontaneous Parity Nonconservation”. In: *Phys. Rev. Lett.* 44 (1980), p. 912. DOI: 10.1103/PhysRevLett.44.912.
- [87] Gino Isidori, Felix Wilsch, and Daniel Wyler. “The standard model effective field theory at work”. In: *Rev. Mod. Phys.* 96.1 (2024), p. 015006. DOI: 10.1103/RevModPhys.96.015006. arXiv: 2303.16922 [hep-ph].

- [88] M. Aker et al. “KATRIN: status and prospects for the neutrino mass and beyond”. In: *J. Phys. G* 49.10 (2022), p. 100501. DOI: 10.1088/1361-6471/ac834e. arXiv: 2203.08059 [nucl-ex].
- [89] F. Capozzi et al. “Neutrino masses and mixings: Status of known and unknown 3ν parameters”. In: *Nucl. Phys. B* 908 (2016), pp. 218–234. DOI: 10.1016/j.nuclphysb.2016.02.016. arXiv: 1601.07777 [hep-ph].
- [90] Susanne Mertens. “Direct Neutrino Mass Experiments”. In: *J. Phys. Conf. Ser.* 718.2 (2016), p. 022013. DOI: 10.1088/1742-6596/718/2/022013. arXiv: 1605.01579 [nucl-ex].
- [91] John Ellis et al. “Updated Global SMEFT Fit to Higgs, Diboson and Electroweak Data”. In: *JHEP* 06 (2018), p. 146. DOI: 10.1007/JHEP06(2018)146. arXiv: 1803.03252 [hep-ph].
- [92] G. D’Ambrosio et al. “Minimal flavor violation: An Effective field theory approach”. In: *Nucl. Phys. B* 645 (2002), pp. 155–187. DOI: 10.1016/S0550-3213(02)00836-2. arXiv: hep-ph/0207036.
- [93] Graham D. Kribs et al. “Custodial symmetry violation in the SMEFT”. In: *Phys. Rev. D* 104.5 (2021), p. 056006. DOI: 10.1103/PhysRevD.104.056006. arXiv: 2009.10725 [hep-ph].
- [94] Elizabeth E. Jenkins, Aneesh V. Manohar, and Michael Trott. “Renormalization Group Evolution of the Standard Model Dimension Six Operators I: Formalism and λ Dependence”. In: *JHEP* 10 (2013), p. 087. DOI: 10.1007/JHEP10(2013)087. arXiv: 1308.2627 [hep-ph].
- [95] Elizabeth E. Jenkins, Aneesh V. Manohar, and Michael Trott. “Renormalization Group Evolution of the Standard Model Dimension Six Operators II: Yukawa Dependence”. In: *JHEP* 01 (2014), p. 035. DOI: 10.1007/JHEP01(2014)035. arXiv: 1310.4838 [hep-ph].
- [96] Rodrigo Alonso et al. “Renormalization Group Evolution of the Standard Model Dimension Six Operators III: Gauge Coupling Dependence and Phenomenology”. In: *JHEP* 04 (2014), p. 159. DOI: 10.1007/JHEP04(2014)159. arXiv: 1312.2014 [hep-ph].
- [97] Gerhard Buchalla et al. “Master Formula for One-Loop Renormalization of Bosonic SMEFT Operators”. In: (Apr. 2019). arXiv: 1904.07840 [hep-ph].
- [98] Alejandro Celis et al. “DsixTools: The Standard Model Effective Field Theory Toolkit”. In: *Eur. Phys. J. C* 77.6 (2017), p. 405. DOI: 10.1140/epjc/s10052-017-4967-6. arXiv: 1704.04504 [hep-ph].
- [99] A. Dedes et al. “Feynman rules for the Standard Model Effective Field Theory in R -gauges”. In: *JHEP* 06 (2017), p. 143. DOI: 10.1007/JHEP06(2017)143. arXiv: 1704.03888 [hep-ph].
- [100] Brian Henning et al. “2, 84, 30, 993, 560, 15456, 11962, 261485, ...: Higher dimension operators in the SM EFT”. In: *JHEP* 08 (2017). [Erratum: *JHEP* 09, 019 (2019)], p. 016. DOI: 10.1007/JHEP08(2017)016. arXiv: 1512.03433 [hep-ph].
- [101] R. V. Harlander, T. Kempkens, and M. C. Schaaf. “Standard model effective field theory up to mass dimension 12”. In: *Phys. Rev. D* 108.5 (2023), p. 055020. DOI: 10.1103/PhysRevD.108.055020. arXiv: 2305.06832 [hep-ph].

- [102] Robert V. Harlander and Magnus C. Schaaf. “AutoEFT: Automated operator construction for effective field theories”. In: *Comput. Phys. Commun.* 300 (2024), p. 109198. DOI: 10.1016/j.cpc.2024.109198. arXiv: 2309.15783 [hep-ph].
- [103] Landon Lehman. “Extending the Standard Model Effective Field Theory with the Complete Set of Dimension-7 Operators”. In: *Phys. Rev. D* 90.12 (2014), p. 125023. DOI: 10.1103/PhysRevD.90.125023. arXiv: 1410.4193 [hep-ph].
- [104] Yi Liao and Xiao-Dong Ma. “Renormalization Group Evolution of Dimension-seven Baryon- and Lepton-number-violating Operators”. In: *JHEP* 11 (2016), p. 043. DOI: 10.1007/JHEP11(2016)043. arXiv: 1607.07309 [hep-ph].
- [105] Yi Liao and Xiao-Dong Ma. “Renormalization Group Evolution of Dimension-seven Operators in Standard Model Effective Field Theory and Relevant Phenomenology”. In: *JHEP* 03 (2019), p. 179. DOI: 10.1007/JHEP03(2019)179. arXiv: 1901.10302 [hep-ph].
- [106] Christopher W. Murphy. “Dimension-8 operators in the Standard Model Effective Field Theory”. In: *JHEP* 10 (2020), p. 174. DOI: 10.1007/JHEP10(2020)174. arXiv: 2005.00059 [hep-ph].
- [107] Hao-Lin Li et al. “Complete set of dimension-eight operators in the standard model effective field theory”. In: *Phys. Rev. D* 104.1 (2021), p. 015026. DOI: 10.1103/PhysRevD.104.015026. arXiv: 2005.00008 [hep-ph].
- [108] Hao-Lin Li et al. “Complete set of dimension-nine operators in the standard model effective field theory”. In: *Phys. Rev. D* 104.1 (2021), p. 015025. DOI: 10.1103/PhysRevD.104.015025. arXiv: 2007.07899 [hep-ph].
- [109] Yi Liao and Xiao-Dong Ma. “An explicit construction of the dimension-9 operator basis in the standard model effective field theory”. In: *JHEP* 11 (2020), p. 152. DOI: 10.1007/JHEP11(2020)152. arXiv: 2007.08125 [hep-ph].
- [110] Gerhard Buchalla, Oscar Catá, and Claudius Krause. “On the Power Counting in Effective Field Theories”. In: *Phys. Lett. B* 731 (2014), pp. 80–86. DOI: 10.1016/j.physletb.2014.02.015. arXiv: 1312.5624 [hep-ph].
- [111] G. Buchalla et al. “Comment on ”Analysis of General Power Counting Rules in Effective Field Theory””. In: (Mar. 2016). arXiv: 1603.03062 [hep-ph].
- [112] Res Urech. “Virtual photons in chiral perturbation theory”. In: *Nucl. Phys. B* 433 (1995), pp. 234–254. DOI: 10.1016/0550-3213(95)90707-N. arXiv: hep-ph/9405341.
- [113] Adam Falkowski and Riccardo Rattazzi. “Which EFT”. In: *JHEP* 10 (2019), p. 255. DOI: 10.1007/JHEP10(2019)255. arXiv: 1902.05936 [hep-ph].
- [114] Rodrigo Alonso, Elizabeth E. Jenkins, and Aneesh V. Manohar. “A Geometric Formulation of Higgs Effective Field Theory: Measuring the Curvature of Scalar Field Space”. In: *Phys. Lett. B* 754 (2016), pp. 335–342. DOI: 10.1016/j.physletb.2016.01.041. arXiv: 1511.00724 [hep-ph].
- [115] Andreas Helset, Adam Martin, and Michael Trott. “The Geometric Standard Model Effective Field Theory”. In: *JHEP* 03 (2020), p. 163. DOI: 10.1007/JHEP03(2020)163. arXiv: 2001.01453 [hep-ph].

- [116] Tyler Corbett, Adam Martin, and Michael Trott. “Consistent higher order $\sigma(\mathcal{GG} \rightarrow h)$, $\Gamma(h \rightarrow \mathcal{GG})$ and $\Gamma(h \rightarrow \gamma\gamma)$ in geoSMEFT”. In: *JHEP* 12 (2021), p. 147. DOI: 10.1007/JHEP12(2021)147. arXiv: 2107.07470 [hep-ph].
- [117] Adam Martin and Michael Trott. “ ggh variations”. In: *Phys. Rev. D* 105.7 (2022), p. 076004. DOI: 10.1103/PhysRevD.105.076004. arXiv: 2109.05595 [hep-ph].
- [118] Grant N. Remmen and Nicholas L. Rodd. “Positively Identifying HEFT or SMEFT”. In: (Dec. 2024). arXiv: 2412.07827 [hep-ph].
- [119] G. Buchalla et al. “Standard Model Extended by a Heavy Singlet: Linear vs. Nonlinear EFT”. In: *Nucl. Phys. B* 917 (2017), pp. 209–233. DOI: 10.1016/j.nuclphysb.2017.02.006. arXiv: 1608.03564 [hep-ph].
- [120] Javier Fuentes-Martín, Ajdin Palavrić, and Anders Eller Thomsen. “Functional matching and renormalization group equations at two-loop order”. In: *Phys. Lett. B* 851 (2024), p. 138557. DOI: 10.1016/j.physletb.2024.138557. arXiv: 2311.13630 [hep-ph].
- [121] Javier Fuentes-Martín et al. “A Guide to Functional Methods Beyond One-Loop Order”. In: (Dec. 2024). arXiv: 2412.12270 [hep-ph].
- [122] Aleksandra Drozd et al. “The Universal One-Loop Effective Action”. In: *JHEP* 03 (2016), p. 180. DOI: 10.1007/JHEP03(2016)180. arXiv: 1512.03003 [hep-ph].
- [123] Benjamin Summ and Alexander Voigt. “Extending the Universal One-Loop Effective Action by Regularization Scheme Translating Operators”. In: *JHEP* 08 (2018), p. 026. DOI: 10.1007/JHEP08(2018)026. arXiv: 1806.05171 [hep-ph].
- [124] Michael Krämer, Benjamin Summ, and Alexander Voigt. “Completing the scalar and fermionic Universal One-Loop Effective Action”. In: *JHEP* 01 (2020), p. 079. DOI: 10.1007/JHEP01(2020)079. arXiv: 1908.04798 [hep-ph].
- [125] Sebastian A. R. Ellis et al. “The Fermionic Universal One-Loop Effective Action”. In: *JHEP* 11 (2020), p. 078. DOI: 10.1007/JHEP11(2020)078. arXiv: 2006.16260 [hep-ph].
- [126] Javier Fuentes-Martín et al. “A proof of concept for matchete: an automated tool for matching effective theories”. In: *Eur. Phys. J. C* 83.7 (2023), p. 662. DOI: 10.1140/epjc/s10052-023-11726-1. arXiv: 2212.04510 [hep-ph].
- [127] Mikhail S. Bilenky and Arcadi Santamaria. “One loop effective Lagrangian for a standard model with a heavy charged scalar singlet”. In: *Nucl. Phys. B* 420 (1994), pp. 47–93. DOI: 10.1016/0550-3213(94)90375-1. arXiv: hep-ph/9310302.
- [128] Zhengkang Zhang. “Covariant diagrams for one-loop matching”. In: *JHEP* 05 (2017), p. 152. DOI: 10.1007/JHEP05(2017)152. arXiv: 1610.00710 [hep-ph].
- [129] Upalaparna Banerjee et al. “One-loop effective action up to dimension eight: integrating out heavy scalar(s)”. In: *Eur. Phys. J. Plus* 139.2 (2024), p. 159. DOI: 10.1140/epjp/s13360-024-04890-0. arXiv: 2306.09103 [hep-ph].
- [130] W. Heisenberg and H. Euler. “Consequences of Dirac’s theory of positrons”. In: *Z. Phys.* 98.11-12 (1936), pp. 714–732. DOI: 10.1007/BF01343663. arXiv: physics/0605038.

- [131] Jeremie Quevillon, Christopher Smith, and Selim Touati. “Effective action for gauge bosons”. In: *Phys. Rev. D* 99.1 (2019), p. 013003. DOI: 10.1103/PhysRevD.99.013003. arXiv: 1810.06994 [hep-ph].
- [132] Christoph Müller-Salditt. “Power counting in the standard model effective field theory with Applications to $gg \rightarrow t\bar{t}$ and $h \rightarrow gg$ ”. PhD thesis. LMU Munich (main), 2023. DOI: 10.5282/edoc.32397.
- [133] Christoph Englert, Peter Galler, and Chris D. White. “Effective field theory and scalar extensions of the top quark sector”. In: *Phys. Rev. D* 101.3 (2020), p. 035035. DOI: 10.1103/PhysRevD.101.035035. arXiv: 1908.05588 [hep-ph].
- [134] M. Beneke and Vladimir A. Smirnov. “Asymptotic expansion of Feynman integrals near threshold”. In: *Nucl. Phys. B* 522 (1998), pp. 321–344. DOI: 10.1016/S0550-3213(98)00138-2. arXiv: hep-ph/9711391.
- [135] Gerhard Buchalla, Oscar Cata, and Claudius Krause. “A Systematic Approach to the SILH Lagrangian”. In: *Nucl. Phys. B* 894 (2015), pp. 602–620. DOI: 10.1016/j.nuclphysb.2015.03.024. arXiv: 1412.6356 [hep-ph].
- [136] Ran Huo. “Standard Model Effective Field Theory: Integrating out Vector-Like Fermions”. In: *JHEP* 09 (2015), p. 037. DOI: 10.1007/JHEP09(2015)037. arXiv: 1506.00840 [hep-ph].
- [137] Matthew J. Dolan et al. “Simplified Models for Higgs Physics: Singlet Scalar and Vector-like Quark Phenomenology”. In: *JHEP* 07 (2016), p. 039. DOI: 10.1007/JHEP07(2016)039. arXiv: 1601.07208 [hep-ph].
- [138] Aneesh Manohar and Howard Georgi. “Chiral Quarks and the Nonrelativistic Quark Model”. In: *Nucl. Phys. B* 234 (1984), pp. 189–212. DOI: 10.1016/0550-3213(84)90231-1.
- [139] Elizabeth E. Jenkins, Aneesh V. Manohar, and Michael Trott. “Naive Dimensional Analysis Counting of Gauge Theory Amplitudes and Anomalous Dimensions”. In: *Phys. Lett. B* 726 (2013), pp. 697–702. DOI: 10.1016/j.physletb.2013.09.020. arXiv: 1309.0819 [hep-ph].
- [140] Aneesh V. Manohar. “An Exactly Solvable Model for Dimension Six Higgs Operators and $h \rightarrow \gamma\gamma$ ”. In: *Phys. Lett. B* 726 (2013), pp. 347–351. DOI: 10.1016/j.physletb.2013.08.072. arXiv: 1305.3927 [hep-ph].
- [141] G. F. Giudice et al. “The Strongly-Interacting Light Higgs”. In: *JHEP* 06 (2007), p. 045. DOI: 10.1088/1126-6708/2007/06/045. arXiv: hep-ph/0703164.
- [142] C. Arzt, M. B. Einhorn, and J. Wudka. “Patterns of deviation from the standard model”. In: *Nucl. Phys. B* 433 (1995), pp. 41–66. DOI: 10.1016/0550-3213(94)00336-D. arXiv: hep-ph/9405214.
- [143] Nathaniel Craig et al. “Loops and Trees in Generic EFTs”. In: *JHEP* 08 (2020), p. 086. DOI: 10.1007/JHEP08(2020)086. arXiv: 2001.00017 [hep-ph].
- [144] Nicolas Deutschmann et al. “Gluon-fusion Higgs production in the Standard Model Effective Field Theory”. In: *JHEP* 12 (2017). [Erratum: *JHEP* 02, 159 (2018)], p. 063. DOI: 10.1007/JHEP12(2017)063. arXiv: 1708.00460 [hep-ph].

- [145] Massimiliano Grazzini, Agnieszka Ilnicka, and Michael Spira. “Higgs boson production at large transverse momentum within the SMEFT: analytical results”. In: *Eur. Phys. J. C* 78.10 (2018), p. 808. DOI: 10.1140/epjc/s10052-018-6261-7. arXiv: 1806.08832 [hep-ph].
- [146] Marco Battaglia et al. “Sensitivity to BSM effects in the Higgs p_T spectrum within SMEFT”. In: *JHEP* 11 (2021), p. 173. DOI: 10.1007/JHEP11(2021)173. arXiv: 2109.02987 [hep-ph].
- [147] Lina Alasfar, Jorge de Blas, and Ramona Gröber. “Higgs probes of top quark contact interactions and their interplay with the Higgs self-coupling”. In: *JHEP* 05 (2022), p. 111. DOI: 10.1007/JHEP05(2022)111. arXiv: 2202.02333 [hep-ph].
- [148] Florian Goertz et al. “Higgs boson pair production in the D=6 extension of the SM”. In: *JHEP* 04 (2015), p. 167. DOI: 10.1007/JHEP04(2015)167. arXiv: 1410.3471 [hep-ph].
- [149] Ramona Grober et al. “NLO QCD Corrections to Higgs Pair Production including Dimension-6 Operators”. In: *JHEP* 09 (2015), p. 092. DOI: 10.1007/JHEP09(2015)092. arXiv: 1504.06577 [hep-ph].
- [150] Fabio Maltoni, Eleni Vryonidou, and Cen Zhang. “Higgs production in association with a top-antitop pair in the Standard Model Effective Field Theory at NLO in QCD”. In: *JHEP* 10 (2016), p. 123. DOI: 10.1007/JHEP10(2016)123. arXiv: 1607.05330 [hep-ph].
- [151] Daniel de Florian, Ignacio Fabre, and Javier Mazzitelli. “Higgs boson pair production at NNLO in QCD including dimension 6 operators”. In: *JHEP* 10 (2017), p. 215. DOI: 10.1007/JHEP10(2017)215. arXiv: 1704.05700 [hep-ph].
- [152] R. Grober, M. Muhlleitner, and M. Spira. “Higgs Pair Production at NLO QCD for CP-violating Higgs Sectors”. In: *Nucl. Phys. B* 925 (2017), pp. 1–27. DOI: 10.1016/j.nuclphysb.2017.10.002. arXiv: 1705.05314 [hep-ph].
- [153] G. Buchalla et al. “Higgs boson pair production in non-linear Effective Field Theory with full m_t -dependence at NLO QCD”. In: *JHEP* 09 (2018), p. 057. DOI: 10.1007/JHEP09(2018)057. arXiv: 1806.05162 [hep-ph].
- [154] Matteo Capozzi and Gudrun Heinrich. “Exploring anomalous couplings in Higgs boson pair production through shape analysis”. In: *JHEP* 03 (2020), p. 091. DOI: 10.1007/JHEP03(2020)091. arXiv: 1908.08923 [hep-ph].
- [155] Gudrun Heinrich et al. “A non-linear EFT description of $gg \rightarrow HH$ at NLO interfaced to POWHEG”. In: *JHEP* 10 (2020), p. 021. DOI: 10.1007/JHEP10(2020)021. arXiv: 2006.16877 [hep-ph].
- [156] Daniel de Florian et al. “Anomalous couplings in Higgs-boson pair production at approximate NNLO QCD”. In: *JHEP* 09 (2021), p. 161. DOI: 10.1007/JHEP09(2021)161. arXiv: 2106.14050 [hep-ph].
- [157] Christoph Müller. “Top-pair production via gluon fusion in the Standard Model effective field theory”. In: *Phys. Rev. D* 104.9 (2021), p. 095003. DOI: 10.1103/PhysRevD.104.095003. arXiv: 2102.05040 [hep-ph].

- [158] Christine Hartmann and Michael Trott. “Higgs Decay to Two Photons at One Loop in the Standard Model Effective Field Theory”. In: *Phys. Rev. Lett.* 115.19 (2015), p. 191801. DOI: 10.1103/PhysRevLett.115.191801. arXiv: 1507.03568 [hep-ph].
- [159] Christine Hartmann and Michael Trott. “On one-loop corrections in the standard model effective field theory; the $\Gamma(h \rightarrow \gamma\gamma)$ case”. In: *JHEP* 07 (2015), p. 151. DOI: 10.1007/JHEP07(2015)151. arXiv: 1505.02646 [hep-ph].
- [160] A. Dedes et al. “The decay $h \rightarrow \gamma\gamma$ in the Standard-Model Effective Field Theory”. In: *JHEP* 08 (2018), p. 103. DOI: 10.1007/JHEP08(2018)103. arXiv: 1805.00302 [hep-ph].
- [161] Wojciech Bizoń et al. “Anomalous couplings in associated VH production with Higgs boson decay to massive b quarks at NNLO in QCD”. In: *Phys. Rev. D* 105.1 (2022), p. 014023. DOI: 10.1103/PhysRevD.105.014023. arXiv: 2106.06328 [hep-ph].
- [162] Ulrich Haisch et al. “NNLO event generation for $pp \rightarrow Zh \rightarrow \ell^+ \ell^- b\bar{b}$ production in the SM effective field theory”. In: *JHEP* 07 (2022), p. 054. DOI: 10.1007/JHEP07(2022)054. arXiv: 2204.00663 [hep-ph].
- [163] Gerhard Buchalla, Marius Höfer, and Christoph Müller-Saldaña. “ $h \rightarrow gg$ and $h \rightarrow \gamma\gamma$ with anomalous couplings at next-to-leading order in QCD”. In: *Phys. Rev. D* 107.7 (2023), p. 076021. DOI: 10.1103/PhysRevD.107.076021. arXiv: 2212.08560 [hep-ph].
- [164] H. M. Georgi et al. “Higgs Bosons from Two Gluon Annihilation in Proton Proton Collisions”. In: *Phys. Rev. Lett.* 40 (1978), p. 692. DOI: 10.1103/PhysRevLett.40.692.
- [165] S. Dawson. “Radiative corrections to Higgs boson production”. In: *Nucl. Phys. B* 359 (1991), pp. 283–300. DOI: 10.1016/0550-3213(91)90061-2.
- [166] A. Djouadi, M. Spira, and P. M. Zerwas. “Production of Higgs bosons in proton colliders: QCD corrections”. In: *Phys. Lett. B* 264 (1991), pp. 440–446. DOI: 10.1016/0370-2693(91)90375-Z.
- [167] Aneesh V. Manohar and Mark B. Wise. “Modifications to the properties of the Higgs boson”. In: *Phys. Lett. B* 636 (2006), pp. 107–113. DOI: 10.1016/j.physletb.2006.03.030. arXiv: hep-ph/0601212.
- [168] G. Buchalla et al. “Effective Field Theory Analysis of New Physics in $e^+e^- \rightarrow W^+W^-$ at a Linear Collider”. In: *Eur. Phys. J. C* 73.10 (2013), p. 2589. DOI: 10.1140/epjc/s10052-013-2589-1. arXiv: 1302.6481 [hep-ph].
- [169] J. de Blas et al. “Impact of the Recent Measurements of the Top-Quark and W-Boson Masses on Electroweak Precision Fits”. In: *Phys. Rev. Lett.* 129.27 (2022), p. 271801. DOI: 10.1103/PhysRevLett.129.271801. arXiv: 2204.04204 [hep-ph].
- [170] Igor P. Ivanov. “Building and testing models with extended Higgs sectors”. In: *Prog. Part. Nucl. Phys.* 95 (2017), pp. 160–208. DOI: 10.1016/j.pnpnp.2017.03.001. arXiv: 1702.03776 [hep-ph].

- [171] G. C. Branco et al. “Theory and phenomenology of two-Higgs-doublet models”. In: *Phys. Rept.* 516 (2012), pp. 1–102. DOI: 10.1016/j.physrep.2012.02.002. arXiv: 1106.0034 [hep-ph].
- [172] John F. Gunion and Howard E. Haber. “The CP conserving two Higgs doublet model: The Approach to the decoupling limit”. In: *Phys. Rev. D* 67 (2003), p. 075019. DOI: 10.1103/PhysRevD.67.075019. arXiv: hep-ph/0207010.
- [173] Hermès Bélusca-Maïto et al. “Higgs EFT for 2HDM and beyond”. In: *Eur. Phys. J. C* 77.3 (2017), p. 176. DOI: 10.1140/epjc/s10052-017-4745-5. arXiv: 1611.01112 [hep-ph].
- [174] Sheldon L. Glashow and Steven Weinberg. “Natural Conservation Laws for Neutral Currents”. In: *Phys. Rev. D* 15 (1977), p. 1958. DOI: 10.1103/PhysRevD.15.1958.
- [175] E. A. Paschos. “Diagonal Neutral Currents”. In: *Phys. Rev. D* 15 (1977), p. 1966. DOI: 10.1103/PhysRevD.15.1966.
- [176] Stephen P. Martin. “A Supersymmetry primer”. In: *Adv. Ser. Direct. High Energy Phys.* 18 (1998). Ed. by Gordon L. Kane, pp. 1–98. DOI: 10.1142/9789812839657_0001. arXiv: hep-ph/9709356.
- [177] Radja Boughezal et al. “Top quark decay at next-to-leading order in the Standard Model Effective Field Theory”. In: *Phys. Rev. D* 100.5 (2019), p. 056023. DOI: 10.1103/PhysRevD.100.056023. arXiv: 1907.00997 [hep-ph].
- [178] Stefan Dittmaier and Carsten Grosse-Knetter. “Deriving nondecoupling effects of heavy fields from the path integral: A Heavy Higgs field in an SU(2) gauge theory”. In: *Phys. Rev. D* 52 (1995), pp. 7276–7293. DOI: 10.1103/PhysRevD.52.7276. arXiv: hep-ph/9501285.
- [179] J. Goldstone. “Field Theories with Superconductor Solutions”. In: *Nuovo Cim.* 19 (1961), pp. 154–164. DOI: 10.1007/BF02812722.
- [180] Yoichiro Nambu. “Quasiparticles and Gauge Invariance in the Theory of Superconductivity”. In: *Phys. Rev.* 117 (1960). Ed. by J. C. Taylor, pp. 648–663. DOI: 10.1103/PhysRev.117.648.
- [181] Yoichiro Nambu. “Axial vector current conservation in weak interactions”. In: *Phys. Rev. Lett.* 4 (1960). Ed. by T. Eguchi, pp. 380–382. DOI: 10.1103/PhysRevLett.4.380.
- [182] Yoichiro Nambu and G. Jona-Lasinio. “Dynamical Model of Elementary Particles Based on an Analogy with Superconductivity. 1.” In: *Phys. Rev.* 122 (1961). Ed. by T. Eguchi, pp. 345–358. DOI: 10.1103/PhysRev.122.345.
- [183] Thomas Appelquist and Claude W. Bernard. “The Nonlinear σ Model in the Loop Expansion”. In: *Phys. Rev. D* 23 (1981), p. 425. DOI: 10.1103/PhysRevD.23.425.
- [184] Steven Weinberg. “Nonlinear realizations of chiral symmetry”. In: *Phys. Rev.* 166 (1968), pp. 1568–1577. DOI: 10.1103/PhysRev.166.1568.
- [185] Sidney R. Coleman, J. Wess, and Bruno Zumino. “Structure of phenomenological Lagrangians. 1.” In: *Phys. Rev.* 177 (1969), pp. 2239–2247. DOI: 10.1103/PhysRev.177.2239.
- [186] Curtis G. Callan Jr. et al. “Structure of phenomenological Lagrangians. 2.” In: *Phys. Rev.* 177 (1969), pp. 2247–2250. DOI: 10.1103/PhysRev.177.2247.

- [187] Heather E. Logan. “Lectures on perturbative unitarity and decoupling in Higgs physics”. In: (July 2022). arXiv: 2207.01064 [hep-ph].
- [188] Benjamin W. Lee, C. Quigg, and H. B. Thacker. “Weak Interactions at Very High-Energies: The Role of the Higgs Boson Mass”. In: *Phys. Rev. D* 16 (1977), p. 1519. DOI: 10.1103/PhysRevD.16.1519.
- [189] Benjamin W. Lee, C. Quigg, and H. B. Thacker. “The Strength of Weak Interactions at Very High-Energies and the Higgs Boson Mass”. In: *Phys. Rev. Lett.* 38 (1977), pp. 883–885. DOI: 10.1103/PhysRevLett.38.883.
- [190] Stefan Scherer and Matthias R. Schindler. *A Primer for Chiral Perturbation Theory*. Vol. 830. 2012. ISBN: 978-3-642-19253-1. DOI: 10.1007/978-3-642-19254-8.
- [191] Mykyta Dmytriiev and Volodymyr Skalozub. “Low-energy effective Lagrangian of the two-Higgs-doublet model”. In: *Journal of Physics and Electronics* 29.2 (2022), pp. 8–20. arXiv: 2206.07770 [hep-ph].
- [192] Ian Banta et al. “Effective field theory of the two Higgs doublet model”. In: *JHEP* 06 (2023), p. 150. DOI: 10.1007/JHEP06(2023)150. arXiv: 2304.09884 [hep-ph].
- [193] Sally Dawson et al. “Matching the 2HDM to the HEFT and the SMEFT: Decoupling and perturbativity”. In: *Phys. Rev. D* 108.5 (2023), p. 055034. DOI: 10.1103/PhysRevD.108.055034. arXiv: 2305.07689 [hep-ph].
- [194] F. Arco et al. “Non-decoupling effects from heavy Higgs bosons by matching 2HDM to HEFT amplitudes”. In: (July 2023). arXiv: 2307.15693 [hep-ph].
- [195] Stefan Dittmaier and Heidi Rzehak. “Electroweak renormalization based on gauge-invariant vacuum expectation values of non-linear Higgs representations. Part II. Extended Higgs sectors”. In: *JHEP* 08 (2022), p. 245. DOI: 10.1007/JHEP08(2022)245. arXiv: 2206.01479 [hep-ph].
- [196] G. Buchalla et al. “Higgs-electroweak chiral Lagrangian: One-loop renormalization group equations”. In: *Phys. Rev. D* 104.7 (2021), p. 076005. DOI: 10.1103/PhysRevD.104.076005. arXiv: 2004.11348 [hep-ph].
- [197] Mikhail A. Shifman et al. “Low-Energy Theorems for Higgs Boson Couplings to Photons”. In: *Sov. J. Nucl. Phys.* 30 (1979), pp. 711–716.
- [198] Gautam Bhattacharyya and Dipankar Das. “Nondecoupling of charged scalars in Higgs decay to two photons and symmetries of the scalar potential”. In: *Phys. Rev. D* 91 (2015), p. 015005. DOI: 10.1103/PhysRevD.91.015005. arXiv: 1408.6133 [hep-ph].
- [199] Joshua Ellis. “TikZ-Feynman: Feynman diagrams with TikZ”. In: *Comput. Phys. Commun.* 210 (2017), pp. 103–123. DOI: 10.1016/j.cpc.2016.08.019. arXiv: 1601.05437 [hep-ph].
- [200] Hiren H. Patel. “Package-X: A Mathematica package for the analytic calculation of one-loop integrals”. In: *Comput. Phys. Commun.* 197 (2015), pp. 276–290. DOI: 10.1016/j.cpc.2015.08.017. arXiv: 1503.01469 [hep-ph].
- [201] Hiren H. Patel. “Package-X 2.0: A Mathematica package for the analytic calculation of one-loop integrals”. In: *Comput. Phys. Commun.* 218 (2017), pp. 66–70. DOI: 10.1016/j.cpc.2017.04.015. arXiv: 1612.00009 [hep-ph].

- [202] Michael E. Peskin and Tatsu Takeuchi. “A New constraint on a strongly interacting Higgs sector”. In: *Phys. Rev. Lett.* 65 (1990), pp. 964–967. DOI: 10.1103/PhysRevLett.65.964.
- [203] Michael E. Peskin and Tatsu Takeuchi. “Estimation of oblique electroweak corrections”. In: *Phys. Rev. D* 46 (1992), pp. 381–409. DOI: 10.1103/PhysRevD.46.381.
- [204] W. Grimus et al. “A Precision constraint on multi-Higgs-doublet models”. In: *J. Phys. G* 35 (2008), p. 075001. DOI: 10.1088/0954-3899/35/7/075001. arXiv: 0711.4022 [hep-ph].
- [205] Abdul Wahab El Kaffas et al. “Consistency of the two Higgs doublet model and CP violation in top production at the LHC”. In: *Nucl. Phys. B* 775 (2007), pp. 45–77. DOI: 10.1016/j.nuclphysb.2007.03.041. arXiv: hep-ph/0605142.
- [206] A. Arhrib et al. “Higgs decays in the two Higgs doublet model: Large quantum effects in the decoupling regime”. In: *Phys. Lett. B* 579 (2004), pp. 361–370. DOI: 10.1016/j.physletb.2003.10.006. arXiv: hep-ph/0307391.
- [207] Francisco Faro, Jorge C. Romão, and João P. Silva. “Nondecoupling in multi-Higgs doublet models”. In: *The European Physical Journal C* 80.7 (July 2020). ISSN: 1434-6052. DOI: 10.1140/epjc/s10052-020-8217-y. URL: <http://dx.doi.org/10.1140/epjc/s10052-020-8217-y>.
- [208] John F. Gunion and Howard E. Haber. “CP-conserving two-Higgs-doublet model: The approach to the decoupling limit”. In: *Phys. Rev. D* 67 (7 2003). DOI: 10.1103/PhysRevD.67.075019.
- [209] H. Hüffel and G. Pócsik. “Unitarity bounds on Higgs boson masses in the Weinberg-Salam model with two Higgs doublets”. In: *Zeitschrift für Physik C Particles and Fields* 8.1 (1981). DOI: 10.1007/BF01429824.
- [210] R. Casalbuoni et al. “Tree-level unitarity violation for large scalar mass in multi-Higgs extensions of the standard model”. In: *Nuclear Physics B* 299.1 (1988). DOI: [https://doi.org/10.1016/0550-3213\(88\)90469-5](https://doi.org/10.1016/0550-3213(88)90469-5).
- [211] J. Maalampi, J. Sirkka, and I. Vilja. “Tree level unitarity and triviality bounds for two Higgs models”. In: *Phys. Lett. B* 265 (1991), pp. 371–376. DOI: 10.1016/0370-2693(91)90068-2.
- [212] Shinya Kanemura, Takahiro Kubota, and Eiichi Takasugi. “Lee-Quigg-Thacker bounds for Higgs boson masses in a two doublet model”. In: *Phys. Lett. B* 313 (1993), pp. 155–160. DOI: 10.1016/0370-2693(93)91205-2. arXiv: hep-ph/9303263.
- [213] Andrew G. Akeroyd, Abdesslam Arhrib, and El-Mokhtar Naimi. “Note on tree level unitarity in the general two Higgs doublet model”. In: *Phys. Lett. B* 490 (2000), pp. 119–124. DOI: 10.1016/S0370-2693(00)00962-X. arXiv: hep-ph/0006035.
- [214] J. Horejsi and M. Kladiva. “Tree-unitarity bounds for THDM Higgs masses revisited”. In: *Eur. Phys. J. C* 46 (2006), pp. 81–91. DOI: 10.1140/epjc/s2006-02472-3. arXiv: hep-ph/0510154.
- [215] Mark D. Goodsell and Florian Staub. “Improved unitarity constraints in Two-Higgs-Doublet-Models”. In: *Phys. Lett. B* 788 (2019), pp. 206–212. DOI: 10.1016/j.physletb.2018.11.030. arXiv: 1805.07310 [hep-ph].

- [216] Vincenzo Cacchio et al. “Next-to-leading order unitarity fits in Two-Higgs-Doublet models with soft \mathbb{Z}_2 breaking”. In: *JHEP* 11 (2016), p. 026. DOI: 10.1007/JHEP11(2016)026. arXiv: 1609.01290 [hep-ph].
- [217] Benjamín Grinstein, Christopher W. Murphy, and Patipan Uttayarat. “One-loop corrections to the perturbative unitarity bounds in the CP-conserving two-Higgs doublet model with a softly broken \mathbb{Z}_2 symmetry”. In: *JHEP* 06 (2016), p. 070. DOI: 10.1007/JHEP06(2016)070. arXiv: 1512.04567 [hep-ph].
- [218] Nilendra G. Deshpande and Ernest Ma. “Pattern of symmetry breaking with two Higgs doublets”. In: *Phys. Rev. D* 18 (7 1978), pp. 2574–2576. DOI: 10.1103/PhysRevD.18.2574. URL: <https://link.aps.org/doi/10.1103/PhysRevD.18.2574>.
- [219] K. G. Klimenko. “On Necessary and Sufficient Conditions for Some Higgs Potentials to Be Bounded From Below”. In: *Theor. Math. Phys.* 62 (1985), pp. 58–65. DOI: 10.1007/BF01034825.
- [220] M. Maniatis et al. “Stability and symmetry breaking in the general two-Higgs-doublet model”. In: *Eur. Phys. J. C* 48 (2006), pp. 805–823. DOI: 10.1140/epjc/s10052-006-0016-6. arXiv: hep-ph/0605184.
- [221] I. P. Ivanov. “Minkowski space structure of the Higgs potential in 2HDM”. In: *Phys. Rev. D* 75 (2007). [Erratum: Phys.Rev.D 76, 039902 (2007)], p. 035001. DOI: 10.1103/PhysRevD.75.035001. arXiv: hep-ph/0609018.
- [222] I. P. Ivanov and Joao P. Silva. “Tree-level metastability bounds for the most general two Higgs doublet model”. In: *Phys. Rev. D* 92.5 (2015), p. 055017. DOI: 10.1103/PhysRevD.92.055017. arXiv: 1507.05100 [hep-ph].
- [223] M. A. Perez, J. J. Toscano, and J. Wudka. “Two photon processes and effective Lagrangians with an extended scalar sector”. In: *Phys. Rev. D* 52 (1995), pp. 494–504. DOI: 10.1103/PhysRevD.52.494. arXiv: hep-ph/9506457.
- [224] Sally Dawson et al. “Role of dimension-eight operators in an EFT for the 2HDM”. In: *Phys. Rev. D* 106.5 (2022), p. 055012. DOI: 10.1103/PhysRevD.106.055012. arXiv: 2205.01561 [hep-ph].
- [225] Jorge de Blas, Otto Eberhardt, and Claudius Krause. “Current and Future Constraints on Higgs Couplings in the Nonlinear Effective Theory”. In: *JHEP* 07 (2018), p. 048. DOI: 10.1007/JHEP07(2018)048. arXiv: 1803.00939 [hep-ph].
- [226] Debtosh Chowdhury and Otto Eberhardt. “Update of Global Two-Higgs-Doublet Model Fits”. In: *JHEP* 05 (2018), p. 161. DOI: 10.1007/JHEP05(2018)161. arXiv: 1711.02095 [hep-ph].
- [227] F. Arco, S. Heinemeyer, and M. J. Herrero. “Triple Higgs couplings in the 2HDM: the complete picture”. In: *Eur. Phys. J. C* 82.6 (2022), p. 536. DOI: 10.1140/epjc/s10052-022-10485-9. arXiv: 2203.12684 [hep-ph].
- [228] Sally Dawson et al. “Is the HEFT matching unique?” In: *Phys. Rev. D* 109.5 (2024), p. 055037. DOI: 10.1103/PhysRevD.109.055037. arXiv: 2311.16897 [hep-ph].
- [229] Fabrizio Caola and Kirill Melnikov. “Constraining the Higgs boson width with ZZ production at the LHC”. In: *Phys. Rev. D* 88 (2013), p. 054024. DOI: 10.1103/PhysRevD.88.054024. arXiv: 1307.4935 [hep-ph].

- [230] Aleksandr Azatov et al. “Taming the off-shell Higgs boson”. In: *Zh. Eksp. Teor. Fiz.* 147 (2015), pp. 410–425. DOI: 10.1134/S1063776115030140. arXiv: 1406.6338 [hep-ph].
- [231] Anisha et al. “Higgs boson off-shell measurements probe nonlinearities”. In: *Phys. Rev. D* 109.9 (2024), p. 095033. DOI: 10.1103/PhysRevD.109.095033. arXiv: 2402.06746 [hep-ph].
- [232] John M. Campbell et al. “Two loop correction to interference in $gg \rightarrow ZZ$ ”. In: *JHEP* 08 (2016), p. 011. DOI: 10.1007/JHEP08(2016)011. arXiv: 1605.01380 [hep-ph].
- [233] Fabrizio Caola et al. “QCD corrections to vector boson pair production in gluon fusion including interference effects with off-shell Higgs at the LHC”. In: *JHEP* 07 (2016), p. 087. DOI: 10.1007/JHEP07(2016)087. arXiv: 1605.04610 [hep-ph].
- [234] Zhenyu Han and Witold Skiba. “Effective theory analysis of precision electroweak data”. In: *Phys. Rev. D* 71 (2005), p. 075009. DOI: 10.1103/PhysRevD.71.075009. arXiv: hep-ph/0412166.
- [235] E. W. Nigel Glover and J. J. van der Bij. “Z Boson Pair Production via Gluon Fusion”. In: *Nucl. Phys. B* 321 (1989), pp. 561–590. DOI: 10.1016/0550-3213(89)90262-9.
- [236] Michael S. Chanowitz and Mary K. Gaillard. “The TeV Physics of Strongly Interacting W’s and Z’s”. In: *Nucl. Phys. B* 261 (1985), pp. 379–431. DOI: 10.1016/0550-3213(85)90580-2.
- [237] J. Kublbeck, M. Bohm, and Ansgar Denner. “Feyn Arts: Computer Algebraic Generation of Feynman Graphs and Amplitudes”. In: *Comput. Phys. Commun.* 60 (1990), pp. 165–180. DOI: 10.1016/0010-4655(90)90001-H.
- [238] Vladyslav Shtabovenko, Rolf Mertig, and Frederik Orellana. “New Developments in FeynCalc 9.0”. In: *Comput. Phys. Commun.* 207 (2016), pp. 432–444. DOI: 10.1016/j.cpc.2016.06.008. arXiv: 1601.01167 [hep-ph].
- [239] Vladyslav Shtabovenko, Rolf Mertig, and Frederik Orellana. “FeynCalc 9.3: New features and improvements”. In: *Comput. Phys. Commun.* 256 (2020), p. 107478. DOI: 10.1016/j.cpc.2020.107478. arXiv: 2001.04407 [hep-ph].
- [240] Vladyslav Shtabovenko, Rolf Mertig, and Frederik Orellana. “FeynCalc 10: Do multiloop integrals dream of computer codes?” In: *Comput. Phys. Commun.* 306 (2025), p. 109357. DOI: 10.1016/j.cpc.2024.109357. arXiv: 2312.14089 [hep-ph].
- [241] E. C. G. Stueckelberg. “Interaction energy in electrodynamics and in the field theory of nuclear forces”. In: *Helv. Phys. Acta* 11 (1938), pp. 225–244. DOI: 10.5169/seals-110852.
- [242] E. C. G. Stueckelberg. “Interaction forces in electrodynamics and in the field theory of nuclear forces”. In: *Helv. Phys. Acta* 11 (1938), pp. 299–328.
- [243] Henri Ruegg and Marti Ruiz-Altaba. “The Stueckelberg field”. In: *Int. J. Mod. Phys. A* 19 (2004), pp. 3265–3348. DOI: 10.1142/S0217751X04019755. arXiv: hep-th/0304245.

- [244] Sally Dawson, Matthew Forsslund, and Marvin Schnubel. “SMEFT matching to Z' models at dimension eight”. In: *Phys. Rev. D* 110.1 (2024), p. 015002. DOI: 10.1103/PhysRevD.110.015002. arXiv: 2404.01375 [hep-ph].
- [245] Abdelhak Djouadi. “The Anatomy of electro-weak symmetry breaking. I: The Higgs boson in the standard model”. In: *Phys. Rept.* 457 (2008), pp. 1–216. DOI: 10.1016/j.physrep.2007.10.004. arXiv: hep-ph/0503172.
- [246] G. Buchalla et al. “Complete One-Loop Renormalization of the Higgs-Electroweak Chiral Lagrangian”. In: *Nucl. Phys. B* 928 (2018), pp. 93–106. DOI: 10.1016/j.nuclphysb.2018.01.009. arXiv: 1710.06412 [hep-ph].
- [247] R. Alonso, K. Kanshin, and S. Saa. “Renormalization group evolution of Higgs effective field theory”. In: *Phys. Rev. D* 97.3 (2018), p. 035010. DOI: 10.1103/PhysRevD.97.035010. arXiv: 1710.06848 [hep-ph].
- [248] T. Hahn and M. Perez-Victoria. “Automatized one loop calculations in four-dimensions and D-dimensions”. In: *Comput. Phys. Commun.* 118 (1999), pp. 153–165. DOI: 10.1016/S0010-4655(98)00173-8. arXiv: hep-ph/9807565.
- [249] Gerard 't Hooft and M. J. G. Veltman. “Scalar One Loop Integrals”. In: *Nucl. Phys. B* 153 (1979), pp. 365–401. DOI: 10.1016/0550-3213(79)90605-9.
- [250] R. Keith Ellis and Giulia Zanderighi. “Scalar one-loop integrals for QCD”. In: *JHEP* 02 (2008), p. 002. DOI: 10.1088/1126-6708/2008/02/002. arXiv: 0712.1851 [hep-ph].

Acknowledgments - Danksagung

Last but not least, I would like to thank everybody who helped me along the way. First and foremost, I would like to thank my advisor, Gerhard Buchalla, for his guidance, encouragement, kindness and patience in answering all my questions. Thank you, Gerhard, for first accepting me as a bachelor's student and later letting me be part of your group as a master's and PhD Student. I will fondly remember all our lunches, discussions, and group excursions together. These were formative years for me in the best possible sense. A big thank you goes to all the awesome members of our group over the years: Marius Höfer, Florian König, and Christoph Müller-Salditt. It was a great pleasure to get to know you, have lunch at Mensa, and collaborate with you guys. The years in the Buchalla group wouldn't have been half as fun without the best office mate imaginable and dear friend Christoph. It has been a great joy to come to the office every day, discuss anything and everything and share the same sense of humor. I also want to acknowledge my other friends with whom I spent time with during my time at LMU. A big thank you goes to Pouria for his friendship and the shared travel experiences over the years. I want to thank Cecilia for the many fun lunches we had together. I am also grateful to Daniel, Martín, and Hrólfur for the nice moments we shared over the years.

I want to thank Gerhard Buchalla, Michael Haack, Bernhard Mayer, Ivo Sachs and Otmar Biebel for being part of my PhD committee.

I also want to thank our secretaries, Herta Wiesbeck-Yonis and Lana Mukhanov, for their administrative support.

Finishing this thesis would not have been possible without the support of my family. I owe a special debt of gratitude to my sister, Marianne; my dad, Franz; and my aunt, Tina, for their continuous emotional support and encouragement over the years. A heartfelt thank you goes to all of you! I wouldn't have come as far without my mom, Nicola, who passed away too soon.